University of Alberta

Detection of mLAPTm4/MTP and hENT Proteins in Mammalian Cells and Investigations into the Regulation of Equilibrative Nucleoside Transporter Proteins

by

Miguel António Cabrita

A thesis submitted to the Faculty of Graduate Studies and Research in partial fulfillment of the requirements for the degree of Doctor of Philosophy

Department of Biochemistry

Edmonton, Alberta

Fall, 2001

National Library of Canada
Acquisitions and Bibliographic Services
395 Wellington Street
Ottawa ON K1A 0N4
Canada

Bibliothèque nationale du Canada
Acquisitions et services bibliographiques
395, rue Wellington
Ottawa ON K1A 0N4
Canada

Your file Votre référence

Our file Notre référence

The author has granted a non-exclusive licence allowing the National Library of Canada to reproduce, loan, distribute or sell copies of this thesis in microform, paper or electronic formats.

The author retains ownership of the copyright in this thesis. Neither the thesis nor substantial extracts from it may be printed or otherwise reproduced without the author's permission.

L'auteur a accordé une licence non exclusive permettant à la Bibliothèque nationale du Canada de reproduire, prêter, distribuer ou vendre des copies de cette thèse sous la forme de microfiche/film, de reproduction sur papier ou sur format électronique.

L'auteur conserve la propriété du droit d'auteur qui protège cette thèse. Ni la thèse ni des extraits substantiels de celle-ci ne doivent être imprimés ou autrement reproduits sans son autorisation.

0-612-68916-6

Canada

University of Alberta

Library Release Form

Name of Author: Miguel António Cabrita

Title of Thesis: Detection of mLAPTm4/MTP and hENT Proteins in Mammalian Cells and Investigations into the Regulation of Equilibrative Nucleoside Transporter Proteins

Degree: Doctor of Philosophy

Year This Degree Granted: 2001

Permission is hereby granted to the University of Alberta Library to reproduce single copies of this thesis and to lend or sell such copies for private, scholarly or scientific research purposes only.

The author reserves all other publication and other rights in association with the copyright in the thesis, and except as herein before provided, neither the thesis nor any substantial portion thereof may be printed or otherwise reproduced in any material form whatever without the author's prior written permission.

Miguel Cabrita

7511-157 Avenue
Edmonton, Alberta
T5Z 2X2

Date: October 2, 2001

"The sole aim of science is the glory of the human spirit"

Gerhard Herzberg
Canadian Nobel Laureate in Chemistry

University of Alberta

Faculty of Graduate Studies and Research

The undersigned certify that they have read, and recommend to the Faculty of Graduate Studies and Research for acceptance, a thesis entitled ***Detection of mLAPTm4/MTP and hENT Proteins in Mammalian Cells and Investigations into the Regulation of Equilibrative Nucleoside Transporter Proteins*** submitted by Miguel António Cabrita in partial fulfillment of the requirements for the degree of Doctor of Philosophy.

Dr. Carol E. Cass
(Supervisor)

Dr. Luis B. Agellon

Dr. Xing-Zhen Chen

Dr. Michael J. Ellison

Dr. Tom C. Hobman

Dr. Marek Michalak

Dr. James D. Young

Dr. James R. Hammond
(External Examiner)

Thesis Approval Date: Oct 2, 2001

This thesis is dedicated to my immediate family, my father, Virgilio, my mother, Maria Encarnação, and my sister, Luisa. Without their love and support, this degree could not have been completed.

ABSTRACT

Membrane transporter proteins mediate the translocation of various solutes. The natural substrates of some transporter proteins, like mLAPTm4, have not yet been identified. Determining the subcellular localization of such proteins may provide clues as to their functions. Described here is the localization of mLAPTm4. Recombinant epitope-tagged mLAPTm4 was localized to lysosomes in transiently transfected cells by confocal immunofluorescence microscopy.

Nucleoside transporter proteins have been divided into five distinct superfamilies. Two of these superfamilies, the equilibrative and concentrative nucleoside transporters, have human representatives. The equilibrative nucleoside transporters (ENTs) are bi-directional transporters that translocate nucleosides down their concentration gradients and are important in the uptake of anticancer and antiviral nucleoside drugs. A major objective of this study was to generate anti-hENT1 and anti-hENT2 antibodies for use in studies of cellular distribution and regulation. Antibodies were raised against a hENT1-specific synthetic peptide and a hENT2-specific fusion protein, which corresponded to residues in the large intracellular loop regions of either hENT1 or hENT2, respectively. These antibodies recognized recombinant hENT1 and hENT2 by immunoblotting and immunofluorescence. Endogenous hENT1 and hENT2 were detected in human cell lines by immunofluorescence microscopy. The anti-hENT1 antibodies gave mostly plasma membrane staining, whereas the anti-hENT2 gave mostly intracellular staining, which was localized to mitochondria. An immunoreactive species was detected in enriched human liver mitochondria with the anti-hENT2 antibodies by immunoblot analysis.

The relationship between hENT2 and hHNP36 was examined. The hHNP36 protein is a truncated version of hENT2 that is produced by alternate splicing. In the process of confirming the structure of the hENT2 gene, a hENT2 pseudogene was discovered.

Two different pertubation methods were used to probe regulatory mechanisms of the ENT proteins in human cell lines. The first involved treating CEM cells with hydroxyurea, which resulted in an increase in hENT1 levels that correlated with the hydroxyurea-induced increase in cell size. The second involved production of hENT1 or hENT2 antisense mRNA in HEK293 cells, which did not result in the ablation of either transport activity. This study has developed important tools for the field of nucleoside transport and attempted to probe the regulation of nucleoside transport proteins.

Acknowledgements

I would first of all like to thank Dr. Carol E. Cass, my supervisor, for her unwavering support, generosity, guidance and optimism. Carol has always been very encouraging and has nurtured my strong work ethic, a sense of perfection and most importantly a perseverant spirit. Carol is a great teacher and writer and I hope that I will remember and use all of the skills that she has taught me. It has been a pleasure to work with her. Another one of Carol's excellent skills has been to surround herself with very talented people who have all played an important role in my scientific training.

My first experience in Carol's laboratory was as a summer student working with a graduate student (now a physician), Dr. Karen King, who took me under her wing. That summer planted the seed in my mind that this laboratory was an excellent place to work and it has been a decision that I have never regretted. The technical personnel, namely Delores Mowles and Milada Selner, have helped me a great deal over the years in a variety of projects. They both apprenticed me in tissue culture and I will forever be in their debt. I would particularly like to thank Milada for all of her hard work and effort in helping to generate the anti-hENT2 monoclonal antibodies and Delores for all of her help in the very beginning and in the final stages of my thesis work. I would also like to thank Patsy-Ann Carpenter, Geraldine Baron and Cheryl Santos for all of their technical assistance. My fellow graduate students, Dr. Karen King, Dawn Fang, Dr. Mark Vickers, Thack Lang, Jacqueline Leithoff, Frank Visser and Jing Zhang, have been extraordinary comrades-in-arms sharing in many laughs and disappointments, scientifically, athletically and otherwise. The laboratory has had the privilege of having expert research associates to help us with many tasks, namely Dr. Kathryn Graham and Dr. Rajam Mani. I would particularly like to thank Kathryn for various discussions and her assistance with the sequencer and the Taqman. A number of post-doctoral fellows have also made an impact on me scientifically, namely Dr. Imogen Coe (localization work), Dr. Douglas Hogue (MTP/LAPTm4 project), Dr. Jihan Marjan (assistance in making antibodies), Dr. Lori L. Jennings (assistance in making antibodies) and Dr. Marilyn Clarke (HPLC analysis). I have had the privilege of meeting some wonderful visiting scientists that Carol has invited to the lab including Dr. Fiona Parkinson, Dr. Lynn Kirkpatrick and Dr. James Hammond. I appreciate the great efforts of Karma Klein, my summer student in 2000, for helping to set up immunoprecipitations in the laboratory. A big thanks also goes out to Ilona (Lily) Zombor, the lab assistant, for preparing tips, tubes and solutions. I shall miss not only the people, but the birthdays and other special occasions when people brought goodies (and the days when I forgot to bring goodies), the many glove fights (not the water fights), the ongoing commentary to solve the world's problems and the great scientific discussions, especially the weekly laboratory meetings.

I would like to thank our collaborators: Drs. John Mackey and Clarence Wong for always reminding us of the clinical relevance of our work; Dr. Xie-Jun Sun for his excellent assistance with the confocal microscope; Dr. James Young and members of his laboratory, especially Mabel Ritzel for early molecular biology coaching and Dr. Syliva Yao for assistance with oocytes; Dr. Liang Li and the ACB Proteomics Facility staff, Dr.

Bernd Keller and Jing Zheng for their efforts and useful discussions; and Dr. Stephen Baldwin.

I would like to thank the members of my supervisory committee, Drs. Mike Ellison, Tom Hobman and James Young for their advice, assistance with methods and generosity with reagents over the years. I would particularly like to thank them and the members of my examining committee, Drs. Marek Michalak, Xing-Zhen Chen and James Hammond, for reading my thesis so carefully and for all of their thoughtful suggestions. It has been a pleasure interacting with them.

I would also like to thank the Department of Biochemistry for all of their assistance over the years, especially in providing tuition fees support. I would also like to thank fellow departmental graduate students for their help along the way: Helen Everett, Glenn Parsons, John Dawson, Chris Rochet and Amir Khan. A big thanks goes out to Perry d'Obrenan, Roger Bradley and Rita Whitford for their help with sequencing, computers and poster printing. I appreciate the warm welcome that was received from the Department of Oncology when we moved to the Cross Cancer Institute in 1996. I would like to thank Drs. Roseline Godbout, Andy Shaw, Joan Turner, David Murray, Charlotte Spencer, Michael Weinfeld, Michael Hendzel, Linda Pilarski and Paul Grundy and the members of their labs (Beth, Chris, Darin, Dwayne, Eva, Heather, John, Jon, Kirk, Laurina, Loretta, Mary, Maryse, Melody, Natalie, Sachin, Sharon, Stacey, and Tanya) for reagents and/or assistance with protocols. I appreciate the assistance of Juanita Wizniak for expert technical assistance in the Flow Cytometry Facility. I would especially like to thank all of those people who volunteered countless times to give blood to enable me to make human erythrocyte membrane preparations. The members of the CIHR (formerly the MRC) Molecular Biology of Membranes Group (weekly Thursday morning meetings) and the Faculty of Medicine Membrane Transport Group (biweekly Tuesday morning meetings) have been very supportive whenever I have presented at these forums and I appreciate everyone's attention and subsequent suggestions.

I appreciate the financial support provided to me by the Department of Biochemisty, the Faculty of Medicine through the 75th Anniversary Graduate Student Scholarships, the Alberta Cancer Foundation through the Alberta Cancer Board studentship and the Faculty of Graduate Studies and Research for providing funds for conference travel.

I would like to express my extreme gratitude to my immediate family and friends for their continued support over these last seven years. My parents, Virgilio and Maria Encarnação, and my sister, Luisa, have always been there for me and have provided me with all sorts of support at home that I can only hope to repay in kind one day. Gostaria também de agradecer aos meus familiares fora de Edmonton que me têm sempre suportado moralemente. This long journey has been made more fun by and would not have been complete without my companion and confidante, Pamela Lagali, a true kindred spirit and a patient one at that. I hope that we will have more journeys together. Thanks for all of your love and support. I would also like to thank Henry and Marilyn Hodysh for friendship, advice, and thoughtfulness over the years. I appreciate the support and encouragement of all of my friends (Adelbert, Arlene, Chantal, Chris, Fitz, Francis,

Glenn, Isabel, Jeff, Jessica, Lindsay, Mateusz, Melanie, Patrick, Quang-Tuan, Ron, Sharlyne, Stephen and Steve).

Best wishes and good health to everyone. May God bless you all! Com muito amor. Muito obrigado a todos.

Table of Contents

Chapters **Page**

1. Introduction 1

1 A. Nucleosides 2
1 A. I. Transporters: An Introduction 2
1 A. II. Physiological Nucleosides and Nucleoside Analogues 2
1 A. II.A. Physiological Nucleosides 3
1 A. II.B. Nucleoside Analogues 4
1 A. III. Nucleoside and Nucleotide Metabolism 4
1 B. Nucleoside Transport 5
1 B. I. Nucleoside Transporter Families 5
1 B. I.A. The Equilibrative Nucleoside Transporter (ENT) Family 5
1 B. I.B. The Concentrative Nucleoside Transporter (CNT) Family 9
1 B. I.C. The Uracil/Allantoin Transporter Family (Microbial Purine-Related Transporter Family) 10
1 B. I.D. The NupG/XapB Nucleoside Transporter Family 11
1 B. I.E. The Putative Nucleoside Permease Family 11
1 B. II. Intracellular Nucleoside Transport Processes and Intracellular Membrane Proteins 12
1 B. II.A. Intracellular Nucleoside Transport 12
1 B. II.B. The mLAPTm4/MTP Protein Family 13
1 B. III. Regulation of Nucleoside Transporters 13
1 C. Hypotheses and Objectives of the Study 14

2. Materials and Methods 50

2 A. Laboratory Chemicals and Isotopes 51
2 B. Cell Culture and Media 51
2 C. Nucleoside Transport Studies 52
2 D. Plasmid Construction, Propagation and Preparation 53
2 D. I. Plasmids used in Chapter 3 54
2 D. II. Plasmids used in Chapter 4 55
2 D. III. Plasmids used in Chapter 6 57
2 E. cDNA Library Screening and Southern Analysis 57
2 F. RNA Synthesis, Isolation and Northern Analysis 58
2 G. Reverse Transcription-PCR (RT-PCR), Taqman Quantitative RT-PCR and GeneScan RT-PCR 58
2 G. I. RT-PCR 58
2 G. II. Taqman Real-time Quantitative RT-PCR 59
2 G. III. GeneScan RT-PCR 60

2 H. Transfections....60
2 H. I. Transient Transfections....60
2 H. II. Stable Transfections....61
2 I. Generation of Anti-hENT2 Polyclonal and Monoclonal Antibodies....61
2 I. I. Production and Purification of Fusion Proteins....61
2 I. II. Injection of Antigens....62
2 I. III. Production of Monoclonal Antibody-secreting Hybridomas....63
2 I. IV. Antibody Screening....63
2 J. Immunoprecipitations....64
2 K. Purification of Monoclonal Antibodies....64
2 L. Labelling of anti-hENT1 Monoclonal Antibodies with Fluorophores....65
2 M. Immunofluorescence Microscopy....65
2 N. Preparation of Crude and Plasma Membranes from Tissue Culture Cells....65
2 O. Isolation of Human Erythrocyte Membranes....66
2 P. Subcellular Fractionation....67
2 Q. Protein Determination....68
2 R. SDS-Polyacrylamide Gel Electrophoresis (SDS-PAGE) Analysis and Immunoblotting....69

3. Localization of mLAPTm4 (MTP)....77

3. Abstract....78
3 A. Introduction....79
3 B. Results....82
3 B. I. Isolation of the Human Orthologue of mLAPTm4 from a Human Kidney cDNA Library....82
3 B. II. Attempts to Improve Recombinant Truncated mLAPTm4 (MTPΔC) Protein Production in *X. laevis* Oocytes....83
3 B. III. Production of Recombinant mLAPTm4 and HA-mLAPTm4 in BHK21 Cells by Transient Transfection....84
3 B. IV. Localization of Recombinant mLAPTm4 and HA-mLAPTm4 in Transiently Transfected BHK21 Cells....85
3 B. V. Absence of Localization of HA-mLAPTm4 to the Golgi Compartment in Transiently Transfected Cells....85
3 B. VI. Localization of HA-mLAPTm4 to Late Endosomes in Transiently Transfected Cells....86
3 B. VII. Localization of HA-mLAPTm4 to Acidic Vesicles in Transiently Transfected Cells....86
3 B. VIII. Localization of HA-mLAPTm4 to Lysosomes in Transfected Cells 87
3 B. IX. Identification of the Rat Orthologue of mLAPTm4 in Subcellular Fractions of Rat Liver....87
3 C. Discussion....88

4. Generation and Assessment of Anti-hENT1 and Anti-hENT2 Antibodies 125

4. Abstract 126
4 A. Introduction 127
4 B. Results 128
4 B. I. Generation of Anti-hENT1 and Anti-hENT2 Antibodies 128
4 B. II. Assessment of the Anti-hENT1 and Anti-hENT2 Antibodies 130
4 C. Discussion 133

5. Detection of hENT1 and hENT2 in HeLa and BeWo Cells 151

5. Abstract 152
5 A. Introduction 153
5 B. Results 154
5 B. I. Immunofluorescence Analysis of Endogenous hENT1 and hENT2 in Human Cell Lines 154
5 B. II. Analysis of Enriched Human Liver Mitochondria and Human Cell Membrane Samples with Anti-hENT1 and Anti-hENT2 Antibodies by Immunoblot Analysis 156
5 B. III. Detection of the hHNP36 Transcript in Four Human Cell Lines using GeneScan RT-PCR Technology 158
5 B. IV. Determination of the hENT2/hHNP36 Exon 11/Intron 11/Exon 12 Boundaries 159
5 B. V. Identification of a hENT2/hHNP36 Pseudogene in the Human Genome 159
5 C. Discussion 160

6. Use of Two Perturbative Methods, Hydroxyurea-treatment and hENT Antisense Production, to study Equilibrative Nucleoside Transporter Regulation 190

6. Abstract 191
6 A. Introduction 192
6 B. Results 194
6 B. I. Flow Cytometric Analysis of Hydroxyurea-treated CEM Cells 194
6 B. II. Analysis of NBMPR-Binding Sites in Hydroxyurea-treated CEM Cells 196
6 B. III. Analysis of hENT1 mRNA Levels in Hydroxyurea-treated CEM Cells 196
6 B. IV. Characterization of Uridine Transport in Hydroxyurea-treated CEM Cells 197
6 B. V. Effect of Hydroxyurea Treatment on the Size of CEM Cells 198
6 B. VI. Characterization of the Nucleoside Transporter Profile of HEK293 Cells. 198

6 B. VII. Characterization of the Nucleoside Transporter Profile of HEK293 Cells Stably Transfected with Sense or Antisense cDNAs for hENT1 and hENT2.....199
6 C. Discussion.....200

7. Summary and Conclusions.....234

7 A. The mLAPTm4 Protein is a Lysosomal/Endosomal Transporter.....235
7 B. Detection and Visualization of Recombinant and Endogenous hENT1 and hENT2.....235
7 C. The hENT2 Gene and Alternate Splice Products.....237
7 D. Potential Regulatory Mechanisms of the ENT family.....238

8. Bibliography.....240

List of Tables

Table 1-1. The ENT Family of Proteins
Table 1-2. Properties of Mammalian ENT Proteins
Table 1-3. Human Nucleoside Transport Activities and Proteins
Table 1-4. The CNT Family of Proteins
Table 1-5. Characteristics of Mammalian CNT Proteins
Table 1-6. The Uracil/Allantoin Family of Proteins
Table 1-7. The NupG/XapB Family of Proteins
Table 1-8. The Nucleoside Permease Family of Proteins
Table 2-1. Description of Plasmids used in this Study
Table 2-2. Primary Antibodies used in this Study
Table 2-3. Secondary Antibodies used in this Study
Table 3-1. Enzyme Marker Assays of Subcellular Fractions
Table 4-1. SurfacePlot Analysis Results
Table 6-1. Flow Cytometry using 5-(SAENTA-x_8)-fluorescein
Table 6-2. Flow Cytometry using Anti-hENT1 Monoclonal Antibodies
Table 6-3. Effects of Hydroxyurea on Site-specific Binding of NBMPR to CEM Cells
Table 6-4. Taqman Real-time Quantitative RT-PCR Analysis of hENT1 in Hydroxyurea-treated CEM Cells
Table 6-5. Comparison of Uridine Transport Rates in Hydroxyurea-treated CEM Cells
Table 6-6. Comparison of Volumes of Hydroxyurea-treated CEM Cells

List of Figures

Figure 1-1. Structures of Physiological Nucleosides
Figure 1-2. Structures of Anticancer Nucleoside Drugs
Figure 1-3. Structures of Antiviral Nucleoside Drugs
Figure 1-4. The ENT Family
Figure 1-5. The Predicted Topological Model of hENT1
Figure 1-6. The Predicted Topological Model of hENT2
Figure 1-7. Structures of Equilibrative Nucleoside Transport Inhibitors.
Figure 1-8. The CNT Family
Figure 1-9. The Predicted Topological Model of hCNT1
Figure 1-10. The Uracil/Allantoin Transporter Family
Figure 1-11. The NupG/XapB Transporter Family
Figure 1-12. The Nucleoside Permease Transporter Family
Figure 3-1. Southern Blot of Human Kidney Clones
Figure 3-2. Human LAPTm4 cDNA Sequence
Figure 3-3. Predicted Human LAPTm4 Protein Sequence
Figure 3-4. Comparison of Predicted Protein Sequences of hLAPTm4 and mLAPTm4
Figure 3-5. Measurement of MTPΔC Activity in *X. laevis* Oocytes
Figure 3-6. Immunodetection of mLAPTm4 and HA-mLAPTm4 in Transfected BHK21 Cells
Figure 3-7. Presence of mLAPTm4 and HA-mLAPTm4 in Juxtanuclear Vesicles
Figure 3-8. Absence of HA-mLAPTm4 in the Golgi Apparatus of Transfected Cells
Figure 3-9. Absence of HA-mLAPTm4 in the Early Endosomes of Transfected Cells
Figure 3-10. Presence of HA-mLAPTm4 in Late Endosomes of Transfected Cells
Figure 3-11. Presence of HA-mLAPTm4 in Late Endosomes of Chloroquine-treated Transfected Cells
Figure 3-12. Presence of HA-mLAPTm4 in Lysosomes of Transfected Cells
Figure 3-13. Presence of HA-mLAPTm4 in Lysosomes of Chloroquine-treated Transfected Cells
Figure 3-14. Immunoblot of Rat Liver Subcellular Fractions
Figure 3-15. ClustalW Alignment of Mammalian LAPTmX Family Members
Figure 4-1. Alignment of hHNP36 and mHNP36
Figure 4-2. Comparison of the hENT1 and hENT2 Large Intracellular Loop Regions
Figure 4-3. Detection of Recombinant hENT1 and hENT2 by Immunoblot Analysis using Anti-hENT1 and Anti-hENT2 Monoclonal Antibodies
Figure 4-4. Detection of Recombinant hENT2 and hHNP36 by Immunoblot Analysis using Anti-hENT2 Polyclonal Antibodies
Figure 4-5. Detection of Recombinant hENT1 by Immunofluorescence Analysis using Anti-hENT1 Monoclonal Antibodies
Figure 4-6. Detection of Recombinant hENT2 and hHNP36 by Immunofluorescence Analysis using Anti-hENT2 Polyclonal Antibodies
Figure 4-7. Detection of Recombinant hENT2 by Immunofluorescence Analysis using

Anti-hENT2 Monoclonal Antibodies
Figure 4-8. Immunoprecipitation of hENT1 from BeWo Cell Lysates
Figure 5-1. Putative Structure of the hENT2/hHNP36 Gene
Figure 5-2. Detection of Endogenous hENT1 and hENT2 in BeWo and HeLa Cells by Immunofluorescence Analysis
Figure 5-3. Detection of Intracellular hENT1 in BeWo Cells by Immunofluorescence Analysis
Figure 5-4. Endogenous hENT2 in BeWo Cells is Not Detected by Immunofluorescence Analysis using Anti-hENT2 Monoclonal Antibodies
Figure 5-5. Mitochondrial Co-localization of Anti-hENT2 Antibody Staining with MitoTracker Red Dye in BeWo and HeLa Cells
Figure 5-6. Mitochondrial Co-localization of Anti-hENT2 Staining with Anti-cytochrome Oxidase (Subunit I) Antibodies in BeWo and HeLa Cells
Figure 5-7. Identification of an Anti-hENT2 Immunoreactive Species in Human Mitochondria
Figure 5-8. Detection of hENT1 in HeLa and BeWo Membranes by Immunoblot Analysis
Figure 5-9. GeneScan Analysis of the hENT2/hHNP36 Transcript
Figure 5-10. GeneScan Analysis Results
Figure 5-11. Corrected Intron/Exon Boundaries for the hENT2/hHNP36 Gene
Figure 5-12. Identification of the hENT2 Pseudogene on Chromosome 11
Figure 5-13. Sequence Comparison of hENT2 Gene and hENT2 Pseudogene
Figure 6-1. hENT1 Probes
Figure 6-2. Analysis of Hydroxyurea-treated CEM Cells using Flow Cytometry and 5-(SAENTA-x_8)-fluorescein
Figure 6-3. Analysis of Hydroxyurea-treated CEM cells using Flow Cytometry and Anti-hENT1 Monoclonal Antibodies
Figure 6-4. NBMPR-binding in Hydroxyurea-treated CEM Cells
Figure 6-5. Taqman Real-time Quantitative RT-PCR Analysis of hENT1 in Hydroxyurea-treated CEM Cells
Figure 6-6. Uridine Transport in Hydroxyurea-treated CEM Cells
Figure 6-7. RT-PCR Analysis of HEK293 Cells
Figure 6-8. Characterization of Nucleoside Transport in HEK293 Cells
Figure 6-9. RT-PCR Analysis of HEK293 Cells Stably Transfected with Plasmids containing Sense and Antisense hENT1 and hENT2 cDNAs
Figure 6-10. Characterization of Nucleoside Transport in HEK293 Cells Stably Transfected with Plasmids containing Antisense hENT1 and hENT2 cDNAs

List of Symbols, Nomenclature and Abbreviations

3TC	3'-thia-2',3'-dideoxcytidine
α-ManII	α-mannosidase II
A_{280}	absorbance at 280 nm
AIDS	acquired immunodeficiency syndrome
AZT	3'-deoxy-3'-azidothymidine
BeWo	human choriocarcinoma cell line
BHK	baby hamster kidney
bp	base pairs
BSA	bovine serum albumin
cDNA	complementary DNA
cib	concentrative, insensitive to NBMPR, broadly selective
cif	concentrative, insensitive to NBMPR, formycin B is a permeant
cit	concentrative, insensitive to NBMPR, thymidine is a permeant
cRNA	capped RNA
cs	concentrative, sensitive to NBMPR
csg	concentrative, insensitive to NBMPR, guanosine is a permeant
CCRF-CEM	human lymphoblastic leukaemia cell line
CHO	Chinese hamster ovary
CNT	concentrative nucleoside transporter
Cy5	indodicarbocyanine
ddC	2', 3'-dideoxycytidine
ddH_2O	distilled, deionized water
ddI	2', 3'-dideoxyinosine
DMEM	Dulbecco's modified Eagle's medium
DMSO	dimethyl sulfoxide
DNA	deoxyribonucleic acid
dNTP	deoxyribonucleotide triphosphate
ECL	enhanced chemiluminescence
EDTA	ethylenediaminetetraacetic acid
ei	equilibrative, insensitive to NBMPR
ELISA	enzyme-linked immunosorbent assay
ENT	equilibrative nucleoside transporter
es	equilibrative, sensitive to NBMPR
EST	expressed sequence tag
FBS	fetal bovine serum
FITC	fluoroisothiocyanin
g	gravity
g	gram
GAPDH	glyceraldehyde phosphate dehydrogenase
GST	glutathione S-transferase
h	human

hf	hagfish
hRBC	human red blood cells/erythrocytes
HA	hemagglutinin
HEK	human embryonic kidney
HeLa	human cervical adenocarcinoma cell line
HEPES	N-2-hydroxyethylpiperazine-N'-2-ethane sulfonic acid
HIV	human immunodeficiency virus
HRP	horseradish peroxidase
HNP	hydrophobic nucleolar protein
INT	*p*-iodonitrotetrazolium violet
kDa	kilodaltons
LAPTm4	lysosomal-associated protein transmembrane 4
LAPTm5	lysosomal-associated protein transmembrane 5
lgp-110	lysosomal glycoprotein-110
µg	microgram
µL	microlitre
µm	micrometre
µM	micromolar
m	mouse
mg	microgram
mm	millimetre
mol	mole
mL	millilitre
mM	millimolar
mRNA	messenger RNA
M	molar
M6PR	mannose-6-phosphate receptor
MBP	maltose-binding protein
MTP	mouse transporter protein
ng	nanogram
NBMPR	nitrobenzylmercaptopurine ribonucleoside (6-[(4 nitrobenzyl)thiol]-9–β-D-ribouranosyl purine)
NMG	N-methyl-D-glucammonium
OD_{600}	optical density at 600 nm
pk	pig kidney
pmol	picomole
PBS	phosphate-buffered saline
PCR	polymerase chain reaction
r	rat
RIPA	radio-immunoprecipiation assay
RNA	ribonucleic acid
RPMI	Roswell Park Memorial Institute

RT-PCR	reverse transcription-PCR
SDS	sodium dodecyl sulfate
SDS-PAGE	sodium dodecyl sulfate - polyacrylamide gel electrophoresis
Tris	tris(hydroxymethyl)aminomethane
TTBS	Tween-20, Tris-buffered saline
VSV-G	vesicular stomatitis virus glycoprotein

Chapter 1

1. Introduction

1 A. Nucleosides

1 A. I. Transporters: An Introduction

Solutes cross membranes by two methods, diffusion and protein-mediated transport. Various non-hydrophobic solutes that cannot diffuse through membranes such as amino acids, sugars, drugs, peptides, nucleosides, ions, and neurotransmitters require the activity of membrane-bound protein transporters for permeation. The majority of well-characterized transport processes occur on plasma membranes, however intracellular solute transporters are becoming more evident as more membrane proteins are studied and as more intracellular transport proteins and processes are identified.

Nucleoside translocation across membranes is usually protein-mediated and the membrane proteins responsible for this activity are termed nucleoside transporters, the main subject of this thesis. The plasma membrane transport of nucleosides is well characterized and is an important step in the salvage pathway in mammalian cells [1-6], while the intracellular transport of nucleosides has been described in a few isolated cases [7, 8] (K. M. King, P. Panayides, and C. E. Cass, unpublished observations) and is not yet well understood. The nucleoside transporter cDNAs isolated to date encode proteins capable of plasma membrane-mediated transport of nucleosides. In contrast, while there are a few potential candidates, to the best of our knowledge, proteins mediating only the intracellular transport of nucleosides have not yet been identified. However, proteins mediating plasma membrane nucleoside transport processes may be responsible for mediating certain intracellular nucleoside transport processes.

Nucleoside transport is required for the salvage of preformed nucleosides from the extracellular milieu. These exogenous precursors are then modified by nucleoside kinases within the cell [9] and utilized by the cellular nucleotide synthesis machinery. Nucleoside transport is also required for the release of physiological nucleosides (*e.g.*, to allow dietary nucleosides to travel through the enterocytes of the intestine and into circulation) and toxic nucleosides that may interfere with cell processes.

1 A. II. Physiological Nucleosides and Nucleoside Analogues

Nucleosides act as signalling molecules, neuromodulators, and precursors of nucleic acids in cells and are synthesized *de novo* or salvaged from the extracellular environment [1-6]. The salvage pathway is particularly vital where the *de novo* synthesis pathway is lacking such as in parasites that are purine auxotrophs [10-12], and in specialized mammalian cells such as enterocytes, bone marrow cells and certain brain cells [13]. Nucleosides and their analogues are generally hydrophilic and thus require a permeation step to enter cells at rates that are sufficient to achieve pharmacological effects, although some pharmacologically active nucleoside analogues such as 3'-deoxy-3'-azidothymidine (AZT) [14, 15] and troxacitabine [16] enter some cell types only by diffusion.

1 A. II.A. Physiological Nucleosides

The physiological nucleosides (Figure 1-1) include purine-containing molecules such as adenosine, guanosine, and inosine, and the pyrimidine-containing molecules such as uridine, thymidine, and cytidine.

Adenosine, Inosine and Guanosine: Adenosine has many pleiotropic effects, particularly in the cardiac and nervous systems, due to a complex system of purinergic receptors that are found on the surfaces of many cell types and bind adenosine, adenine nucleotides and inosine [17-19]. Adenosine is an important nucleoside since it acts as a cardioprotector during periods of hypoxia and ischemia [20, 21]. While having beneficial effects on some cell types, adenosine has also been demonstrated to mediate growth inhibition [22, 23] and apoptosis [24-27] in other cell types. Inosine, an adenosine metabolite, binds only a certain subset of purinergic receptors such as those found on mast cells, and interaction with its receptors causes mast cells to degranulate leading to microvascular vasoconstriction [18]. Adenosine accumulates in solid tumours at high concentrations causing immunosuppression [28, 29] and promotion of tumour growth [29]. Adenosine also manifests this cytoprotective/cytotoxic duality in the central nervous system where its concentrations are tightly regulated [17, 30]. These opposing effects have been observed in glial cells [31]. Adenosine is seen as a neuroprotector since it prevents release of neurotransmitters [17]. Guanosine has also been demonstrated to be a neuroprotector by modulating glutamate uptake via an unknown mechanism [32]. Adenosine, formed by degradation of adenosine nucleotides on the surface of the cell, also regulates nephron activity via activation of adenosine receptors [33]. Most recently, adenosine, via its interactions with three adenosine receptors in human airway epithelial cells, has been demonstrated to regulate the activity of K^+ channels [34]. However, not all effects of adenosine are due to purinergic receptor activation since permeation of adenosine into cells plays an important role in some of the actions mediated by adenosine [22, 23, 26, 27, 35]. Adenosine concentrations in blood and in tissues, which range from 80 nM to 1.2 μM, are tightly regulated [36], presumably because of the potent extracellular effects of adenosine.

Uridine and Thymidine: Uridine also has a multitude of biological activities; it can act as a signalling molecule and a therapeutic agent [37-39]. Uridine, which is found in humans (*i.e.,* in plasma, cerebro-spinal fluid and bone marrow) at concentrations of 3-8 μM, is used therapeutically to treat hereditary orotic aciduria and to protect against the side effects (*e.g.*, myelosuppresion) of 5-fluorouracil cancer therapy [38]. Uridine (and uridine nucleotides) are in clinical trials alone and in combination with other drugs to treat a host of other diseases such as schizophrenia, epilepsy, cystic fibrosis and peripheral nerve neuropathy induced by diabetes [38]. Uridine nucleotides, like adenine nucleotides, are bound on the surface of cells by pyrimidinoceptors [40] and regulate many cell processes, such as depolarization and hormone release [37]. Recently, uridine has been demonstrated to induce differentiation of human neuroblastoma cells via a protein kinase

Cε-dependant pathway [39]. In this case, permeation of uridine into cells was necessary for differentiation, which coincided with growth inhibition. Thymidine has also been used therapeutically to modulate the activity of various anti-metabolite drugs such as 5-fluorouracil, cytarabine and methotrexate [41].

1 A. II.B. Nucleoside Analogues

Anticancer Drugs: Nucleoside analogues are used as drugs in the treatment of cancer (Figure 1-2) and viral diseases (Figure 1-3) [42-46]. The purine-containing anticancer analogues, cladribine and fludarabine, are used to treat hematologic malignancies [46, 47]. Cladribine is active against hairy cell leukaemia and is used to treat B-cell lymphoid diseases, while fludarabine is used to treat chronic lymphocytic leukaemia and other indolent lymphocytic diseases [46, 47]. The pyrimidine-containing anticancer analogues, cytarabine and gemcitabine, are used to treat a variety of cancers. Cytarabine, which has been widely tested and studied, is mainly used to treat acute myelogenous leukaemia [46, 47] and is ineffective against solid tumours. In contrast, gemcitabine, a fluoropyrimidine nucleoside, has activity against solid tumours, such as breast, head and neck, pancreatic, bladder, colon and non-small cell lung cancers [46-49].

Antiviral Drugs: Various viral infections caused by the herpes, hepatitis B and human immunodeficiency viruses are treated with nucleoside analogues (Figure 1-3). Once phosphorylated, these nucleoside analogues inhibit viral reverse transcriptases and thus prevent viral replication. Acquired immunodeficiency syndrome (AIDS) caused by the human immunodeficiency virus (HIV) is treated with various combinations of nucleoside analogues and viral protease inhibitors. Nucleoside drugs used in these combination therapies include 3'-deoxy-3'-azidothymidine (AZT), 2', 3'-dideoxyinosine (ddI), 2', 3'-dideoxycytidine (ddC) and 3'-thia-2',3'-dideoxcytidine (3TC) [50] (Figure 1-3). In addition, 3TC (also known as lamivudine) is active against hepatitis B [51]. Nucleoside analogues must enter cells to be effective and thus nucleoside transporters are often critical determinants of drug entry into diseased cells.

1 A. III. Nucleoside and Nucleotide Metabolism

Cells obtain nucleotides and their precursors by two major pathways, the *de novo* synthesis pathway and the salvage pathway. The *de novo* synthesis pathway is highly conserved from bacteria to humans [52]. Most cell types synthesize their own purine and pyrimidine nucleotides. The enzymes involved in purine and pyrimidine nucleotide biosynthesis are highly regulated and create nucleotides from low-molecular weight precursors [52]. The enzymes of the *de novo* synthesis pathway can be inhibited with a variety of agents, including many derived from nucleoside or nucleobase analogues that are used for therapeutic purposes [53].

The salvage pathway is important for organisms such as parasites [10, 54, 55] and cells such as enterocytes and bone marrow cells [13] that lack or have impaired *de novo*

pathways. Precursors such as nucleosides and nucleobases are obtained from either inside the cell or outside the cell. The salvage pathway reutilizes intracellular precursors such as nucleosides and nucleobases that result from degradation of nucleic acids. Extracellular nucleotides cannot be transported across the plasma membrane in most cases, and thus must be degraded to nucleosides or nucleobases by extracellular enzymes. The transport of nucleosides and nucleobases is an important first step in the salvage pathway. Once inside cells, nucleosides are phosphorylated by nucleoside kinases [9], and nucleobases are transformed into nucleoside monophosphates by phosphoribosyltransferases [52]. Also, various therapeutic strategies that exploit the reliance on the salvage pathway and the lack of *de novo* purine synthesis pathways in parasites have been employed in attempts to treat parasitic disease [55-65].

1 B. Nucleoside Transport

1 B. I. Nucleoside Transporter Families

Because the majority of nucleosides and nucleoside analogues are hydrophilic compounds, extracellular nucleosides diffuse slowly through the plasma membrane to enter cells. The passive diffusion of most nucleosides is too slow to sustain nucleotide pools by salvage pathways in the absence of *de novo* nucleotide synthesis or to achieve pharmacologically active levels of activated nucleoside drugs. Thus, the salvage of physiological nucleosides and the entry of therapeutic nucleoside drugs into cells are achieved via nucleoside transporter proteins. Over the last seven years, the expression cloning of over 20 cDNAs encoding nucleoside transporter proteins and the sequencing of various genomes including the human genome [66, 67] have resulted in the identification and GenBank database entry of over 70 nucleoside transporter cDNA sequences derived from different species. These sequences have been classified into five distinct protein families. This cloning explosion has led to a greater understanding of the proteins that are responsible for mediating the nucleoside transport processes.

1 B. I.A. The Equilibrative Nucleoside Transporter (ENT) Family

Family Structural Characteristics: The original member of the equilibrative nucleoside transporter (ENT) family is human ENT1 (hENT1) protein, whose cDNA was first isolated from placenta in 1996 [68]. Subsequently, the equilibrative nucleoside transporter family has grown to include members from *Caenorhabditis elegans* [6], *Saccharomyces cerevisiae* [69],various parasites [70-74], other animals [75, 76] and plants [77]. See Table 1-1 for a list of family members and GenBank accession numbers. There are now over 40 full-length sequences in GenBank as shown in the dendogram shown in Figure 1-4. The majority of mammalian ENT family members have a distinct putative membrane topology comprised of 11 transmembrane domains with two large

loops that are predicted to be extracellular between transmembrane domains 1 and 2 and intracellular between transmembrane domains 6 and 7. The extracellular loop (found in the mammalian proteins) usually has one or two signals for glycosylation [68, 78-81]. See Figures 1-5 and 1-6 for schematics of the predicted hENT1 and hENT2 topologies and Table 1-2 for a list and summary of the properties of the known mammalian ENT proteins.

Functional Characteristics: In mammalian cells, equilibrative transport processes appear to be ubiquitous and are distinguished by their sensitivity to specific inhibitors. The mammalian equilibrative nucleoside transporters exhibit nucleoside transport activities of broad permeant selectivity that are either sensitive (*es*) or insensitive (*ei*) to nitrobenzylthioinosine, otherwise known as nitrobenzylmercaptopurine ribonucleoside (NBMPR), a nucleoside transport inhibitor. Both *es* and *ei* activities are inhibited by dipyridamole, dilazep and draflazine (Figure 1-7). Dilazep and draflazine are used medically in coronary care as vasodilators [1-4, 20]. The *es* and *ei* transport processes are found in human cells (Table 1-3*A*). Studies with intact cultured human K562 leukaemia cells have shown that at physiological temperatures the *es* process has higher affinities, higher maximal velocities and higher efficiencies for adenosine and uridine than the *ei* process [82].

There are species differences in the sensitivities of equilibrative nucleoside transporters to the various inhibitors, with the most well known example being the difference between rat and human cells [83, 84]. Also, rat *es* and *ei* activities are less sensitive to dipyridamole when compared to their human counterparts [85]. The only member of the ENT family found in *S. cerevisiae* is FUN26, a prevaculolar membrane protein that was demonstrated to stimulate the uptake of a broad range of nucleosides when its cDNA was injected into *X. laevis* oocytes [69]. Some of the parasitic ENT proteins have also been shown to differ from their mammalian counterparts: i) the trypanosomal and leishmanial transporters have higher substrate affinities than the mammalian transporters [10, 12, 86], ii) the trypanosomal and leishmanial transporters have limited substrate specificities, whereas the mammalian transporters have broad substrate specificities [10, 12, 86], and iii) the parasitic ENTs appear to be proton-dependent, concentrative transporters due to the electrochemical gradient, while the mammalian ENTs are equilibrative [10].

Human Proteins: This study focuses on the two human nucleoside transporters hENT1 and hENT2. The proteins have primary sequences of 456 amino acids and are 49% identical and 69% similar at the amino acid level with highly conserved transmembrane regions. hENT1 and hENT2, when produced recombinantly in *X. laevis* oocytes, transport uridine, adenosine and thymidine and a series of nucleoside analogues [68, 78]. hENT2 also transports nucleobases [87, 88].

hENT1: hENT1 mediates the *es* transport activity that was first described in human erythrocytes [89] and has subsequently been studied in many other cell types [2-4]. The hENT1-mediated *es* process is sensitive to the highly specific and tight-binding inhibitor, NBMPR [90] at nanomolar concentrations (0.1-1 nM) and has broad permeant selectivity. The hENT1 gene has been localized to chromosome 6p21 [91]. hENT1 has

been purified from human erythrocytes [92] and is known to be glycosylated near one end of the protein [93]. The glycosylation site is now known to exist on the N-terminus of the protein where there is an N-glycosylation site at N48 [78] in the large extracellular loop between transmembrane domains 1 and 2 [94, 95] (See Figure 1-5). Studies with cells grown in tunicamycin, a drug which prevents glycosylation, demonstrated that *es* activity is not dependent on glycosylation of the protein [96]. The *es* transport activity is thought to be ubiquitous [2-4] and this conclusion is supported by the presence of hENT1 mRNA in all tissues probed thus far [68, 97] (See Table 1-2).

hENT2: The human cDNA encoding the hENT2 protein, which mediates *ei* activity, was isolated independently by two groups: one using a placental cDNA library [78] and the other using a HeLa cell cDNA library [98, 99]. The *ei* process was first described in L1210 murine leukaemia cells and Walker 256 rat cells [100, 101] and is inhibited only by high (>100 nM) concentrations of NBMPR [3-5, 102]. hENT2 is less well characterized and, unlike hENT1, has not yet been purified. Like hENT1, hENT2 has consensus glycosylation sites on the extracellular face of the protein [78, 99], which have been shown to be glycsolyated (M. F. Vickers. K. Wong, S. A. Baldwin, J. D. Young and C. E. Cass, unpublished observations) (Figure 1-6). hENT2 mRNA and activity are not as widespread as that of hENT1, but there is an abundance of hENT2 mRNA in skeletal muscle [97, 99] (See Table 1-2).

Although a truncated version of the hENT2 cDNA was isolated before either of the two full-length hENT2 cDNAs [78, 99], it was not recognized as encoding a nucleoside transporter [103]. A series of mouse cDNAs were isolated that represented products of delayed early response genes upon growth factor stimulation [104], including a mouse cDNA that encoded a putative 36-kDa hydrophobic nucleolar protein (HNP36), which was used to identify human HNP36 [103]. The mouse and human HNP36 cDNAs encode truncated mouse and human ENT2 proteins [78, 98, 99] that are missing the first 130 amino acids (the first three transmembrane domains) of the ENT2 proteins. The hHNP36 gene has been localized to chromosome 11q13 [105]. Analysis of the gene structure and transcripts from human cell lines and tissue samples suggested that cells produce multiple transcripts from the HNP36 gene by alternate splicing [105].

Unlike hENT1, hENT2 also transports nucleobases [87, 88]. A recent study has shown that hENT2, when expressed in *X. laevis* oocytes, transports hypoxanthine, uracil, adenine and thymine with K_m values ranging from 0.74-2.6 mM [106]. More recently, hENT2 was demonstrated to differ from hENT1 in the transport of antiviral 3'-deoxynucleoside drugs [107]. hENT2 transported AZT, ddI and ddC, whereas hENT1 only transported ddI and ddC. Since AZT is so hydrophobic and its transport was not inhibited by dilazep, NBMPR or excess amounts of uridine, thymidine or guanosine in human erythrocytes [15] or in CaCo2 cells [14], it had been postulated that its primary route of entry into cells was passive diffusion, although AZT could inhibit *es* transport of thymidine in human erythrocytes [108]. The recent results of Yao *et al.*, [107] suggest that AZT transport may be protein-mediated and implicate hENT2 as playing an important role in the transport of the aforementioned antiviral drugs when the concentrative nucleoside transporters are not present.

hENT3: More recently, cDNA sequences encoding hENT3 and mENT3 were isolated [75]. When the corresponding transcripts encoding the hENT3 or mENT3 protein were injected into oocytes [75], no nucleoside uptake was observed. The presence of two potential dileucine lysosomal targeting motifs [109] on the intracellular, highly positively charged N-termini of both hENT3 and mENT3 suggest that these proteins may be targeted to intracellular membranes and thus may function as organellar transporters. If this hypothesis is correct, functional production of the full-length transcripts of hENT3 and mENT3 in *X. laevis* oocytes cannot be used to determine their transport characteristics, since this model system can only characterize transport proteins that localize to the plasma membrane.

Structure-Function Studies of ENT Proteins: In addition to human and mouse ENTs, rat cDNAs (rENT1 and rENT2) have been isolated from intestine [79]. rENT1 is not as sensitive to NBMPR as hENT1, and both rENT1- and rENT2-mediated activities are less sensitive to dipyridamole when compared to their human counterparts [79]. Chimaeric proteins have been generated from the hENT1, rENT1 and rENT2 cDNAs, and regions important for inhibitor-binding have been identified by producing the chimaeras in *X. laevis* oocytes and performing transport inhibition studies. For example, the characteristics of hENT1 and rENT1 chimaeras indicate that transmembrane domains 3-6 comprised of amino acids 100-231 in hENT1 are important for interaction with dilazep and dipyridamole [110]. Also, the characteristics of rENT1 and rENT2 chimaeras have indicated that transmembrane domains 3-6 of rENT1 are important for interactions with NBMPR [95]. The same chimaeras have been used to demonstrate that transmembrane domains 5 and 6 in rENT2 are important for nucleobase translocation [88]. Furthermore, the characteristics of these chimaeras have established that transmembrane domains 1-6 of ENT2 are required in the transport of the 3'-deoxynucleoside drugs [107].

More recently, inhibitor binding to hENT1 has been investigated using site-directed mutagenesis. When the amino acid at position 154 of hENT1, a glycine, was modified to a serine residue, NBMPR binding was lost [6, 111]. Also, when a random mutagenesis strategy was used to probe dipyridamole inhibition of transport, the methionine at position 33 of hENT1 was modified to isoleucine, leading to decreased dipyridamole inhibition of uridine transport [112]. In hENT2, the amino acid at that position is isoleucine and the reciprocal mutant in hENT2 was more sensitive to dipyridamole [112].

Location of Transporters: The physiological significance of the presence of both hENT1-mediated *es* and hENT2-mediated *ei* activities in some cell types is unknown. Now that hENT2 has been shown to also transport nucleobases, it may be that in some cells hENT2 is the main nucleobase transporter, although other different nucleobase transport processes are known to exist [88]. Most cell lines examined, such as BeWo, derived from a human choriocarcinoma [7, 113], K562, derived from a human erythroleukaemia [82], HeLa, derived from a human cervical adenocarcinoma [98, 114], and tissues such as brain [115-117] and intestine [118, 119], possess both types of transporters. The hENT1-mediated activity appears to always be the larger of the two activities, accounting for as much as 80% of total nucleoside transport [7, 82, 98, 113,

114]. Also, there are only a few examples of cell types or tissues that possess only one type of nucleoside transport process. One such cell line is CEM, derived from a human leukaemia, that possesses only hENT1-mediated *es* ıransport activity [120].

1 B. I.B. The Concentrative Nucleoside Transporter (CNT) Family

Family Structural Characteristics: The founding member of the CNT family was the rat concentrative nucleoside transporter 1 (rCNT1) [121]. Subsequently, the CNT family has expanded rapidly to include homologues from different bacteria, *C. elegans*, *Drosophila melanogaster* and other animals (see Table 1-4 for a list of family members and GenBank accession numbers). To date there are 29 full-length sequences in GenBank as shown in the dendogram in Figure 1-8. The distinct membrane topology of rCNT1 has been determined to consist of 13 transmembrane domains with a large, putatively extracellular glycosylated C-terminus [122]. All of the mammalian CNT proteins are predicted to have putative membrane topologies that are similar to that of rCNT1 (hCNT1 is depicted in Figure 1-9). See Table 1-5 for a list and summary of the properties of known mammalian CNT proteins.

Once the sequence of rCNT1 was elucidated, it became apparent that it was related to NupC [123, 124], one of the *Escherichia coli* nucleoside transport proteins. *E. coli* NupC has many bacterial homologues in other organisms including *Bacillus subtilis*, *Haemophilus influenzae* and *Helicobacter pylori* [125]. The prokaryotic NupC proteins are predicted to have ten transmembrane domains (the last ten transmembrane domains of the eukaryotic CNT family members) and a much shorter C-terminus than the eukaryotic CNTs and thus tend to be smaller [122]. The architecture of the CNT protein family is quite different from that of the ENT protein family (compare Figure 1-9 with Figures 1-5 and 1-6), as would be expected since these protein families are not related and have different ancestries.

Family Functional Characteristics: In human cells, five functionally distinct concentrative sodium:nucleoside co-transport activities have been described [3-5, 102, 126-134]. Three different proteins have been described that are responsible for the *cit* (hCNT1), *cif* (hCNT2) and *cib* (hCNT3) activities. However, the molecular entities mediating the renal *cit* activity that transports guanosine [127-129], the *cs* activity [130], and the *csg* activity [126] have yet to be identified (Table 1-3*B*). The cDNAs encoding all of the mammalian CNTs have been injected into *X. laevis* oocytes [79, 121, 131, 133-136]. The first cDNA to be injected, encoding rCNT1, was shown to preferentially stimulate sodium-dependent uptake of pyrimidine nucleosides [121], and subsequent mammalian CNT1 proteins were shown to transport mainly pyrimidine nucleosides [121, 131]. In contrast, the mammalian CNT2 proteins transport purine nucleosides as well as uridine and thus mediate the *cif* transport process [134, 136, 137]. The mammalian CNT3 proteins and the hagfish (hf) CNT protein transport a broad range of nucleosides and thus mediate the *cib* transport process [132, 133, 138]. The CNT3 proteins also differ from the CNT1 and CNT2 proteins in that the sodium:nucleoside coupling ratio is 2:1 for the former and is 1:1 for the latter [133]. The main functional difference between

the known mammalian and bacterial CNT proteins is that transport mediated by NupC (and presumably by other related bacterial transporter proteins) is proton-dependent [123], whereas transport mediated by mammalian CNT proteins is sodium-dependent [131-134, 136]. Studies with hCNT1- and hCNT2-encoding plasmids stably transfected into transport-deficient cells revealed that these transporter proteins are important in mediating nucleoside drug uptake into cells [139] (T. Lang, J. D. Young and C. E. Cass, unpublished observations).

Structure-Function Studies of CNT Proteins: Structure function studies have been performed using CNT chimaeric proteins. Uptake experiments using a rCNT1/rCNT2 chimaera expressed in *X. laevis* oocytes demonstrated that the chimaera had the transport characteristics of both proteins [140]. This result also demonstrated that transmembrane domains 8 and 9 in both proteins were important for binding of purine and pyrimidine nucleosides. Subsequent to these studies, amino acids 318 and 319 in rCNT1 and 319 and 320 in hCNT1 (a serine and glutamine residue, respectively) were shown to be necessary for the pyrimidine specificity of rCNT1- and hCNT1-mediated transport [138, 141]. Replacement of the serine with a glycine (the corresponding residue in rCNT2 and hCNT2) resulted in rCNT1 and hCNT1 becoming purine-specific transporters. In the human protein, substitution of the glutamine with methionine increased the specificity of the mutated transporter towards purine nucleosides [138], whereas in the rat protein, the glutamine was shown to be important in mediating the affinity for the substrates [141].

Location of Transporters: Mammalian CNT family members are found in highly differentiated tissues (see Table 1-5). For example, rCNT1 has been immunolocalized not only to rat jejunum, but also to hepatocytes and kidney [122]. No naturally occurring cell type has yet been identified that only possesses concentrative nucleoside transport activity. In tissues such as the intestine, the concentrative transporters are known to be on brush border membranes [118, 142, 143]. Intestinal cells also possess equilibrative nucleoside transport activity and this activity is not found on the brush border membrane but on the basolateral membrane [118, 119]. Work from Giacomini's group has demonstrated that green fluorescent protein-tagged rCNT1 and rCNT2 are targeted to the apical membrane of polarized kidney cells [144], suggesting that these transporters contain targeting elements that direct them to the appropriate membrane of polarized cells.

1 B. I.C. The Uracil/Allantoin Transporter Family (Microbial Purine-Related Transporter Family)

Family Characteristics: Most members of the uracil/allantoin transporter family are found exclusively in yeast, either *S. cerevisiae* or *Schizosaccharomyces pombe*. The founding member of this family is FUR4, the yeast uracil permease [145]. The members of this family include the allantoin transporter, DAL4, and the thymine transporter, THI10 (Table 1-6). Recently, de Koning and Diallinas proposed that these proteins are members of a larger family, called the microbial purine-related transporter family [146].

The rationale for this proposal lies in the identification of conserved residues when members of the uracil/allantoin family are aligned with the yeast FCY2 protein and the *E. coli* codB protein [146]. The dendogram shown in Figure 1-10 includes FCY2 and codB to reflect the latest observation of de Koning and Diallinas [146]. The proteins in this family are predicted by the hidden Markov model [147, 148] to have 10-13 transmembrane domains.

FUI1, the Yeast Nucleoside Transporter: Another member of the uracil/allantoin transporter family is the FUI1 protein. The FUI1 sequence is quite different from that of the ENT and CNT proteins [76]. FUI1 is 70% similar to FUR4, the yeast uracil permease, and 69% similar to DAL4, the allantoin permease [76]. The FUI1 gene locus was first described in *S. cerevisiae* mutants that were resistant to the cytotoxic drug, 5-fluorouridine [149]. Subsequent analysis revealed that *fui1* knock-out strains were viable and that disruption of the *fui1* gene resulted in 5-fluorouridine resistance [150]. More recently, Vickers and co-workers [69] have demonstrated that FUI1 is indeed a uridine-specific nucleoside transporter on the yeast plasma membrane. The uptake mediated by FUI1 was not inhibited by NBMPR, dilazep or dipyridamole.

1 B. I.D. The NupG/XapB Nucleoside Transporter Family

Family Characteristics: The last recognized family of nucleoside transporters is limited to bacteria and has only four members that are found in *E. coli* or in *Caulobacter crescentus* (see Table 1-7). NupG and XapB have been demonstrated to be nucleoside [151, 152] and xanthosine [153] transporters, respectively, in *E. coli*. The other two proteins, yegT and the *C. crescentus* protein Cc1628, are predicted to be nucleoside transporters based on their homology to NupG and XapB (see dendogram in Figure 1-11). The proteins in this family are predicted by the hidden Markov model [147, 148] to have 12 transmembrane domains.

1 B. I.E. The Putative Nucleoside Permease Family

Family Characteristics: There are four cDNAs, three of which are related, in GenBank that encode putative nucleoside transporters that are not homologous to any of the aforementioned protein families (see Table 1-8). One of these "orphan" transporters has been characterized functionally. The *Candida albicans* protein is a broad selectivity transporter that transports both adenosine and guanosine in a *S. cerevisiae* complementation system [154]. The other three sequences (from *Giardia intestinalis*, *S. pombe*, and *C. crescentus*) were obtained from searches of GenBank and two of these sequences are related to the *C. albicans* protein (see dendogram in Figure 1-12). The GenBank entry for the *G. intestinalis* sequence mentions functional data, but these are unpublished findings. Similarly, the *S. pombe* sequence has been cloned (F. Visser, N. Lutic, J. D. Young and C. E Cass, unpublished observations), but functional activity was not observed in a *S. cerevisiae* complementation system previously developed to screen for nucleoside transporters [155, 156]. The hidden Markov model [147, 148] predicts

only 1 putative transmembrane domain for these proteins, while the TopPredII program [157] predicts 1-3 putative transmembrane domains. It remains to be seen whether or not these open reading frames encode membrane proteins that translocate nucleosides in these lower organisms.

1 B. II. Intracellular Nucleoside Transport Processes and Intracellular Membrane Proteins

1 B. II.A. Intracellular Nucleoside Transport

Nucleosides are required for many cellular processes and may be required to cross membranes before they can be utilized. Intracellular nucleoside transport was first reported in studies with lysosomes isolated from human fibroblasts [8]. This lysosomal nucleoside transport process preferred purine nucleosides over pyrimidine nucleosides and was also inhibited by NBMPR. However, it differed from the plasma membrane process in two major ways. First, the lysosomal activity had a K_m value (approximately 9 mM) for adenosine uptake that was 25-100 fold larger than that of the hENT1-mediated *es* process [8]. Second, the concentrations of NBMPR (25 μM) or dipyridamole (25 μM) required to inhibit 50% of the lysosomal process were much higher than those (1-10 nM) that are required to inhibit 50% of transport at the plasma membrane in human cells. These characteristics suggest that a lysosomal member of the ENT family exists, but is different from hENT1. The molecular identity of this transporter remains unknown, but hENT3 is a candidate.

Evidence of mitochondrial nucleoside transporters also exists. Mitochondria possess their own DNA and the machinery necessary to replicate it. Nucleoside kinases, specifically deoxyguanosine kinase [158] and deoxythymidine kinase 2 [159], have been localized to mitochondria. Mitochondrial toxicity of antiviral drugs [160] and anticancer drugs [161] is well-documented, although it is not known if the nucleoside or the nucleotide version of drug enters mitochondria. NBMPR binding has been reported in mitochondria isolated from rat testis [162], but adenosine transport in isolated mitochondria is not inhibited by NBMPR [163]. Studies in human and rat liver mitochondria have demonstrated mediated uptake of uridine and nucleoside analogues (K. M. King, P. Panayides, and C. E. Cass, unpublished observations). These studies have also demonstrated that NBMPR binds to rat liver mitochondria and that NBMPR inhibition of transport is not as complete as that seen with plasma membrane transport processes (K. M. King, P. Panayides, and C. E. Cass, unpublished observations). Thus, although protein-mediated nucleoside transport exists in mitochondria, the protein or proteins responsible for this activity have not yet been identified.

Functional *es* and *ei* transporters have been reconstituted from

nuclear/endoplasmic reticulum membranes [7], and the *es* transporters present in various subcellular fractions were quantitated by the [^{3}H]-NBMPR-binding technique. The study by Mani and colleagues [7] supported earlier studies of NBMPR binding in reticulocytes, BeWo, and chromaffin cells that suggested that there are intracellular pools of *es* transporters (*i.e.*, hENT1) that may be recruited to the cell surface [113, 164, 165].

1 B. II.B. The mLAPTm4/MTP Protein Family

In attempts to identify cDNAs encoding nucleoside transporters, a *S. cerevisiae* complementation system [156] was used to screen various cDNA libraries. A screen of a mouse L1210 library resulted in the identification of mouse transporter protein (MTP), a protein of intracellular membranes [156]. Also, a screen of a human kidney cDNA library resulted in the identification of a mitochondrial protein, ND4, that was identified as part of a fusion protein [155]. This fusion protein consisted of UDP-galactose-4'-epimerase and a truncated version of ND4, a mitochondrially encoded component of Complex I of the respiratory chain [155]. The ND4 fusion protein and a truncated version of MTP [156] complemented the *S. cerevisiae* nucleoside transport deficiency.

MTP, now known as murine lysosome-associated protein transmembrane 4 (mLAPTm4), was the first member of a four transmembrane domain-containing protein family to be identified. There are now known orthologues in human, rat, *C. elegans, Bombyx mori* and *D. melanogaster*. The exact function of these membrane proteins is not known. Subsequent studies with mLAPTm4/MTP, including the determination of its subcellular localization, which is part of this study [166, 167], have suggested that mLAPTm4/MTP is involved in drug sequestration and is probably not a nucleoside transport protein [168].

1 B. III. Regulation of Nucleoside Transporters

Regulation of membrane transport processes occurs by one or both of two general mechanisms [169, 170]. In the first instance, transporter proteins are modified such that their activities change. An example of this type of regulation is the reversible modification of proteins by covalent phosphorylation [170]. In the second instance, the amount of active transporters present in plasma membranes is modified either by modulating protein synthesis and/or degradation rates or by recruiting transporters from a pre-existing intracellular pool [170]. These two modes of regulation are not mutually exclusive.

Regulation of hENT1-mediated *es* and hENT2-mediated *ei* activities has been demonstrated in some cell types. In some cases, the results are conflicting, which suggests that regulation is cell-type specific. Rat fibroblasts expressing a transforming protein tyrosine kinase exhibited increased levels of *es* and *ei* activities compared to wild-type fibroblasts [171]. Protein kinase C activation in chromaffin cells results in decreased

adenosine transport by reducing transporter abundance, as measured by quantitating the number of NBMPR-binding proteins in preparations of plasma membrane vesicles [172]. Protein kinase A and protein phosphatases, which may be regulated by protein kinase C, have been implicated in the ethanol sensitivity of adenosine transport in neuroblastoma x glioma hybrid cells [173, 174]. More recently, protein kinase C inhibition was accompanied by a decrease in adenosine efflux from rat smooth muscle cells preloaded with [^{3}H]-adenosine [175]. It is not yet known whether these kinases achieve their effects directly by phosphorylation of nucleoside transporter proteins or indirectly by phosphorylation of accessory proteins.

The levels of *es* and *ei* activities differ depending on the proliferative and differentiation state of cells. In quiescent murine macrophages, *es* and *ei* activities are low, but when the cells are stimulated to enter the cell cycle, the activities increase [176]. In synchronized HeLa cells [177, 178], *es* transport activity and NBMPR-binding sites remain constant relative to cell size as HeLa cells progress through the cell cycle. Differentiation of HL-60 cells has been used successfully to examine the regulation of nucleoside transport. Stoeckler and co-workers were the first to notice that *es* transport activity decreased when dimethylformamide was added to HL-60 cells to induce myeloid differentiation [179]. Comparison of uptake rates of cytarabine in retinoic acid-differentiated and undifferentiated HL-60 cells demonstrated differences which were associated with changes in the proliferative status of the cell [180]. Also, *es* and *ei* activities decreased when HL-60 cells were induced to differentiate by treatment with phorbol esters or dimethylsulfoxide [165, 181-184]. In differentiated human neuroblastoma cells, formycin B uptake increased by 26% due to the appearance of an *ei* nucleoside transport component that was not observed in undifferentiated cells [185]. More recently, studies in a human B-lymphocyte-derived cell line, Raji, and in mouse bone marrow lymphocytes have demonstrated that lipopolysaccharide and phorbol esters downregulate *es* transport activity and are capable of upregulating concentrative nucleoside transport activities [186-188]. Changes in the amount of hENT1 at cell surfaces, as monitored by NBMPR binding, have been observed in cells when thymidine triphosphate levels were altered by treatment with thymidylate synthase inhibitors [189] or 5-fluorouracil and hydroxyurea [190].

1 C. Hypotheses and Objectives of the Study

The hypotheses were that:

1. mLAPTm4/MTP is an intracellular transporter involved in transport of, as yet, unidentified molecules across organellar membranes.
2. In addition, to their roles as plasma membrane transporters, hENT1 and hENT2 function inside cells to transport nucleosides across organellar membranes.
3. The hHNP36 protein is a splice product of the hENT2 gene.
4. hENT1 and/or hENT2 activities are regulated in response to changes in cellular deoxyribonucleotide levels or in response to changes in the activity or levels of the other ENT transporter when both proteins are present in the same cell type.

The objectives of this work were to characterize the subcellular localization of membrane transporter proteins of the LAPTm4 and ENT families and to probe potential regulatory mechanisms of equilibrative nucleoside transporters. The specific goals were to:

1. **Assess the function and define the intracellular location of mLAPTm4/MTP.**
2. **Examine hENT1 and hENT2 in tissue culture cells using the newly generated anti-hENT1 and anti-hENT2 antibodies.**
3. **Define the relationship between hENT2 and hHNP36.**
4. **Use perturbatory metabolism- and antisense-based methods to probe for potential avenues of regulation of hENT1 and hENT2 activities.**

Figure 1-1. Structures of Physiological Nucleosides. The chemical structures of the purine and pyrimidine nucleosides are depicted.

Figure 1-1

Structures of Physiological Nucleosides

Purine nucleosides

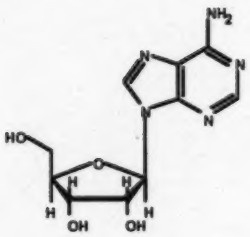

adenosine

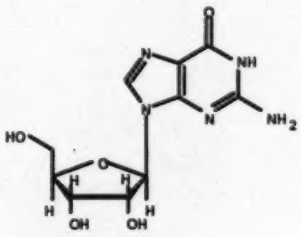

guanosine

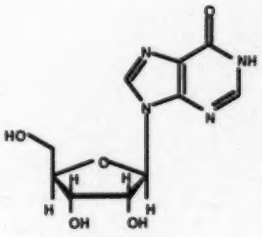

inosine

Pyrimidine nucleosides

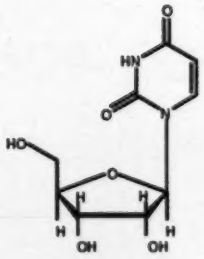

uridine

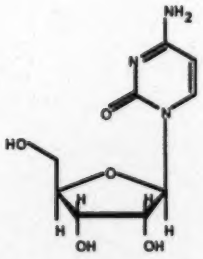

cytidine

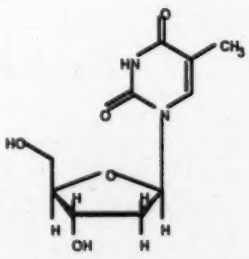

thymidine

Figure 1-2. Structures of Anticancer Nucleoside Drugs. The structures of two purine-based drugs, cladribine (2-chloro, 2'-deoxyadenosine) and fludarabine (2'-fluoro adenine arabinoside), and two pyrimidine-based nucleoside drugs, cytarabine (cytosine arabinoside) and gemcitabine (difluorodeoxycytidine) are depicted.

Figure 1-2

Structures of Anticancer Nucleoside Drugs

Purine nucleoside drugs

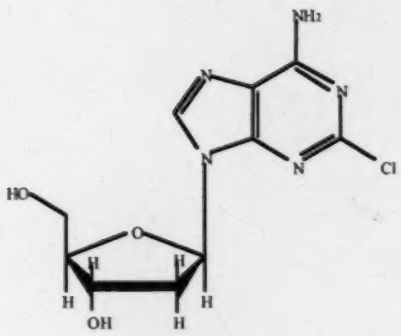

cladribine

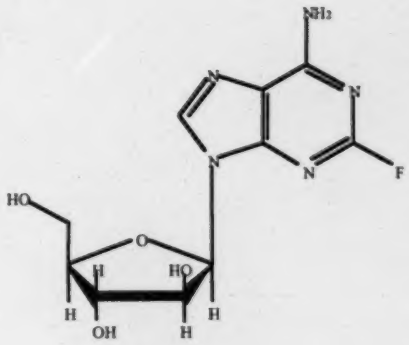

fludarabine

Pyrimidine nucleoside drugs

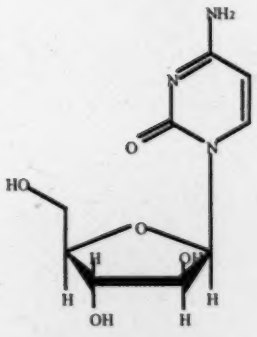

cytarabine

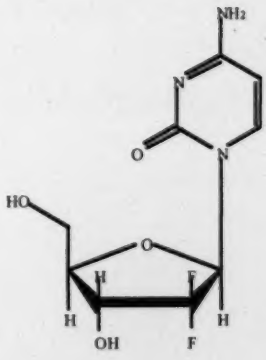

gemcitabine

Figure 1-3. Structures of Antiviral Nucleoside Drugs. The structures of three purine-based drugs, 3'-deoxy-3'-azidothymidine (AZT), 2', 3'-dideoxycytidine (ddC), and 3'-thia-2',3'-dideoxcytidine (3TC) and the pyrimidine-based nucleoside drug 2', 3'-dideoxyinosine (ddI) are depicted.

Figure 1-3

Structures of Antiviral Nucleoside Drugs

Purine nucleoside drugs

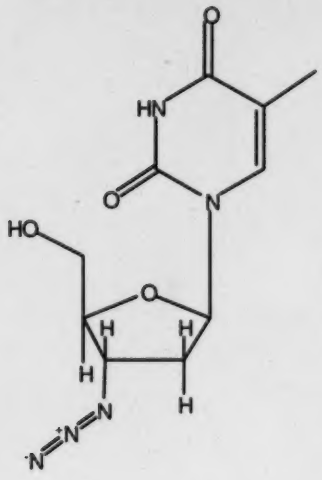

AZT

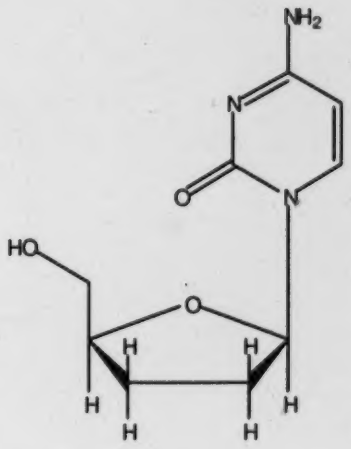

ddC

Pyrimidine nucleoside drug

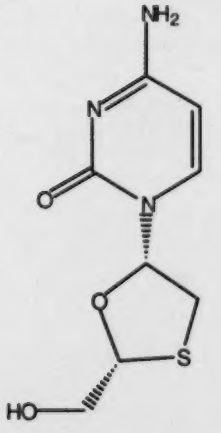

3TC

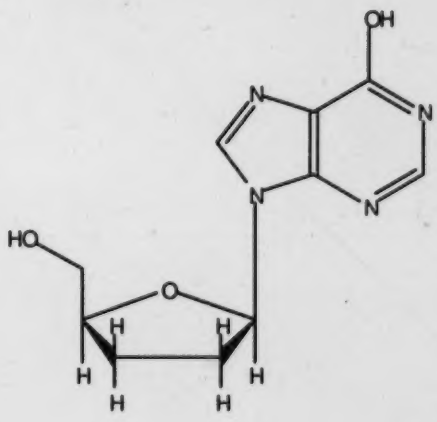

ddI

Figure 1-4. The ENT Family. The members of the ENT family (see Table 1-1) were aligned using ClustalW and grouped into an evolutionary tree using parsimony on WebPhylip at the Canadian Bioinformatics Resource website (http://www.cbr.nrc.ca). The transporters depicted in red have been functionally characterized.

Figure 1-4 The ENT Family

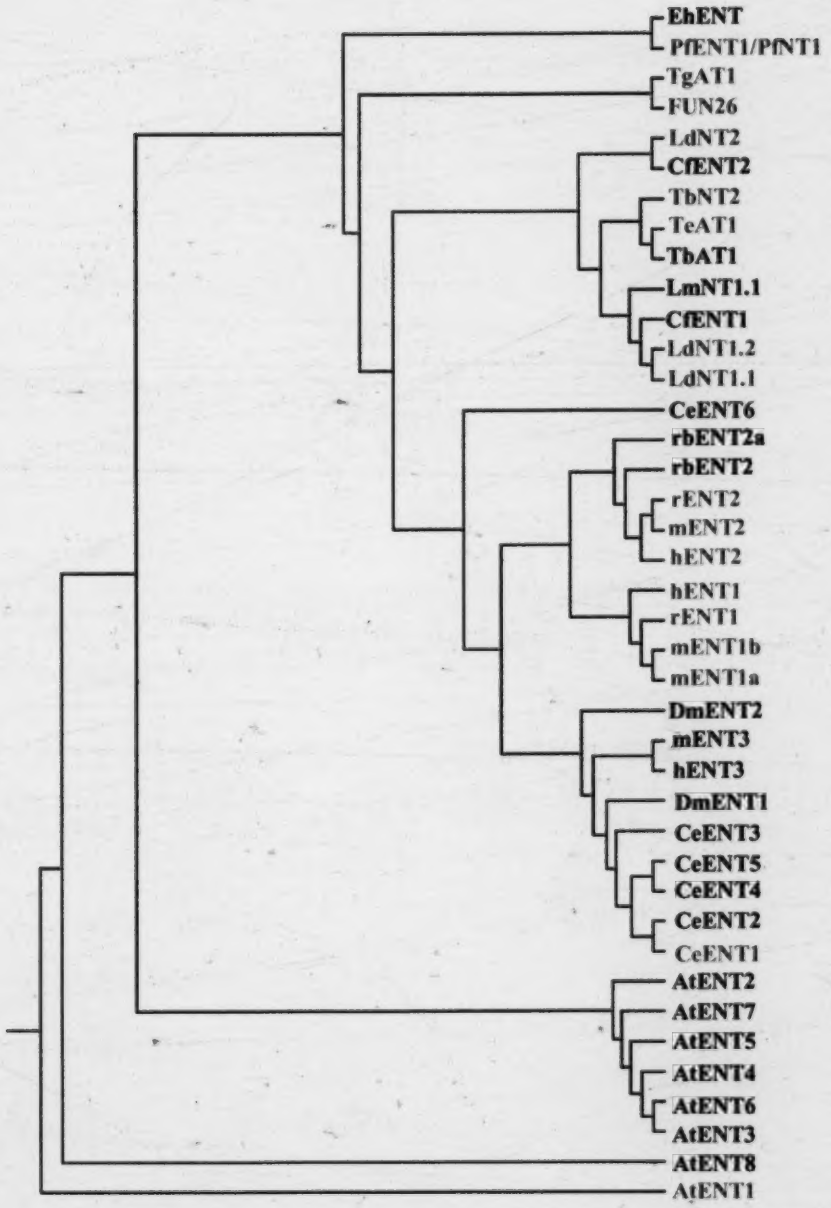

Figure 1-5. The Predicted Topological Model of hENT1. The topology model of hENT1 predicted by Baldwin and co-workers [75, 86] using the hidden Markov model of Sonnhammer and colleagues [147, 148] is shown with 11 transmembrane domains along with the glycosylation site on the extracellular N-terminal loop between transmembrane domains 1 and 2. The amino acids implicated in NBMPR- and dipyridamole-binding are highlighted. Depicted in red is the synthetic peptide epitope used to generate anti-hENT1 polyclonal and monoclonal antibodies [115].

Figure 1-5 The Predicted Topological Model of hENT1

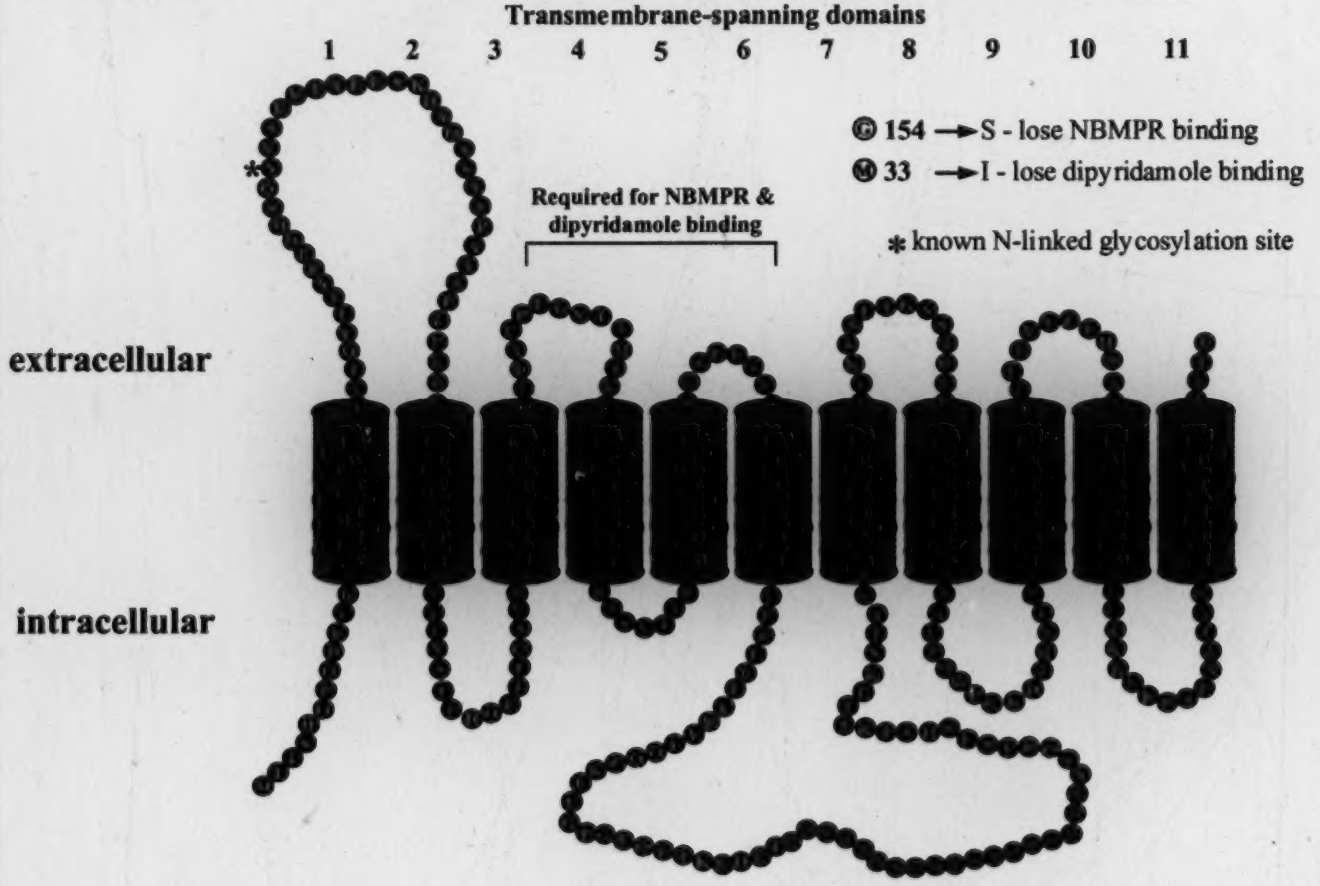

Figure 1-6. The Predicted Topological Model of hENT2. The topology model of hENT2 predicted by Baldwin and co-workers [75, 86] using the hidden Markov model of Sonnhammer and colleagues [147, 148] is shown with 11 transmembrane domains along with the two glycosylation sites on the extracellular N-terminal loop between transmembrane domains 1 and 2. Depicted in red is the fusion protein epitope used to generate anti-hENT2 polyclonal and monoclonal antibodies.

Figure 1-6 The Predicted Topological Model of hENT2

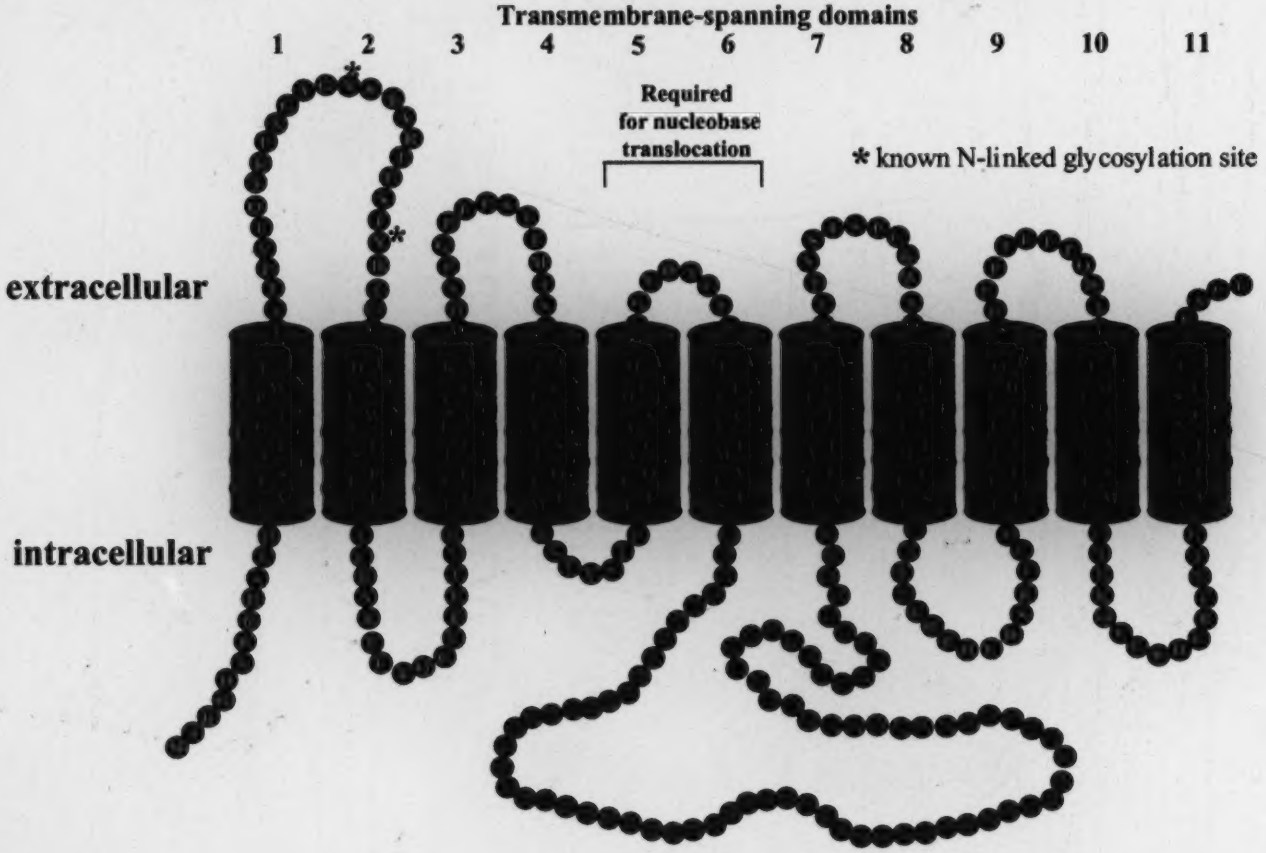

Figure 1-7. Structures of Equilibrative Nucleoside Transport Inhibitors. The chemical structures of the most common ENT inhibitors are depicted.

Figure 1-7

Structures of Equilibrative Nucleoside Transport Inhibitors

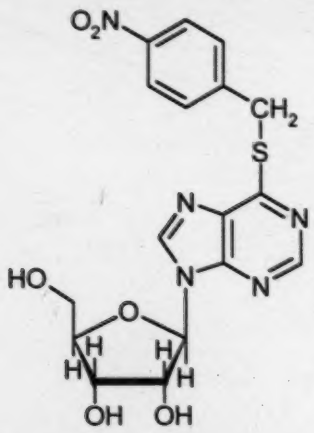

nitrobenzylthioinosine/ nitrobenzylmercaptopurine ribonucleoside (NBMPR)

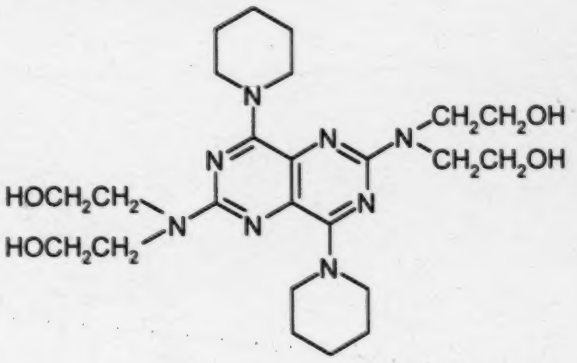

dipyridamole

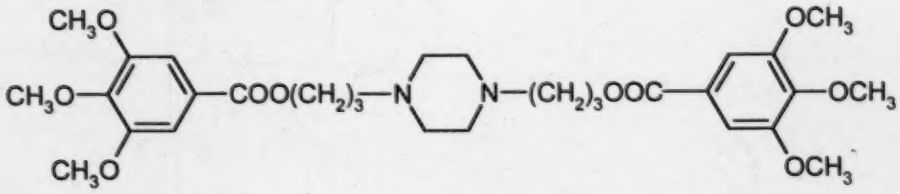

dilazep

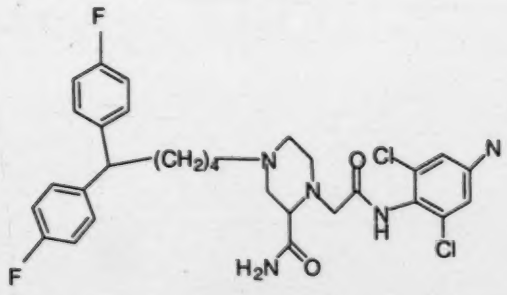

draflazine

Figure 1-8. The CNT Family. The members of the CNT family (see Table 1-3) were aligned using ClustalW and grouped into an evolutionary tree using parsimony on WebPhylip at the Canadian Bioinformatics Resource website (http://www.cbr.nrc.ca). The transporters depicted in red have been functionally characterized.

Figure 1-8 The CNT Family

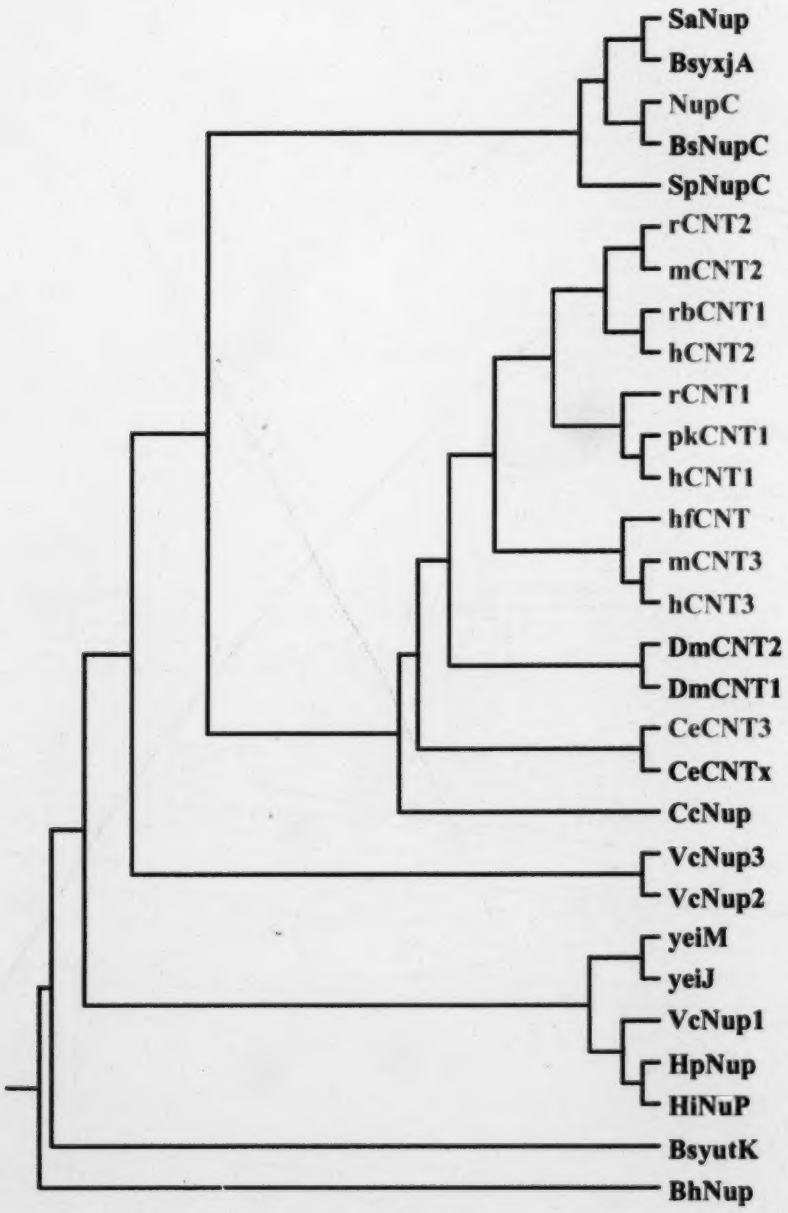

Figure 1-9. The Predicted Topological Model of hCNT1. The topology model of hCNT1 by Baldwin and co-workers [122, 133] using the hidden Markov model of Sonnhammer and colleagues [147, 148] is shown with 13 transmembrane domains along with the glycosylation sites on the C-terminal extracellular tail. Model courtesy of Dr. Mark Vickers [76].

Figure 1-9 The Predicted Topological Model of hCNT1

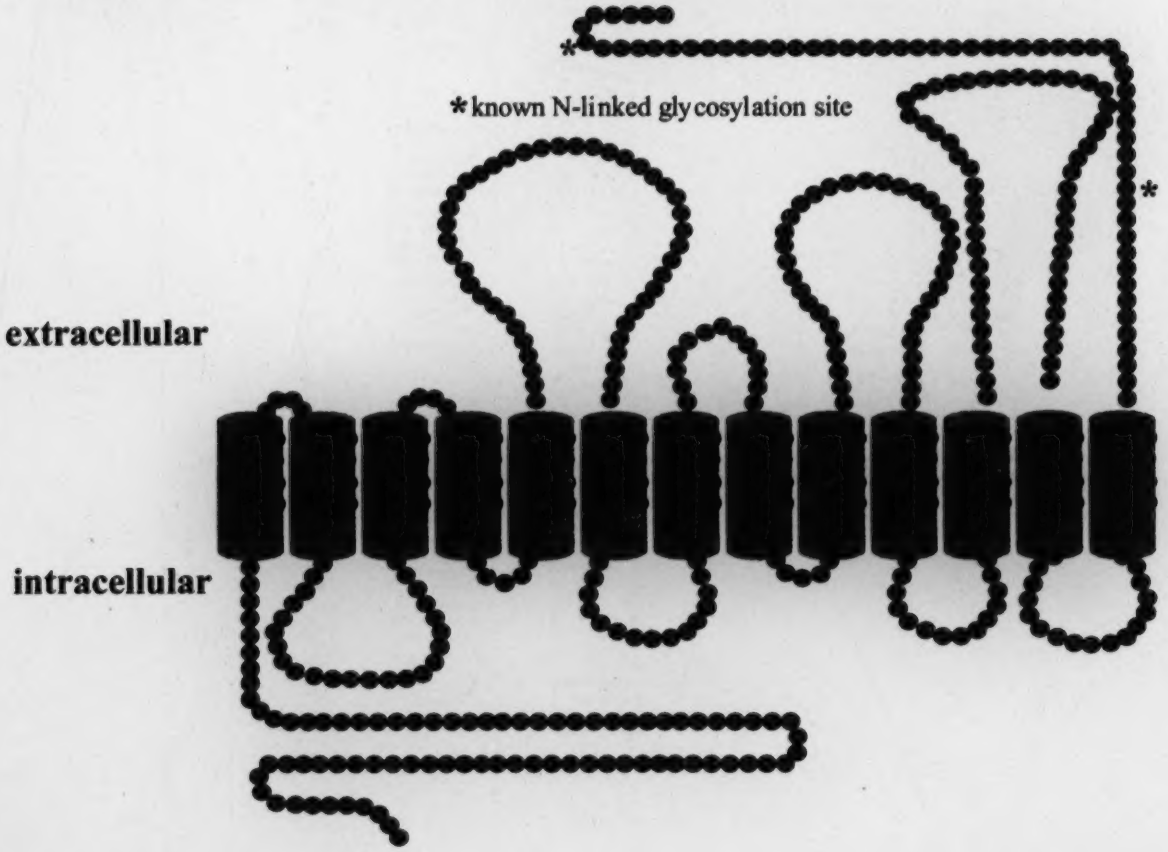

Figure 1-10. The Uracil/Allantoin Transporter Family. The members of the uracil/allantoin transporter family (see Table 1-6) were aligned using ClustalW and grouped into an evolutionary tree using parsimony on WebPhylip at the Canadian Bioinformatics Resource website (http://www.cbr.nrc.ca). The transporters depicted in red have been functionally characterized.

Figure 1-10

The Uracil/Allantoin Transporter Family

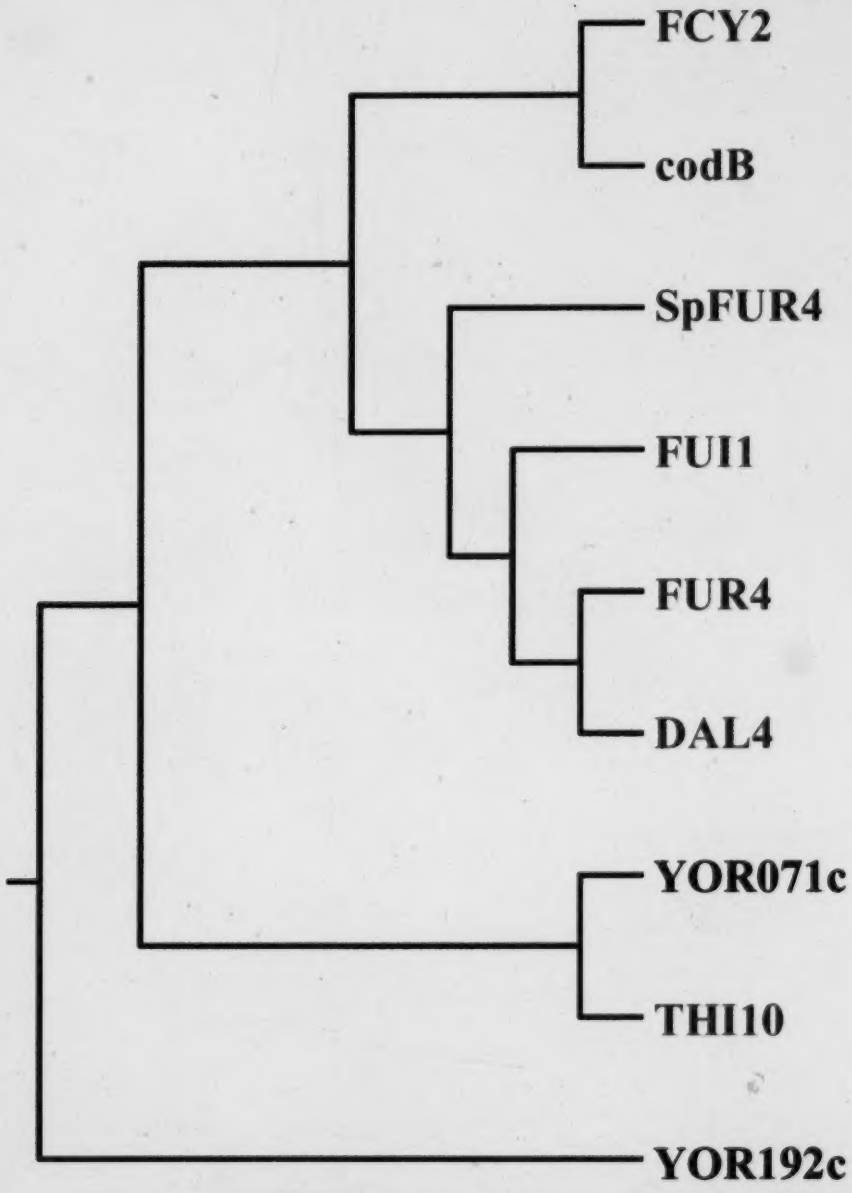

Figure 1-11. The NupG/XapB Transporter Family. The members of the NupG/XapB family (see Table 1-7) were aligned using ClustalW and grouped into an evolutionary tree using parsimony on WebPhylip at the Canadian Bioinformatics Resource website (http://www.cbr.nrc.ca). The transporters depicted in red have been functionally characterized.

Figure 1-11

The NupG/XapB Transporter Family

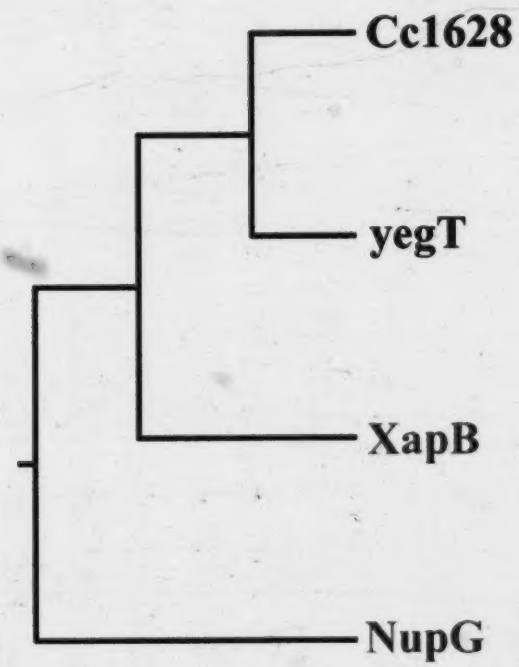

Figure 1-12. The Nucleoside Permease Transporter Family. The members of the putative nucleoside permease family (see Table 1-8) were aligned using ClustalW and grouped into an evolutionary tree using parsimony on WebPhylip at the Canadian Bioinformatics Resource website (http://www.cbr.nrc.ca). The transporters depicted in red have been functionally characterized.

Figure 1-12

The Nucleoside Permease Transporter Family

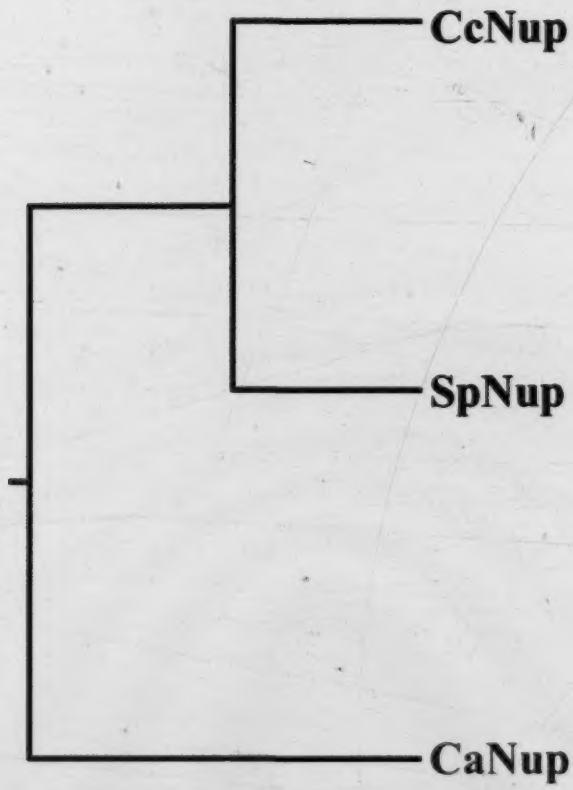

Table 1-1. The ENT Family of Proteins

Protein	GenBank Accession Number(s)	Gene name (if applicable)	Organism	Reference
1. hENT1	Q99808		*Homo sapiens*	[68]
2. rENT1	O54698		*Rattus norvegicus*	[79]
3. mENT1a/ mENT1.2[1]	AAF76430, AAF64036, AAF78452, NP_075018		*Mus musculus*	[80, 81, 191]
4. mENT1b/ mENT1.1[1]	AAF76429, AAF64035, AAG22828		*M. musculus*	[80, 81, 191]
5. hENT2	Q14542		*H. sapiens*	[68, 98, 99]
6. rENT2	O54699		*R. norvegicus*	[79]
7. mENT2	AAF76431, AAF78477 NP_031880		*M. musculus*	[80, 81, 191]
8. hENT3	AAK00958		*H. sapiens*	[75]
9. mENT3	AAK00957		*M. musculus*	[75]
10. DmENT1	AAF52405		*Drosophila melanogaster*	
11. DmENT2	AAF51506*		*D. melanogaster*	
12. CeENT1	CAA92642*	ZK809.4	*Caenorhabditis elegans*	[6]
13. CeENT2	CAB01882	K09A9.3	*C. elegans*	
14. CeENT3	CAB01223*	K02E11.1	*C. elegans*	
15. CeENT4	CAB62793*	C47A4.2	*C. elegans*	
16. CeENT5	AAA98003	F16H11.3	*C. elegans*	
17. CeENT6	CAB03075	F36H2.2	*C. elegans*	
18. AtENT1	AAF26446, AAC18807	F17O7.13	*Arabidopsis thaliana*	[77]
19. AtENT2	AAF04424	T22K18.20	*A. thaliana*	
20. AtENT3	CAB81054	AT4g05120	*A. thaliana*	
21. AtENT4	CAB81055	AT4g05130	*A. thaliana*	
22. AtENT5	CAB81056	AT4g05140	*A. thaliana*	
23. AtENT6	CAB81053	AT4g05110	*A. thaliana*	

24. AtENT7	AAD45278	T25B24.2	*A. thaliana*	
25. AtENT8	AAG10625	T14P4.9	*A. thaliana*	
26. TbAT1	AAD45278		*Trypanosoma brucei brucei*	[192]
27. TbNT2	AAF04490		*T. brucei brucei*	[71]
28. LdNT1.1	AAC32597		*Leishmania donovani*	[70]
29. LdNT1.2	AAC32315		*L. donovani*	[70]
30. LdNT2	AAF74264		*L. donovani*	[73]
31. LmNT1.1	CAB96736		*L. major*	
32. LmNT2			*L. major*	
33. CfNT1	AAG22610		*Crithidia fasciculata*	
34. CfNT2	AAG22611		*C. fasciculata*	
35. TgAT	AAF03427/ AAF02894		*Toxoplasma gondii*	[72]
36. PfNT1/ PfENT1[1]	AAF67613/ AAG09713		*Plasmodium falciparum*	[74, 86]
37. rbENT2	AAK11605		*Oryctolagus cuniculus*	
38. rbENT2a	AAK11606		*O. cuniculus*	
39. TbAT1r	AAD45279		*T. brucei brucei*	[192]
40. EhENT1	S49592		*Entamoeba histolytica*	
41. FUN26	P31381		*S. cerevisiae*	[69]
42. TeAT1	CAC41330		*T. equiperdum*	
43. TeAT1r	CAC41331		*T. equiperdum*	

[1]These cDNAs were found by two independent groups and were thus given two different names and two different sets of GenBank numbers.

N.B. Due to the annotation of entries within the GenBank database, some of the original GenBank accession numbers have been replaced by a new number that in some cases combines a set of original GenBank entries.

Table 1-2. Properties of Mammalian ENT Proteins

Transporter Protein	Amino Acids	Tissue Distribution	Chromosomal location of gene	Reference
hENT1	456	Ubiquitous	6p21.1-21.2	[68, 97, 115, 118, 193]
hENT2	456	Skeletal muscle, heart, pancreas, brain, kidney, small intestine, lung, fetal heart, fetal kidney, salivary gland, thyroid gland, thymus, prostate, colon, kidney	11q13	[68, 97-99, 105, 115, 118]
hENT3	475	placenta	10	[75]
mENT1a (mENT1.2)[1]	458	Heart, brain, NG108-15 cells, spleen, lung, liver, skeletal muscle, testis	17C	[80, 81, 191]
mENT1b (mENT1.1)[1]	460	Heart, brain, NG108-15 cells, spleen, lung, liver, skeletal muscle, testis	17C	[80, 81, 191]
mENT2	456	brain, NG108-15 cells	nd[2]	[80, 81, 191]
mENT3	474	kidney	nd[2]	[75]
rENT1	457	intestine, brain, epididymis	nd[2]	[79, 117, 194, 195]
rENT2	456	intestine, brain, epididymis	nd[2]	[79, 116, 195]
rbENT2	456	nd[2]	nd[2]	
rbENT2a	415	nd[2]	nd[2]	

[1]These cDNAs were found by two independent groups and were thus given two different names.
[2]not determined

Table 1-3. Human Nucleoside Transport Activities and Proteins

A. Equilibrative Nucleoside Transport

Transporter Protein	Transport Process	Permeant selectivity	Reference
hENT1	*es*[1]	purine and pyrimidine nucleosides	[68]
hENT2	*ei*[2]	purine and pyrimidine nucleosides & nucleobases	[68, 88, 98, 99]
hENT3	nd[3]	nd[3]	[75]

B. Concentrative Nucleoside Transport

Transporter Protein	Transport Process	Permeant selectivity/ Sodium:Substrate Ratio	Reference
hCNT1	*cit*[4]	pyrimidine nucleosides/ 1:1	[131]
hCNT2	*cif*[5]	purine nucleosides, uridine/ 1:1	[134, 136]
hCNT3	*cib*[6]	purine and pyrimidine nucleosides/ 2:1	[102, 132, 133]
nd[3]	*cit*[4]	pyrimidine nucleosides, adenosine and guanosine	[127, 128]
nd[3]	*cs*[7]	formycin B, fludarabine, cladribine	[130]
nd[3]	*csg*[8]	guanosine	[126]

[1]equilibrative, sensitive to nitrobenzylthioinosine
[2]equilibrative, insensitive to nitrobenzylthioinosine
[3]not determined
[4]concentrative, insensitive to nitrobenzylthioinosine, thymidine-selective
[5]concentrative, insensitive to nitrobenzylthioinosine, formycin B-selective
[6]concentrative, insensitive to nitrobenzylthioinosine, broadly selective
[7]concentrative, sensitive to nitrobenzylthioinosine
[8]concentrative, sensitive to nitrobenzylthioinosine, guanosine-selective

Table 1-4. The CNT Family of Proteins

Protein	GenBank Accession Number(s)	Gene Name (if applicable)	Organism	Reference
1. BhNupC	BAB05165	BH1446	*Bacillus halodurans*	
2. BsNupC	CAA57663	NupC	*B. subtilis*	
3. BsyutK	CAB15208	yutK	*B. subtilis*	
4. BsyxjA	CAB15938	yxjA	*B. subtilis*	
5. CcCNT	AAK24060	CC2089	*Caulobacter crescentus*	
6. CeCNTx	AAB65255, AAF80461	F27E11.1	*C. elegans*	
7. CeCNT3	AAB65256, AAF80462	F27E11.2	*C. elegans*	[196]
8. DmCNT1	AAF58996	CG11778	*D. melanogaster*	
9. DmCNT2	AAF58997	CG8083	*D. melanogaster*	
10. NupC	CAA52821	NupC	*E. coli*	[123, 124]
11. yeiJ	AAC75222	yeiJ	*E. coli*	
12. yeiM	AAC75225	yeiM	*E. coli*	
13. hfCNT	AAD52151	hfCNT	*Eptatretus stouti*	[138]
14. hCNT1	O00337	cit/N2	*H. sapiens*	[131]
15. hCNT2	O43868	SPNT, cif/N1	*H. sapiens*	[134, 136]
16. hCNT3	AAG22551	cib/N3	*H. sapiens*	[132, 133]
17. HiNupC	AAC22177	HI0519	*Haemophilus influenzae*	[125]
18. HpNupC	AAD08224	HP1180	*Helicobacter pylori*	[125]
19. mCNT2	O88627	cif/N1	*M. musculus*	[197]
20. mCNT3	AAG22552	cib	*M. musculus*	[132, 133]
21. pCNT1	O62667	cit/N2	*Sus scrofa*	[198]
22. rbCNT1	Q9MZT2	cit/N2	*O. cuniculus*	
23. rCNT1	Q62674	cit/N2	*R. norvegicus*	[121]
24. rCNT2	Q62773	cif/N1	*R. norvegicus*	[137]
25. SaNupC[1]	BAB41833, BAB56807	SA0600, SAV0645	*Staphylococcus aureus*	
26. SpNupC	AAK34582	nupC	*Streptococcus pyogenes*	
27. VcNupC1	AAF95495	VC2352	*Vibrio cholerae*	

28. VcNupC2	AAF95101	VC1953	*V. cholerae*	
29. VcNupC3	AAF96092	VCA0179	*V. cholerae*	

[1]This sequence has two GenBank entries because two identical sequences were isolated from different strains.

N.B. Due to the annotation of entries within the GenBank database, some of the original GenBank accession numbers have been replaced by a new number that in some cases combines a set of original GenBank entries.

Table 1-5. Characteristics of Mammalian CNT Proteins

Transporter Protein	Amino Acids	Tissue distribution	Chromosomal location of gene	References
hCNT1	649	kidney, liver, intestine, placenta, fetal kidney, brain	15q25-26	[97, 118, 131, 142]
hCNT2	658	kidney, brain, placenta, lung, liver, skeletal muscle, pancreas, intestine, heart	15q15 (15q13-14)	[97, 118, 134, 136, 142]
hCNT3	691	bone marrow, intestine, pancreas, trachea, mammary gland, HL-60 cells, prostate, testis, liver, lung, kidney, placenta	9q22.2	[133]
rCNT1	648	intestine, liver, kidney, brain (protein seen in kidney, liver and intestine)	nd[1]	[121, 122, 199, 200]
rCNT2	659	liver, intestine, kidney, brain, epididymis	nd[1]	[121, 137, 195, 199-201]
rbCNT2	658	small intestine	nd[1]	[135]
mCNT2	660	spleen	2e3	[202]
mCNT3	703	liver	nd[1]	[132, 133]
pCNT1	647	kidney	nd[1]	[198]

[1]not determined

Table 1-6. The Uracil/Allantoin Family of Proteins

Protein	GenBank Accession Number	Organism	Reference
1. FUI	P38196	*S. cerevisiae*	[69, 149, 150]
2. YOR192c	CAA99401	*S. cerevisiae*	
3. YOR071c	CAA99264	*S. cerevisiae*	
4. THI10	BAA09504	*S. cerevisiae*	[203]
5. FUR4	CAA53678	*S. cerevisiae*	[150]
6. DAL4	CAA86188	*S. cerevisiae*	[204]
7. SpFUR4	CAA67256	*Schizosaccharomyces pombe*	[145, 205]
8. FCY2	NP_010976	*S. cerevisiae*	[206]
9. codB	P25525	*E. coli*	[207]

Table 1-7. The NupG/XapB Family of Proteins

Protein	GenBank Accession Number	Organism	Reference
1. yegT	P76417	*E. coli*	
2. NupG	P09452	*E. coli*	[151, 152]
3. XapB	P45562	*E. coli*	[153]
4. Cc1628	AAK23606	*C. crescentus*	

Table 1-8. The Nucleoside Permease Family of Proteins

Protein	GenBank Accession Number	Gene Name	Organism	Reference
1. CaNup	AAC64324	Nup	*Candida albicans*	[154]
2. SpNup	T41251	SPCC285.05	*S. pombe*	
3. CcNup	AAK22174	CC0187	*C. crescentus*	
GiNup	AAA29158	tpt1	*Giardia intestinalis*	

Chapter 2

2. Materials and Methods

2 A. Laboratory Chemicals and Isotopes

Unless otherwise noted, chemicals described in this study were purchased from either Sigma-Aldrich (Oakville, ON) or Fisher Scientific (Nepean, ON). All solutions were prepared with distilled, deionized water (ddH_2O). Isotopes purchased from Moravek Biochemicals (Brea, CA) were: [methyl-^{3}H]-thymidine, [5-^{3}H]-uridine, [^{3}H]-H_2O, [^{14}C(U)]-sucrose, [^{3}H(G)]-NBMPR. The isotope [α-^{32}P]-dCTP was purchased from Amersham Pharmacia Biotech.

2 B. Cell Culture and Media

General: Cells were grown as adherent or suspension cultures at 37°C in 5% CO_2 in the absence of antibiotics. Cells were subcultured at regular intervals either by trypsinization for adherent cell lines (3-7 days, 2 x 10^5 cells/flask) or by dilution for suspension cell lines (2-4 days, 1 x 10^5 cells/mL) in T-25 flasks. Cultures were discarded after ≤ 30 passages and new cultures were reinitiated from mycoplasma-free, low-passage stock cultures stored in 10% dimethyl sulfoxide (DMSO) in liquid nitrogen. Routine mycoplasma testing was performed by the Provincial Health Laboratory (Edmonton, AB). Media and sera were obtained from Gibco/BRL Life Technologies (Burlington, ON). All tissue culture flasks and plates were obtained from either Corning (Corning, NY), Falcon (Becton Dickinson Labware, Franklin Lakes, NJ) or Nunc (Roskilde, Denmark). Cells were enumerated using a Model Zf or Z2 electronic particle counter (Beckman-Coulter, Miami, FL). The electronic particle counter was also used to measure cell diameters for use in cell volume calculations.

Human Cell Lines: BeWo (choriocarcinoma) and HeLa (cervical adenocarcinoma) were obtained by Dr. C. E. Cass from the American Tissue Culture Collection (Bethesda, MD) and were cultured in Roswell Park Memorial Institute (RPMI) 1640 medium supplemented with 10% fetal bovine serum (FBS) or 10% calf serum, respectively. Human embryonic kidney (HEK) 293 cells were a gift from Dr. J. R. Casey (Physiology, University of Alberta), who obtained them from the American Tissue Culture Collection (Bethesda, MD). HEK 293 cells were cultured in Dulbecco's modified Eagle's medium (DMEM) supplemented with 5% FBS and 5% calf serum. CCRF-CEM (lymphoblastic leukaemia) cells were obtained by Dr. C. E. Cass from Dr. W. T. Beck (University of Illinois, Chicago, IL) and were cultured in RPMI 1640 medium supplemented with 10% FBS.

Hamster Cell Lines: Chinese Hamster Ovary (CHO) K1 cells were a gift from Dr. Jean Vance (Medicine, University of Alberta) and were cultured in F-12 (Ham's) medium supplemented with 10% FBS. Baby hamster kidney (BHK) 21 cells were a gift from Dr. T. C. Hobman (Cell Biology, University of Alberta), who obtained them from the American Tissue Culture Collection (Bethesda, MD), and were cultured in DMEM supplemented with 10% FBS.

2 C. Nucleoside Transport Studies

Xenopus laevis Oocytes: The transport of 10 μM or 100 μM thymidine or 100 μM uridine into oocytes, injected with either water alone or water that contained RNA transcripts produced *in vitro* from transporter cDNAs (see Chapter 2 F. I), was measured at room temperature using established methods [208]. rCNT1 RNA was used as a positive control in these experiments since its activity in the *X. laevis* expression system was well characterized [121]. Oocytes were prepared in and obtained from the laboratory of Dr. James D. Young (Physiology, University of Alberta) and injections were performed by Dr. Sylvia Y. M. Yao (Physiology, University of Alberta). Transport was measured 3-5 days after oocyte injections. Oocytes were incubated in oocyte transport buffer (100 mM NaCl, 2 mM KCl, 1mM $CaCl_2$, 1 mM $MgCl_2$, 10 mM HEPES, pH 7.5) containing either 10 μM or 100 μM [^{3}H]-thymidine or 100 μM [^{3}H]-uridine (500, 000 cpm/400 μL) for 30 min at room temperature, after which the oocytes were washed three times with 1 mL ice-cold oocyte transport buffer and then lysed in 5.0% sodium dodecyl sulfate (SDS) at 37°C for 2 h in scintillation vials. Ecolite (ICN, Costa Mesa, CA) scintillation fluid (5 mL/vial) was added and the radioactive content of the oocytes was determined by scintillation counting (Beckman-Coulter, Palo Alto, CA).

HEK 293 and CCRF-CEM Cells: The transport of 10 μM [^{3}H]-uridine into proliferating HEK293 cells was measured at room temperature by the oil-stop method previously described [209] with some modifications. Briefly, HEK293 cells cultured as described above were trypsinized, washed by centrifugation (850 X *g*, 5 min, room temperature) in DMEM medium with serum, enumerated, centrifuged again and resuspended in sodium buffer (5 mM glucose, 20 mM, tris(hydroxymethyl)aminomethane (Tris)-HCl , 3 mM K_2HPO_4, 144 mM NaCl, 1.8 mM $CaCl_2$, 1 mM $MgCl_2{\cdot}6H_20$, pH 7.4) or N-methyl-D-glucammonium (NMG) buffer (5 mM glucose, 20 mM Tris-HCl, 3 mM K_2HPO_4, 120 mM NMG, 1.8 mM $CaCl_2$, 1 mM $MgCl_2{\cdot}6H_20$, pH 7.4). Transport assays were initiated by rapidly adding 1 x 10^6 cells in 100 μL transport buffer to microcentrifuge tubes that contained [^{3}H]-uridine in 100 μL transport buffer. At regular time intervals, transport was stopped by rapid addition of ice-cold 200-μL portions of sodium or NMG buffer containing 400 μM dilazep followed immediately by centrifugation (12, 000 X *g*, 2 min, room temperature) through 200 μL of transport oil (a mixture of 75% 550 silicon oil (Dow Chemical, ON) and 15% light paraffin oil; specific gravity, 1.03 g/mL). The transport buffer above the transport oil was removed by aspiration. Next, tubes were washed above the oil three times each with ddH_2O after which the transport oil was removed by aspiration. The pellet water volume was determined under identical conditions by incubating cells with [^{3}H]-H_2O for 45 s, followed by centrifugation and washing of tubes as described above. The extracellular volume of the pellet space was determined under identical conditions by incubating with [^{14}C]-sucrose for 10 s, followed by centrifugation and washing of tubes as described above. For all conditions, the cell pellets were solubilized with 0.5 mL 5% (v/v) Triton X-100 and transferred to scintillation vials where they were mixed with 5 mL Ecolite

scintillation fluid. The radioactive content of the pellets was determined by scintillation counting. The CEM uptake experiments were designed by M. A. Cabrita and were performed by Ms. Delores Mowles (Oncology, University of Alberta).

HeLa and BeWo Cells: The transport was measured at room temperature by determining the rates of uptake of 10 μM [^{3}H]-uridine by replicate adherent cultures (3 plates for each condition) of proliferating HeLa and BeWo cells [113] with some modifications. Briefly, HeLa and BeWo cells cultured as described above were trypsinized, enumerated, centrifuged again and resuspended in RPMI medium with serum. Cells (approximately 5 x 10^5) were plated onto 60-mm culture dishes 2 days before the transport experiments were performed. One day prior to performing the transport experiments, the medium was removed by aspiration and medium containing hydroxyurea (either 50, 100, 200 or 500 μM final concentration) was added to the HeLa and the BeWo cells. On the day of transport, each culture was processed individually. Medium was removed by aspiration and transport was commenced by addition of sodium buffer containing 10 μM [^{3}H]-uridine. At regular time intervals, transport was stopped by aspiration of the transport medium, followed immediately by immersion of the culture dishes in a large volume of ice-cold sodium buffer. The dishes were drained, and the cells were solubilized with 1.0 mL 5% (v/v) Triton X-100 and transferred to scintillation vials where they were mixed with 5 mL Ecolite scintillation fluid. The radioactive content of the cell lysates was determined by scintillation counting. The HeLa and BeWo uptake experiments were designed by M. A. Cabrita and were performed by Ms. Delores Mowles (Oncology, University of Alberta).

2 D. Plasmid Construction, Propagation and Preparation

General: The molecular biology techniques (polymerase chain reaction (PCR) amplification, cDNA cloning, cDNA library screening) used in this study were adopted from procedures described in Chapter 3 of Ausubel *et al.*, [210]. DNA primers were synthesized using Perkin Elmer/Applied Biosystems DNA synthesizers (Foster City, CA) and cyanoethyl chemistry. The identity of PCR products was confirmed by DNA sequencing using PRISM Dye Terminator chemistry (fluorescent-dideoxy cycle sequencing) with a Perkin Elmer/Applied Biosystems Model 373A DNA sequencer (Foster City, CA) at the DNA Core Facility, Department of Biochemistry, University of Alberta, or an automated Perkin Elmer/Applied Biosystems 310 Genetic Analyzer (Foster City, CA) at the Cross Cancer Institute (Department of Oncology, Division of Experimental Oncology). DNA sequencing results were analysed using MacVector (Oxford Molecular, Cambridge, England), EditView/AutoAssembler software (PE Biosytems) and/or the Wisconsin Package (Genetics Computer Group/Oxford Molecular, Madison, WI). The use of the ClustalW and WebPhylip programs to generate alignments and evolutionary trees, respectively, from the Canadian Bioinformatics Resource (http://www.cbr.nrc.ca) in this research is acknowledged. Plasmids were transformed into the *E. coli* strain TOP10F' or TOP10 (Invitrogen, San Diego, CA) by the heat-shock

method [210] and grown in Luria broth (1% (w/v) bacto-tryptone, 0.5% (w/v) bacto-yeast extract, 1% (w/v) NaCl, pH 7.0) with ampicillin (50 μg/mL) at 37°C in a shaker at 250 rpm overnight. Stocks of untransformed and transformed *E. coli* cultures (grown overnight) were stored (1:1) in *E. coli* freezing solution (65% glycerol, 0.1 M $MgSO_4$, 0.025 M Tris-Cl, pH 8.0) [210] at –70°C. Plasmid DNA was isolated using either the alkaline lysis method [210] or Qiagen DNA Mini, Midi or Maxi columns (Qiagen, Mississauga, ON) according to the manufacturer's protocols. Microbiological media were obtained from Difco/BD Diagnostic Systems (Sparks, MD). Restriction enzymes and T4 ligase were obtained from Gibco/BRL Life Technologies (Burlington, ON) unless otherwise noted. DNA was electrophoretically resolved on 1% (w/v) agarose or 1% (w/v) low melting point agarose (Gibco/BRL Life Technologies) in Tris/acetate/(ethylenediaminetetraacetic acid) EDTA electrophoresis buffer (40 mM Tris-acetate, 2 mM $Na_2EDTA{\cdot}2H_20$, pH 8.5) alongside *Hin*dIII-cut λ phage DNA or 1-kilobase DNA molecular weight markers (Gibco/BRL Technologies). *Taq* polymerase was obtained from either Gibco/BRL Life Technologies or Amersham-Pharmacia Biotech (Baie d'Urfé, PQ). *Vent* polymerase was obtained from New England BioLabs (Mississauga, ON). *Pwo* polymerase was obtained from Boerhinger Mannheim/Roche Molecular Biochemicals (Laval, PQ).

A list of the plasmids used for the work described in this thesis is presented in Table 2-1.

2 D. I. Plasmids used in Chapter 3

pcDMTPΔC: pcDMTPΔC was previously constructed by ligating the *Bam*HI-MTPΔC-*Xba*I fragment generated by PCR [156] into the pcDNA1-AMP mammalian expression vector (Invitrogen). MTPΔC lacks amino acid residues 198-233.

pcDMTPΔCΔ5'UTR: pcDMTPΔCΔ5'UTR was constructed by excising the 5' untranslated sequence of the MTPΔC cDNA using the *Bsp*EI (New England Biolabs, Mississauga, ON) and *Bam*H1 restriction enzymes. The ends were blunt-ended using the Klenow fragment of DNA polymerase I (Gibco/BRL Life Technologies) according to the manufacturer's instructions and religated. The expected orientation was confirmed using the restriction enzymes *Eco*RI and *Xba*I.

pcDMTPΔCKB: pcDMTPΔCKB was prepared by PCR using a *Taq/Vent* (1:100 ratio) polymerase mixture. The oligonucleotide primer MTPKB1 (5'-AACGAGGATCCCGAGGGCCACCATGGTGTC-3') was used to introduce a BamHI site and a Kozak box [211] (GCCACCATG) before the translational start site (underlined). The MTPΔCKB construct, obtained by amplification of pcDMTPΔC [156] using the oligonucleotides MTPKB1 and SP6 (5'-ATTTAGGTGACACTATAGAATAG-3'), was digested with *Bam*HI and *Xba*I and subsequently ligated into pcDNA1-AMP.

pSP64T/MTPΔC: pSP64T/MTPΔC was constructed in the following manner. MTPΔC was obtained from pcDMTPΔC by restriction digestion using *Xba*I and blunt-ended using the Klenow fragment of DNA polymerase I (Gibco/BRL Life Technologies) according to the manufacturer's instructions. *Bgl*II linkers (New England Biolabs) were ligated to the blunt-ended MTPΔC fragment and the subsequent product was digested with *Bgl*II. The *Bgl*II-MTPΔC fragment was ligated into the *Bgl*II site of the pSP64T vector [212, 213], which was obtained as a gift in the form of the pSPGT1 vector (pSP64T vector with glucose transporter 1 cDNA sequence) from Dr. Gwyn W. Gould (Division of Biochemistry and Molecular Biology, Institute of Biomedical and Life Sciences, University of Glasgow), by Dr. James D. Young (Physiology, University of Alberta). The expected orientation of the insert was confirmed using *Pvu*II.

pcDNA3/β-gal: pcDNA3/β-gal was constructed by ligating the *Hin*dIII-β-galactosidase cDNA-*Xho*I fragment from pcDNA1-AMP/β-gal into the pcDNA3 mammalian expression vector (Invitrogen).

pcDNA3/MTP3: pcDNA3/MTP3 was constructed by ligating the *Eco*RI-MTP3-*Not*I fragment from pcDMTP3 [156] into the pcDNA3 mammalian expression vector.

pcDNA3/HA-MTP: The hemagglutinin (HA)-tagged version of MTP (termed HA-MTP) was prepared by PCR using the *Pwo* polymerase. The oligonucleotide primer, MTPHA1 (5'-GGGATCCGCCACCATGTACCCATACGATGTTCCAGATTACGCTATGGTGTCCATGAGTTTCAAGCGG-3'), was used to introduce a *Bam*HI site (GGATCC), the nonapeptide (YPYDVPDYA) HA epitope tag [214, 215] and a consensus ribosomal binding domain (GCCACCATG) [211] at the 5' end of the MTP cDNA. The translational start site is underlined. A second oligonucleotide primer, MTP-P2 (5'-GCAGAGAATTCTCAGGCAGGCAGGTAAGGAGG-3'), was used to introduce an *Eco*RI site (GAATTC) after the stop codon on the 3' end of the MTP cDNA. The HA-MTP construct, obtained by amplification from pcDMTP3 [156] using the oligonucleotides MTPHA1 and MTP-P2, was digested with *Bam*HI and *Eco*RI and subsequently ligated into pcDNA3 to produce pcDNA3/HA-MTP.

These plasmids were designed and constructed by M. A. Cabrita except for the pcDNA3/β-gal plasmid which was constructed with the assistance of Ms. Delores Mowles (Oncology, University of Alberta).

2 D. II. Plasmids used in Chapter 4

pMALc2-es fusion: The primers ESF2 (5'-GGCGGATCCCGCCTGCAATTCTACCG-3'), containing a *Bam*HI site (underlined) on the 5' end, and ESF3 (5'-GAAAGCGTCGACTCAGATATTTTTCAGG-3'), containing a stop codon (in bold) followed by a *Sal*I site (underlined) on the 3' end, were used in a reaction catalysed by *Pwo* polymerase, in which pBluescript II KS(+)/c17.1 (contains hENT1 cDNA) [68] was used as the template. The resulting single PCR product was digested with *Bam*HI and *Sal*I and then ligated in-frame into the pMALc2 plasmid (New England BioLabs), a gift

from Dr. Haralabia Boleti (Institute Pasteur, Athens, Greece).

pGEX4T1-es fusion: The primers ESF4 (5'-GGCGGATCCCGCCTGGAATTCTACCG-3'), containing a *Bam*HI site (underlined) on the 5' end, and ESF3 (5'-GAAAGCGTCGAC**TCA**GATATTTTTCAGG-3'), containing a stop codon (in bold) followed by a *Sal*I site (underlined) on the 3' end, were used in a reaction catalysed by *Pwo* polymerase in which pBluescript II KS(+)/c17.1 (contains hENT1 cDNA) [68] was used as the template. The resulting single PCR product was digested with *Bam*HI and *Sal*I and then ligated in-frame into the pGEX-4T1 (Amersham-Pharmacia Biotech), a gift from Dr. Haralabia Boleti (Institute Pasteur, Athens, Greece).

pcDNA3/hENT1-HA: The HA-tagged version of hENT1 (termed hENT1-HA) was prepared by PCR amplification. The primers, ES2KPN (5'-ATGGTACCATGACAA CCAGTCACCAGCCT -3'), containing a *Kpn*I site (GGTACC) before the translational start site (underlined) at the 5' end, and ESHA1-C (5'-GGCGGTACC**TCA**AGCGTAATCTGGAACATCGTATGGGTACACAATTGCCC GGAACAGGAAGG-3'), containing the cDNA encoding the nonapeptide (YPYDVPDYA) HA epitope tag [214, 215], a stop codon (in bold) and a *Kpn*I site (GGTACC) on the 3' end, were used in an amplification reaction catalysed by the *Taq/Vent* polymerase mixture in which pBluescript II KS(+)/c17.1 (contains hENT1 cDNA) [68] was the template. The construct was digested with *Kpn*I and subsequently ligated into the pcDNA3 expression vector to produce pcDNA3/hENT1-HA. The expected orientation of the insert was confirmed using *Bst*XI.

pMALc2-ei fusion and pGEX4T1-ei fusion: The primers EIF1 (5'-GGGCGGATCCCTGCCTCACCTGAAGTTTG-3'), containing a *Bam*HI site (underlined) on the 5' end, and EIF2 (5'-GGAGTCGAC**TCA**GATCTTCTGGAAGACAG-3'), containing a stop codon (in bold) followed by a *Sal*I site (underlined) on the 3' end, were used in a reaction using *Pwo* polymerase, in which pHNPc7 (contains hENT2 cDNA) [78] was used as the template. The resulting single PCR product was digested with *Bam*HI and *Sal*I and then ligated in-frame into both the pMALc2 (New England BioLabs) and pGEX-4T1(Amersham-Pharmacia Biotech) plasmids.

pcDNA3/hENT2-VSV-G: The vesicular stomatitis virus glycoprotein (VSV-G)-tagged version of hENT2 (termed hENT2-VSV-G) was prepared by PCR. The primers, *Kpn*I5'ei (5'-CGGGGTACCGCCACCATGGCCCGAGGAG-3'), containing a *Kpn*I (GGTACC) site and a consensus ribosomal binding domain (GCCACCATG) [211] at the 5' end, and eiVSVG3' (5'-GCCGCTCGAGTCACTTCTCGAGACGATTCATTTCGATATCGGTGTAGAGCA GCGCCTTGAAGAGGAAGG-3'), containing the cDNA encoding the 11-amino acid (YTDIEMNRLGK) epitope [214, 216], a stop codon and a *Xho*I site (CTCGAG) after the stop codon on the 3' end were used in a reaction catalysed by *Pwo* polymerase in which pHNPc7 (contains hENT2 cDNA) [78] was the template. The construct was digested with *Kpn*I and *Xho*I and subsequently ligated into the pcDNA3 expression vector to produce pcDNA3/hENT2-VSV-G.

pcDNA3/hHNP36-VSV-G: The VSV-G-tagged version of HNP36 (termed HNP36-VSV-G) was prepared by PCR. The primers, HNP365'*Kpn*I (5'-CGGGGTACCATGGCCTCCGTC-3'), containing a *Kpn*I (GGTACC) site at the 5' end, and eiVSVG3', containing the cDNA encoding the 11-amino acid (YTDIEMNRLGK) epitope [214, 216], a stop codon and a *Xho*I site (CTCGAG) after the stop codon on the 3' end, were used in a reaction catalysed by *Pwo* polymerase in which pHNPc7 (contains hENT2 cDNA) [78] was the template. The construct was digested with *Kpn*I and *Xho*I and subsequently ligated into the pcDNA3 expression vector to produce pcDNA3/HNP36-VSV-G.

2 D. III. Plasmids used in Chapter 6

pcDNA3/hENT1: pcDNA3/hENT1 was constructed by ligating the *Xho*I-hENT1-*Xho*I fragment from pBluescript II KS(+)/c17.1 (contains the hENT1 cDNA) [68] into the pcDNA3 mammalian expression vector. The expected orientation of the insert was confirmed using *Hin*dIII.
pcDNA3/hENT2: pcDNA3/hENT2 was constructed by ligating the *Hin*dIII-hENT2-*Eco*RI fragment from pHNPc7 (contains the hENT2 cDNA) [78] into the pcDNA3 mammalian expression vector.
pcDNA3/hENT1as: pcDNA3/hENT1as was constructed by ligating the *Xho*I-hENT1-*Xho*I fragment from pBluescript II KS(+)/c17.1 (contains the hENT1 cDNA) [68] into the pcDNA3 mammalian expression vector. The expected orientation of the insert was confirmed using *Hin*dIII.
pcDNA3/hENT2as: pcDNA3/hENT2as was constructed by ligating the *Eco*RI-hENT2-*Xho*I fragment from pHNPc7 (contains the hENT2 cDNA) [78] into the pcDNA3 mammalian expression vector.

2 E. cDNA Library Screening and Southern Analysis

The human kidney 5'-STRETCH PLUS cDNA library (Clontech, Palo Alto, CA) cloned unidirectionally into pcDNA1 was screened by colony hybridization ([210] and manufacturer's directions). DNA was resolved electrophoretically on a 1% (w/v) agarose gel (Gibco/BRL Life Technologies) and transferred by upward capillary transfer [210] to nylon membranes. The DNA used to screen the library and probe the Southern blot was a fragment of the MTP cDNA (88-804 bp). The probe was made by PCR using the SP6 (5'-ATTTAGGTGACACTATAGAATAG-3') and DH10 (5'-CTCAGGAATCTTCACAGCCATT-3') primers and pcDMTP3 [156] as the template. The resulting amplicon was digested with *Hin*dIII to remove vector sequence and labelled with 5'-[α-^{32}P]-dCTP by random-priming labelling using the T7 Quick Prime Labelling Kit according to the manufacturer's instructions. The radioactively labelled probe was purified by either a custom- or commercially-made Sephadex G-50/Nick column. Southern blotting was performed [210] using the same probe as described above. Autoradiography was used to detect the positive colonies and hybridization complexes

on Southern blots [210] using X-OMAT AR film (Kodak, Toronto, ON) processed in a Kodak developer (Departments of Biochemistry and Oncology, University of Alberta). The Hybond-N nylon membranes, [α-^{32}P]-dCTP, T7 Quick Prime Labelling Kit, Sephadex–G50 and Nick columns used in the colony hybridization and blotting experiments were obtained from Amersham-Pharmacia Biotech.

2 F. RNA Synthesis, Isolation and Northern Analysis

Synthesis of RNA Transcripts: Plasmid DNA containing transporter cDNA was linearized by restriction digestion at a unique restriction site. Next, the sample was treated with Proteinase K (2 µL of 5 mg/mL stock; Gibco/BRL Life Technologies or Ambion (Austin, TX)) in the presence of 2 µL of 10% SDS and incubated at 50°C for 30 min. The DNA was extracted using phenol/chloroform (19:1 ratio) and the DNA was precipitated from the aqueous layer (2.5 volumes of 95% ethanol and 0.1 volume of 3 M sodium acetate). The resulting linearized, concentrated DNA was transcribed to RNA by using cap analog, $m^7G(5')ppp(5')G$ (Ambion or Gibco/BRL Life Technologies), in conjunction with the Ambion Megascript High Yield T7 or SP6 Transcription kits or the Ambion mMESSAGE mMACHINE High Yield Capped RNA kit alone, according to manufacturer's instructions. Newly synthesized RNA was electrophoretically resolved along with Novagen RNA size markers (Madison, WI) on a denaturing agarose/formaldehyde gel [210] in borate buffer. The resulting capped RNA transcripts are hereafter designated "cRNAs".

RNA Isolation: Total RNA was isolated from tissue culture cells using either the TRIzol reagent (Gibco/BRL Life Technologies) or the Qiagen RNeasy columns according to the manufacturer's instructions. mRNA was isolated from total RNA with an oligo(dT)-based FASTTrack mRNA isolation kit (Invitrogen), according to the manufacturer's instructions.

Northern Blotting: Total RNA (20 µg) was resolved electrophoretically on a denaturing 1.0% (w/v) agarose/formaldehyde gel, blotted onto Hybond-N membranes by upward capillary transfer [210] and probed with labelled cDNA fragments obtained by random-priming labelling and purified as described above. Membranes were incubated with labelled probes in ExpressHyb hybridization solution (Clontech) according to the manufacturer's instructions. Autoradiography was used to detect the hybridization complexes on the northern blot [210] using X-OMAT AR film (Kodak) processed in a Kodak developer (Departments of Biochemistry and Oncology, University of Alberta).

2 G. Reverse Transcription-PCR (RT-PCR), Taqman Quantitative RT-PCR and GeneScan RT-PCR

2 G. I. RT-PCR

RT-PCR was performed using the Gibco/BRL Life Technologies Superscript RT-PCR kit or the Pharmacia single tube RT-PCR kit according to the manufacturer's instructions. The hENT1-specific primers used were ESF3 and ESF4 (sequences are given in Chapter 2 D). The hENT2-specific primers used were EIF1and EIF2 (sequences are given in Chapter 2 D). For RT-PCR screening of stable transfectants, the following primer pairs were used: i) for **pcDNA3/hENT1** stably transfected cells: T7 (5'-AATACGACTCACTATAGGGA-3'), 15bRA (5'-GAAACACCAGCAGGAT-3'), ii) for **pcDNA3/hENT2**: T7 and hENT2-83' (5'-GGTGATAGGAGAAGAAG-3'), iii) for **pcDNA3/hENT1as**: T7 and 24aFE (5'-AAGGACAGCCGCTGGCT-3'), iv) for **pcDNA3/hENT2as**: T7 and KG27 (5'-CCCTCTTCATGCTGCCACGTGCC-3').

2 G. II. Taqman Real-time Quantitative RT-PCR

Total RNA was isolated from CEM cells, which were either untreated or treated with various concentrations of hydroxyurea, using RNeasy columns (Qiagen) as described in Chapter 2 F, and cDNA was produced using the Applied Biosystems Reverse Transcription kit according to manufacturer's instructions. The resulting cDNAs were used as templates in Taqman PCR [217-219] and the levels of various transporter mRNAs were quantitated by detection of the PCR products in real-time using the Taqman 7700 sequence detection system (Applied Biosystems). Experiments were performed in triplicate using purchased DNA primers and probes (Applied Biosystems) that were designed with Primer Express software (Applied Biosystems) to be specific for either hENT1 or hENT2. The primers and probe used to detect hENT1 were hENT1-F (5'-CACCAGCCTCAGGACAGATACAA-3'), hENT1-R (5'-GTGAAATACTGAGTGGCCGTCAT-3') and hENT1-Probe (5'-6-FAM-CCACGGGAGCAGCGTTCCCA-3'), where 6-FAM represents 6-carboxy-fluorescein. The primers and probe used to detect hENT2 were hENT2-F (5'-ATGAGAACGGGATTCCCAGTAG-3'), hENT2-R (5'-GCTCTGATTCCGGCTCCTT-3') and hENT2-Probe (5'-TET-CCACGGGAGCAGCGTTCCCA-3', where TET represents tetrachloro-6-carboxy-fluorescein. The primers- and probe-combinations used for the glyceraldehyde-3-phosphate dehydrogenase (GAPDH) and ribosomal 18S control reactions were purchased from Applied Biosystems as the Taqman RNA Control Reagent kit. These control mRNAs are assumed to change very little when cells are manipulated and are used to control for the amount of DNA (representing the original mRNA) produced in the RT-PCR reaction. The assumption is that all mRNAs will be reverse transcribed at the same efficiency.

The relative RNA amounts for each treated sample were determined in the following manner. A cycle threshold (C_t) value was obtained from the number of PCR cycles required to reach an arbitrary level of fluorescence. The level of fluorescence is arbitrary since the C_t value is always set empirically for each experimental run within the linear phase of the PCR reaction and is determined independently. RNA concentration differences were taken into account by subtracting the C_t values for either the GAPDH or

ribosomal 18S reactions from each sample C_t value resulting in a ΔC_t value (treated or untreated sample C_t - control C_t = ΔC_t). Next, mRNA levels in treated cells were normalized to the mRNA level in untreated cells by the following manipulation (untreated ΔC_t - treated ΔC_t = $\Delta\Delta C_t$). The data were expressed as $2^{-(\Delta\Delta C)}_t$ to normalize the data to the untreated sample (untreated ΔC_t - untreated ΔC_t = 0, therefore 2^0=1) as has been done previously [133]. The Taqman reactions were prepared by Dr. Kathryn Graham and Ms. Delores Mowles (Oncology, University of Alberta).

2 G. III. GeneScan RT-PCR

Total RNA was isolated from BeWo, CEM, HeLa and HEK293 cells using either RNeasy columns (Qiagen) or TRIzol (Gibco/Life Technologies BRL) as described in Chapter 2 F, and cDNA was produced using the Applied Biosystems Reverse Transcription kit according to manufacturer's instructions. The cDNAs were used as template in GeneScan PCR [220] to detect small quantities of transcripts. Experiments were performed in triplicate using one fluorescently-tagged primer (purchased from Applied Biosystems) and another untagged primer (made as described in Chapter 2 B). Both primers were designed with Primer Express software (Applied Biosystems). These primers were designed to distinguish between the hENT2 and the hHNP36 transcripts. The primers used to detect hENT1 and hHNP36 were: GShENT2-F (5'-6-FAM-TCCTGAGCACCAACCACACGGG-3') and GShENT2-R (5'-ATGGTGATGGAGAAGAAG-3'). RT-PCR samples along with GENESCAN-500 ROX standards (Applied Biosystems) were applied to the 310 Genetic Analyzer and then analysed using GeneScan software (Applied Biosystems).

2 H. Transfections

2 H. I. Transient Transfections

CHOK1 or BHK21 cells were plated at 2 x 10^5 cells/well in 6-well tissue culture dishes and grown at 37°C for 18-24 h until approximately 60-80% confluency was reached. DNA used in the transfections was prepared using Qiagen DNA columns (as described in Chapter 2 D). The cells were transfected with 1 μg of either pcDNA3/HA-MTP, pcDNA3/MTP3, pcDNA3/β-gal, pcDNA3/hENT1-HA, pcDNA3/hENT2-VSV-G, pcDNA3/hHNP36-VSV-G or pcDNA3 and either 5 μg of Lipofectamine (Gibco/BRL Life Technologies) or 6 μL of DOSPER (Boerhinger Mannheim/Roche Molecular Biochemicals) according to the manufacturer's instructions. Cells were incubated with the DNA/lipid complex for 6-24 h after which the medium was aspirated and replaced with fresh medium. Cells transfected for the mLAPTm4 experiments in Chapter 3 were sometimes treated with 40 μM chloroquine [221-223] for 1 h post-transfection before being processed. Transfection efficiencies were monitored by β-galactosidase-staining

CHOK1 or BHK21 cells that had been transiently transfected with pcDNA3/β-gal in parallel with the cells above [224]. Transfection efficiencies with lipofectamine ranged from 20-50%, while transfection efficiencies with DOSPER ranged from 20-80%.

2 H. II. Stable Transfections

HEK 293 cells were plated at 1 x 10^6 cells/well in 100-mm dishes and grown at 37°C for 18-24 h until approximately 60-80% confluency was reached. DNA used in the transfections was purified using Qiagen columns (Qiagen) according to the manufacturer's instructions. The cells were transfected with 1.5 μg of either pcDNA3/hENT1, pcDNA3/hENT2, pcDNA/hENT1as, pcDNA3/hENT2as or pcDNA3/β-gal (plasmids were linearized using the restriction enzyme *Pvu*I) and 6 μL of Fugene (Boehringer Mannheim/Roche Molecular Biochemicals) according to the manufacturer's instructions. Transfection efficiencies were monitored by staining the pcDNA3/β-gal-transfected cells for β-galactosidase expression [224]. Two days after transfection, cells were collected by trypsinization, combined and subcultured into six 100-mm dishes at various dilutions containing DMEM medium (supplemented as described in Chapter 2 B) and Geneticin (Gibco/BRL Life Technologies) (0.5 mg/mL). Approximately 10 days later, single colonies were selected [225] and subcultured in the presence of Geneticin until sufficient cell numbers were obtained for freezing cultures for storage and for protein and RNA isolation. The selected cultures were assessed by RT-PCR as described in Chapter 2 G I and immunoblot analysis of crude cell lysates as described in Chapter 2 T to verify that the transfection was successful. Functional characterization of the stable transfectants using nucleoside uptake assays was carried out as described in Chapter 2 C.

2 I. Generation of Anti-hENT2 Polyclonal and Monoclonal Antibodies

2 I. I. Production and Purification of Fusion Proteins

Polyclonal antibodies were raised as described against the hENT2 protein using a strategy previously employed by Boleti and co-workers [226]. The plasmids pMALc2-*ei* fusion (producing the maltose binding protein (MBP)-eif protein) and pGEX4T1-*ei* fusion (producing the glutathione S-transferase (GST)-eif protein) were transformed into the *E. coli* strain UT580 (*Δ(lac-pro), rK-, mK+, Tn10, supD, lac^{Iq}, F', traD, pro+, 'LacZ ΔM15*) [227] (a gift from Dr. Bernard Lemire (Biochemistry, University of Alberta)). MBP and GST proteins were purified according to the protocol of Boleti and co-workers [226] and the instructions provided by New England BioLabs and Amersham-Pharmacia Biotech, respectively.

Briefly, an overnight culture of UT580 cells transformed with either plasmids that contained an insert encoding the fusion protein or plasmids that lacked the insert was incubated at 37°C with shaking in Luria broth with ampicillin (50 μg/mL) overnight. In

the morning, cultures were diluted 1:100 in 1 L of Luria broth with ampicillin (50 μg/mL) and incubated for approximately 1 h at 37°C until the OD_{600} was equal to 0.4. Isopropyl-β-D-thiogalactoside was then added to a final concentration of 0.3 mM and the induced cells were allowed to grow at 30°C in a shaker at 250 rpm and harvested after 6 h by centrifugation (2, 000 X *g*, 30 min, 4°C).

For MBP fusion proteins, cells were resuspended in 1:20 volumes of column buffer (20 mM Tris-HCl, pH 7.4, 200 mM NaCl and 1 mM EDTA) plus COMPLETE protease inhibitors (1 tablet/50 mL of solution; Boerhinger Mannheim/Roche Molecular Biochemicals). For GST fusion proteins, cells were resuspended in 1:20 volumes of phosphate-buffered saline (PBS; 137 mM NaCl, 5.5 mM KCl, 1 mM Na_2HPO_4, 1 mM KH_2PO_4, pH7.4) plus COMPLETE protease inhibitors. Cells were frozen by rapid immersion in liquid nitrogen and stored at -70°C until needed, when cells were thawed and subsequently incubated with lysozyme (1 mg/mL; 1 h, 4°C). Cell lysates were then sonicated using a probe sonicator (Branson, Danbury, CT) at setting 6 for 6 min at 30 s intervals. Triton X-100 was added to cell lysates to a final concentration of 1%, and lysates were centrifuged (10, 000 X *g*, 30 min, 4°C). Lysates containing MBP fusions were passed through prepacked amylose resin columns (New England Biolabs, Mississauga, ON) and MBP fusions that bound to the resin were eluted with column buffer containing 10 mM maltose and COMPLETE protease inhibitors. Lysates containing GST proteins were passed through prepacked glutathione sepharose 4 fast-flow columns (Amersham Pharmacia Biotech), and GST proteins that bound to the resin were eluted with 50 mM Tris-HCl and 10 mM reduced glutathione, pH 8.0. Proteins were stored at 4°C and subsequently quantitated as described in Chapter 2 Q.

2 I. II. Injection of Antigens

Rabbits and mice were immunized with MBP-eif proteins or synthetic peptides according to a modified protocol of Harlow and Lane [228] and the standard operating procedures of the Cross Cancer Institute Vivarium. Animal procedures were performed under the approval of the Cross Cancer Institute Animal Care Committee. Gail Hipperson, Vivarium Manager, or vivarium personnel, under the supervision of Ms. Hipperson, performed the animal procedures. Virus antibody-free, barrier-maintained female New Zealand White rabbits were obtained from Charles River Laboratories (St. Constant, PQ). Female Balb/cCR//Alt barrier-maintained mice were obtained from the Health Sciences Laboratory Animal Services (Faculty of Medicine, University of Alberta). Animals were maintained in quarantine for acclimatization for at least one week before procedures were started. For rabbits and mice, blood (5-10 mL and 0.1–0.2 mL, respectively) was collected one week prior to immunization.

For intramuscular immunization of rabbits, the primary injection contained 50-100 μg of antigen along with Freund's complete adjuvant (Gibco/BRL Life Technologies) in a volume not larger than 0.4 mL. Blood (5-10 mL) was collected 10 days after the first injection. Next, three booster immunizations containing 100 μg of purified MBP-eif

protein and Freund's incomplete adjuvant (Gibco/BRL Life Technologies) were given 4-6 weeks apart from each other and blood was collected 10 days after each booster immunization. The animals were then euthanized by injection and a cardiac puncture was performed to collect blood. Blood samples were incubated at room temperature for 30 min, placed at 4°C overnight and then centrifuged (1, 000 X *g*, 30 min, 4°C) the following day. Sera were collected from each tube, distributed into 100-µL portions in 1.5-mL tubes and stored at –20°C.

For intraperitoneal immunization of mice, the primary injections contained 50 µg of antigen along with Freund's Complete Adjuvant (Gibco/BRL Life Technologies) in a volume not larger than 0.1 mL. At days 14 and 35, mice received intraperitoneal booster injections containing 50 µg of purified MBP-eif protein along with Freund's incomplete adjuvant (Gibco/BRL Life Technologies). Blood (0.1 mL) was collected from tail veins on days 24 and 45. On day 56 (or on the day of the final injection if a mouse was not used on day 56), 50 µg of purified MBP-eif protein was injected intravenously. Four days later, the mouse was euthanized and the spleen was aseptically removed. Blood samples were incubated at 37°C for 30 min, placed at 4°C overnight and then centrifuged (1, 000 X *g*, 30 min, 4°C) the following day. Sera were collected from each tube (1 tube/mouse) and stored at –20°C.

2 I. III. Production of Monoclonal Antibody-secreting Hybridomas

Hybridomas were generated by Mrs. Milada Selner using established protocols [228] as described previously for the generation of anti-hENT1 monoclonal antibodies, specifically clone 10D7G2 [115]. Hybridomas were generated by fusing splenocytes from the immunized mouse and cells of the non-secreting mouse myeloma cell line, P3/NSI/1-AG4-1 [229, 230] using polyethylene glycol (Sigma) as the fusing agent. The hybridomas were subcultured in 100 µM hypoxanthine, 0.4 µM aminopterin and 16 µM thymidine selection medium supplemented with 20% heat-inactivated FBS, 2 mM L-glutamine, 0.5 mM oxaloacetic acid, 1 mM sodium pyruvate in the presence of 50 µg/mL gentamycin in 96-well tissue culture plates. After positive clones were identified (see Chapter 2 I. IV below) and recloned by serial dilution into 96-well plates, the cultures were maintained in 100 µM hypoxanthine and 16 µM thymidine selection medium supplemented with the same compounds as described above. After a few weeks, the recloned hybridomas were transferred and expanded in hybridoma growth medium that consisted of RPMI supplemented with the same components as described above. To obtain serum-free antibody preparations, hybridomas were grown in serum-free growth medium (Gibco/BRL Life Technologies). Cultures were frozen in 10% DMSO and stored in liquid nitrogen.

2 I. IV. Antibody Screening

Rabbit and mouse test sera and supernatants from hybridomas were examined for antibody production by enzyme-linked immunosorbent assays (ELISA) where GST-eif protein (50 ng/well) was placed into Linbro EIA II (ICN) 96-well plates. IgG-gamma specific secondary antibodies conjugated to horseradish peroxidase (Jackson ImmunoResearch Laboratories, West Grove, PA) were used in conjunction with tetramethyl benzidene (Sigma) to give a blue end product that could be measured spectrophotometrically. The end product was detected at 650 nm using a Uvmax 96-well plate reader along with the SOFTmax software (both from Molecular Devices, Sunnyvale, CA). The isotype of the monoclonal antibodies was determined using a mouse monoclonal antibody isotyping kit (Sigma).

2 J. Immunoprecipitations

Immunoprecipitations were performed according to the protocol of Harlow and Lane [231]. Cells were lysed directly in 100-mm tissue culture dishes on ice with cold radio-immunoprecipiation assay (RIPA) buffer which consisted of 0.1% SDS, 0.5% sodium deoxycholate, 1% Nonidet P-40 (Calbiochem, San Diego, CA), 150 mM NaCl, and 50 mM Tris-HCl, pH 8.0 in the presence of 10% Mammalian Protease Inhibitors Cocktail (Sigma). The resulting lysates were transferred to 1.5-mL microcentrifuge tubes and centrifuged (13, 000 X *g*, 15 min, 4°C), and equal portions of the supernatants were transferred to fresh tubes. Antibodies (1 µL of antisera or 10 µL of hybridoma supernatant) were added and the resulting mixtures were incubated on a Nutator end-over-end rocker (Clay Adams, Becton Dickinson, Oakville, ON) overnight at 4°C. The next day, 100 µL of a 10% (v/v) suspension of Protein G (Amersham-Pharmacia Biotech) (v/v) in RIPA buffer was added to each tube and the tubes were incubated on the Nutator at 4°C for 1-3 h. The resulting precipitates were centrifuged (13, 000 X *g*, 1 min, 4°C) and supernatants were removed by careful aspiration. The Protein G pellets were washed 3 times with 1 mL of RIPA buffer. The immunoprecipated complexes were then dissociated by addition of loading buffer (10% glycerol, 2% SDS, 0.065 M Tris-HCl, 0.05% bromophenol blue and 1% beta-mercaptoethanol), heated at 65°C for 5 min and analysed by immunoblotting as described in Chapter 2 S.

2 K. Purification of Monoclonal Antibodies

Monoclonal antibodies were purified using custom-made Protein G columns (Amersham-Pharmacia Biotech) by the protocol of Harlow and Lane [228]. Briefly, supernatants from hybridoma cultures were placed on PBS-equilibrated Protein G columns and recirculated using a peristaltic pump at 4°C overnight. The columns were then washed with PBS (pH 7.4) until no more protein was detected (monitored by absorbance at 280 nm). Antibodies were eluted from the column using 100 mM glycine (pH 2.5) and were neutralized with 100 µL of 1 M Tris-HCl (pH 9.0) (that was already in 1.5-mL collection tubes) per 900 µL fraction eluted. The antibody-containing fractions

were identified by A_{280}. Antibodies were stored at 4°C and quantitated as described in Chapter 2 Q.

2 L. Labelling of anti-hENT1 Monoclonal Antibodies with Fluorophores

Purified monoclonal antibodies were labelled with Alexa 546 (in the case of anti-hENT1 monoclonal antibodies [115]) and Alexa 488 (in the case of anti-hENT2 monoclonal antibodies) according to the manufacturer's instructions (Molecular Probes, Eugene, OR). The anti-hENT1 (clone 10D7G2) monoclonal antibodies [115] were labelled by Ms. Geraldine Barron (Oncology, University of Alberta).

2 M. Immunofluorescence Microscopy

Cells were grown on 12-mm coverslips (5 coverslips per well) contained in 35-mm wells as described in Chapter 2 B. Cells were fixed and permeabilized with either i) 100% methanol at –20°C for 6 min or ii) 4% paraformaldehyde (w/v) and 10 µg/mL digitonin [232-234]. The cells (on coverslips) were washed twice with PBS and incubated at room temperature for 1 h or 4°C overnight with 2% goat serum (Sigma) in PBS (pH 7.4) to block non-specific binding of antibodies. The cells were then incubated with either one or more primary antibodies (see Table 2-2 for a list of antibodies used). For the anti-hENT2 polyclonal antibody competition experiments, the primary antibodies were incubated overnight at 4°C on a rocker with either GST or GST-eif proteins in 20-fold excess of the antibodies prior to incubations with the cells. Cells were washed with 1 mL PBS three times and (if necessary) incubated with fluorescently-labelled secondary antibodies that were diluted 1:250 (see Table 2-3 for a list of antibodies used). Antibodies were diluted in PBS and incubations were for 30 min at room temperature. In some instances, MitoTracker Red (Molecular Probes; final concentration 100 nM), a gift from Dr. Joan Turner (Oncology, University of Alberta), was used according to the manufacturer's instructions. Coverslips were mounted onto slides in 1 mg/mL paraphenylenediamine/90% glycerol in PBS. Cells were examined with an Axioskop immunofluorescence microscope (Carl Zeiss, Toronto, ON) or an LSM-510 laser-scanning confocal microscope (Carl Zeiss). Images were acquired either by photography (Axioskop) or by using the LSM-510 software and printed on a NP-1600 sublimation printer (Codonics, Middleburg Heights, OH). All of the immunofluorescence experiments shown were repeated at least three times.

2 N. Preparation of Crude and Plasma Membranes from Tissue Culture Cells

Crude membranes and plasma membranes were obtained using a modified version of the protocol of Johnstone and colleagues [235-237]. BeWo, HeLa or HEK293 cells (3×10^8 - 1×10^9 cells) were harvested by trypsinization, washed twice in ice-cold PBS (900 X *g*, 10 min, 4°C), enumerated and centrifuged again. The resulting cell pellets were resuspended in 10 volumes of swelling buffer (1 mM $ZnCl_2$, pH to 4.8-5.2 with 200 mM

succinic acid) on ice for 10 min and then lysed with a Polytron homogenizer (Brinkmann Instruments, Mississauga, ON). Unbroken cells and nuclei were removed by centrifugation (900 X *g*, 10 min, 4°C), the supernatants were collected, and the unbroken cell pellets were resuspended in swelling buffer and homogenized. This step was repeated. The supernatants were combined and membranes were collected by centrifugation (11, 000 X *g*, 30 min, 4°C). The resulting crude membrane preparations were resuspended in a small volume of cell homogenization buffer (5 mM K_2HP0_4, 0.5 mM $ZnCl_2$, pH 4.8-5.2) with 9.25% (w/v) sucrose, Dounce homogenized, brought to the original volume with 9.25% sucrose solution (approximately 40 mL) and centrifuged (11, 000 X *g*, 30 min, 4°C). The resulting membrane pellets were resuspended in 1.5 mL of 9.25% (w/v) sucrose solution and either frozen at –70°C or used to obtain plasma membranes.

For isolation of plasma membranes, the crude membranes were layered onto a discontinuous sucrose (w/v in cell homogenization buffer) gradient (4.5 mL of 45% sucrose, 6 mL of 30% sucrose, 10.5 mL of 25% sucrose, 10 mL of 20% sucrose and 3 mL of 15% sucrose) and centrifuged (3500 X *g*, 45 min, 4°C) in a swinging bucket rotor with no brake. Plasma membranes were collected between the 20% and 30% sucrose layers and diluted with 1.5 volumes of ice-cold water. 100 mM EDTA was added to a concentration of 0.66 mM to chelate the zinc and the resulting mixture was centrifuged (11, 000 X *g*, 60 min 4°C). Plasma membrane pellets were resuspended in freshly made 15% DMSO (v/v) and centrifuged (27, 000 X *g*, 20 min, 4°C). The resulting plasma membrane-enriched pellets were resuspended in a small volume (0.2-0.5 mL) of 15% DMSO and stored at –70°C.

2 O. Isolation of Human Erythrocyte Membranes

Human erythrocyte ghosts and membranes treated to remove peripheral membrane proteins were prepared by the protocol of Hanahan and Ekholm [238]. Briefly, human blood was collected in heparinized tubes from normal volunteers (under an approved protocol) by medical laboratory staff at the Cross Cancer Institute. The blood was centrifuged (1, 000 X *g*, 30 min, 4°C) and the plasma and buffy coats were removed by aspiration. The remaining erythrocytes were resuspended in ice-cold isotonic Tris buffer (172 mM, pH 7.6) and centrifuged (1, 000 X *g*, 30 min, 4°C). This wash was repeated two more times. Next, erythrocytes were resuspended in ice-cold hypotonic Tris buffer (11.1 mM, pH 7.6) and centrifuged (20, 000 X *g*, 30 min, 4°C). The supernatants were removed and the washing and centrifugation steps were repeated at least 4 more times until the membranes were colourless. Next, 1 volume of erythrocyte membranes was mixed with 7 volumes of alkaline extraction buffer (0.1 mM EDTA, pH 11.2) and incubated for 15 min, after which the mixtures was centrifuged (22, 000 X *g*, 25 min, 4°C) to remove peripheral membrane proteins. The supernatants were removed and discarded, and the membranes were then resuspended and washed with 50 mM Tris-HCl, pH 8.2 and centrifuged (22, 000 X *g*, 25 min, 4°C). This washing step was repeated once and the membranes were resuspended in a small volume of 50 mM Tris-HCl, pH 8.2 and

stored at 4°C in the presence of Mammalian Protease Inhibitors Cocktail (100 µL/1 mL) (Sigma).

2 P. Subcellular Fractionation

Rat livers were donated by Dr. William F. Colmers (Pharmacology, University of Alberta) or by Gail Hipperson (Vivarium, Cross Cancer Institute). Rats were euthanized by guillotine and livers were immediately removed. Golgi membranes were isolated according to the protocol of Morré and Morré [239] with minor modifications. Three freshly isolated rat livers were placed in ice-cold homogenization buffer (0.5 M sucrose, 50 mM Tris-HCl, pH 6.9, 5 mM β-mercaptoethanol, 1% dextran (Sigma, 500, 000 g/mol)), minced with scissors and homogenized with a Polytron homogenizer. Homogenates were filtered through cheesecloth, combined and centrifuged (5, 000 X *g*, 15 min, 4°C). Most of the resulting supernatant was discarded and the upper one-third of the pellet was resuspended in a small amount of supernatant. The resulting suspension was layered over a gradient solution (1.2 M sucrose in ddH_2O containing 3% dextran) and centrifuged (100, 000 X *g*, 30 min, 4°C). The Golgi-enriched membranes were removed from the top of the 1.2 M sucrose gradient, collected by centrifugation (5000 X *g*, 15 min, 4°C) and resuspended in homogenization buffer.

Preparation of lysosomes was performed according to the instructions accompanying the density gradient media, Nycodenz (Gibco/BRL Life Technologies) and Graham *et al.*, [240]. Freshly isolated rat livers were placed in ice-cold lysosome buffer A (0.25 M sucrose, 5 mM Tris-HCl, pH 7.6, 1 mM EDTA), cut into small pieces and homogenized with a Polytron homogenizer. Homogenates were filtered through cheesecloth, combined and centrifuged (1, 000 X *g*, 10 min, 4°C) and the resulting postnuclear supernatants were centrifuged (15, 000 X *g*, 10 min, 4°C). The resulting 15, 000*g* pellet was resuspended in 11 mL of lysosome buffer A and was then combined with an equal volume of 50% Nycodenz (w/v in buffer A). A discontinuous Nycodenz gradient was assembled (0.5 mL of 40% Nycodenz, 1.0 mL of 30% Nycodenz, 3.5 mL of 15, 000*g* pellet in 25% Nycodenz, 2.0 mL of 23% Nycodenz, 2.0 mL of 20% Nycodenz, 2.0 mL of 15% Nycodenz, 1.0 mL of 10% Nycodenz) and centrifuged (52, 000 X *g* for 1.5 h at 4°C) in a swinging bucket rotor. Lysosome-enriched membranes were collected from the 15/20% Nycodenz interface.

Mitochondria were isolated from rat livers using the procedure of Rickwood *et al.*, [241] and Fleischer *et al.*, [242]. Freshly isolated livers were placed in ice-cold liver homogenization buffer (0.3 M sucrose, 1 mM ethyleneglycol-bis(β-aminoethyl ether)N,N,N',N'-tetraacetic acid, 5 mM 3-(N-morpholino)-propane sulfonic acid, 5 mM potassium phosphate monobasic, 0.1% bovine serum albumin (BSA) (fatty acid free), 1 mM phenylmethylsulfonyl fluoride, pH 7.4) and rinsed with liver homogenization buffer to remove excess blood. The remainder of the procedure was carried out on ice. Livers were minced, washed with liver homogenization buffer, suspended in the same buffer (2 mL/g liver), and disrupted for 1 min using a Polytron homogenizer. The resulting

homogenate was strained through cheesecloth and centrifuged (1000 X *g*, 10 min, 4°C), the supernatant was decanted and centrifuged (10, 000 X *g*, 10 min, 4°C) and the supernatant from the latter centrifugation was discarded. The resulting crude mitochondrial pellet was separated from the pelleted contaminating erythrocytes by scraping it away from the erythrocytes using a glass rod and was then resuspended in liver homogenization buffer (35 mL). Centrifugation as described above was repeated until the erythrocytes were removed. The crude mitochondrial pellet was further purified using centrifugation (4, 000 X *g*, 40 min, 4°C) through a continuous sucrose gradient (0.75-1.75 M sucrose in 1 mM ethyleneglycol-bis(β-aminoethyl ether)N,N,N',N'-tetraacetic acid, 5 mM 3-(N-morpholino)-propane sulfonic acid, 5 mM potassium phosphate monobasic, 0.1% BSA, pH 7.4). The resulting fractions were collected, resuspended in liver homogenization buffer, centrifuged (10, 000 X *g*, 20 min, 4°C), and resuspended at concentrations of 10-20 mg/mL. The functionality of the mitochondria was determined by measurement of the respiratory control ratio using a Clarke-type oxygen electrode (Rank Brothers, Bottisham, United Kingdom) [241] courtesy of Dr. Bernard Lemire (Biochemistry, University of Alberta).

Portions of normal human liver were obtained (under an approved protocol) after surgical procedure performed by Dr. Norman Kneteman (Surgery, University of Alberta). Mitochondria from human livers were isolated as described in the paragraph above using the appropriate precautions for handling human tissues. Rat and human mitochondria were isolated by Dr. Karen M. King (Biochemistry and Medicine, University of Alberta).

Golgi and lysosomal preparations were either used immediately or frozen by immersion in liquid nitrogen and stored at –70°C. Mitochondria were resuspended in liver homogenization buffer containing 10 mg/mL BSA, frozen by immersion in liquid nitrogen and stored at –70°C. The various organelle-enriched preparations were tested for β-galactosidase (lysosome-specific enzyme) and succinate *p*-iodonitrotetrazolium violet (INT) reductase (mitochondria-specific enzyme) as described in Graham *et al.*, [240] and for galactosyl transferase (Golgi-specific enzyme) as described in Bergeron *et al.*, [243].

2 Q. Protein Determination

Protein concentrations were determined by either the bicinchoninic acid assay (Sigma) [244] (for samples in Chapter 3) or by the Bradford assay using the BioRad Reagent (Bio-Rad Technologies, Mississauga, ON) (for all subsequent chapters) [245] according to the manufacturers' instructions. Assays were performed in 96-well plates and the absorbance of samples for both methods was measured at 600 nm using a UVmax 96-well plate reader along with the SOFTmax software (both from Molecular Devices). The protein concentrations of test samples were determined from a standard curve using BSA as the protein standard.

2 R. SDS-Polyacrylamide Gel Electrophoresis (SDS-PAGE) Analysis and Immunoblotting

Cells plated in 35-mm wells as described in Chapter 2 B were harvested by trypsinization and collected by centrifugation. Cells were lysed in the tissue culture dishes in 100 µL of sample loading buffer (50 mM Tris-HCl, pH 6.8, 100 mM dithiothreitol (Calbiochem), 2% SDS, 0.1% bromophenol blue, 10% glycerol) [246]. The DNA in the samples was sheared using a 1-mL syringe with a 22-gauge needle. Cell lysates were collected by centrifugation (15, 800 X *g*, 3 min, 24°C) in the absence of protease inhibitors. Protein samples from other sources (*e.g.*, cell membranes and rat liver samples) were quantitated and mixed with an equal volume of 2X sample loading buffer [246].

Membrane protein samples were heated at 65°C for 5 min, and soluble protein samples were boiled for 5 min; both sample types were centrifuged (15, 800 X *g*, 1 min, 24°C). Membrane protein samples were not boiled to prevent aggregation of the sample. The resulting supernatants were subjected to electrophoresis on 12% SDS-polyacrylamide gels [210, 247] along with prestained broad-range (~6-175 kDa) protein markers (New England Biolabs, Mississauga, ON, Canada) or low range (~20-120 kDa) protein markers (BioRad). If SDS-PAGE gels were not used for immunoblot analysis (see below), they were incubated with Coomassie Blue stain [210] for 0.5-1.0 h and then incubated with destain (10% acetic acid/30% methanol) overnight at room temperature.

Proteins were electroblotted (400 mA, 1 h; Tyler Electronics, Edmonton, AB or Owl Scientific, Portsmouth, NH) onto polyvinylidene fluoride membranes (Immobilon-P, Millipore, Bedford, MA) in the presence of cold semi-dry blotting solution (10% methanol, 100 mM glycine, 10 mM Tris-HCl). Membranes were incubated overnight at 4°C, first with 5% skim milk powder (Carnation, Nestlé Canada, Toronto, ON) in TTBS (Tween-20, Tris-Buffered Saline; 0.2% Tween-20, 0.137 mM NaCl, 20 mM Tris-HCl, pH 7.5), and then for 12-18 h with 5% skim milk powder in TTBS that also contained primary antibodies. The membranes were then washed three times with TTBS and incubated for 2 h at room temperature with the appropriate secondary antibodies conjugated to horseradish peroxidase, diluted 1:10, 000 (see Table 2-3). Membranes were washed with TTBS three times and visualized using the enhanced chemiluminescence (ECL) reagents (Amersham-Pharmacia Biotech) according to the manufacturer's instructions. Membranes were stripped and reprobed according to the instructions for use with the ECL reagents. Fuji RX film was obtained from Fuji Medical Systems (Stamford, CT) and developed in a Kodak developer.

2 S. Flow Cytometry Experiments

All samples were analysed on a FACSort flow cytometer (Becton Dickinson). A minimum sample size of 10, 000 cells was used for each reading. Forward angle and side-scatter signals were used for cell gating.

2 S. I. Flow Cytometric Analysis using Anti-hENT1 Antibodies

CEM cells were enumerated and processed as follows. Cells were washed twice with 2 mL of PBS (pH 7.4), permeabilized with 0.5% saponin in PBS on ice for 5 min, centrifuged (800 X *g*, 8 min, 4°C) and washed twice with 4 mL of PBS. Cells were resuspended in PBS (2 x 10^6 cells/tube) and incubated with primary antibodies for 45 min at 4°C after which they were washed with 4 mL of PBS and incubated with the appropriate secondary antibodies (see Table 2-3) diluted 1:250 in PBS for 30 min at 4°C. Tubes were washed twice with 2 mL of PBS and resuspended cells were fixed with 0.1% formaldehyde. Cells were then placed at 4°C and wrapped in foil until the following day for analysis with the FACSort.

2 S. II. Flow Cytometric Analysis using 5-(SAENTA-x_8)-fluorescein

CEM cells (5 x 10^6/tube) were resuspended in SAENTA buffer (140 mM NaCl, 5 mM KCl, 10 mM HEPES, pH 7.4, 0.1% glucose and 0.1% BSA) [248, 249] and then incubated for 30 min at room temperature with 20 nM 5-(SAENTA-x_8)-fluorescein (from a 50 μM stock) in the dark in the presence or absence of 6 μM NBMPR as described elsewhere [249, 250]. Cells were then analysed using the FACSort.

2 T. [^{3}H(G)]-NBMPR-Binding Experiments

CCRF-CEM cells were cultured as described in Chapter 2 B. [^{3}H]-NBMPR-binding experiments were performed in triplicate by a modified version of a previously described filtration assay [7, 251, 252]. Cells were centrifuged (1, 000 X *g*, 10 min, 24°C) and resuspended in 50 mL of binding buffer (10 mM Tris-HCl, 100 mM KCl, 0.1 mM $MgCl_2 \cdot 6H_20$, 0.1 mM $CaCl_2 \cdot 2H_20$, pH 7.4) twice. Cells were enumerated and the cell concentration was adjusted to 1 x 10^7 cells/mL. The cell suspensions (100 μL/15 x 85 mm borosilicate tube) were then incubated with 12 different concentrations (0.24, 0.48, 0.75, 1.50, 2.25, 3.00, 4.50, 6.00 7.50, 12.00, 18.00, 24.00 nM) of [^{3}H]-NBMPR in the presence (to determine non-specific binding) or absence (to determine total binding) of 10 μM unlabelled NBMPR at room temperature for 50 min. Ice-cold binding buffer (4 mL/tube) was added to the tubes and the resulting mixtures were poured onto GF/B glass microfibre filters (Whatman) in a vacuum manifold (Millipore). The filters were then washed twice with 4 mL of ice-cold binding buffer for each filter; the first wash was a 4-mL rinse of the corresponding glass tube. Filters were placed in scintillation vials to which 10 mL of Ecolite (ICN) scintillation fluid was added. The same volume of [^{3}H]-NBMPR that was used for each condition described was added to a scintillation vial with 10 mL Ecolite scintillation fluid to determine the concentration of [^{3}H]-NBMPR for each condition. Vials were shaken gently at room temperature overnight to ensure proper mixing of the radioactivity with the scintillation fluid and counted in a scintillation counter

(Beckman-Coulter). The amount of specifically-bound [^{3}H]-NBMPR was calculated as the difference between the amount of [^{3}H]-NBMPR that bound in the presence of 10 μM non-radioactive NBMPR and the amount that bound in its absence. The binding isotherms (calculated using a non-linear one-site binding equation) and the Scatchard analyses were calculated using the GraphPad Prism 3.0 software (San Diego, CA).

Table 2-1. Description of Plasmids used in this Study

Plasmid	Insert Name	Product of Insert	Application	Used in Chapter
pcDMTPΔC [156]	MTPΔC	MTP lacking residues 198-233	Making cRNA for oocyte injections	3
pcDMTPΔCΔ5'UTR	MTPΔCΔ5'UTR	MTP lacking residues 198-233	Making cRNA for oocyte injections	3
pcDMTPΔCKB	MTPΔCKB	MTP lacking residues 198-233	Making cRNA for oocyte injections	3
pSP64T/MTPΔC	MTPΔC	MTP lacking residues 198-233	Making cRNA for oocyte injections	3
pcDNA3/β-gal	β-gal	β-galactosidase	Transient and stable transfections	3/4/6
pcDNA3/MTP3	MTP3	MTP	Transient transfections	3
pcDNA3/HA-MTP	HA-MTP	HA-tagged MTP	Transient transfections	3
pGEX4T1-*es* fusion	*es* fusion	Residues 228-289 of hENT1	Recombinant protein production	4
pMALc2-*es* fusion	*es* fusion	Residues 228-289 of hENT1	Recombinant protein production	4
pGEX4T1-*ei* fusion	*ei* fusion	Residues 213-290 of hENT2	Recombinant protein production	4
pMALc2-*ei* fusion	*ei* fusion	Residues 213-290 of	Recombinant protein	4

		hENT2	production	
pcDNA3/hENT1-HA	hENT1-HA	HA-tagged hENT1	Transient transfections	4
pcDNA3/hENT2-VSV-G	hENT2-VSVG	VSV-G-tagged hENT2	Transient transfections	4
pcDNA3/hHNP36-VSV-G	hHNP36-VSV-G	VSV-G-tagged hHNP36	Transient transfections	4
pcDNA3/hENT1	hENT1 sense	hENT1	Stable transfections	6
pcDNA3/hENT2	hENT2 sense	hENT2	Stable transfections	6
pcDNA3/hENT1as	hENT1 antisense	n/a[1]	Stable transfections	6
pcDNA3/hENT2as	hENT2 antisense	n/a[1]	Stable transfections	6

[1]n/a = not applicable

Table 2-2. Primary Antibodies used in this Study

Antibody	Species	Target (Antigen, if known)	Source	References
α-HA (3F10)	Rat	Hemagglutinin (YPYDVPDYA)	Roche Molecular Biochemical	[215]
α-VSV-G (P5D4)	Mouse	vesicular stomatitis virus glycoprotein (YTDIEMNRLGK)	Roche Molecular Biochemical	[216]
α-MTP	Rabbit	MTP (amino acids 5-19)	Dr. Douglas Hogue[1]	[156]
α-lgp110	Rabbit	Lysosomal glycoprotein 110	Drs. B. Reaves and P. Luzio[2]	[253]
α-α-Man II	Rabbit	α-mannosidase II	Dr. M. Farquhar[3]	[254]
α-M6PR	Rabbit	mannose-6-phosphate receptor	Dr. M. Farquhar[3]	[221, 222]
α-rab5A	Rabbit	rab5A	Santa Cruz Biotechnology	[255]
α-hENT1 polyclonal (041)	Rabbit	hENT1 (amino acids 254-270)	Cass Laboratory[4]	[115]
α-hENT1 monoclonal (10D7G2)	Mouse	hENT1 (amino acids 254-270)	Cass Laboratory[5]	
α-hENT2 polyclonal (9801)	Rabbit	hENT2 (amino acids 213-290)	This study, Cass Laboratory[6]	
α-hENT2 monoclonal (5C7B8, 10H11B10)	Mouse	hENT2 (amino acids 213-290)	This study, Cass Laboratory[7]	

[1]Antibodies developed by Dr. Douglas Hogue, Department of Biochemistry, Dalhousie University.

[2]A gift from Drs. Barbara Reaves and J.P. Luzio, University of Cambridge, England, United Kingdom.

[3]A gift from Dr. Marilyn Farquhar, Department of Cellular and Molecular Medicine Biology, University of San Diego, CA, USA.

[4]Antibodies raised against a synthetic peptide and developed by Dr. Lori L. Jennings, Cross Cancer Institute/Department of Oncology, University of Alberta.

[5]Antibodies raised against a synthetic peptide and developed by Dr. Lori L. Jennings and Mrs. Milada Selner, Cross Cancer Institute/Department of Oncology, University of Alberta.

[6]Antibodies raised against a fusion protein for this study developed by Miguel A. Cabrita, Cross Cancer Institute/Department of Biochemistry, University of Alberta.

[7]Antibodies raised against a fusion protein for this study developed by Miguel A. Cabrita and Mrs. Milada Selner, Cross Cancer Institute/Departments of Biochemistry and Oncology, University of Alberta.

Table 2-3. Secondary Antibodies used in this Study

Secondary Antibodies	Species	Target	Source
α-mouse FITC	goat	Mouse IgG	Jackson Immunoresearch Laboratories
α-mouse Alexa 488	goat	Mouse IgG	Molecular Probes
α-mouse Cy5	goat	Mouse IgG	Jackson Immunoresearch Laboratories
α-rabbit Cy5	donkey	Rabbit IgG	Jackson Immunoresearch Laboratories
α-rabbit FITC	goat	Rabbit IgG	Jackson Immunoresearch Laboratories
α- rat FITC	goat	Rat IgG	Jackson Immunoresearch Laboratories
α- rabbit rhodamine	donkey	Rabbit IgG	Jackson Immunoresearch Laboratories
α- rabbit Alexa 594	goat	Rabbit IgG	Molecular Probes
α- mouse HRP	goat	Mouse IgG	Jackson Immunoresearch Laboratories
α- rabbit HRP	goat	Rat IgG	Jackson Immunoresearch Laboratories
α- rat HRP	goat	Rabbit IgG	Jackson Immunoresearch Laboratories

Chapter 3

3. Localization of mLAPTm4 (MTP)[1]

[1]A version of this chapter has been published [166, 167].

3. Abstract

Mouse transporter protein (MTP), a small, highly conserved mammalian intracellular membrane protein with four putative transmembrane domains, has been implicated in the transport of nucleosides and other related molecules across intracellular membranes. In this study, the human version of the MTP cDNA was isolated from a kidney cDNA library. Different cDNA constructs encoding the truncated form of MTP were injected in *X. laevis* oocytes with the goal of improving production of the protein and thus enhancing transport activity. However, little or no thymidine or uridine uptake was observed with any of the cDNA constructs tested, suggesting that thymidine may not be the true biological substrate of MTP. Experiments were then undertaken to define the intracellular location of MTP in mammalian cells to assist in defining its biological function. Because native MTP was not detected by indirect immunofluorescence in cell types that expressed MTP mRNA, a HA-tagged version of MTP was produced in cultured BHK21 cells. The subcellular distribution of the recombinant, tagged protein was determined by confocal immunofluorescence microscopy using antibodies directed against the HA epitope and various organellar proteins. Antibodies directed against HA-MTP co-localized with antibodies against late endosomal and lysosomal proteins, but not with antibodies against either Golgi or early endosomal proteins. Analysis of subcellular fractions from rat liver by immunoblotting with antibodies directed against MTP demonstrated the presence of an MTP-like protein in Golgi- and lysosome-enriched membranes, but not in mitochondria. However, since no staining of Golgi was observed in cells transiently transfected with the HA-tagged MTP, the presence of rat MTP in the Golgi fraction of liver was probably due to newly synthesized MTP and/or contaminating endosomes in the Golgi fraction. These results indicated that MTP resides in late endosomes and lysosomes, a finding that is consistent with a role for MTP in the movement of small molecules across endosomal and lysosomal membranes. MTP and the human orthologue share a number of characteristics with other lysosome-associated proteins and consequently have been redesignated murine and human lysosome-associated protein transmembrane 4 (LAPTm4), respectively.

3 A. Introduction

A novel protein with nucleoside transport activity was identified by the ability of a partial cDNA isolated from mouse leukaemia L1210 cells to complement a thymidine transport deficiency in the yeast, *S. cerevisiae* [156]. The full-length cDNA (GenBank accession number U34259) encodes a small hydrophobic protein with 233 amino acids and four predicted transmembrane domains that was initially named mouse transporter MTP [156], and is now known as murine lysosome-associated protein transmembrane 4 (mLAPTm4) [166]. mLAPTm4 is highly conserved, with 97% identity at the amino acid level to a human protein of unknown function, HUMORF13 (GenBank accession number D14696) [256, 257], suggesting an essential role in cells.

Recombinant mLAPTm4 localized to the plasma membrane and exhibited low levels of nucleoside transport activity when produced in truncated form, but not when produced in full-length form, in oocytes of *X. laevis* [156]. The functional results, together with the demonstration of mLAPTm4 in intracellular membranes of liver subcellular fractions, led to the suggestion by Hogue *et al.*, [156] that mLAPTm4 plays a role in the transport of nucleosides and/or related molecules across intracellular membranes. mLAPTm4 is structurally unrelated to the ENT and CNT protein families, whose molecular identities have been determined by isolation and functional characterization of cDNAs in several heterologous expression systems (reviewed in [1, 4, 76]).

Full-length mLAPTm4 was produced in drug-sensitive strains of *S. cerevisiae* and found to mediate a multidrug resistance phenotype [168]. Yeast cells harbouring mLAPTm4 exhibited a collateral i) increased resistance towards anthracyclines, carboxylic and neutral ionophores, dihydropyrines and steroids and ii) increased sensitivity towards hydrophobic cations (e.g., ethidium, tetraphenylphosphonium), 5-fluorouracil, 5-fluorouridine, and trifluoperazine. mLAPTm4 was also shown to alter the subcellular distribution of steroids in yeast. These observations indicated that mLAPTm4-mediated alterations in subcellular drug distribution lead to a multidrug resistance phenotype in yeast and suggested that a similar function is carried out by endogenous LAPTm4 in mammalian cells [168].

Multidrug resistance can arise in mammalian cells by several different types of biochemical changes that alter sensitivity to cytotoxic drugs [258]. One of the most well-studied and widely accepted mechanisms for the generation of multidrug resistance is the overproduction of the ATP-dependent drug pump, p-glycoprotein [259], which works primarily by mediating the efflux of drugs from cells. Many forms of multidrug resistance, including p-glycoprotein-dependent multidrug resistance, have been associated with the sequestration of drugs into subcellular compartments [260-271]. Some studies have demonstrated that drug-resistant cell lines differ from parental cell lines by accumulating drugs in different subcellular compartments [262, 264-270]. In some cases, lysosomes have been implicated in the subcellular compartmentalization of the drugs [264-268, 270], whereas in other cases, the vesicular compartment has not been clearly defined [262, 269]. Compartmentalization of cationic amphiphilic drugs into acidic

organelles was originally thought to be only due to the action of proton pumps [272], wherein the transmembrane proton gradient leads to the intra-organelle trapping of protonated drug. However, recent evidence for the presence of active drug transport processes in lysosomes [273] and the involvement of mLAPTm4 in the subcellular redistribution of drugs in yeast [168] suggest that protein-mediated processes are responsible for the accumulation of certain drugs within acidic vesicles.

The goals of the work described in this chapter were to:

1) isolate the cDNA encoding the human orthologue of mLAPTm4,

2) improve the level of activity of truncated mLAPTm4 in X. laevis oocytes, and

3) define the intracellular location of transfected mLAPTm4 in mammalian cells.

Goal 1: Approach. Searches in the GenBank database revealed the existence of a human orthologue of mLAPTm4, the HUMORF13 protein [256, 257]. HUMORF13 mRNA was shown to be distributed widely amongst human tissues [256, 257]. To confirm its existence and to see if it exhibited characteristics similar to mLAPTm4, a human cDNA library was screened to obtain the human orthologue of mLATPm4.

Goal 2: Approach. In a previous study [156], low levels of thymidine uptake activity were observed in *X. laevis* oocytes injected with *in vitro*-transcribed RNAs encoding a truncated form of mLAPTm4. A possible explanation for low protein levels was inefficient translation of the injected mLAPTm4 transcripts. The truncated mLATPm4 construct was modified in three different ways in attempts to improve efficiency of translation: i) the 5' untranslated region of the cDNA was removed by restriction enzyme digestion, ii) a Kozak box [211] was added by PCR to increase the efficiency of initiation of translation, and iii) the truncated mLAPTm4 cDNA was inserted into the pSP64T vector that contains the 5' and 3' flanking regions of the β-globin gene of *X. laevis* [212, 213]. These constructs were transcribed *in vitro* and the resulting transcripts were injected into *X. laevis* oocytes.

Goal 3: Approach. The observation that an mLAPTm4-like protein was detected by immunoblot analysis [156] in subcellular membrane fractions of rat liver enriched in Golgi membranes led to the conclusion that LAPTm4 normally resides in intracellular membranes. However, endogenous mLAPTm4 is a low-abundance protein and could not be detected in the cell line (mouse leukaemia L1210) from which its cDNA was initially obtained by either indirect immunofluorescence of cells or immunoblot analysis of solubilized membranes with mLAPTm4-specific antibodies. To circumvent this difficulty, baby hamster kidney cells (BHK21) were transfected with cDNA encoding an epitope-tagged version of mLAPTm4 and then examined for localization by double-label indirect immunofluorescence using anti-tag antibodies and antibodies to various organellar proteins. The transfected cells were also treated with chloroquine, a lysosomotropic reagent that causes the formation of enlarged endosomal and lysosomal vesicles, to determine if acidic vesicles were associated with anti-mLAPTm4 staining. In addition, subcellular fractions obtained from rat liver were examined for the presence of native LAPTm4 by immunoblotting with anti-mLAPTm4 antibodies.

Summary: The human orthologue of mLAPTm4 was isolated and found to be identical to the HUMORF13 cDNA that was deposited in GenBank. The modifications

to the 5'UTR of mLAPTm4 did not improve nucleoside uptake. Using double label immunofluorescence, epitope-tagged mLAPTm4 was co-localized to lysosomes in cells that had been transiently transfected with the mLAPTm4 cDNA. Also, the highest levels of rat LAPTm4 (rLAPTm4) were found in late endosomes and lysosomes, indicating that rLAPTm4 is a resident protein of lysosomes, thereby substantiating the recent suggestion [168] that mLAPTm4 plays a role in the subcellular distribution of drugs associated with multidrug resistance.

3 B. Results

3 B. I. Isolation of the Human Orthologue of mLAPTm4 from a Human Kidney cDNA Library

The reagents (*e.g.*, antibodies and plasmids) used in this study were all named prior to the name change of MTP to LAPTm4. Thus, while LAPTm4 terminology is used in the text to describe the protein, the original names of the reagents, which were based on the MTP terminology, have been retained.

A predicted human protein with 97% sequence identity to mLAPTm4 was found in GenBank, and was, therefore, assumed to be the human orthologue of mLAPTm4. The HUMORF13 cDNA was isolated from cells of a human acute myelogenous leukaemia cell line (KG1) and the HUMORF13 gene was found on chromosome number 2 [256, 257]. The HUMORF13 mRNA (also known as clone KIAA0108) was found in RNA from all tissues that were probed in northern blots (heart, brain, placenta, lung, liver, skeletal muscle, kidney, pancreas, spleen, thymus, prostate, testis, ovary, small intestine, colon, peripheral blood leukocytes) as well as in RNA from cultured HeLa cells [256, 257].

In this study, a human kidney cDNA library (Clontech) was screened using a fragment of the mLAPTm4 cDNA (88-804 bp) as a probe and the colony hybridization method described in Chapter 2 E. Seven potential clones were obtained and the positive inserts were confirmed by Southern blot analysis (Figure 3-1), which demonstrated that at least 3 of the 7 clones were positive. Plasmids containing the mLAPTm4 sequence were used as the positive controls for the experiment. Clone 6.1 had been previously sequenced and was shown to be empty vector, so this plasmid was used as the negative control. The clone that gave the strongest signal (6.8) had an insert of approximately 1000 bases. The insert found in clone 6.8 was sequenced in its entirety and was comprised of 962 bases with an open reading frame starting at base 53 and ending with a stop codon (TGA) at 752 (Figure 3-2).

The human cDNA encodes a protein of 233 amino acids with 4 putative transmembrane domains (Figure 3-3) and is 100% identical to the HUMORF13 cDNA that was found in GenBank. The human protein is 97% similar and 97% identical to mLAPTm4 and thus has been designated hLAPTm4 (Figure 3-4). Of the seven amino acid residues that differ between the human and mouse versions of LAPTm4, four are semi-conserved and occur at positions 5 (mT/hS), 9 (mS/hN), 171 (mV/hL) and 221 (mI/hM) and two are unconserved and occur in the N-terminus and C-terminus tails at positions 23 (mF/hC) and 206 (mT/hA), respectively. Two differences occur in the middle of the fourth putative transmembrane domain at positions 170 (mV/hA) and 171 (mV/hL). Three differences occur on the N-terminus and two differences occur on the C-terminus, possibly reflecting species differences that affect binding sites where other proteins may interact with LAPTm4 or the function of these proteins.

During the course of this study, two papers described the isolation of expressed sequence tags (ESTs) encoding fragments of LAPTm4 from rat and rabbit cells. The first paper described the downregulation of a series of ESTs in pheochromocytoma cells

induced to differentiate into sympathetic-like neurons by treatment with nerve growth factor [274]. Six rat ESTs exhibiting nearly 100% sequence identity with the HUMORF13 cDNA (and therefore also with the mLAPTm4 cDNA) were isolated [274] and two of these ESTs (105428 and 106134) correspond to the N-terminus of the rat protein. In the initial mLAPTm4 study [156], anti-mLAPTm4 antibodies were raised against an N-terminal peptide (amino acids 5-19) and were found to cross-react against the rat orthologue. The sequence identity of the rat ESTs with mLAPTm4 establishes the basis for the cross-species reactivity of the antibodies. The second paper describes the isolation of cDNAs obtained from highly abundant mRNAs in rabbit osteoclasts and one of the ESTs isolated in this study is almost 100% identical to the C-termini of the human, mouse and rat LATPm4 proteins [275]. The highly conserved nature of the ESTs from rat and rabbit are further proof that LAPTm4 must play a critical biological role.

The original intent of isolating the cDNA encoding the human version of LAPTm4 was to enable studies of the properties of the human protein in parallel with those of the mouse protein. However, since the functional studies with the mouse protein were not successful (see next section), no further work was done with the human cDNA.

3 B. II. Attempts to Improve Recombinant Truncated mLAPTm4 (MTPΔC) Protein Production in *X. laevis* Oocytes

A truncated version of mLAPTm4 protein (MTPΔC) was shown to have a low level of thymidine transport activity in *X. laevis* oocytes injected with the MTPΔC RNA [156]. One possible explanation for the low levels of activity previously observed was that the messenger RNA transcripts encoding the recombinant protein were not efficiently translated in oocytes.

Three strategies were employed to improve the efficiency of translation of the MTPΔC RNA, The first strategy involved removing the 5' untranslated region immediately upstream of the ATG start site to eliminate any sequences that were potentially interfering with the efficient translation of the protein. The second strategy involved adding a Kozak box (GCCACCATG) [211], which represents the consensus sequence for optimal translation initiation, immediately upstream to the start site. The third strategy involved cloning the MTPΔC cDNA into the pSP64T vector [212, 213]. This vector contains the 5' and 3' flanking regions of the β-globin gene from *X. laevis* and has been used to enhance translation of mRNA sequences that have their own translation initiation sequence [212, 213].

The three resulting constructs were transcribed *in vitro* and the resulting cRNAs were injected into *X. laevis* oocytes. Uptake of thymidine (and in one case uridine) was measured 3-5 days later. Several different incubation times were selected to allow for sufficient amount of the proteins to be produced. The control oocytes injected with transcripts encoding rCNT1 [121] demonstrated substantially greater uptake of the radiolabelled nucleoside when compared to the water-injected (control) oocytes. In contrast, the truncated mLAPTm4 transcript-injected oocytes demonstrated uptake levels

that were low and virtually identical to those of water-injected oocytes (Figure 3-5*A*, *B*, *E*, and *F*). Thus, little or no transport was detected in oocytes injected with the various cRNAs from these constructs. In addition, when uptake of 10 and 100 μM thymidine was measured in oocytes injected with MTPΔC cRNA, the accumulation of radioactivity was similar in cRNA-injected and water-injected oocytes, suggesting little, if any, transport activity was detected (Figure 3-5 *C* and *D*). Thus, modification of MTPΔC cRNAs did not improve the detection of transport activity in the *X. laevis* system. These results suggest that translation efficiency was not the explanation for the lack of transport activity of the injected transcripts.

A possible explanation for the lack of transport in the truncated mLAPTm4 transcript-injected oocytes is that the protein produced may not have been processed properly or was degraded before it could reach the plasma membrane of the oocytes. Protein production in truncated mLAPTm4 transcript-injected oocytes had been verified in the earlier study [156] using anti-mLAPTm4 sera. However, protein production and oocyte plasma membrane localization of the truncated mLAPTm4 proteins were not confirmed in this study due to scarcity of the anti-mLAPTm4 sera. Also, despite the truncation of the mLAPTm4 protein, the protein may not have been localized to the plasma membrane of the oocytes.

3 B. III. Production of Recombinant mLAPTm4 and HA-mLAPTm4 in BHK21 Cells by Transient Transfection

The biological role of mLAPTm4 is unknown and it was felt that determination of its subcellular localization would provide clues as to the function of this highly conserved protein. The LAPTm4 protein could not be detected in mouse L1210 leukaemia cells (the source of the cDNA library from which the mLAPTm4 cDNA was obtained) or in freshly isolated rat hepatocytes by either immunoblotting of membrane preparations or indirect immunofluorescence of cells [156]. Experiments were therefore undertaken with cells producing recombinant mLAPTm4 to identify its intracellular membrane location. Recombinant mLAPTm4 and an epitope-tagged version, HA-mLAPTm4, were overproduced by transient transfection in BHK21 cells with plasmids that contained the cDNA encoding either full length mLAPTm4 (pcDNA3/MTP3) or the HA-tagged version of mLAPTm4 (pcDNA3/HA-MTP) to determine whether these proteins could be visualized and thus determine their subcellular localization.

Lysates of solubilized membranes of transfected cells were analysed by immunoblotting with antibodies directed against a synthetic peptide derived from the N-terminus of the mLAPTm4 sequence [156] (Figure 3-6*A*) or against the HA epitope [215] (Figure 3-6*B*). The anti-mLAPTm4 antibodies recognized a protein of ~20-22 kDa in cells transfected with the mLAPTM4-encoding plasmid (pcDNA3/MTP3) and a protein with a slightly higher apparent molecular weight in cells transfected with the HA-mLAPTM4-encoding plasmid (pcDNA3/HA-MTP). The faint bands at ~ 17 kDa may have been due to degradation of the sample. The anti-HA antibodies, which did not

detect any proteins in cells transfected with the mLAPTM4-encoding plasmid (pcDNA3/MTP3), recognized proteins of ~21-23 kDa in cells transfected with the HA-mLAPTM4-encoding plasmid (pcDNA3/HA-MTP). The anti-mLAPTm4 and anti-HA antibodies did not detect any proteins in preparations from cells transfected with pcDNA3 alone. The failure of the anti-mLAPTm4 antibodies to detect material in the lysates suggested that either endogenous levels of native protein were too low or the antibodies against mLAPTm4 were not cross-reactive with hamster LAPTm4.

3 B. IV. Localization of Recombinant mLAPTm4 and HA-mLAPTm4 in Transiently Transfected BHK21 Cells

Immunofluorescence studies with antibodies against mLAPTm4 or HA-mLAPTm4 were undertaken to determine if the recombinant proteins produced in transiently transfected hamster cells could be visualized by fluorescence microscopy.

In the experiments of Figure 3-7, double-label indirect immunofluorescence experiments using anti-mLAPTm4 and anti-HA antibodies were carried out on cells transiently transfected as described in Chapter 2 H I. These experiments demonstrated that both mLAPTm4 and HA-mLAPTm4 were localized to vesicular structures concentrated in the perinuclear region (Figure 3-7*A*, *D*, *E*, *G* and *H*). As expected, HA-mLAPTm4-containing vesicles were detected by both anti-mLAPTm4 and anti-HA antibodies (Figure 3-7*A*, *D* and *G*). These studies also failed to detect native hamster LAPTm4 in BHK21 (Figure 3-7*F*), since vesicular staining was not observed in cells transfected with vector alone (Figure 3-7*C*, *F* and *I*). These observations suggested that the HA epitope tag did not affect the targeting of mLAPTm4, since the vesicles in both HA-mLAPTm4- and mLAPTm4-producing cells were similar in both size and location. Recombinant HA-mLAPTm4 and mLAPTm4 were only found in vesicular structures and were not detected at the plasma membrane.

At the time that these experiments were being performed, the majority of anti-organelle antibodies available were rabbit polyclonal antibodies. Since the anti-mLAPTM4 antibodies were also rabbit polyclonal antibodies, they could not be used in double-label indirect immunofluorescence experiments with the anti-organelle antibodies. Thus, to facilitate the use of rabbit anti-organelle antibodies for double-label indirect immunofluorescence, experiments were thereafter conducted with cells that produced the epitope-tagged recombinant protein, HA-mLAPTm4, since the anti-HA antibodies used to detect this protein were of a rat monoclonal origin.

3 B. V. Absence of Localization of HA-mLAPTm4 to the Golgi Compartment in Transiently Transfected Cells

The observation that the anti-mLATPm4 and the anti-HA antibodies labelled distinct perinuclear vesicles and not more crescent-shaped, elongated structures associated with Golgi staining [254] seemed to contradict the observation that mLAPTm4 was found in Golgi membranes [156]. To verify that the mLAPTm4-containing vesicles were not

part of other perinuclear membranes such as Golgi, cells transfected with either the HA-mLAPTM4-encoding plasmid (pcDNA3/HA-MTP) or the plasmid lacking an insert (pcDNA3) were subjected to double-labeling with anti-HA antibodies and antibodies raised against the Golgi oligosaccharide-processing enzyme, α-mannosidase II (α-ManII) [254]. The Golgi apparatus in cells transfected with either plasmid exhibited a normal appearance, being crescent-shaped and juxtanuclear (Figure 3-8*C* and *D*). The structures labelled with the anti-HA and the anti-α-ManII antibodies were clearly different and consequently there was no co-localization between these antibodies (Figure 3-8*A*, *C*, *D*, *E* and *F*). Thus, recombinant HA-mLAPTm4 was not detected in the Golgi apparatus by this technique.

3 B. VI. Localization of HA-mLAPTm4 to Late Endosomes in Transiently Transfected Cells

The experiments of Figures 3-9 and 3-10 were undertaken to determine if mLAPTm4 could be detected in early or late endosomes, respectively. Antibodies against the early endosomal marker, rab5A [255], and the late endosomal marker, cation-independent mannose-6-phosphate receptor (M6PR) [221, 222], were used with the anti-HA antibodies to examine, by double-indirect immunofluorescence, cells that had been transfected with either the HA-mLAPTM4-encoding plasmid (pcDNA3/HA-MTP) or the plasmid lacking an insert (pcDNA3). The rab5A protein is a member of the large GTP-binding family that is required for membrane fusion and regulates transport between the plasma membrane and early endosomes [255]. The cation-independent M6PR mediates the transport of soluble lysosomal enzymes from the *trans*-Golgi network to lysosomes and is concentrated in late endosomes/prelysosomes [221, 222]. The production of HA-mLAPTm4 did not modify the staining pattern of either anti-rab5A (Figure 3-9*C* and *D*) or anti-M6PR antibodies (Figure 3-10*C* and *D*). In cells transfected with pcDNA3/HA-MTP, the staining pattern of the anti-HA antibodies partially overlapped with that of the anti-M6PR antibodies (Figure 3-10*A*, *C* and *E*) but not with that of the anti-rab5A antibodies (Figure 3-9*A*, *C* and *E*). Thus, although recombinant HA-MTP could not be detected by immunofluorescence in early endosomes, it was present in late endosomes.

3 B. VII. Localization of HA-mLAPTm4 to Acidic Vesicles in Transiently Transfected Cells

Chloroquine is a lysosomotropic reagent that causes the formation of enlarged endosomal and lysosomal vesicles [221-223]. It prevents M6PR from recycling and thus M6PR accumulates in acidic vesicles. In the experiments of Figure 3-11, cells were transfected with either the HA-mLAPTM4-encoding plasmid (pcDNA3/HA-MTP) or the plasmid lacking an insert (pcDNA3) and subsequently treated with chloroquine (Figure 3-11). Antibodies against M6PR were used with the anti-HA antibodies to

examine, by double indirect immunofluorescence, cells that had been transfected. In the absence of chloroquine (Figure 3-11*B*, *C*), the punctate vesicular staining pattern of the anti-M6PR antibodies was identical in both types of transfected cells. In contrast, cells that were treated with chloroquine (Figure 3-11*A*) had larger endosomes than untreated cells (Figure 3-11*B*, *C*), evidently due to sequestering of the M6PR [221-223]. In cells transfected with the HA-mLAPTM4-encoding plasmid (pcDNA3/HA-MTP), the staining pattern of the anti-HA antibodies overlapped in most cells with that of the anti-M6PR antibodies, in both the chloroquine-treated (Figure 3-11*A*, *D*) and chloroquine-untreated (Figure 3-11*B*, *E*) cells. The co-localization of the anti-HA and anti-M6PR antibodies in most cells suggested that recombinant HA-mLAPTm4 was localized to vesicles that were of an acidic nature and thus part of the endosomal/lysosomal pathway [221-223].

3 B. VIII. Localization of HA-mLAPTm4 to Lysosomes in Transfected Cells

The experiments of Figure 3-12 were undertaken to determine if HA-mLAPTm4 was also present in lysosomes. Anti-lgp-110 [253] is an antibody that recognizes the type I lysosomal membrane glycoprotein 110 [276], which is also known as the lysosomal associated membrane protein 2 [277]. The anti-lgp110 antibodies recognized large vesicular structures in cells transfected with either plasmid (Figure 3-12*C* and *D*). In cells transfected with the HA-mLAPTM4-encoding plasmid (pcDNA3/HA-MTP), the anti-HA antibodies labelled many of the same large juxtanuclear vesicles as the anti-lgp-110 antibodies (Figure 3-8*A*, *C* and *E*). The anti-HA antibodies did not recognize any structures in cells transfected with the plasmid lacking an insert (pcDNA3) (Figure 3-12*B*).

Since the chloroquine experiments of Chapter 3 B. VII suggested the localization of HA-mLAPTm4 to the endosomal/lysosomal pathway, the chloroquine experiments were repeated to verify the acidic nature of the anti-lgp-110-labelled vesicles. In the transfected cells, the anti-lgp-110 antibodies labelled the same large juxtanuclear vesicles in both chloroquine-treated and -untreated cells (Figure 3-13*A*, *B*, *C*). The lysosomes were noticeably larger in the cells treated with chloroquine (Figure 3-13*A* and *B*). Co-localization of anti-lgp-110 and anti-HA antibodies was observed in cells expressing the HA-mLAPTM4-encoding plasmid (pcDNA3/HA-MTP) in both chloroquine-treated (Figure 3-13*A*, *D*) and -untreated (Figure 3-13*B*, *E*) cells. The anti-HA antibodies did not recognize any structures in cells transfected with empty vector (Figure 3-13*F*). These results demonstrated the presence of recombinant HA-mLAPTm4 protein in lysosomes.

3 B. IX. Identification of the Rat Orthologue of mLAPTm4 in Subcellular Fractions of Rat Liver

As was noted in Chapter 3 B. I, the anti-mLAPTm4 antibodies are cross-reactive against rat LAPTm4 (rLAPTm4) due to the high sequence identity of the rat protein with mLAPTm4 and hLAPTm4. Thus, subcellular fractions of rat liver were prepared using

established protocols and examined for the presence of rLAPTm4. The identities of the membrane fractions enriched for lysosomes, mitochondria and Golgi were verified by measurement of β-galactosidase, succinate INT reductase and galactosyl transferase activities, respectively (Table 3-1). Although, the lysosome-, mitochondria- and Golgi-enriched membrane fractions each exhibited high activity for the particular marker enzyme known to be associated with that organelle, they also exhibited low levels of activity of the other marker enzymes indicating some cross-contamination between the fractions.

The presence of rLAPTm4 in these fractions was determined by immunoblotting (Figure 3-14). Cell lysates from BHK21 cells that were transiently transfected with either pcDNA3/MTP3 or pcDNA3 were included as positive and negative controls for antibody reactivity, respectively. Proteins of ~20-22 kDa were observed in the Golgi- and lysosome-enriched membrane fractions, but not in the mitochondria-enriched membrane fraction. These results demonstrated the presence of the rat equivalent of mLAPTm4 in the Golgi- and lysosome-enriched membranes.

3 C. Discussion

The cDNA encoding the human orthologue of mLAPTm4 was isolated and the sequence (HUMORF13/hLAPTm4) that was initially deposited in GenBank was confirmed. Rat and rabbit ESTs that exhibit high sequence identity to mLAPTm4 have also been deposited in GenBank [274, 275]. More recently, two homologues of LAPTm4 have been deposited in GenBank, one human protein of 226 amino acids (named hLAPTm4beta; GenBank accession number AAK69595) which is 45% identical and 55% similar to hLAPTm4 and one mouse protein of 227 amino acids (named mLAPTm4beta; GenBank accession number AAK69596) which is 45% identical and 56% similar to mLAPTm4. The LAPTm4beta proteins are 92% identical to each other. Such high identity between the newly discovered LAPTm4beta proteins and the 97% identity between the original human and mouse LAPTm4 proteins suggests an important role for members of this protein family. Other highly conserved (95-97% identical) membrane transporter proteins include the sodium-dependent excitatory amino acid transporter 2, which is required for the reuptake of secreted amino acid neurotransmitters such as glutamate and aspartate in brain tissues [278], and the vesicular acetylcholine transporter, which loads synaptic vesicles with acetylcholine from the cytoplasm [279].

The evidence that mLAPTm4 has nucleoside transport activity is based on studies in heterologous expression systems in which thymidine uptake was observed with the truncated proteins, MTP1 and MTPΔC [156]. The truncated MTP1 protein lacked the first 83 amino acids of mLAPTm4 and allowed rescue of yeast in a thymidine complementation assay. As a result of the 83-amino acid deletion, MTP1 was missing the first transmembrane domain of mLAPTm4 and was probably inserted into the membrane improperly and therefore not targeted to the correct intracellular location. This could have resulted in the truncated protein being inserted into the yeast plasma membrane and allowing thymidine uptake into cells. Uptake of thymidine into oocytes

was not detected in this study despite various attempts to improve the efficiency of translation of the truncated protein. Four different versions of the truncated form of mLAPTm4 were injected into *X. laevis* oocytes, yet no activity was observed. These results suggest that mLAPTm4 cannot transport uridine or thymidine when produced recombinantly in this truncated form.

It was determined that mLAPTm4 resides in late endosomes and lysosomes by two independent approaches: localization of an epitope-tagged version of recombinant mLAPTm4 in intracellular membranes of transiently transfected cultured cells by indirect immunofluoresence and identification of a native mLAPTm4-like molecule by immunoblotting of subcellular fractions from rat liver. In the immunofluoresence experiments, recombinant HA-mLAPTm4 and mLAPTm4 were both found in large juxtanuclear vesicular structures, indicating that the epitope-tagged protein was targeted to the same intracellular location as the untagged protein. HA-mLAPTm4 was specifically shown to be present in acidic vesicles, which could be enlarged by treating transfected cells with chloroquine, notably the late endosomes and lysosomes, but not in the Golgi apparatus nor in early endosomes. Because both recombinant HA-mLAPTm4 and mLAPTm4 were produced at high levels in BHK21 cells, transient levels of these proteins are expected in late endosomes en route to lysosomes. In the subcellular fractionation experiments, rLAPTm4 was found in the Golgi- and lysosome-enriched preparations from rat liver. In both the earlier study [156] and this study, it is likely that the rat orthologue of mLAPTm4 was observed in Golgi-enriched fractions because such preparations are likely to contain late endosomes and the enriched fractions also contained lysosomal membranes. Also, some lysosomal membrane proteins can be localized to late endosomes en route to their final destination [280].

mLAPTm4 and hLAPTm4 (*i.e.*, HUMORF13 protein) share features with several mammalian proteins with related sequences that were identified in the GenBank database using the BLAST algorithm [281]. The five transmembrane domain lysosomal proteins, hLAPTm5 and mLAPTm5 (GenBank accession numbers U51240 and U51239, respectively) [282], the retinoic acid-induced murine and human hematopoietic E3 proteins (GenBank U29539 and U30498, respectively) [283], and the rat neuronal GCD-10 protein (GenBank AB046592) [284] are all homologous to each other and also have carboxy termini that contain the tyrosine-based motifs, YXXØ, where Y is tyrosine, X can be any amino acid and Ø is a bulky hydrophobic amino acid residue. The newly discovered LAPTm4beta proteins also contain this motif (see Figure 3-15 for an alignment of the mammalian LAPTmX family). This tyrosine-based motif has been implicated as an internalization and a lysosomal targeting signal [280, 285-289]. One of the tyrosine-based motifs that is present in all family members (Figure 3-15) is immediately downstream from the last putative transmembrane domain that is predicted to be facing the cytosol, an arrangement that resembles that of the tyrosine-based lysosomal targeting signal in Lamp1 [288]. The importance of the tyrosine-based motifs in the targeting of mLATPm4 to lysosomes has not been established.

An important lysosomal cystine transporter protein, cystinosin, was recently discovered and shown to require a similar tyrosine-based motif for its targeting to

lysosomes [290]. Mutations in cystinosin cause the autosomal recessive disease cystinosis, which results in the intra-lysosomal accumulation of cystine, leading to renal failure in the infantile/severe form or renal impairment or corneal cystine-crystal deposits in the less severe forms. The tyrosine-based motifs have also been shown to interact with the μ chains of adaptor proteins required for organellar targeting, in particular the adaptor proteins, AP-3, which mediates the targeting of many lysosomal proteins [291]. Lastly, all of the members of the LAPTm family possess a proline-rich PY motif (PPXY) on their C-termini [292]. This motif has been implicated in the regulation of degradation of other transporter proteins and is thought to be important in ubiquitination via the Nedd4 family of ubiquitin-protein ligases [293-296]. Preliminary experiments using GST-fusion proteins have shown that Nedd4 family members can bind mLAPTm4 *in vitro* (Douglas Hogue, Dalhousie University, personal communication).

Based upon the lysosomal localization of mLAPTm4, the four predicted transmembrane domains and the description of LAPTm5 proteins, the mouse and human proteins were redesignated mLAPTm4 and hLAPTm4, respectively. This nomenclature more accurately reflects characteristics of the proteins and allows for simplified cross-species naming.

There is no mLAPTm4 orthologue in the *S. cerevisiae* genomic database although sequences similar to LAPTm4 and LAPTm5 have been submitted to GenBank from other species, including *C. elegans* (GenBank accession number AAK69599), *B. mori* (GenBank accession number AAK69598) and *D. melanogaster* (GenBank accession numbers AAF59049 and AAF59050) with low homology to the LAPTmX family [281]. Also, ESTs with high homology have been identified in the zebrafish genome.

What is the physiological function of LAPTm4 family members? Lysosomes are responsible for turnover of intracellular macromolecules as well as extracellular material that enters cells through phagocytosis and endocytosis. Human lysosomes have several well-described transport systems that function to release breakdown products into the cytosol [297], at least one of which is specialized for transport of nucleosides [8]. The lysosomal nucleoside transport process, which was studied in lysosomes isolated from human fibroblasts, has a preference for purine nucleosides (*e.g.*, 2'-deoxyadenosine, inosine) over pyrimidine nucleosides (*e.g.*, uridine), exhibits lower affinities for nucleosides than the plasma membrane nucleoside-transport processes and is inhibited by the well known transport inhibitors, dipyridamole and nitrobenzylthioinosine. The LAPTm4 proteins are probably not responsible for the nucleoside transport activity in lysosomes. A more plausible candidate for this activity would be the recently isolated hENT3, since the protein has two potential dileucine lysosomal-targeting motifs on its putative N-terminus [75].

Some preliminary evidence also exists for possible modes of regulation of LAPTm4 proteins. Rat ESTs encoding rLAPTm4 are downregulated when pheochromcytoma cells are treated with nerve growth factor [274]. This observation suggests that more differentiated cell types may have lower amounts of LAPTm4 protein than less differentiated ones.

The study by Hogue [168] showed that production of recombinant full length mLAPTm4 in yeast confers increased resistance or sensitivity to a wide variety of drugs. Drug-sensitive yeast producing recombinant mLAPTm4 were found to have increased resistance to daunorubicin, doxorubicin, erythromycin, progesterone and rhodamine 123 and increased sensitivity to 5-fluorouracil, 5-fluorouridine and trifluoperazine. Several studies in mammalian cells have demonstrated drug accumulation in lysosomes [260, 263-268, 270, 272, 273, 298], probably due to a variety of mechanisms. The demonstration that mLAPTm4 is a resident protein of mammalian lysosomes, combined with its functional activity when produced in yeast, suggests that mLAPTm4 plays a role in sequestering structurally unrelated amphiphilic molecules in lysosomes by transporting these compounds into lysosomes. Drug compartmentalization and subsequent accumulation in lysosomes is an important determinant of the multidrug resistance phenotype [258, 260, 261, 264-268, 270, 271], however little is known about the resident transporter proteins of lysosomes that are responsible for this process. Identification of the physiological substrates of mLAPTm4 awaits development of a system in which the transport characteristics of the full length, functional protein can be studied in isolation from other transporters, for example, by functional reconstitution of recombinant mLAPTm4 in proteoliposomes or by expression in heterologous systems.

Figure 3-1. Southern Blot of Human Kidney Clones. Clones (6.1, 6.2., 6.4, 6.5, 6.6, 6.7, 6.8) were isolated from a tertiary screen of a human kidney cDNA library that was probed with a portion of the mLAPTm4 cDNA as described in Chapter 2 E. DNA was isolated from the clones and digested with the restriction endonuclease *Bst*XI. The positive controls were uncut pcDMTP3 and pcDMTP3 that was digested with the restriction endonucleases *Bam*HI and *Hin*dIII. Clone 6.1 was known to be negative for the insert by PCR analysis and restriction digest analysis. The DNA was separated on a 1% agarose gel and analysed by Southern analysis as described in Chapter 2 E.

Figure 3-1

Southern Blot of Human Kidney Clones

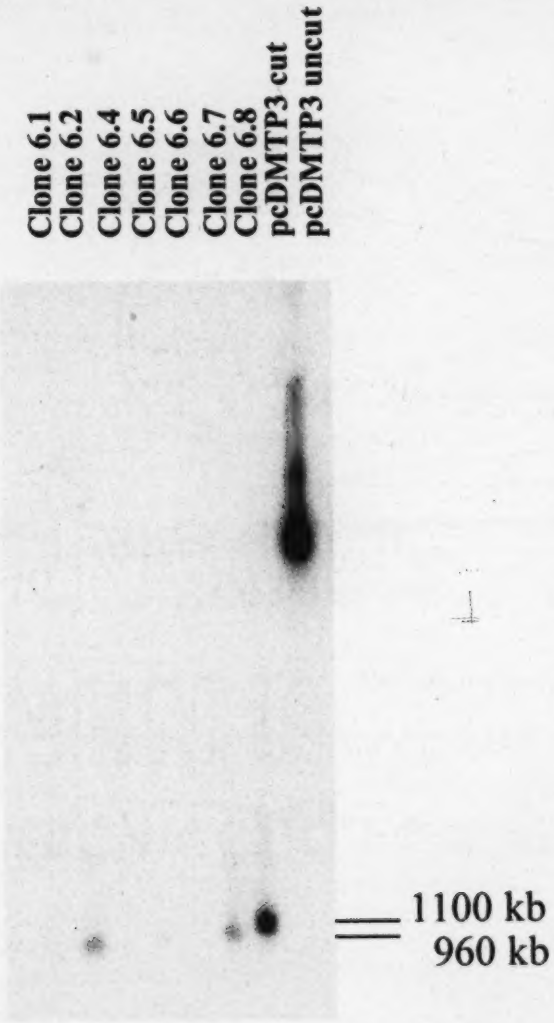

Figure 3-2. Human LAPTm4 cDNA Sequence. Clone 6.8 isolated from a hybridization screen of a human kidney cDNA library. The plasmid containing the clone was sequenced as described in Chapter 2 D. The open reading frame encoding hLAPTm4 is in bold and the stop codon is underlined.

Figure 3-2. Human LAPTm4 cDNA Sequence.

1 AAACTCAAAC GGCTGTCAGG GGCCCGGCCA AGAAGGAGGC CCGCCTGTTA

51 CGATGGTGTC CATGAGTTTC AAGCGGAACC GCAGTGACCG GTTCTACAGC

101 ACCCGGTGCT GCGGCTGTTG CCATGTCCGC ACCGGGACGA TCATCCTGGG

151 GACCTGGTAC ATGGTAGTAA ACCTATTGAT GGCAATTTTG CTGACTGTGG

201 AAGTGACTCA TCCAAACTCC ATGCCAGCTG TCAACATTCA GTATGAAGTC

251 ATCGGTAATT ACTATTCGTC TGAGAGAATG GCTGATAATG CCTGTGTTCT

301 TTTTGCCGTC TCTGTTCTTA TGTTTATAAT CAGTTCAATG CTGGTTTATG

351 GAGCAATTTC TTATCAAGTG GGTTGGCTGA TTCCATTCTT CTGTTACCGA

401 CTTTTTGACT TCGTCCTCAG TTGCCTGGTT GCTATTAGTT CTCTCACCTA

451 TTTGCCAAGA ATCAAAGAAT ATCTGGATCA ACTACCTGAT TTTCCCTACA

501 AAGATGACCT CCTGGCCTTG GACTCCAGCT GCCTCCTGTT CATTGTTCTT

551 GTGTTCTTTG CCTTATTCAT CATTTTTAAG GCTTATCTAA TTAACTGTGT

601 TTGGAACTGC TATAAATACA TCAACAACCG AAACGTGCCG GAGATTGCTG

651 TGTACCCTGC CTTTGAAGCA CCTCCTCAGT ACGTTTTGCC AACCTATGAA

701 ATGGCCGTGA AAATGCCTGA AAAAGAACCA CCACCTCCTT ACTTACCTGC

751 CTGAAGAAAT TCTGCCTTTG ACAATAAATC CTATACCAGC TTTTTGTTTG

801 TTTATGTTAC AGAATGCTGC AATTCAGGGC TCTTCAAACT TGTTTGATAT

851 AAAATATGTT GTCTTTTGTT TAAGCATTTA TTTTCAAACA CTAAGGAGCT

901 TTTTGACATC TGTTAAAAAG CTCCTTAGTG TTTGAAAATA AATGCTTAAA

951 AAAAAAAAAA AA

Figure 3-3. Predicted Human LAPTm4 Protein Sequence. Shown here is the protein predicted by the open reading frame of the cDNA from clone 6.8. The four transmembrane domains are underlined as predicted by the hidden Markov model of Sonnhammer *et al.*, [147, 148].

Figure 3-3. Predicted Human LAPTm4 Protein Sequence.

```
  1  MVSMSFKRNR SDRFYSTRCC GCCHVRTGTI ILGTWYMVVN LLMAILLTVE

 51  VTHPNSMPAV NIQYEVIGNY YSSERMADNA CVLFAVSVLM FIISSMLVYG

101  AISYQVGWLI PFFCYRLFDF VLSCLVAISS LTYLPRIKEY LDQLPDFPYK

151  DDLLALDSSC LLFIVLVFFA LFIIFKAYLI NCVWNCYKYI NNRNVPEIAV

201  YPAFEAPPQY VLPTYEMAVK MPEKEPPPPY LPA
```

Figure 3-4. Comparison of Predicted Protein Sequences of hLAPTm4 and mLAPTm4. The sequences of hLAPTm4 and mLAPTm4 were aligned using the BESTFIT program (Wisconsin Package Version 9.1, Genetics Computer Group) and found to be 97% similar and 97% identical. The dissimilar amino acids are in bold print below the asterisks (*).

Figure 3-4. Comparison of Predicted Protein Sequences of hLAPTm4 and mLAPTm4.

```
                  *.  *       .       *  .           .           .
mLAPTm4     1 MVSMTFKRSRSDRFYSTRCCGCFHVRTGTIILGTWYMVVNLLMAILLTVE 50
              ||||.|||.|||||||||||||| |||||||||||||||||||||||||||
hLAPTm4     1 MVSMSFKRNRSDRFYSTRCCGCCHVRTGTIILGTWYMVVNLLMAILLTVE 50

                  .       .       .       .       .
mLAPTm4    51 VTHPNSMPAVNIQYEVIGNYYSSERMADNACVLFAVSVLMFIISSMLVYG 100
              ||||||||||||||||||||||||||||||||||||||||||||||||||||
hLAPTm4    51 VTHPNSMPAVNIQYEVIGNYYSSERMADNACVLFAVSVLMFIISSMLVYG 100

                  .       .       .       .       .
mLAPTm4   101 AISYQVGWLIPFFCYRLFDFVLSCLVAISSLTYLPRIKEYLDQLPDFPYK 150
              ||||||||||||||||||||||||||||||||||||||||||||||||||||
hLAPTm4   101 AISYQVGWLIPFFCYRLFDFVLSCLVAISSLTYLPRIKEYLDQLPDFPYK 150

                  .       .  **   .       .       .
mLAPTm4   151 DDLLALDSSCLLFIVLVFFVVFIIFKAYLINCVWNCYKYINNRNVPEIAV 200
              ||||||||||||||||||  .||||||||||||||||||||||||||||||
hLAPTm4   151 DDLLALDSSCLLFIVLVFFALFIIFKAYLINCVWNCYKYINNRNVPEIAV 200

                  *       .   *   .
mLAPTm4   201 YPAFETPPQYVLPTYEMAVKIPEKEPPPPYLPA 233
              ||||| |||||||||||||.||||||||||||
hLAPTm4   201 YPAFEAPPQYVLPTYEMAVKMPEKEPPPPYLPA 233
```

Figure 3-5. Measurement of MTPΔC Activity in *X. laevis* Oocytes. For each experiment, oocytes were injected with water as a negative control or with rCNT1 cRNA as a positive control as described in Chapter 2 C. The cRNAs were transcribed *in vitro* as described in Chapter 2 F. *A*, Oocytes were injected with MTPΔCΔ5'UTR cRNA and 10 μM [^{3}H]-thymidine uptake was measured on Day 4. *B*, Oocytes were injected with MTPΔCKB cRNA and 10 μM [^{3}H]-thymidine uptake was measured on Day 5. *C*, Oocytes were injected with MTPΔC cRNA and 10 μM [^{3}H]-thymidine uptake was measured on Day 4. *D*, Oocytes were injected with MTPΔC cRNA and 100 μM [^{3}H]-thymidine uptake was measured on Day 3. *E*, Oocytes were injected with SP64TMTPΔC cRNA and 100 μM [^{3}H]-thymidine uptake was measured on Day 3. *F*, Oocytes were injected with MTPΔCΔ5'UTR cRNA and 10 μM [^{3}H]-thymidine uptake was measured on SP64TMTPΔC cRNA and 100 μM [^{3}H]-uridine uptake was measured on Day 3. Each figure shows representative results from 2-3 separate experiments conducted under similar conditions except for figures *E* and *F* which were only conducted once. Each experimental condition involved 8-24 oocytes, depending on the day of the experiment. Error bars represent standard error and some error bars are not shown because the values were too small to be visible.

Figure 3-5
Measurement of MTPΔC Activity in *X. laevis* Oocytes

A. 10 μM Thymidine Uptake

***X. laevis* oocytes - Day 4**

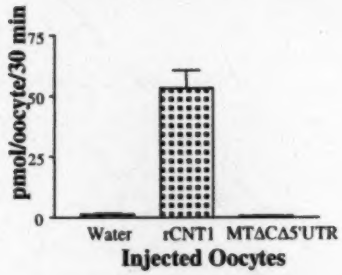

B. 10 μM Thymidine Uptake

***X. laevis* oocytes - Day 5**

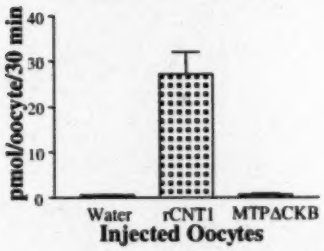

C. 10 μM Thymidine Uptake

***X. laevis* oocytes- Day 4**

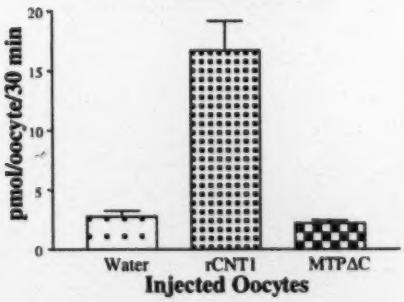

Figure 3-5
Measurement of MTPΔC Activity in *X. laevis* Oocytes

D. 100 μM Thymidine Uptake

***X. laevis* oocytes - Day 3**

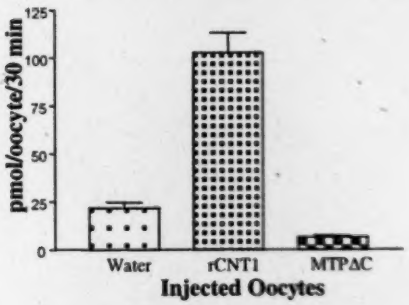

E. 100 μM Thymidine Uptake

***X. laevis* oocytes - Day 3**

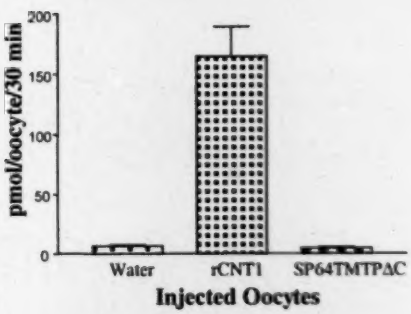

F. 100 μM Uridine Uptake

***X. laevis* oocytes - Day 3**

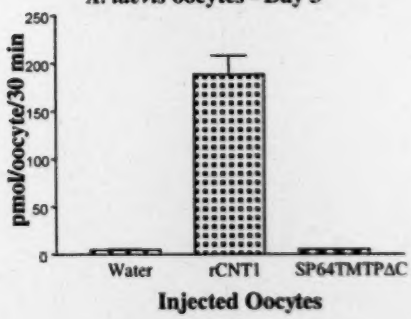

Figure 3-6. Immunodetection of mLAPTm4 and HA-mLAPTm4 in Transfected BHK21 Cells. Cell lysates were prepared from BHK21 cells that had been transfected with pcDNA3/HA-MTP, pcDNA3/MTP3 or pcDNA3 as described in Chapter 2 R. *A*, The immunoblot was incubated first with anti-mLAPTm4 rabbit antibodies and then with horseradish peroxidase-conjugated goat anti-rabbit IgG antibodies. *B*, The immunoblot shown in A was stripped, blocked, incubated with anti-HA rat antibodies and then with horseradish peroxidase-conjugated goat anti-rat IgG antibodies. Detection was by ECL as described in Chapter 2 R. *Left*, positions of the protein markers (in kDa).

Figure 3-6
Immunodetection of mLAPTm4 and HA-mLAPTm4 in Transfected BHK21 Cells

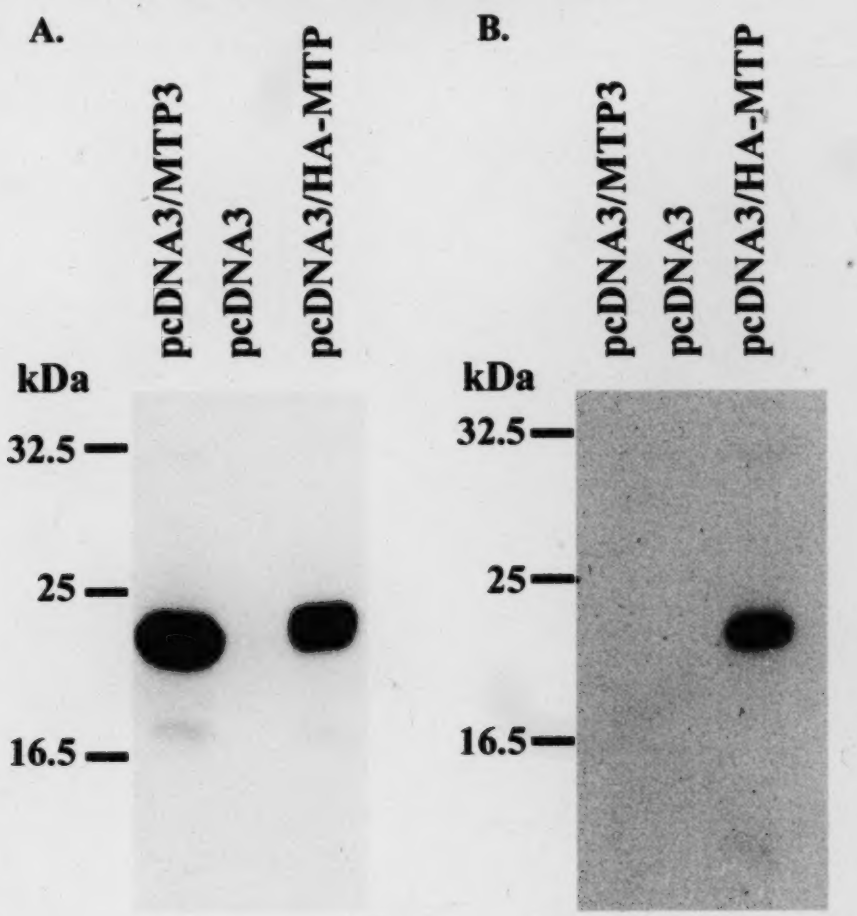

Figure 3-7. Presence of mLAPTm4 and HA-mLAPTm4 in Juxtanuclear Vesicles. BHK21 cells were transfected with pcDNA3/HA-MTP, pcDNA3/MTP3 or pcDNA3 as described in Chapter 2 H I. Cells were fixed, permeabilized, and incubated first with anti-HA antibodies (*A*, *B*, and *C*) or anti-mLAPTm4 antibodies (*D*, *E*, and *F*), then with FITC-conjugated donkey anti-rat IgG antibodies (*A*, *B*, and *C*) or Cy5-conjugated goat anti-rabbit IgG antibodies (*D*, *E*, and *F*). Cells were visualized using laser-scanning confocal microscopy. Overlapping images are shown in Panels *G*, *H*, and *I*. *Bars*, 20 μm.

Figure 3-7

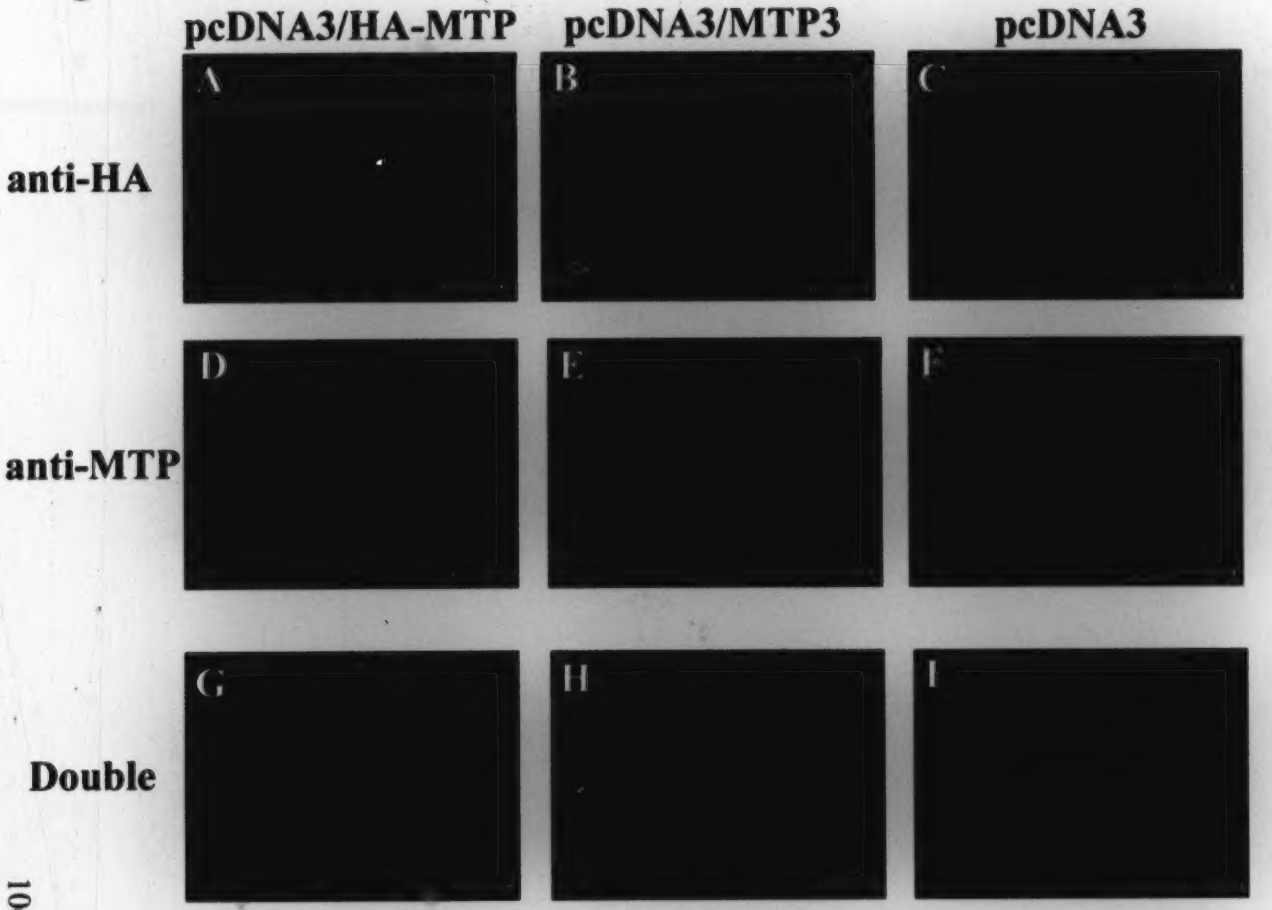
pcDNA3/HA-MTP
pcDNA3/MTP3
pcDNA3
anti-HA
anti-MTP
Double
A
B
C
D
E
F
G
H
I

Figure 3-8. Absence of HA-mLAPTm4 in the Golgi Apparatus of Transfected Cells. BHK21 cells were transfected with pcDNA3/HA-MTP or pcDNA3 as described in Chapter 2 H I. Cells were fixed, permeabilized, and incubated with monoclonal anti-HA antibodies (*A* and *B*) or with polyclonal anti-α-ManII antibodies (*C* and *D*), then with FITC-conjugated goat anti-rat IgG antibodies (*A* and *B*) or Cy5-conjugated donkey anti-rabbit IgG antibodies (*C* and *D*). Cells were visualized using laser-scanning confocal microscopy. Overlapping images are shown in *E* and *F*. *Bars*, 20 μm.

Figure 3-8

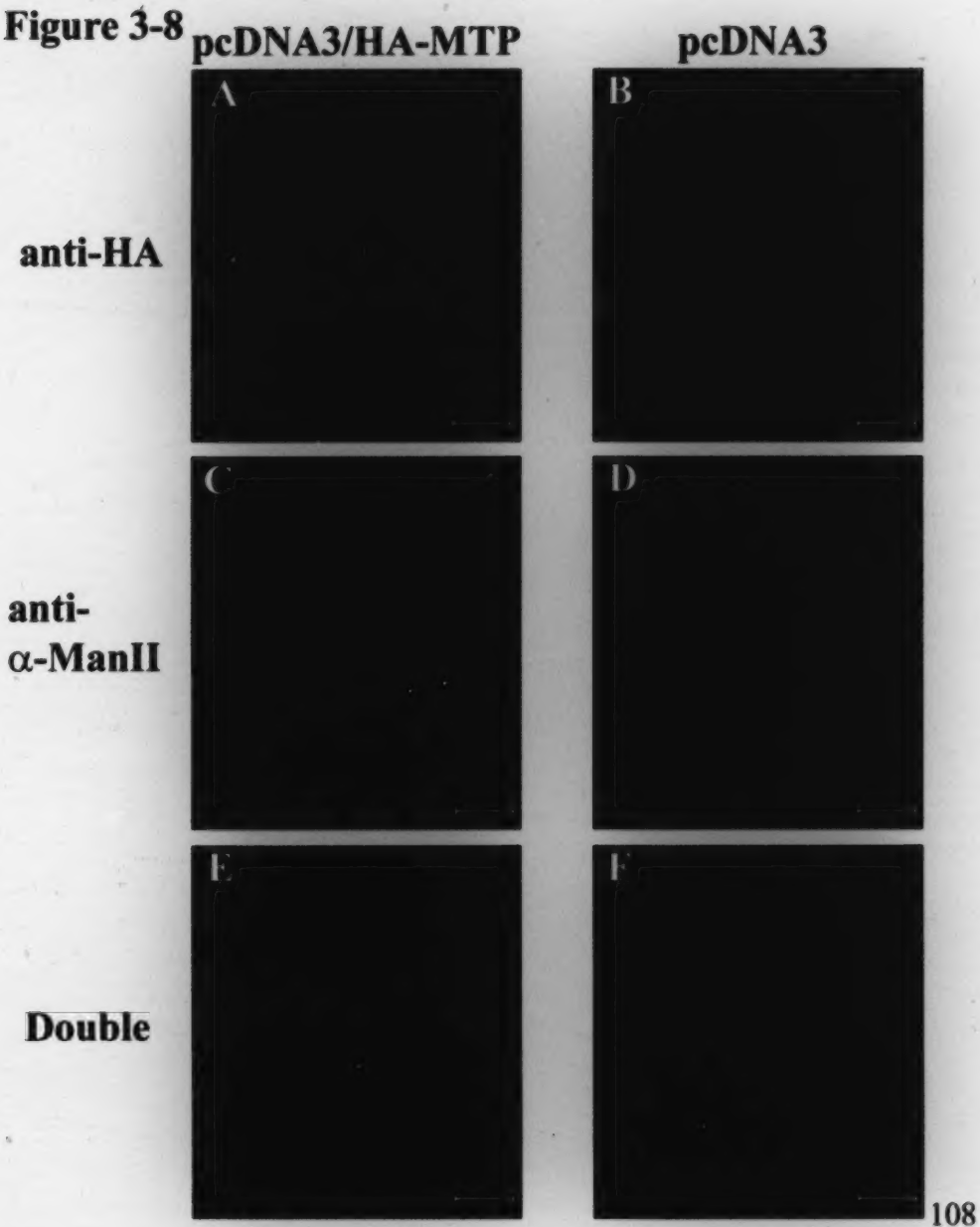

Figure 3-9. Absence of HA-mLAPTm4 in the Early Endosomes of Transfected Cells. BHK21 cells were transfected with pcDNA3/HA-MTP or pcDNA3 as described in Chapter 2 H I. Cells were fixed, permeabilized, and incubated with rat anti-HA antibodies (*A* and *B*) or with polyclonal anti-rab5A antibodies (*C* and *D*), then with FITC-conjugated goat anti-rat IgG antibodies (*A* and *B*) or Cy5-conjugated donkey anti-rabbit IgG antibodies (*C* and *D*). Cells were visualized using laser-scanning confocal microscopy. Overlapping images are shown in *E* and *F*. *Bars*, 20 μm.

Figure 3-9

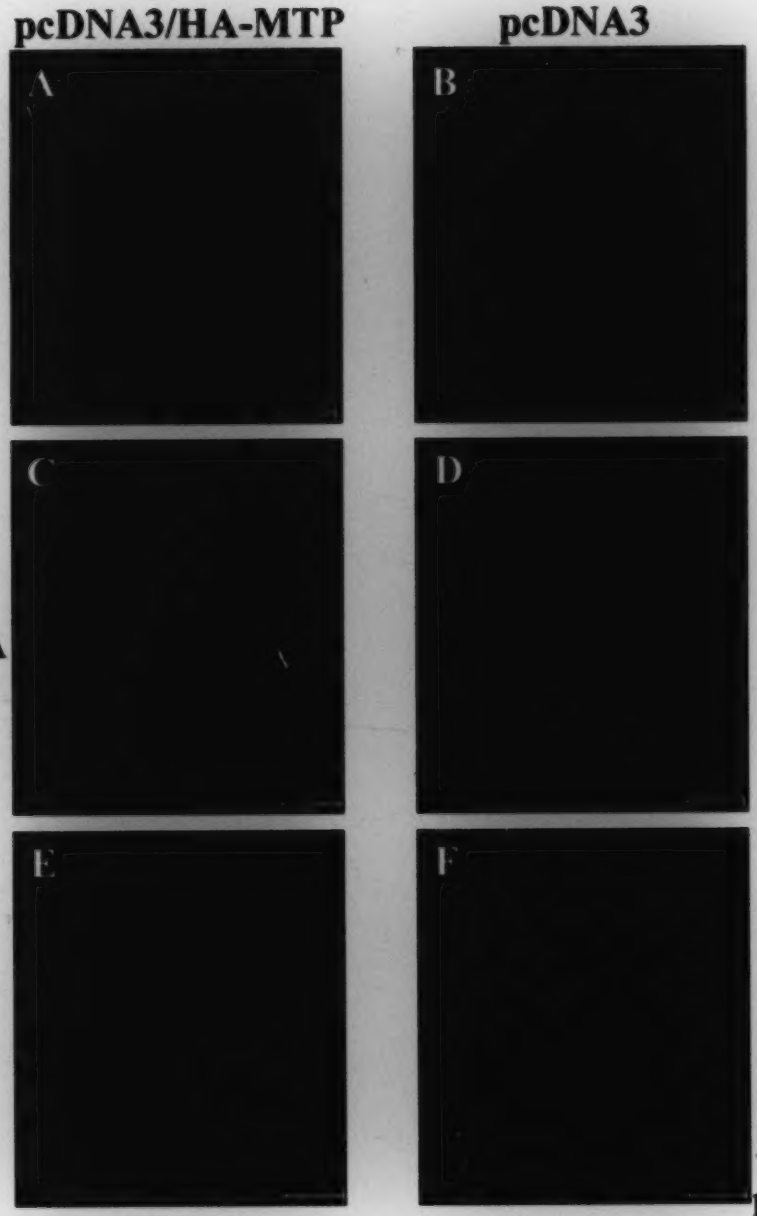

Figure 3-10. Presence of HA-mLAPTm4 in Late Endosomes of Transfected Cells. BHK21 cells were transfected with pcDNA3/HA-MTP or pcDNA3 as described in Chapter 2 H I. Cells were fixed, permeabilized, and double-labelled for HA-mLAPTm4 (anti-HA; *A* and *B*) and late endosomes (anti-M6PR; *C* and *D*). The secondary antibodies were FITC-conjugated goat anti-rat IgG antibodies (*A* and *B*) or Cy5-conjugated donkey anti-rabbit IgG antibodies (*C* and *D*). Cells were visualized using laser-scanning confocal microscopy. Overlapping images are shown in *E* and *F*. *Bars*, 20 μm.

Figure 3-10

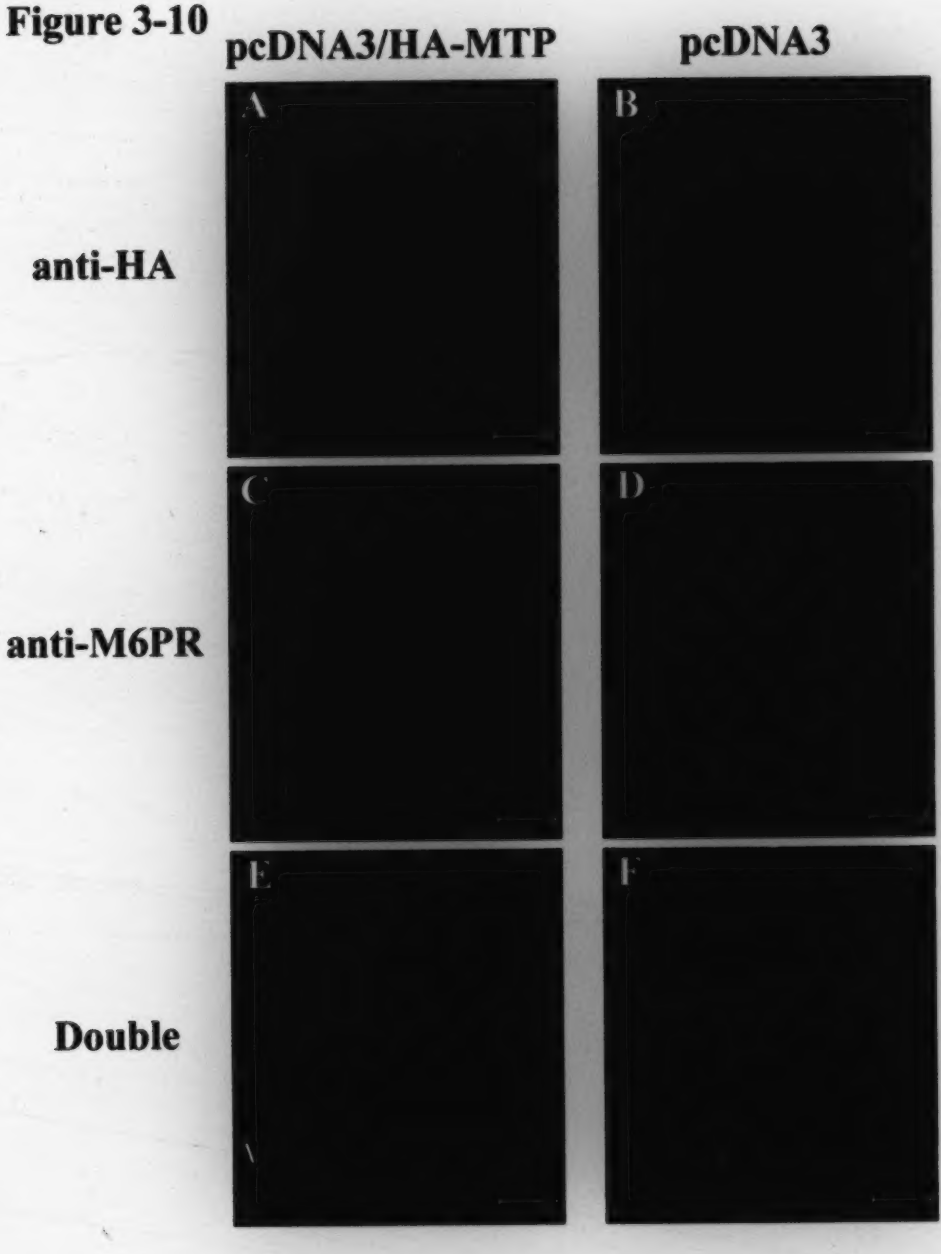

Figure 3-11. Presence of HA-mLAPTm4 in Late Endosomes of Chloroquine-treated Transfected Cells. BHK21 cells were transfected with pcDNA3/HA-MTP or pcDNA3 and treated with 40 μM chloroquine for 1 h as described in Chapter 2 H I. Cells were fixed, permeabilized, and double-labelled for HA-mLAPTm4 (anti-HA; *A*, *B* and *C*) and late endosomes (anti-M6PR; *D*, *E* and *F*). The secondary antibodies were FITC-conjugated goat anti-rat IgG antibodies (*A*, *B* and *C*) or Cy5-conjugated donkey anti-rabbit IgG antibodies (*D*, *E* and *F*). Cells were visualized using immunofluorescence microscopy.

Figure 3-11

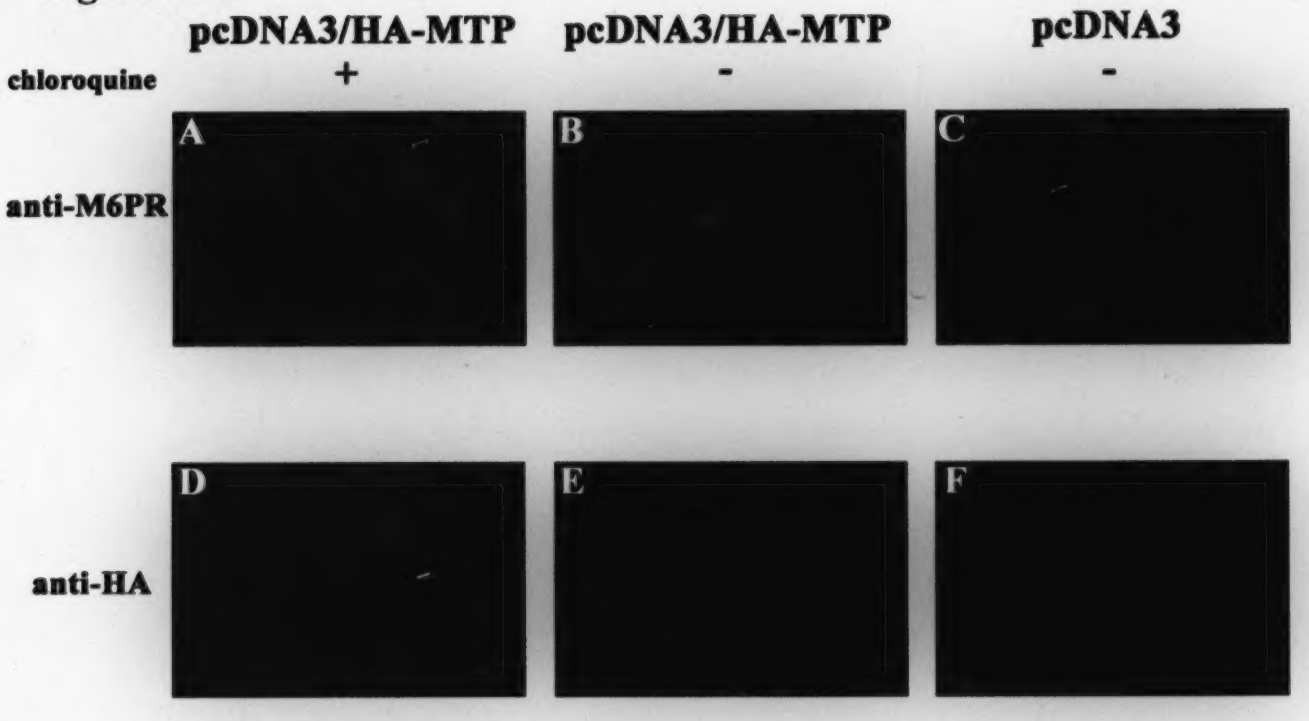
pcDNA3/HA-MTP
pcDNA3/HA-MTP
pcDNA3
chloroquine
+
-
-
A
B
C
anti-M6PR
D
E
F
anti-HA

Figure 3-12. Presence of HA-mLAPTm4 in Lysosomes of Transfected Cells. BHK21 cells were transfected with pcDNA3/HA-MTP or pcDNA3 as described in Chapter 2 H I. Cells were fixed, permeabilized, and double-labelled for HA-MTP (anti-HA; *A* and *B*) and for lysosomes (anti-lgp110; *C* and *D*). The secondary antibodies were FITC-conjugated goat anti-rat IgG antibodies (*A* and *B*) or Cy5-conjugated donkey anti-rabbit IgG antibodies (*C* and *D*). Cells were visualized using laser-scanning confocal microscopy. Overlapping images are shown in *E* and *F*. *Bars*, 20 μm.

Figure 3-12

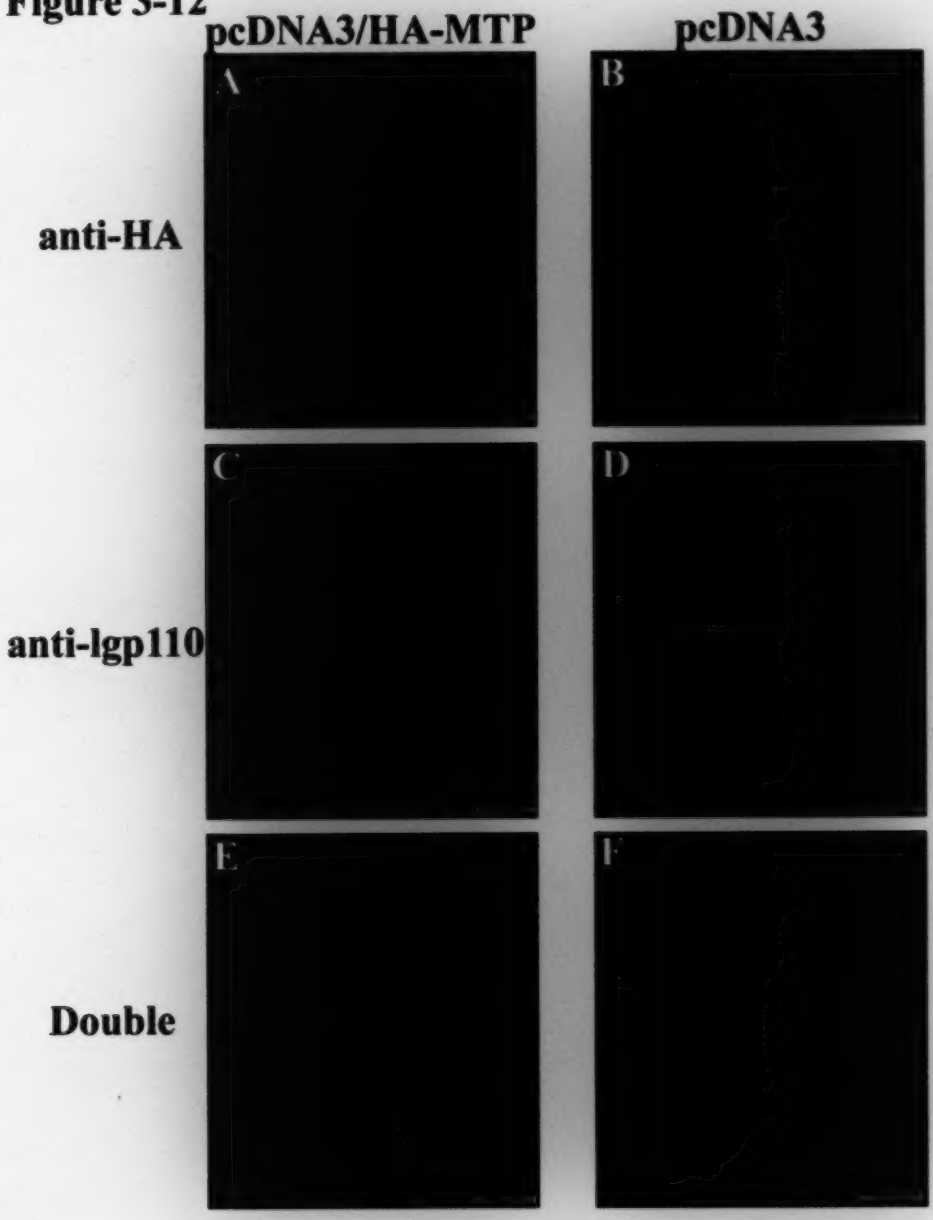

Figure 3-13. Presence of HA-mLAPTm4 in Lysosomes of Chloroquine-treated Transfected Cells. BHK21 cells were transfected with pcDNA3/HA-MTP or pcDNA3 and treated with 40 μM chloroquine for 1 h as described in Chapter 2 H I. Cells were fixed, permeabilized, and double-labelled for HA-mLAPTm4 (anti-HA; *A*, *B* and *C*) and lysosomes (anti-lgp110; *D*, *E* and *F*). The secondary antibodies were FITC-conjugated goat anti-rat IgG antibodies (*A*, *B* and *C*) or Cy5-conjugated donkey anti-rabbit IgG antibodies (*D*, *E* and *F*). Cells were visualized using immunofluorescence microscopy.

Figure 3-13

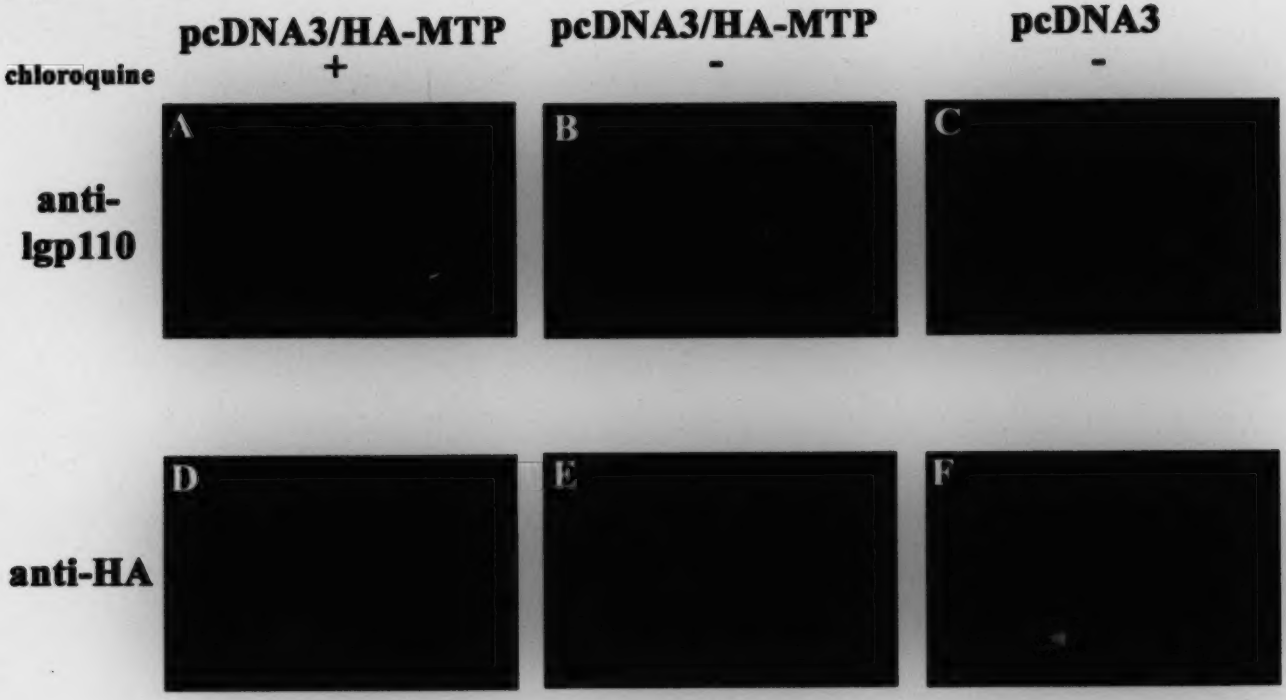
pcDNA3/HA-MTP
pcDNA3/HA-MTP
pcDNA3
chloroquine
+
-
-
A
B
C
anti-
lgp110
D
E
F
anti-HA

Figure 3-14. Immunoblot of Rat Liver Subcellular Fractions. Samples from rat liver and transfected BHK21 cells were prepared as described in Chapter 2. For electrophoresis (12% gels), 100 μg of protein from each membrane fraction and 10 μL from cell lysates for each transfected sample were loaded into the sample wells. The immunoblot was probed first with anti-mLAPTm4 antibodies and then with horseradish peroxidase-conjugated goat anti-rabbit IgG antibodies. Detection was by ECL as described in Chapter 2 R. *Left* and *right*, positions of the protein markers (in kDa).

Figure 3-14

Immunoblot of Rat Liver Subcellular Fractions

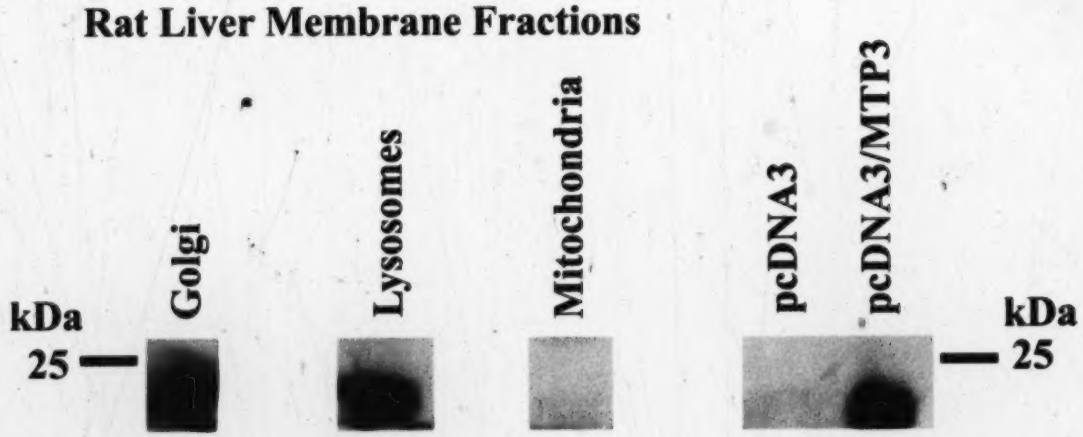

Figure 3-15. ClustalW Alignment of Mammalian LAPTmX Family Members. Sequences other than those of hLAPTm4 and mLAPTm4 were obtained from GenBank and aligned using the ClustalW program at the Canadian Bioinformatics Resource website (http://www.cbr.nrc.ca). Identical residues are depicted in bold type and the YXXØ motifs are underlined.

Figure 3-15. ClustalW Alignment of Mammalian LAPTmX Family Members

```
mLAPTm5          ........MA SRAAPVRQTC CCFNIRVATI ALAIYHIVMS VLLFIEHVVE
mE3              ........MA SRAAPVRQTC CCFNIRVATI ALAIYHIVMS VLLFIEHVVE
rGCD10           ........MA SRAVPVRQTC CCFNVRVATV ALAIYHIVMS VLLFIEHVVE
hLAPTm5          ........MD PRLSTVRQTC CCFNVRIATT ALAIYHVIMS VLLFIEHSVE
hE3              ........MD PRLSTVRQTC CCFNVRIATT ALAIYHVIMS VLLFIEHSVE
mLAPTm4          MVSMTFKRSR SDRFYSTRCC GCFHVRTGTI ILGTWYMVVN LLMAILLTVE
hLAPTm4          MVSMSFKRNR SDRFYSTRCC GCCHVRTGTI ILGTWYMVVN LLMAILLTVE
mLAPTm4b         ....MKMVAP WTRFYSHSCC LCCHVRTGTI LLGVWYLIIN AVVLLILLSA
hLAPTm4b         ....MKMVAP WTRFYSNSCC LCCHVRTGTI LLGVWYLIIN AVVLLILLSA

mLAPTm5          VARGKVSCRF FKMPYLRMAD LLSS...... ....FLLIGV LFIISISLLF
mE3              VARGKVSCRF FKMAYLRMAD LLSS...... ....FLLIGV LFIISISLLF
ratGCD10         VARGKVSCRF SKMPYLRLAD LLSS...... ....FLLIGV LFIISLSLLF
hLAPTm5          VAHGKASCKL SQMGYLRIAD LISS...... ....FLLITM LFIISLSLLI
hE3              VAHGKASCKL SQMGYLRIAD LISS...... ....FLLITM LFIISLSLLI
mLAPTm4          VTH.PNSMPA VNIQYEVIGN YYSSERMADN ACVLFAVSVL MFIISSMLVY
hLAPTm4          VTH.PNSMPA VNIQYEVIGN YYSSERMADN ACVLFAVSVL MFIISSMLVY
mLAPTm4b         LAD.PNQYHF SGSELGGEFE FMDD....AN MCIAIAISLL MILICAMATY
hLAPTm4b         LAD.PDQYNF SSSELGGDFE FMDD....AN MCIAIAISLL MILICAMATY

mLAPTm5          GVVKNREKYL IPFLSLQIMD FLLCLLTLLG SYIELPAYLK LAR.PRPGPS
mE3              GVVKNREKYL IPFLSLQIMD FLLCLLTLLG SYIDLPAYLK LAR.SRPGPS
rGCD10           GVVKNREKYL IPFLSLQIMD FLLCLLTLLG SYIELPAYLK FAR.PRPGPS
hLAPTm5          GVVKNREKYL LPFLSLQIMD YLLCLLTLLG SYIELPAYLK LASRSRASSS
hE3              GVVKNREKYL LPFLSLQIMD YLLCLLTLLG SYIELPAYLK LASRSRASSS
mLAPTm4          GAISYQVGWL IPFFCYRLFD FVLSCLVAIS SLTYLPRIKE YLD.......
hLAPTm4          GAISYQVGWL IPFFCYRLFD FVLSCLVAIS SLTYLPRIKE YLD.......
mLAPTm4b         GAYKQHAAWI IPFFCYQIFD FALNTLVAIT VLVYPNSIQE YIR.......
hLAPTm4b         GAYKQRAAWI IPFFCYQIFD FALNMLVAIT VLIYPNSIQE YIR.......

mLAPTm5          KVPLMTLQLL DFCLSILTLC SSYMEVPTYL NFKSMNHMNY LPSQEGVPHS
mE3              KVPLMTLQLL DFCLSILTLC SSYMEVPTYL NFKSMNHMNY LPSQEGVPHS
rGCD10           KVPLMTLQLL DFCLSILTLC SSYMEVPTYL NFKSMNHMNY LPSQEGMPRS
hLAPTm5          KFPLMTLQLL DFCLSILTLC SSYMEVPTYL NFKSMNHMNY LPSQEDMPHN
hE3              KFPLMTLQLL DFCLSILTLC SSYMEVPTYL NFKSMNHMNY LPSQEDMPHN
mLAPTm4          .......... .......... .......... .....QLP.D FPYKDDLLAL
hLAPTm4          .......... .......... .......... .....QLP.D FPYKDDLLAL
mLAPTm4b         .......... .......... .......... .....QLPPS FPYRDDIMSV
hLAPTm4b         .......... .......... .......... .....QLPPN FPYRDDVMSV
```

Figure 3-15. ClustalW Alignment of LAPTmX Family Members

```
mLAPTm5          QFINMMLIFS VAFITVLILK VYMFKCVYTC YKFLKHMN.. SAMEDSSSKM
mE3              QFINMMLIFS VAFITVLILK VYMFKCVYTC YKFLKHMN.. SAMEDSSSKM
rGCD10           QFINMMLIFS VAFITVLILK VYMFKCVWTC YRFMKHMN.. SAVEDSSSKL
hLAPTm5          QFIKMMIIFS IAFITVLIFK VYMFKCVWRC YRLIKCMN.. SVEEKRNSKM
hE3              QFIKMMIIFS IAFITVLIFK VYMFKCVWRC YRLIKCMN.. SVEEKRNSKM
mLAPTm4          DSSCLLFIVL VFFVVFIIFK AYLINCVWNC YKYINNRNVP EIAVYPAFET
hLAPTm4          DSSCLLFIVL VFFALFIIFK AYLINCVWNC YKYINNRNVP EIAVYPAFEA
mLAPTm4b         NPTCLVLIIL LFIGILLTLK GYLISCVWSC YRYINGRNSS DVLVYVTSND
hLAPTm4b         NPTCLVLIIL LFISIILTFK GYLISCVWNC YRYINGRNSS DVLVYVTSND

mLAPTm5          FLKVALPSYE EALS.LPPKT PEGDPAPPPY SEV
mE3              FLKVALPSYE EALS.LPPKT PEGDPAPPPY SEV
rGCD10           FLKVALPSYE EALS.LPTKT PEGDPAPPPY SEV
hLAPTm5          LQKVVLPSYE EALS.LPSKT PEGGPAPPPY SEV
hE3              LQKVVLPSYE EALS.LPSKD PEGGPAPPPY SEV
mLAPTm4          PPQYVLPTYE MAVK.IPEKE P.....PPPY LPA
hLAPTm4          PPQYVLPTYE MAVK.MPEKE P.....PPPY LPA
mLAPTm4b         TTVLLPPYDD ATAVPSTAKE P.....PPPY VSA
hLAPTm4b         TTVLLPPYDD ATVN.GAAKE P.....PPPY VSA
```

Table 3-1. Enzyme Marker Assays of Subcellular Fractions. Established procedures were used to enrich for lysosomes [240], Golgi [239] and mitochondria [241, 242]. The values (mean ± standard deviation, n = 3 except where noted otherwise) are units/100 mg of protein, where units represent absorbance at 405 μm for β-galactosidase (lysosomal marker), absorbance at 490 μm for succinate INT reductase (mitochondrial marker) and cpm for galactosyl transferase (Golgi marker). Enzyme assays were conducted as described in Chapter 2 P. Background values, which were obtained using reaction mixtures that did not contain subcellular fractions, were subtracted from experimental values.

	Specific Activity of Enzyme Markers		
Subcellular Fractions	**β-Galactosidase** ($x10^3$)	**Succinate INT Reductase** ($x10^4$)	**Galactosyl Transferase** ($x10^{-3}$)
Lysosomes	228 ± 15	48.6 ± 4.9	83.1‡
Golgi	55.0 ± 1.9	14.5 ± 1.2	221 ± 28.3
Mitochondria	46.7 ± 2.9	117.6 ± 17.5	14.0 ± 2.0*

‡n = 2
*n = 4

Chapter 4

4. Generation and Assessment of Anti-hENT1 and Anti-hENT2 Antibodies

4. Abstract

Antibodies specific for hENT1 and hENT2 were generated using synthetic peptides and fusion proteins, respectively. These antibodies were assessed for reactivity using recombinant, epitope-tagged versions of hENT1 and hENT2 produced in hamster cell lines by transient transfection. The antibodies were used in immunoblot and confocal immunofluorescence microscopy analyses. Both sets of antibodies recognized recombinant proteins of the predicted size, ~50 kDa in immunblots. The anti-hENT1 and anti-hENT2 antibodies also recognized the recombinant proteins in the immunofluorescence experiments.

4 A. Introduction

The production of antibodies to hENT1 and hENT2 was the main goal of the research described in this chapter. The availability of antibodies specific for hENT1 and hENT2 would enable detection and visualization of the transporter proteins using a variety of techniques.

There have been numerous attempts to raise antibodies against hENT1, the protein responsible for mediating *es* transport activity. The first efforts concentrated on using preparations of band 4.5 from human erythrocytes as the antigen [299]. Unfortunately, these efforts resulted in the repeated generation of antibodies directed against the human glucose transporter, which is present in human erythrocyte band 4.5 membrane preparations in >20-fold excess of the equilibrative nucleoside transporter [299]. Antibodies against the nucleoside transporter of pig erythrocytes, which lack glucose transport activity, were generated, but these were not cross reactive with the NBMPR-binding protein (*i.e.*, the nucleoside transporter) in human erythrocytes [300]. These experiments and those of others also demonstrated that while both the human and pig erythrocyte nucleoside transporters bound NBMPR, the apparent molecular weights of these entities were different (55, 000 (human) and 64, 000 (pig), versus 45, 000 (human) and 57, 000 (pig) for the glycosylated versus deglycosylated proteins, respectively) [300, 301].

Anti-hENT1 polyclonal antibodies were successfully raised by Baldwin and co-workers both prior to [301-303] and after the isolation [94, 304] of the hENT1 cDNA. The antibodies obtained prior to the cloning of the hENT1 cDNA were obtained using purified equilibrative nucleoside transporter from human erythrocytes [301] and provided three important pieces of information. First, they reacted with polypeptides from human erythrocyte membranes that were the same size as the NBMPR-binding protein [301, 302]. Second, the antibodies were cross-reactive and highlighted size similarities and differences between proteins from other species such as rat, rabbit and pig [301, 302]. Third, in immunolocalisation experiments in human placenta, the antibodies did not recognize all the known NBMPR-binding sites. NBMPR bound to both basal and brush-border membranes of human syncytiotrophoblasts, whereas the polyclonal antibodies raised against the human erythrocyte nucleoside transporter only bound to polypeptides from brush-border membranes. The latter study suggested that there are at least two isoforms of the human equilibrative nucleoside transporters in placental tissue that can bind NBMPR [302, 303]. Thus, the early polyclonal antibodies established that antibodies could be raised against the NBMPR-binding protein, that more than one isoform of the NBMPR-binding protein probably existed in human tissues and that transporters from different species contained common antigens. The anti-hENT1 polyclonal antibodies raised after the isolation of the hENT1 cDNA were raised against a synthetic peptide corresponding to amino acid residues 254-272 from the large loop between transmembranes domains 6 and 7. The antibodies have been used to determine that the large loop is on the intracellular side of the plasma membrane [304].

Prior to the isolation of the hENT2 cDNA by two independent groups [78, 99],

there was a report in the literature describing the isolation of two cDNAs, encoding related human and mouse proteins [103]. The two proteins were predicted to be about 36 kDa in size and had seven or eight putative transmembrane domains that were highly conserved. These proteins, called human hydrophobic nucleolar protein 36 (hHNP36) and mouse hydrophobic nucleolar protein 36 (mHNP36), respectively, bore resemblance to the yeast open reading frame of unknown function, FUN26 [103]. The mouse cDNA was isolated in a screen of delayed early response genes that were activated when mouse fibroblasts were stimulated by serum [104]. When antibodies raised against a 54-amino acid region in the large hydrophilic portion of mHNP36 were used in immunocytochemistry experiments with mouse fibroblasts, the antibodies bound to nucleoli. The same antibodies immunoprecipitated *in vitro* translated mHNP36 [103]. The hHNP36 open reading frame encodes a truncated version of hENT2 that corresponds to amino acids 131-456 (or the last eight transmembrane domains) of hENT2 (Figure 4-1).

The goals of the work described in this chapter were *to generate and characterize anti-hENT1 and anti-hENT2 polyclonal and monoclonal antibodies.*

To generate hENT1 antibodies, synthetic peptides (corresponding to amino acids 55-64 and 254-271 of hENT1, which reside in the extracellular loop between transmembrane domains 1 and 2 and the intracellular loop between transmembrane domains 6 and 7, respectively (see Figure I-5)) conjugated to keyhole limpet haemocyanin and a fusion protein comprised of the majority of the large putative intracellular loop of hENT1 (amino acids 226-289) and the maltose-binding protein of *E. coli* were used as antigens. Reactivity and specificity of the antibodies were tested by ELISA and immunoblot analysis using the corresponding synthetic peptides conjugated to bovine serum albumin and using fusions of the same hENT1-derived polypeptide with glutathione-S-transferase (GST), respectively. Work on the antibodies directed against the intra- and extracellular loops of hENT1 was a collaborative effort involving M. A. Cabrita, Dr. J. M. J. Marjan, Dr. L. L. Jennings and M. Selner.

To generate anti-hENT2 antibodies, a fusion protein comprised of the majority of the large putative intracellular loop of hENT2 (amino acids 213-290 or amino acids 83-160 of hHNP36; see Figure I-6) and the maltose-binding protein of *E. coli* was used as the immunogen. Reactivity and specificity of the antibodies were tested by immunoblot analysis using fusions of the same hENT2-derived polypeptide with GST.

The specificities of the anti-hENT1 and anti-hENT2 antibodies were also tested by immunofluorescence and immunoblot analysis using recombinant, HA-tagged hENT1 [215, 305], VSV-G-tagged hENT2 [216], and VSV-G-tagged hHNP36 [216] proteins that were produced by transient transfection in mammalian cells.

4 B. Results

4B. I. Generation of Anti-hENT1 and Anti-hENT2 Antibodies

Both the hENT1 and hENT2 protein sequences were analysed at the University

of Alberta by the Alberta Peptide Institute's SurfacePlot algorithm [306, 307]. This algorithm identified stretches of polypeptides that had a high probability of being antigenic, and thus were good choices for use as antigens to be conjugated with an immunogenic carrier protein and injected into animals. In Table 4-1, the potential antigenic sites are given for hENT1 and hENT2.

hENT1: Although intracellular sequences had already been utilized to generate anti-hENT1 antibodies [94, 304], antibodies that could be used with intact cells were desired and an extracellular epitope was therefore chosen as the potential antigen. A synthetic peptide, corresponding to amino acids 55-64 of hENT1, was synthesized, conjugated to keyhole limpet haemocyanin and injected into two rabbits and twelve mice. Unfortunately, the polyclonal antibodies that were generated in this effort only recognized the antigen that was injected (when tested by enzyme-linked immunosorbent assays (ELISA)) and not the recombinant, epitope-tagged hENT1 produced in *S. cerevisiae* or by transient transfection in mammalian cells by immunoblot analyses. In collaboration with Dr. J. M. J. Marjan and M. Selner, a potentially useful monoclonal antibody-producing hybridoma was generated from one fusion, but the resulting monoclonal antibodies were of the IgM subtype and were reactive only in flow cytometry assays [7] and were not reactive in either immunoblotting or immunofluorescence experiments.

Because of the failure to obtain antibodies that recognized hENT1 using the synthetic peptide corresponding to part of the large extracellular loop, antibodies were raised against the large intracellular loop of hENT1 by two approaches. First, recombinant fusion proteins containing amino acids 228-289 of hENT1 fused to the C-terminus of the *E. coli* maltose-binding protein were produced in *E. coli* as described in Chapter 2 I. This antigen was injected into two rabbits and also did not produce useful antisera. The polyclonal antibodies that were generated in this effort only recognized the antigen that was injected (when tested using fusions of the same hENT1-derived polypeptide with GST) and not the recombinant, epitope-tagged hENT1 produced in *S. cerevisiae* or by transient transfection in mammalian cells by immunoblotting.

A second approach to raising anti-hENT1 antibodies used a synthetic peptide corresponding to amino acids residues 254-271 of the large intracellular loop of hENT1 [115], similar to the peptide epitope used by Baldwin and colleagues [94, 304]. This effort, which was led by Dr. L. L. Jennings in collaboration with M. Selner, resulted in the generation of hENT1 polyclonal and monoclonal antibodies. For the experiments described below, the anti-hENT1 monoclonal antibodies utilized were those generated by this initiative [115].

hENT2: Because the SurfacePlot algorithm predicted three antigenic sites in the large intracellular loop region of hENT2 between transmembrane domains 6 and 7 (see Table 4-1), the whole intracellular loop of hENT2 was used as the antigen. Also, successful anti-hENT1 antibodies had been raised twice against a portion of the intracellular loop between transmembrane domains 6 and 7 [94, 115, 304]. The large intracellular loop regions of hENT1 and hENT2 are predicted to be quite different in size, 64 and 78 amino acids long, respectively (see Figure 4-2), and since these loop sequences

are 28% identical and 48% similar, a lack of cross-reactivity between the two proteins was expected. A recombinant fusion protein containing amino acids 213-290 of hENT2 fused to the C-terminus of the *E. coli* maltose-binding protein was produced in *E. coli* as described in Chapter 2 I. This antigen was injected into two rabbits and twelve mice to generate polyclonal and monoclonal antibodies as described in Chapter 2 I. Only one of the immunized rabbits generated antisera that detected both the immunizing antigen and the recombinant protein (see the following section). Antibody-secreting hybridoma cells that were generated as described in Chapter 2 I in collaboration with M. Selner produced anti-hENT2 monoclonal antibodies (see the following section). The antibodies that were raised against the hENT2 amino acids (residues 213-290) were expected to also recognize hHNP36, since it contains the identical sequence (residues 83-160).

4 B. II. Assessment of the Anti-hENT1 and Anti-hENT2 Antibodies

To test the specificity and usefulness of the anti-hENT1 and anti-hENT2 antibodies for immunoblotting and immunofluorescence, recombinant epitope-tagged versions of all three proteins were produced by transient transfection in CHOK1 and BHK21 cells. These cell lines were used because preliminary and previous experiments, respectively, had established that they lacked reactivity with the antibodies against the ENT proteins and epitope-tags (Chapter 3 and data not shown). All of the proteins were epitope-tagged at their C-termini, with the HA-tag being added to hENT1 and the VSV-G tag to hENT2 and hHNP36. The plasmids containing the cDNAs encoding the epitope-tagged proteins were transiently transfected into CHOK1 or BHK21 cells. CHOK1 cells are known to have both *es* and *ei* activities and NBMPR-binding proteins [308, 309], while the nucleoside transport profile of BHK21 cells is unknown. Crude solubilized membranes from transiently transfected cells were analysed by immunoblotting using anti-hENT1 monoclonal antibodies or anti-hENT2 polyclonal or monoclonal antibodies. Production of the recombinant proteins in the transiently transfected cells was then analysed by double indirect immunofluorescence using anti-hENT1 monoclonal or anti-hENT2 polyclonal or monoclonal antibodies and anti-HA or anti-VSV-G monoclonal antibodies to ensure that the antibodies were recognizing the appropriate target protein. Also, hENT1 immunoprecipitation reactions were undertaken with the anti-hENT1 polyclonal antibodies using BeWo cells as a source of hENT1 followed by immunoblot analysis with anti-hENT1 monoclonal antibodies.

Anti-hENT1 and hENT2 Monoclonal Antibodies: Demonstration of Reactivity with hENT1 and hENT2 by Immunoblot Analysis. To determine if the anti-hENT1 and anti-hENT2 monoclonal antibodies could recognize recombinant hENT1 and hENT2, respectively, immunoblotting experiments were undertaken with membranes isolated from cells transiently transfected with plasmids encoding epitope-tagged versions of hENT1 and hENT2. Solubilized membranes of transiently transfected cells were analysed by immunoblotting with anti-hENT1 and anti-hENT2 monoclonal antibodies (Figure 4-3). The anti-hENT1 monoclonal antibodies recognized proteins of ~50-55 kDa in cells transfected with the hENT1-HA-encoding plasmid (pcDNA3/hENT1-HA) (Panel *A*),

whereas they did not recognize any proteins from cells transfected with either pcDNA3 or pcDNA3/VSV-G-hENT2. The anti-hENT2 monoclonal antibodies recognized proteins of ~50-55 kDa in cells transfected with the hENT2-encoding plasmid (pcDNA3/hENT2-VSV-G) (Panel *B*), whereas they did not recognize any proteins from cells transfected with either pcDNA3 or pcDNA3/hENT1-HA. The bands below the 50 kDa marker may have been degradation products of either protein, while the slower-migrating bands above the 80 kDa marker may have been aggregates of either protein. These experiments demonstrated the specificity and lack of cross-reactivity of the anti-hENT1 and anti-hENT2 monoclonal antibodies for hENT1 and hENT2, respectively.

Anti-hENT2 Polyclonal Antibodies: Demonstration of Reactivity with hENT2 and hHNP36 by Immunoblot Analysis. To determine if the anti-hENT2 polyclonal antibodies could recognize hENT2 and hHNP36, respectively, immunoblotting experiments were undertaken similar to those described above. Solubilized membranes of transiently transfected cells were analysed by immunoblotting with anti-hENT2 polyclonal antibodies (Figure 4-4). The anti-hENT2 polyclonal antibodies recognized proteins of ~50-55 kDa in cells transfected with the hENT2-encoding plasmid (pcDNA3/hENT2-VSV-G) and proteins of ~38-40 kDa in cells transfected with the hHNP36-VSV-G encoding plasmid (pcDNA3/hENT2-VSV-G), whereas they did not recognize any proteins of these sizes from cells transfected with either pcDNA3, pcDNA3/hENT1-HA, or pcDNA3/β-gal. Recombinant hHNP36 may have migrated more slowly than expected due its high hydrophobicity. When incubated with the electroblotted proteins at room temperature, the anti-hENT2 polyclonal antibodies recognized slowly migrating bands (~80-90 kDa) from the CHOK1 cells. The intensity of these bands decreased or disappeared when the antibodies were incubated at 4°C overnight. These experiments demonstrated the specificity of the anti-hENT2 polyclonal antibodies for hENT2 and hHNP36 and the lack of cross-reactivity with hENT1.

Anti-hENT1 Monoclonal Antibodies: Demonstration of Reactivity with hENT1 by Immunofluorescence. To determine if the anti-hENT1 monoclonal antibodies could recognize recombinant hENT1, immunofluorescence experiments were undertaken with cells transiently transfected with plasmids encoding epitope-tagged versions of hENT1. In the experiments of Figure 4-5, CHOK1 cells were transfected with pcDNA3/hENT1-HA and analysed by double-label indirect immunofluorescence using the anti-hENT1 monoclonal antibodies [115] and the anti-HA monoclonal antibodies [215, 305]. These experiments demonstrated that hENT1-HA was recognized by both anti-hENT1 (Panel *A*) and anti-HA (Panel *B*) antibodies. The superimposed images from Panels *A* and *B* are shown in Panel *C* and the antibody-staining patterns showed co-localization indicating that both antibody preparations were recognizing the same immunoreactive species. The staining pattern of hENT1-HA resembles that of the endoplasmic reticulum. Neither of the antibody preparations bound to CHOK1 cells that were transfected with the pcDNA3 vector alone (Panel *D*). Also, no fluorescent signal was observed in transiently transfected cells incubated with secondary antibodies alone (Panel *E*). These experiments demonstrated that the anti-hENT1 monoclonal antibodies recognized recombinant hENT1-HA by immunofluorescence. Similar results were obtained with transfected

BHK21 cells (data not shown).

Anti-hENT2 Polyclonal Antibodies: Demonstration of Reactivity with hENT2 and hHNP36 by Immunofluorescence. To determine if the anti-hENT2 polyclonal antibodies could recognize recombinant hENT2 and hHNP36, immunofluorescence experiments were undertaken with cells transiently transfected with plasmids encoding epitope-tagged versions of hENT2. In the experiments of Figure 4-6, CHOK1 cells were transfected with pcDNA3/hENT2-VSV-G and pcDNA3/hHNP36-VSV-G and analysed by double-label indirect immunofluorescence using anti-hENT2 polyclonal antibodies and anti-VSV-G monoclonal antibodies [216]. These experiments demonstrated that hENT2 and hHNP36 were recognized by both anti-hENT2 (Panels *A* and *D*) and anti-VSV-G (Panels *B* and *E*) antibodies. The superimposed images from Panels *A* and *B*, and *D* and *E* and are shown in Panels *C* and *F* and the antibody-staining patterns showed co-localization indicating that both antibody preparations bound to the same immunoreactive species. The staining patterns of both constructs resembled that expected for endoplasmic reticulum. Neither of the antibody preparations bound to CHOK1 cells that were transfected with the pcDNA3 vector (same result as in Figure 4-5, Panel *D*) and no fluorescent signal was observed in transiently transfected cells incubated with secondary antibodies alone (same result as in Figure 4-5, Panel *E*). These experiments demonstrated that the anti-hENT2 polyclonal antibodies recognized recombinant HA-hENT2 by immunofluorescence. These experiments also established that hHNP36-VSV-G could be produced as a recombinant protein in mammalian cells, and demonstrated that the anti-hENT2 polyclonal antibodies recognized recombinant hHNP36-VSV-G by immunofluorescence. Similar results were obtained when the hENT-HA- and hENT2-VSV-G-containing plasmids were transiently transfected into BHK21 cells (data not shown).

Anti-hENT2 Monoclonal Antibodies: Demonstration of Reactivity with hENT2 by Immunofluorescence. To determine if the anti-hENT2 monoclonal antibodies could recognize recombinant hENT2, immunofluorescence experiments were undertaken with cells transiently transfected with plasmids encoding epitope-tagged versions of hENT2. In the experiments of Figure 4-7, CHOK1 cells were transfected with pcDNA3/hENT2-VSV-G and analysed by indirect immunofluorescence using anti-hENT2 monoclonal antibodies. Double-label immunofluorescence could not be used as in these experiments because the anti-VSV-G monoclonal antibodies were also of murine origin [216]. The anti-hENT2 monoclonal antibodies recognized immunoreactive material in cells transfected with the plasmid encoding hENT2-VSV-G (Panel *A*), whereas they did not bind to CHOK1 cells that were transfected with the pcDNA3 vector alone (Panel *B*). Once again, the staining pattern resembled that expected for endoplasmic reticulum. These experiments demonstrated that the anti-hENT2 monoclonal antibodies, like the anti-hENT2 polyclonal antibodies, could be used to detect recombinant hENT2 by immunofluorescence.

Immunoprecipitation of hENT1 from BeWo Cell Lysates. To determine if the anti-hENT1 polyclonal antibodies were suitable for immunoprecipitations, the following experiment was undertaken. BeWo cells, which are known to possess both hENT1 and

hENT2 [7], were used since they possess a large number of NBMPR-binding sites and are expected to have a high abundance of hENT1 protein [113]. BeWo cell lysates were incubated with either anti-hENT1 polyclonal antisera or preimmune rabbit antisera and then with Protein G beads, which bind specifically to rabbit IgG. The antigen-antibody-Protein G complexes were washed, incubated with loading buffer, and the proteins released from the protein G beads were analysed by immunoblotting with anti-hENT1 monoclonal antibodies (Figure 4-8). The anti-hENT1 monoclonal antibodies recognized proteins of ~50-55 kDa, as well as high molecular weight species (>116 kDa) that were only present in the lane that contained material from the sample with anti-hENT1 polyclonal antisera. The preimmune sera and the PBS sample did not contain any immunoreactive material. Thus, this experiment demonstrated that the anti-hENT1 polyclonal antibodies could be used to immunoprecipitate endogenous hENT1 from BeWo cells.

4 C. Discussion

The main objective of the work described in this chapter was to design and generate antibodies specific for hENT1 and hENT2 for use in studies of cells that produced recombinant or endogenous hENT1 or hENT2. Unfortunately, anti-hENT1 antibodies specific for the extracellular loop between transmembrane domains 1 and 2 of hENT1 were not obtained despite multiple attempts using rabbits and mice. It was thought that perhaps the presence of the carbohydrate moiety on this loop may have prevented antibodies from recognizing the epitope. Anti-hENT1 and anti-hENT2 monoclonal and polyclonal antibodies were raised against the intracellular loops between transmembrane domains 6 and 7 of both proteins.

The anti-hENT1 monoclonal antibodies raised by Jennings *et al.*, [115] and the anti-hENT2 antibodies raised in this study were used to probe cells transiently transfected with plasmids encoding either hENT1-HA, hENT2-VSV-G or hHNP36-VSV-G. The anti-hENT1 monoclonal antibodies detected recombinant hENT1-HA in immunofluorescence and immunoblotting experiments. The anti-hENT1 polyclonal antibodies immunoprecipitated hENT1 from BeWo cell lysates. Both anti-hENT2 monoclonal and polyclonal antibodies detected recombinant hENT2-VSV-G and hHNP36 VSV-G in immunoblotting and immunofluorescence experiments. Thus, the anti-hENT1 and anti-hENT2 antibodies were specific and did not cross react with hENT2 or hENT1, respectively. This is the first time that anti-hENT2 antibodies have been generated.

Figure 4-1. Alignment of hHNP36 and mHNP36. The sequences of hHNP36 (GenBank accession number X86681) and mHNP36 (GenBank accession number X86682) were aligned using the BESTFIT program (Wisconsin Package Version 9.1, Genetics Computer Group) and found to be 92% similar and 90% identical. The seven transmembrane domains (underlined) were predicted using the hidden Markov model [147, 148]. The residues highlighted in bold type in the mouse protein were used to generate anti-mHNP36 antibodies as part of a glutathione-S-transferase fusion protein [103].

Figure 4-1

Alignment of hHNP36 and mHNP36

```
hHNP36     1 MASVCFINSFSAVLQGSLFGQLGTMPSTYSTLFLSGQGLAGIFAALAMLL 50
             |||| ||||| ||||||||||||||||||||||||||||||||||||||:
mHNP36     1 MASVWFINSFCAVLQGSLFGQLGTMPSTYSTLFLSGQGLAGIFAALAMLM 50

hHNP36    51 SMASGVDAETSALGYFITPYVGILMSIVCYLSLPHLKFARYYLANKSSQA 100
             |:|||||||:|||||||||| ||||:||||||||||||||||  | |||
mHNP36    51 SLASGVDAQTSALGYFITPCVGILLSIVCYLSLPHLKFARYYLTEKLSQA 100

hHNP36   101 QAQELETKAELLQSDE.NGIPSSPQKVALTLDLDLEKEPESEPDEPQKPG 149
             |||||||||||.|| ||:| |||. . ||||| ||||  ||:||||||
mHNP36   101 PTQELETKAELLQADEKNGVPISPQQASPTLDLDPEKEP..EPEEPQKPG 148

hHNP36   150 KPSVFTVFQKIWLTALCLVLVFTVTLSVFPAITAMV.TSSTSPGKWSQFF 198
             ||||| ||.|||||||||||||||||||||||||| ||| |||||  ||
mHNP36   149 KPSVFVVFRKIWLTALCLVLVFTVTLSVFPAITAMVTTSSNSPGKWGLFF 198

hHNP36   199 NPICCFLLFNIMDWLGRSLTSYFLWPDEDS.RLLPLLVCLRFLFVPLFML 247
             ||||||||||:|||||||||||||||||| .|||||||||||||||||||
mHNP36   199 NPICCFLLFNVMDWLGRSLTSYFLWPDEDSQQLLPLLVCLRFLFVPLFML 248

hHNP36   248 CHVPQRSRLPILFPQDAYFITFMLLFAVSNGYLVSLTMCLAPRQVLPHER 297
             ||||| .||||:| ||||||||||||||||||||||||||||||||||||
mHNP36   249 CHVPQHARLPIIFRQDAYFITFMLLFAVSNGYLVSLTMCLAPRQVLPHER 298

hHNP36   298 EVAGALMTFFLALGLSCGASLSFLFKALL 326
             |||||||||||||||||||||||||||||
mHNP36   299 EVAGALMTFFLALGLSCGASLSFLFKALL 327
```

Figure 4-2. Comparison of the hENT1 and hENT2 Large Intracellular Loop Regions. The sequences of the large intracellular loops of hENT1 and hENT2 were aligned using the BESTFIT program (Wisconsin Package Version 9.1, Genetics Computer Group) and found to be 48% similar and 28% identical. The sequences corresponding to the antigens used to generate the anti-hENT1 and anti-hENT2 antibodies are in bold print.

Figure 4-2

Comparison of the hENT1 and hENT2 Large Intracellular Loop Regions

```
                                                                  .
hENT1 226 LPRLEFYRYYQQLK..LEGPGEQETKLDLISKGEEPRAGK..... 263
          ||:|.| ||| . |   ..:.| ||| :|: .:|:. ::.
hENT2 213 LPHLKFARYYLANKSSQAQAQELETKAELLQSDENGIPSSPQKVALTLDL 262

                                  .
hENT1 264 ..EESGVSVSNSQPTNESHSIKAILKNI 289
            |... | .:.... :..|: .::..|
hENT2 263 DLEKEPESEPDEPQKPGKPSVFTVFQKI 290
```

Figure 4-3. Detection of Recombinant hENT1 and hENT2 by Immunoblot Analysis using Anti-hENT1 and Anti-hENT2 Monoclonal Antibodies. Cell lysates were prepared from CHOK1 cells that had been transiently transfected with pcDNA3/hENT1-HA, pcDNA3/hENT2-VSV-G or pcDNA3 as described in Chapter 2 H. Panels *A* and *B* depict immunoblots analyses performed in parallel. *A*, The immunoblot was incubated first with anti-hENT1 monoclonal mouse antibodies and then with horseradish peroxidase-conjugated donkey anti-mouse IgG antibodies. *B*, The immunoblot was incubated first with anti-hENT2 monoclonal antibodies and then with horseradish peroxidase-conjugated donkey anti-mouse IgG antibodies. Detection was by ECL as described in Chapter 2 R. In each panel, positions of the protein markers (in kDa) are shown on the left.

Figure 4-3

Detection of Recombinant hENT1 and hENT2 by Immunoblot Analysis using anti-hENT1 and anti-hENT2 Monoclonal Antibodies

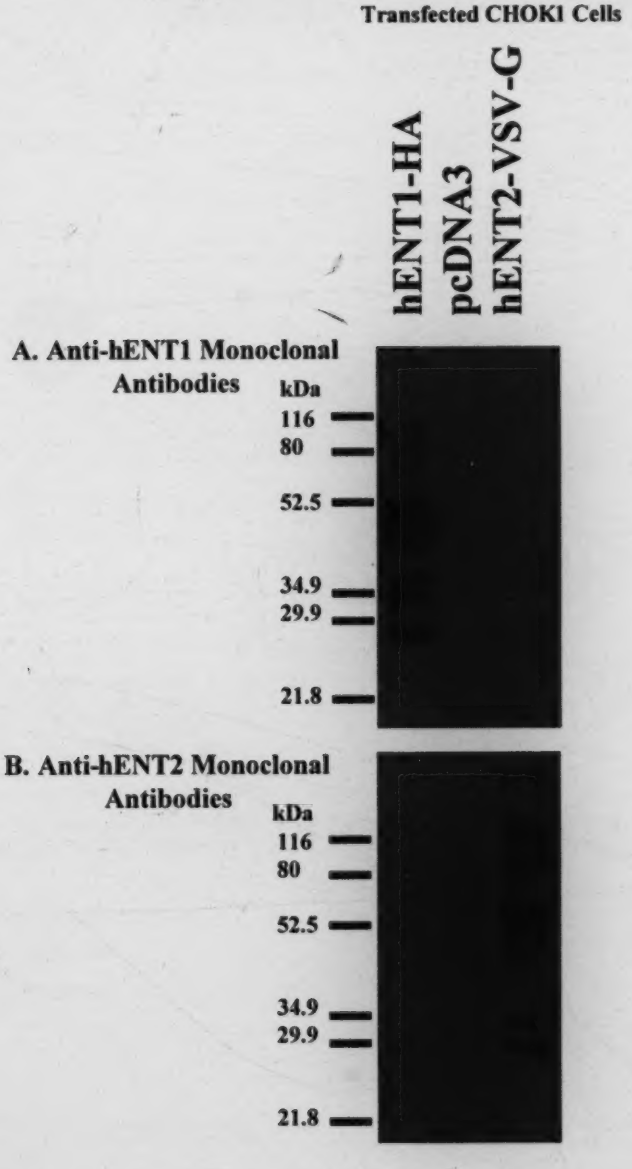

Figure 4-4. Detection of Recombinant hENT2 and hHNP36 by Immunoblot Analysis using Anti-hENT2 Polyclonal Antibodies. Cell lysates were prepared from CHOK1 cells that had been transiently transfected with pcDNA3/hENT1-HA, pcDNA3, pcDNA3/hENT2-VSV-G, pcDNA3/β-gal, pcDNA3/hHNP36, or pcDNA3 as described in Chapter 2 H. The immunoblot was incubated first with anti-hENT2 monoclonal mouse antibodies and then with horseradish peroxidase-conjugated donkey anti-mouse IgG antibodies. Detection was by ECL as described in Chapter 2 R. In each panel positions of the protein markers (in kDa) are shown on the right.

Figure 4-4

Detection of Recombinant hENT2 and hHNP36 by Immunoblot Analysis using Anti-hENT2 Polyclonal Antibodies

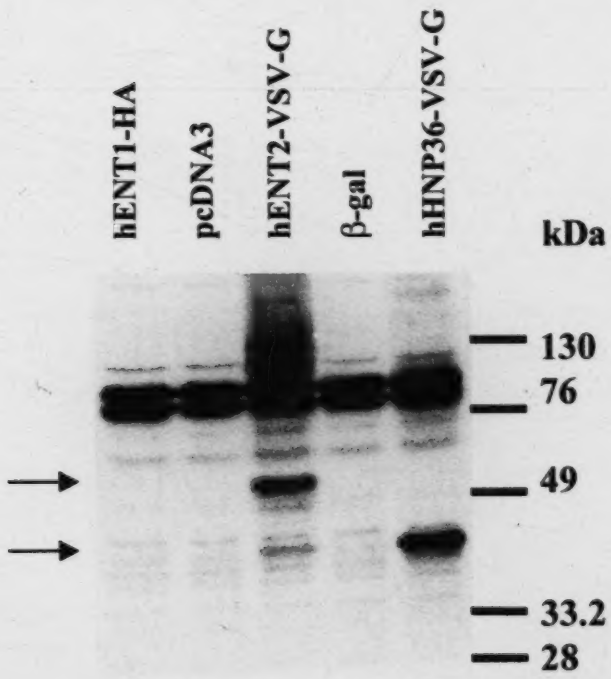

Figure 4-5. Detection of Recombinant hENT1 by Immunofluorescence Analysis using Anti-hENT1 Monoclonal Antibodies. CHOK1 cells transiently transfected with pcDNA3/hENT1-HA or pcDNA3 as described in Chapter 2 H. Cells were fixed, permeabilized, and incubated first with anti-hENT1 (*A*, *C* and *D*) and anti-HA antibodies (*B*, *C*, and *D*), then with Cy5-conjugated donkey anti-mouse IgG antibodies (*A*, *C*, *D*, and *E*) and Alexa 488-conjugated goat anti-rat IgG antibodies (*B*, *C*, *D*, and *E*). Cells were visualized using laser-scanning confocal microscopy. Overlapping images are shown in Panels *C*, *D*, and *E*. *Bars*, 10 μm.

Figure 4-5

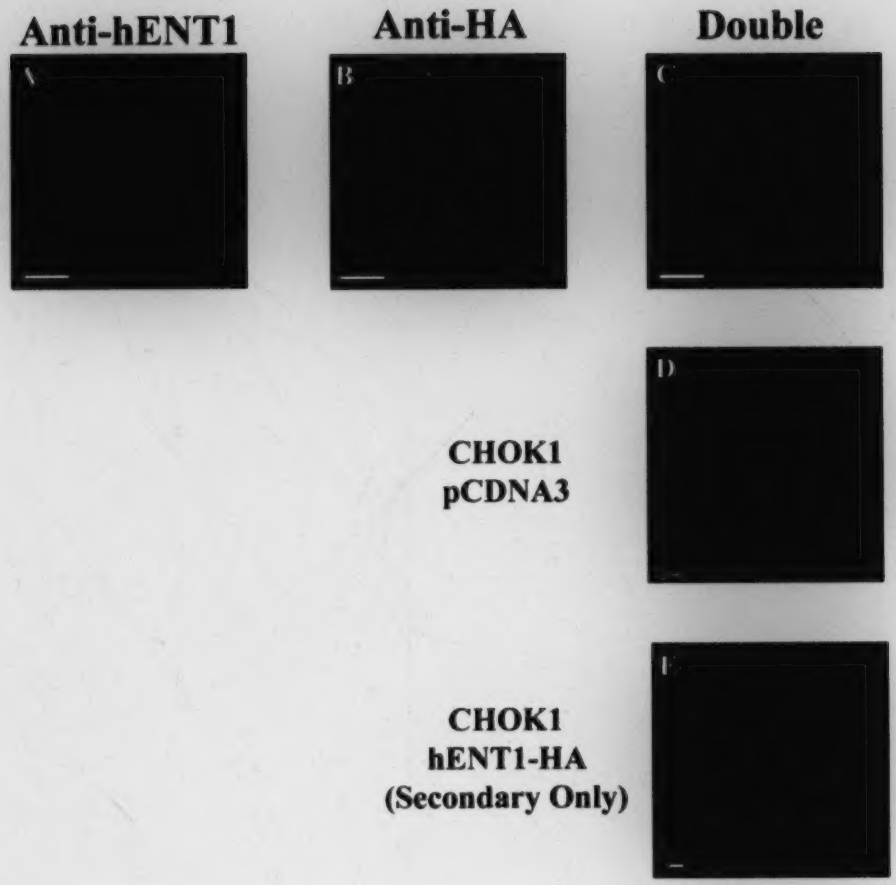
Anti-hENT1
Anti-HA
Double
A
B
C
D
E
CHOK1
hENT1-HA
CHOK1
pCDNA3
CHOK1
hENT1-HA
(Secondary Only)

Figure 4-6. Detection of Recombinant hENT2 and hHNP36 by Immunofluorescence Analysis using Anti-hENT2 Polyclonal Antibodies. CHOK1 cells were transiently transfected with pcDNA3/hENT2-VSV-G or pcDNA3/hHNP36-VSV-G as described in Chapter 2 H. Cells were fixed, permeabilized, and incubated first with anti-hENT2 (*A*, *C*, *D*, and *F*) and anti-VSV-G antibodies (*B*, *C*, *E*, and *F*), then with Alexa 488-conjugated donkey anti-rabbit IgG antibodies (*A*, *C*, *D*, and *F*) and Cy5-conjugated goat anti-mouse IgG antibodies (*B*, *C*, *E*, and *F*). Cells were visualized using laser-scanning confocal microscopy. Overlapping images are shown in Panels *C* and *F*. *Bars*, 10 μm.

Figure 4-6

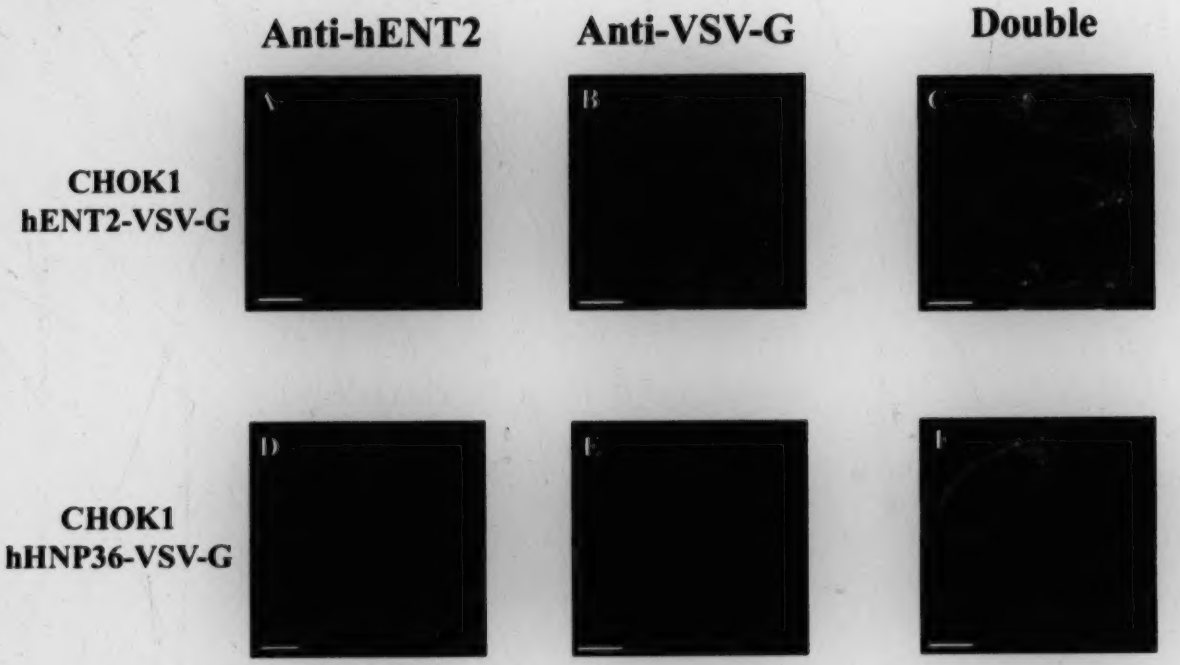
Anti-hENT2
Anti-VSV-G
Double
CHOK1
hENT2-VSV-G
CHOK1
hHNP36-VSV-G

Figure 4-7. Detection of Recombinant hENT2 by Immunofluorescence Analysis using Anti-hENT2 Monoclonal Antibodies. CHOK1 cells were transiently transfected with pcDNA3/hENT2-VSV-G or pcDNA3 as described in Chapter 2 H. Cells were fixed, permeabilized, and incubated first with anti-hENT2 (*A* and *B*) then with Cy5-conjugated donkey anti-mouse IgG antibodies (*A* and *B*). Cells were visualized using laser-scanning confocal microscopy. *Bars*, 10 μm.

Figure 4-7

Anti-hENT2 Monoclonal Antibody

CHOK1 hENT2-VSV-G

CHOK1 pcDNA3

Figure 4-8. Immunoprecipitation of hENT1 from BeWo Cell Lysates. BeWo cell lysates were prepared using RIPA buffer as described in Chapter 2 J. BeWo lysates were cleared by centrifugation and 200 µL-portions were incubated with either anti-hENT1 polyclonal antisera, preimmune sera or with PBS overnight at 4°C with continuous mixing. Protein G beads (100 µL of 10% v/v in RIPA buffer) were added to each tube and incubated at room temperature for 1 h. The antigen-antibody-Protein G bead complexes were washed 3 times with RIPA buffer. The proteins were solubilized and dissociated from the beads by the addition of 25 µL SDS-PAGE loading buffer to each sample followed by heating at 65°C. The proteins were resolved by SDS-PAGE and the immunoblot was prepared as described in Chapter 2 R. The immunoblot was incubated first with anti-hENT1 monoclonal mouse antibodies and then with horseradish peroxidase-conjugated donkey anti-mouse IgG antibodies. Detection was by ECL as described in Chapter 2 R. The positions of the protein markers (in kDa) are shown on the left.

Figure 4-8

Immunoprecipitation of hENT1 from BeWo Cell Lysates

Table 4-1. SurfacePlot Analysis Results. The amino acid sequences of hENT1 and hENT2 were submitted to the Alberta Peptide Institute (University of Alberta) for identification of potential antigens using the SurfacePlots algorithm [306, 307]. The amino sequences shown below for each protein were identified as being suitable for peptide synthesis as well as being antigenic. The lowercase "i" or "e" refers to the putative location of the amino acids (either intracellular or extracelllular).

hENT1		hENT2	
Residues	Sequence	Residues	Sequence
1-10 (i)	MTTSHQPQDR	1-10 (i)	MARGDAPRDS
55-64 (e)	ELSKDAQASA	226-235 (i)	KSSQAQAQEL
193-202 (e)	AIASGSELSE	246-255 (i)	ENGIPSSPQS
259-273 (i)	RAGKEESGVSVSNSQ	271-280 (i)	EPDEPQKPGK
419-428 (i)	KKVKPAEAET	314-323 (e)	MVTSSTSPGK

Chapter 5

5. Detection of hENT1 and hENT2 in HeLa and BeWo Cells

5. Abstract

The equilibrative nucleoside transporters, hENT1 and hENT2, mediate the well-studied *es* and *ei* activities. They are both comprised of 456 amino acids and have 11 putative transmembrane domains. Although, hENT1 has been detected before in placenta by immunohistochemistry and in human erythrocytes by immunoblotting, hENT2 has never been visualized. Endogenous hENT1 and hENT2 were detected by immunofluorescence studies in cultured BeWo and HeLa cells. hENT1 was mostly observed on the plasma membrane, while hENT2 was mostly observed in intracellular membranes. The staining patterns of the anti-hENT2 antibodies in HeLa and BeWo were shown to match those of two mitochondrial markers, MitoTracker Red dye and anti-cytochrome oxidase (subunit I) antibodies. In immunoblots, anti-hENT2 antibodies recognized proteins of ~45 kDa in enriched human liver mitochondrial preparations, suggesting the presence of an mitochondrial ENT protein. Anti-hENT2 antibodies failed to detect endogenous hENT2 in crude membrane fractions from either HeLa or BeWo cells, suggesting that hENT2 proteins are low abundance in these cell lines. The hHNP36 protein is a truncated version of hENT2 that was identified before hENT2 was isolated. *In silico* analysis revealed that hHNP36 may be a splice product of the hENT2/hHNP36 gene and this prediction was confirmed using a GeneScan RT-PCR technique. Also, analysis of the hENT2/hHNP36 gene, which resides on chromosome 11q13, revealed discrepancies at a few intron/exon boundaries, when compared to the sequence of the hENT2 cDNA. Searches of the Human Genome Project data in GenBank using the hENT2 and hHNP36 cDNA sequences confirmed that the initial description of the gene structure was incorrect and revealed the existence of a hENT2-like pseudogene.

5 A. Introduction

hENT1 and hENT2 mediate transport activities that are on the cell surface. However, results of recent studies suggest that intracellular nucleoside transporters may also be important. Nucleoside transport has been observed in at least two organelles, lysosomes [8] and mitochondria (K. M. King, P. Panayides, and C. E. Cass, unpublished observations), and NBMPR-binding sites have been detected in mitochondria [162, 163] (K. M. King, P. Panayides, and C. E. Cass, unpublished observations). Additionally, Mani and co-workers have described the isolation of crude nuclear and endoplasmic reticulum membranes from BeWo cells that contained functional *es* and *ei* activities [7]. These results suggest that the proteins mediating intracellular nucleoside transport processes may be related to the plasma membrane ENT proteins. To determine where endogenous hENT1 and hENT2 proteins are localized within cells, the antibodies that were raised in the previous chapter were used to detect and visualize hENT1 and hENT2.

hENT2 and hHNP36 are related in some fashion, since the latter protein contains is an abbreviated form of hENT2 (see Figure 4-1). The chromosomal location of hHNP36 gene is 11q13 [105]. The exon/intron boundaries were sequenced and it was demonstrated that the hHNP36 gene had 12 exons [105]. Multiple smaller transcripts were detected in pituitary and parathyroid glands, suggesting that the hHNP36 gene was differentially spliced in different tissues. The hENT2 open reading frame is found within the hHNP36 sequence and thus the hHNP36 gene is probably the hENT2 gene.

There are two discrepancies in the cDNA sequence of hHNP36 compared to that of the two isolated hENT2 cDNAs [78, 99]. The first discrepancy is a 43-base pair "deletion" in the hHNP36 cDNA that caused the hENT2 open reading frame to be missed in the initial description of hHNP36 [99] because it results in an open reading frame encoding a very short transcript. As a result of this deletion, the assignment of the splice site at intron 3/exon 4 boundary [105] fell into a region of what is now known to be the hENT2 cDNA sequence (Figure 5-1). The second discrepancy is in the region of the intron 11/exon 11/intron 12 boundary. Examination of that region in the two independently isolated hENT2 cDNA sequences [78, 99] revealed differences between those two sequences and the hHNP36 sequence identified by Williams and coworkers [105].

Belt and co-workers attempted to determine if the hHNP36 cDNA could encode a protein that transported nucleosides, by transiently transfecting the hHNP36 cDNA into COS-1 cells and testing for uridine uptake. Transfection of hHNP36 cDNAs into COS-1 cells did not lead to measurable nucleoside transport activity in COS-1 cells [99]. Thus, the question remained, was the hHNP36 mRNA a real transcript or was it a cloning artifact? If it was a real transcript, could it be produced and detected in cells? The experiments in this chapter provided answers to these questions.

The goals of the work described in this chapter were to:

1) detect endogenous hENT1 and hENT2 in human cell lines by immunofluorescence and immunoblot analysis and

2) identify hHNP36 transcripts in RNA isolated from human cell lines and to detect recombinant hHNP36 produced by transient transfection.

The newly created anti-hENT1 and anti-hENT2 antibodies were used to probe HeLa and BeWo cells in two different ways. HeLa and BeWo cells were analysed by indirect and direct immunofluorescence. Crude membranes were prepared and used for immunoblotting with the anti-hENT1 and anti-hENT2 antibodies. The anti-hENT1 antibodies recognized endogenous proteins in immunoblotting experiments, unlike the anti-hENT2 antibodies which did not recognize endogenous proteins from cell lines. In immunofluorescence experiments, endogenous hENT1 was mostly found on the plasma membrane of BeWo and HeLa cells, the nuclei/endoplasmic reticulum membranes of HeLa cells also contained hENT1. The anti-hENT2 polyclonal antibodies reacted mostly with intracellular epitopes, which were found to be mitochondrial upon closer examination using mitochondrial-specific antibodies and dyes, while the anti-hENT2 monoclonal antibodies did not give a signal in immunofluorescence experiments.

To determine if hHNP36 transcripts exists, a fluorescent-based RT-PCR method was used because it detects small amounts of DNA and discriminates between similarly-sized, small fragments (<200 bp). Two primers were designed such that both the hHNP36 and the hENT2 transcript would be detected. The relationship between hENT2 and hHNP36 was clarified and hHNP36 mRNA was found to varying degrees in all cell lines examined thus far. Lastly, while attempting to verify the structure of the hENT2 gene, a hENT2 pseudogene was identified.

5 B. Results

5 B. I. Immunofluorescence Analysis of Endogenous hENT1 and hENT2 in Human Cell Lines

Two cell lines, HeLa and BeWo, both of which are known to possess *es* and *ei* transport activities and also hENT1 and hENT2 mRNA [7] (K. A. Graham, D. Mowles and C. E. Cass, unpublished observations) were selected for studies of the endogenous transporters. To visualize hENT1 and hENT2 in HeLa and BeWo cells and to determine the locations of hENT1 and hENT2 in the HeLa and BeWo cells, immunofluorescence confocal microscopy experiments using anti-hENT1 monoclonal and anti-hENT2 polyclonal antibodies were undertaken. These experiments represented the first attempts to visualize endogenous hENT1 and hENT2 in these cell lines by immunofluorescence.

Using the same methanol fixation/permeabilization conditions of the experiments described in Chapter 4 B II, BeWo and HeLa cells were labelled with either anti-hENT1 monoclonal or anti-hENT2 polyclonal antibodies and examined using confocal immunofluorescence microscopy (Figure 5-2). For BeWo cells (Panels *A* and *B*), anti-hENT1 antibodies stained mainly the plasma membrane (Panel *A*), whereas anti-hENT2 antibodies stained mainly intracellular membranes (Panel *B*). Similar results were found for HeLa cells (Panels *C* and *D*); anti-hENT1 antibodies stained mainly the plasma membrane and the nucleoplasm (Panel *C*), whereas anti-hENT2 antibodies stained mainly

intracellular membranes (Panel *D*). Comparison of the two staining patterns in both cell lines suggested that there was very little overlap of anti-hENT1 and anti-hENT2 staining. Although the mainly plasma membrane localization of the hENT1 staining was expected, the hENT2 staining pattern (absence on plasma membranes and mainly intracellular staining) was unexpected since hENT2 is known to mediate transport across plasma membranes.

Next, two different methods were employed to determine if more structured internal anti-hENT1 staining could be detected in BeWo cells. First, gentler fixation and permeabilization conditions (paraformaldehyde and digitonin) were used and BeWo cells were analysed by indirect immunofluorescence with anti-hENT1 monoclonal antibodies examined using confocal immunofluorescence microscopy (Figure 5-3). Although anti-hENT1 antibodies stained mainly the plasma membrane of BeWo cells, intense intracellular staining was also observed in most cells (Panel *A*). Thus, by using different fixation and permeabilization conditions, the intracellular hENT1 sites became visible, demonstrating that fixation and permeabilization may change the epitope recognized by the anti-hENT1 monoclonal antibodies. Secondly, BeWo cells were fixed and permeabilized using methanol fixation and analysed by direct immunofluorescence with anti-hENT1 monoclonal antibodies directly conjugated to the fluorophore Alexa 546. Once again, the anti-hENT1 antibodies stained mainly the plasma membrane of BeWo cells, but intense intracellular staining was also observed in most cells (Panel *B*). The anti-hENT1 antibodies conjugated to Alexa 546 were used at a higher concentration than the antibody preparations used in indirect immunofluorescence, suggesting that antibody concentration may also make a difference in the visualization of the internal hENT1 in BeWo cells.

The methanol fixation/permeabilization conditions were used in the experiments of Figure 5-4 to assess the reactivity of the anti-hENT2 monoclonal antibodies with BeWo and HeLa cells by confocal immunofluorescence microscopy. However, no signals were obtained using antibodies produced by three different hybridoma clones, all of which were isolated from the same successful fusion. Other hybridoma clones are currently being investigated, but thus far, the anti-hENT2 monoclonal antibodies have only detected overproduced recombinant hENT2 (see Figure 4-4*B*). These results were consistent with the conclusion that hENT2 is a low abundance protein in BeWo and HeLa cells, and may also indicate that the monoclonal antibodies have low affinities for hENT2.

Mitochondrial localization of anti-hENT2 polyclonal antibody staining. To further investigate the intracellular staining seen with the anti-hENT2 antibodies, double-label immunofluorescence experiments with the anti-hENT2 polyclonal antibodies and organellar markers were undertaken. Mitochondria were examined first since they are distributed throughout cells and the anti-hENT2 staining pattern had suggested a wide-spread distribution. The two mitochondrial markers used were the mitochondrial-specific MitoTracker Red dye and anti-cytochrome oxidase (subunit I) antibodies. In the experiments of Figure 5-5, BeWo cells were incubated with MitoTracker Red dye prior to fixation and then incubated with anti-hENT2 polyclonal antibodies. In Panels *A* and *B*, both the MitoTracker Red dye and the anti-hENT2 antibodies, respectively, stained the

intracellular membranes of BeWo cells. When the images in Panels *A* and *B* were superimposed in Figure 5-5 *C*, co-localization was observed, suggesting that the anti-hENT2 antibodies were staining mitochondria.

The mitochondrial-hENT2 co-localization experiments were repeated in HeLa cells. In Panels *D* and *E*, both the MitoTracker Red dye and the anti-hENT2 antibodies, respectively, stained the intracellular membranes of HeLa cells. When the images in Panels *D* and *E* were superimposed in Panel *F*, co-localization was observed, again suggesting that the anti-hENT2 antibodies were staining mitochondria.

To confirm the finding that the anti-hENT2 antibodies were staining mitochondria, a second set of immunofluorescence experiments were undertaken with a different mitochondrial marker, anti-cytochrome oxidase (subunit I) antibodies. In the experiments of Figure 5-6, BeWo and HeLa cells were incubated with anti-cytochrome oxidase (subunit I) and anti-hENT2 antibodies. In Panels *A* and *D*, the cells were stained with anti-cytochrome oxidase (subunit I) antibodies, while in Panels *B* and *E*, they were stained with anti-hENT2 antibodies. Incubations with both antibodies gave similar intracellular staining patterns. When the images in Panels *A* and *D*, and in *B* and *E* were superimposed (Panels *C* and *F*, respectively), co-localization was seen in both BeWo and HeLa cells. The results from these experiments suggested the presence of a hENT2-like protein in mitochondria.

In immunofluorescence experiments in which the anti-hENT2 polyclonal antibodies were incubated with polypeptides that contained the immunizing epitope prior to incubation with cells, the intracellular staining was not diminished. The anti-hENT2 polyclonal antibodies were incubated with either GST or the GST-eif fusion proteins (both at 20 times the protein concentration of the antibodies) overnight at 4°C on a rocker. The next day, methanol-fixed BeWo and HeLa cells were incubated with either i) anti-hENT2 polyclonal antibodies and the appropriate secondary antibodies, ii) anti-hENT2 polyclonal antibodies with 20-fold more GST-eif fusion protein and the appropriate secondary antibodies, iii) the anti-hENT2 polyclonal antibodies with 20-fold more GST protein and the appropriate secondary antibodies, iv) preimmune sera and the appropriate secondary antibodies or v) the appropriate secondary antibodies only and immunofluorescence was determined as described in Chapter II M. The intracellular staining pattern for the first three conditions was the same was seen in Figure 5-2 (Panels *B* and *D*) for BeWo and HeLa cells, respectively. Also, there was no staining observed in cells incubated with either the preimmune sera or the secondary antibodies only. These results suggested that the mitochondrial staining observed with the anti-hENT2 antibodies may be due to interaction with mitochondrial proteins other than hENT2. Additional experimental work will be required to determine the relationship of the immunoreactive material in mitochondria with hENT2.

5 B. II. Analysis of Enriched Human Liver Mitochondria and Human Cell Membrane Samples with Anti-hENT1 and Anti-hENT2 Antibodies by Immunoblot Analysis

To confirm the observation that anti-hENT2 antibodies reacted with an immunoreactive species in mitochondria, enriched human and rat liver mitochondria were analysed by immunoblotting techniques using anti-hENT1 and anti-hENT2 monoclonal antibodies. Crude membrane preparations from BeWo, HeLa and human erythrocytes were also analysed simultaneously.

Crude membranes were prepared from HeLa and BeWo cells as described in Chapter 2 N. Enriched human and rat mitochondrial fractions were isolated from liver samples as described in Chapter 2 P. The controls for the experiments were solubilized membranes from CHOK1 cells transiently transfected with the plasmids encoding either hENT1-HA or hENT2-VSV-G and human erythrocyte membranes, which contain only hENT1, that were prepared as described in Chapter 2 O.

In Figure 5-7*A*, the anti-hENT1 monoclonal antibodies recognized proteins from CHOK1 cells transfected with plasmids containing the hENT1-HA cDNA, where the main reactive species were ~50-55 kDa, and proteins from human erythrocyte membranes, where the reactive species were ~60-70 kDa. The anti-hENT1 monoclonal antibodies did not detect any proteins in CHOK1 cells that were transfected with the pcDNA3 vector or with the plasmid carrying the hENT2-VSV-G cDNA nor any proteins in human or rat mitochondria.

In Figure 5-7*B*, the anti-hENT2 monoclonal antibodies recognized proteins from CHOK1 cells transfected with plasmids containing the hENT2-VSV-G cDNA, where the main reactive species were ~52-57 kDa and protein from enriched human mitochondria, where the reactive species were ~48-50 kDa. The anti-hENT2 monoclonal antibodies did not detect proteins in CHOK1 cells that were transfected with vector alone or with the plasmid carrying the hENT1-HA cDNA or proteins in human erythrocyte membranes or proteins in rat liver mitochondria.

In Figure 5-8*A*, the anti-hENT1 monoclonal antibodies recognized proteins from CHOK1 cells transfected with plasmids containing the hENT1-HA cDNA, where the main reactive species were ~50-55 kDa. The protein bands detected below 50 kDa may have been due to the degradation of the sample. The antibodies also recognized proteins from human erythrocyte ghosts and membranes, where the reactive species were ~60-70 kDa, and proteins from HeLa and BeWo cell crude membranes, where the reactive species were ~50-55 kDa. The human erythrocyte ghost sample did not contain protease inhibitors, thus there was some degradation as can be seen by the band migrating at ~20 kDa. However, the human erythrocyte membrane sample contained protease inhibitors, and little or no degradation products were detected. The anti-hENT1 monoclonal antibodies did not detect any proteins in CHOK1 cells that were transfected with the plasmid carrying the hENT2-VSV-G cDNA.

In Figure 5-8*B*, the anti-hENT2 monoclonal antibodies recognized proteins from CHOK1 cells transfected with plasmids containing the hENT2-VSV-G cDNA, where the main reactive species were ~52-57 kDa . The anti-hENT2 monoclonal antibodies did not detect any proteins in CHOK1 cells that were transfected with the plasmid carrying the hENT1-HA cDNA, in human erythrocyte membranes, or in HeLa or BeWo crude membranes. The protein bands below 50 kDa may have been due to the degradation of

the sample.

5 B. III. Detection of the hHNP36 Transcript in Four Human Cell Lines using GeneScan RT-PCR Technology

The basis for the putative existence of the hHNP36 transcript lies in the discovery of a potential alternative splice site that was reported by Williams and colleagues [105]. The sequence at the intron 3/exon 4 boundary of hHNP36 assigned by Williams *et al.* [105] corresponds to the hENT2 coding sequence, suggesting that there may be alternative splicing at this site. If an alternate splice site does exist within this region, it would explain how Williams *et al.*, [103] isolated the hHNP36 cDNA rather than the hENT2 cDNA[103]. The hHNP36 cDNA was isolated from a human heart cDNA library by hybridization screening using the mHNP36 cDNA as a probe [103]. The hHNP36 cDNA differs from the hENT2 cDNA in that it lacks 43 bases near the 5' end of the sequence [99]. According to the consensus sites for splicing [310], introns must end with an "AG" and the putative splice site does have an "AG" at the end of the putative intron (Figure 5-9).

Thus, to demonstrate that hENT2 and hHNP36 were the splice products from the same gene, two primers, GShENT2-F and GShENT2-R (sequences are described in Chapter 2 G II), were selected to distinguish between hHNP36 and hENT2 transcripts (Figure 5-9). If the hHNP36 transcript was produced, the expected PCR product size would be approximately 170 bp, whereas the expected PCR product size for the hENT2 transcript would be approximately 230 bp (Figure 5-9). Because the size difference between these two PCR products was so small and the likelihood that hHNP36 transcripts were low abundance, a sensitive RT-PCR methodology using GeneScan software on the ABI 310 Genetic Analyzer was employed to detect both transcripts. The GeneScan technique resolves and detects small fragments of DNA (<200 bp) by capillary electrophoresis and fluorescence technology, respectively.

Total RNA was isolated from four human cell lines: BeWo, HeLa, HEK293 and CEM, of which BeWo, HeLa, and HEK293 cells possess hENT1-mediated *es* and hENT2-mediated *ei* activities and CEM cells possess only hENT1-mediated *es* activity [7, 113, 114, 120, 139] (K. A. Graham, D. Mowles and C. E. Cass, unpublished observations; for more information on HEK293 cells, see the next chapter). The RNA was reverse transcribed using an oligo dT primer and the resulting single-stranded DNAs were used in a PCR reaction that contained the two primers described above (GShENT2-F and GShENT2-R). The results are shown in Figure 5-10. hENT2 and hHNP36 transcripts were detected in all four cell lines. The existence of hENT2 mRNA in CEM cells was unexpected, since CEM cells do not possess detectable *ei* activity [120, 139]. Also the amount of hENT2 and hHNP36 mRNA differed for each cell line. The hENT2 transcripts were always the most dominant transcripts, while the hHNP36 transcripts were found in small quantities. HeLa and HEK293 cells had the most hHNP36 transcripts relative to hENT2 transcripts and BeWo and CEM cells had the least. The PCR products obtained from each cell line were isolated and the sequences were shown to

correspond to those expected for the hENT2 and hHNP36 sequences by DNA sequencing.

5 B. IV. Determination of the hENT2/hHNP36 Exon 11/Intron 11/Exon 12 Boundaries

A second sequence discrepancy was noted between the hENT2 and hHNP36 cDNAs (see Figure 5-11) in the region of the exon 11/intron 11/exon 12 boundaries. This sequence difference was examined more closely by comparing the two hENT2 cDNAs and hHNP36 with the draft of the human genome project [66] using the BLAST algorithm [281].

Each cDNA was entered into the BLAST algorithm page found at the National Center for Biotechnology Information website (http://www.ncbi.nlm.nih.gov/genome/seq/HsBlast.html). The searches resulted in the identification of a contig from human chromosome 11q13 that contained the various cDNA sequences (GenBank accession number NT_009296). This stretch of DNA sequence also contained the hENT2/hHNP36 gene (designated SLC29A2, which stands for Solute Carrier Family 29 member 2). When the intron/exon boundary sequences in the Williams paper [105] were compared to the sequence found in the contig, there were sequence differences (possibly due to sequencing errors in the former) in the region of the exon 11/intron 11/exon 12 boundaries. The corrected exon 11/intron 11/exon 12 boundaries are given in Figure 5-11 Panel *A* according to the sequence contig that was retrieved from GenBank. Also, when the other intron/exon boundaries were verified against the human genome draft sequence, it was found that the intron 6 donor had been incorrectly identified [105] and was lacking two base pairs (See Figure 5-11 Panel *B*).

5 B. V. Identification of a hENT2/hHNP36 Pseudogene in the Human Genome

A graphical view (see Figure 5-12) of the comparison of the hENT2 cDNA sequences to the draft human genome sequence confirmed that there were twelve exons in the hENT2/hHNP36/SLC29A2 gene. However approximately 77, 000 bp upstream there were 10 nearly exact matches with the first 10 exons of hENT2/hHNP36. These 10 sequences were organized in a similar manner to that of SLC29A2 (the actual hENT2/hHNP36 gene), suggesting the existence of a pseudogene or perhaps a different, but closely related, gene. Closer examination of the 10 sequences revealed that their coding sequences corresponded to only a portion of the first exon and to exons 2-10 of the hENT2 gene. The first exon of the pseudogene, in addition to lacking the first 50 bp of exon 1 of SLC29A2 (which corresponded to the 5' untranslated region), also had a "C" inserted at the potential exon 1/intron 1 boundary (see Figure 5-13) which breaks the consensus splice site described by Padgett [310]. This insertion creates a defective splice site, which would probably result in a non-functional gene or pseudogene. A defect at such an important point in the gene structure is a distinguishing feature of pseudogenes

[311]. Thus, this sequence should be designated ΨhENT2/hHNP36/SLC29A2 since it is next to the homologous functional gene and has a highly similar organization to the functional gene, two characteristics of pseudogenes [311]. This type of pseudogene, probably caused by gene duplication, has been reported before as in the case of BRCA1 [311].

5 C. Discussion

The anti-hENT1 and anti-hENT2 antibodies were used to detect hENT1 and hENT2 in tissue culture cells by immunofluorescence and immunoblotting experiments. The localization of endogenous hENT1 and hENT2 was similar in two human cell lines, BeWo and HeLa. The anti-hENT1 monoclonal antibodies stained mostly plasma membranes in BeWo and HeLa cells, although there was also staining of nuclear membranes in HeLa cells and when BeWo cells were fixed with paraformaldehyde and permeabilized with digitonin, intracellular staining also became apparent. Direct immunofluorescence analysis of BeWo cells also demonstrated intracellular staining. This intracellular staining may have reflected transporters that were being synthesized and processed in the endoplasmic reticulum membrane which is contiguous with the nuclear membrane. The *es* and *ei* nucleoside transport activities have been reported in crude nuclear/endoplasmic reticulum membranes from BeWo cells [7].

In experiments with both BeWo and HeLa cells, the anti-hENT2 polyclonal antibodies did not stain plasma membranes as was expected, but rather stained intracellular membranes. Further experiments demonstrated that the anti-hENT2 intracellular membrane staining co-localized with two different mitochondria-specific markers, MitoTracker Red and anti-cytochrome oxidase (subunit I) antibodies. These results were consistent with the conclusion that the proteins recognized by anti-hENT1 monoclonal and anti-hENT2 polyclonal antibodies have different subcellular locations in both BeWo and HeLa cells. The anti-hENT2 monoclonal antibodies, which had detected recombinant hENT2 in the immunofluorescence experiments of Chapter IV, did not detect endogenous protein in HeLa and BeWo cells by immunofluorescence analysis, but did detect recombinant protein. These results suggested either that hENT2 was present in very low amounts at the plasma membrane or perhaps the anti-hENT2 monoclonal antibodies had low affinity for hENT2. Also, the inability of the anti-hENT2 polyclonal antibody staining to be blocked by using GST-eif polypeptide suggests that the mitochondrial staining may not be specific, despite the lack of staining with the preimmune sera.

Crude membranes from BeWo and HeLa cells, human erythrocytes and enriched human mitochondria were probed with anti-hENT1 and anti-hENT2 antibodies. The anti-hENT1 monoclonal antibodies recognized proteins of ~50 kDa in the BeWo and HeLa preparations, but did not recognize any proteins in the enriched human mitochondrial fraction. The differences in hENT1 mobility among the tissue culture cell lines and erythrocytes were probably due to differences in glycosylation. In contrast, the anti-hENT2 antibodies, which recognized recombinant hENT2-VSV-G and hHNP36-

VSV-G in transiently transfected cells (see Figures 4-6 and 4-7), did not detect immunoreactive material in crude membrane fractions of HeLa or BeWo cells, suggesting that endogenous hENT2 was present in very low quantities. However, the anti-hENT2 antibodies detected immunoreactive material in enriched human mitochondrial fractions that migrated with an apparent molecular weight of 45 kDa, suggesting that there was a hENT2-like protein in mitochondria. The specificity of the reactivity of the antibodies with the 45 kDa material will need to be determined by the demonstration that immunostaining can be blocked by addition of an excess of GST-eif polypeptide. The intracellular versions of hENT1 and hENT2 may be important in maintaining nucleoside concentrations in different parts of the cell. The rationale for having a nucleoside transporter in mitochondria would be to provide precursors for use by the mitochondrial DNA replication machinery. Mitochondria possess nucleoside kinases, such as deoxyguanosine kinase [158] and deoxythymidine kinase 2 [159], which convert nucleosides to nucleotides.

Using anti-hENT1 monoclonal and anti-hENT2 polyclonal antibodies in immunoblotting experiments, Jennings *et al.*, [115] demonstrated that the hENT1 and hENT2 proteins have a reciprocal distribution among various parts of the human brain. Crude membranes were prepared from different regions of a human brain obtained and dissected at autopsy. The anti-hENT1 monoclonal antibodies recognized proteins that were approximately 45 kDa , while the anti-hENT2 polyclonal antibodies recognized proteins, of approximately 50 kDa and ~38-40 kDa in the human brain membrane preparations; the latter may have been endogenous hHNP36. hENT1 was more abundant in the frontal and parietal lobes of the cerebral cortex, thalamus, midbrain and basal ganglia while hENT2 was concentrated in the cerebellum and brainstem regions, especially in the pons. The hENT1 distribution pattern seemed to mirror that of the adenosine A(1) receptor suggesting that the two proteins play an important role together in modulating adenosine concentration in those areas of the brain. The reason for this particular distribution of hENT1 and hENT2 in the brain is unknown.

The relationship between hENT2 and hHNP36 has not been established. The initial description of hHNP36 and mHNP36 [103] was hard to interpret after the isolation of the hENT2 cDNAs [78, 99], since the two shorter hydrophobic and clearly membrane proteins had been reported to be in nucleoli. [103] The mHNP36 cDNA was used for hybridization screening of a human heart library, which resulted in the isolation of a similar human cDNA [103]. The hHNP36 cDNA, when compared to the two independently isolated hENT2 cDNAs, exhibits a 43-base pair deletion. In contrast, the mHNP36 cDNA [103] contains the 43 base-pairs that are absent from the hHNP36 cDNA. Examination of the hHNP36 gene structure reported by Williams *et al.*, [105] revealed, since known hENT2 coding sequence was present in putative intronic sequence, that alternative splicing could be the explanation for the existence of hHNP36.

Comparison of the two sequences of the independently isolated hENT2 cDNAs with the hHNP36 gene structure as described by Williams *et al.*, [105] revealed another discrepancy at the exon 11/intron 11/exon 12 boundary. There seemed to be DNA sequence missing from this exon/intron/exon boundary, which was present in the two

hENT2 cDNAs as well as in the hHNP36 cDNA. The initial report describing the hHNP36 gene made reference to non-consensus donor and acceptor splice sites for introns 6 and 11, respectively [105], which was unlikely, since the donor sites always have a GT and acceptor sites are always C/TAG, where the AG are always conserved [310].

The GeneScan RT-PCR strategy was used to determine if hHNP36 transcripts existed in RNA isolated from human tissue culture cells. These experiments demonstrated that all of the cell lines tested (HeLa, BeWo, CEM and HEK293) had transcripts for hENT2 and, to a much lesser degree, hHNP36, suggesting that alternative splicing was occurring in the gene. The amount of hENT2 PCR product was always found in greater quantities than that of hHNP36, suggesting that more hENT2 mRNA was present. The amount of hHNP36 PCR product differed from cell line to cell line, suggesting that different amounts of hHNP36 mRNA were produced in each cell line and that the degree of splicing of the hENT2/hHNP3 gene was probably regulated in each line.

The GenBank database was frequently searched using the hENT2 cDNAs during the course of this study to verify the structure of the hENT2 gene. Recently, with the completion of the draft version of the human DNA sequencing project [66], a positive result was found. The results of this search enabled the identification of the correct exon 11/intron 11/exon 12 and intron 6/exon 7 boundaries. The search of the human genome also identified a potential human nucleoside transporter pseudogene in a stretch of DNA that is upstream of the hENT2 gene, and is nearly identical to the first 10 exons and 9 introns of the hENT2 gene. The crucial difference between the two DNA sequences is the presence of an insertion at the splice site at the end of the first exon and the deletion of 50 base pairs from the 5' untranslated region of exon 1 of the pseudogene. This insertion would result in a non-functional splice site, resulting in either a protein different from hENT2 or non-functional gene. A pseudogene, such as this one, that is adjacent to its functional homologue was probably created by a gene duplication event [311].

The studies in this chapter represent the first attempts to detect endogenous hENT1 and hENT2 in human tissue culture cells by immunofluorescence and immunoblotting. The fact that hENT2 may be a low abundance protein is not surprising given that *ei* activity is the smaller equilibrative nucleoside transport component in BeWo and HeLa cells [113, 114]. Also, the presence of a hENT2-like immunoreactive species as well as the potential for alternate splicing of the hENT2 gene suggest that this gene may encode for proteins that have different functions as well as different locations.

Figure 5-1. Putative Structure of the hENT2/hHNP36 Gene. Shown here is the exon gene map of the hENT2/HNP36 gene adapted from [105]. The single asterisk denotes the putative alternative splice site in exon 4, which results in the HNP36 transcript. The double asterisk denotes that a discrepancy lies in the assignment of the exon 11, intron 11 and exon 12 boundaries.

Figure 5-1 Exon Structure of hENT2/HNP36 Gene

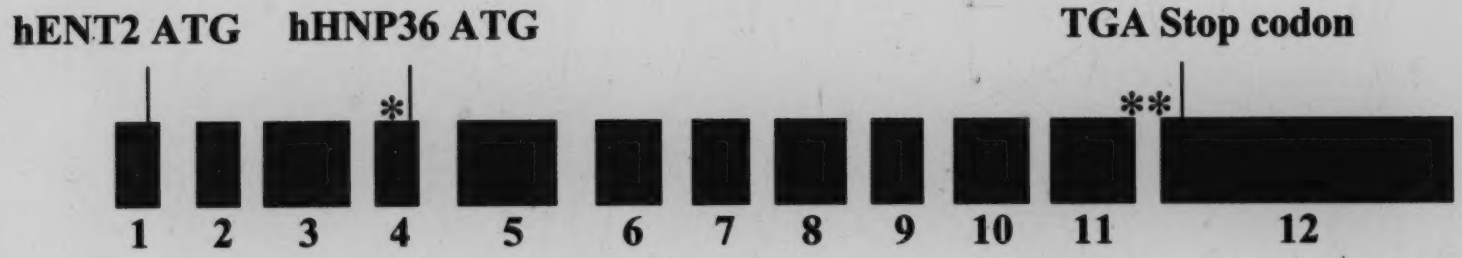

* Putative alternative splice site in exon 4.

** Discrepancy between cDNA sequence and published exon/intron boundaries.

Figure 5-2. Detection of Endogenous hENT1 and hENT2 in BeWo and HeLa Cells by Immunofluorescence Analysis. BeWo and HeLa cells were fixed, permeabilized, and incubated first with anti-hENT1 monoclonal (*A* and *C*) and anti-hENT2 polyclonal antibodies (*B* and *D*) then with Cy5-conjugated donkey anti-mouse IgG (*A* and *C*) and Alexa 488-conjugated donkey anti-rabbit IgG antibodies (*B* and *D*). Cells were visualized using laser-scanning confocal microscopy. *Bars*, 10 μm.

Figure 5-2

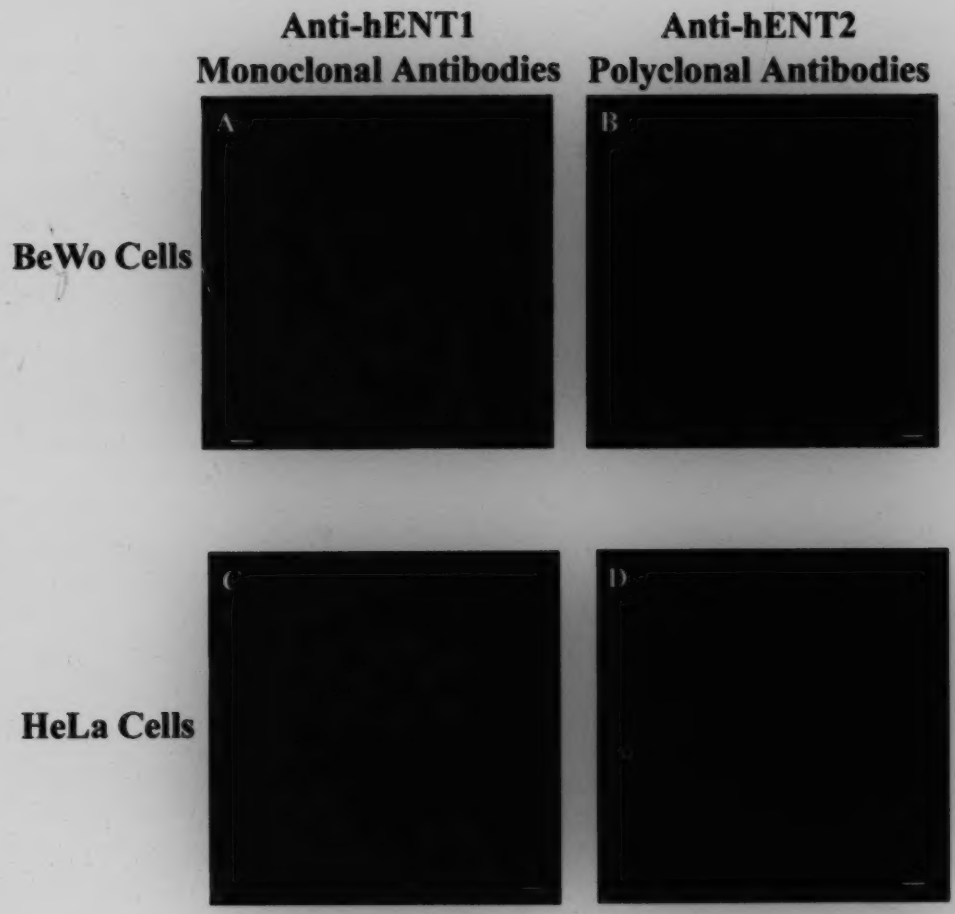
Anti-hENT1
Monoclonal Antibodies
Anti-hENT2
Polyclonal Antibodies
A
B
BeWo Cells
C
D
HeLa Cells

Figure 5-3. Detection of Intracellular hENT1 in BeWo Cells by Immunofluorescence Analysis. In Panel *A*, BeWo cells were fixed with 4% paraformaldehyde, permeabilized with 10 μg/mL digitonin as described in Chapter 2 M and incubated first with anti-hENT1 monoclonal and then with Alexa 594-conjugated donkey anti-mouse IgG. In Panel *B*, BeWo cells were fixed and permeabilized with 100% cold methanol and then incubated with anti-hENT1 monoclonal antibodies conjugated to Alexa 546. Cells were visualized using laser-scanning confocal microscopy. *Bars*, 10 μm.

Figure 5-3

BeWo Cells

Indirect immunofluorescence using anti-hENT1 monoclonal antibodies in digitonin-permeabilized cells

Direct immunofluorescence using Alexa 546-conjugated anti-hENT1 monoclonal antibodies in methanol-permeablized cells

Figure 5-4. Absence of Detection of Endogenous hENT2 in BeWo Cells by Immunofluorescence Analysis using Anti-hENT2 Monoclonal Antibodies. BeWo cells were fixed, permeabilized, and incubated first with anti-hENT2 (*A*, *B*, and *C*) then with Cy5-conjugated donkey anti-mouse IgG antibodies (*A*, *B*, and *C*). Cells were visualized using laser-scanning confocal microscopy. *Bars*, 10 μm.

Figure 5-4

BeWo Cells

Anti-hENT2 Monoclonal Antibodies (10H11G10)

Anti-hENT2 Monoclonal Antibodies (10H11B7)

Anti-hENT2 Monoclonal Antibodies (10 H1A10)

Figure 5-5. Mitochondrial Co-localization of Anti-hENT2 Antibody Staining with MitoTracker Red Dye in BeWo and HeLa Cells. BeWo and HeLa cells were incubated with MitoTracker Red Dye (100 nM final concentration) for 30 min and washed with media twice prior to fixation and permeabilization. The MitoTracker Red signal is seen in Panels *A*, *C*, *D*, and *F*. Next, cells were incubated first with anti-hENT2 (*B*, *C*, *E*, and *F*) then with Alexa 488-conjugated donkey anti-rabbit IgG antibodies (*B*, *C*, *E*, and *F*). Cells were visualized using laser-scanning confocal microscopy. Overlapping images are shown in Panels *C* and *F*. *Bars*, 10 μm.

Figure 5-5

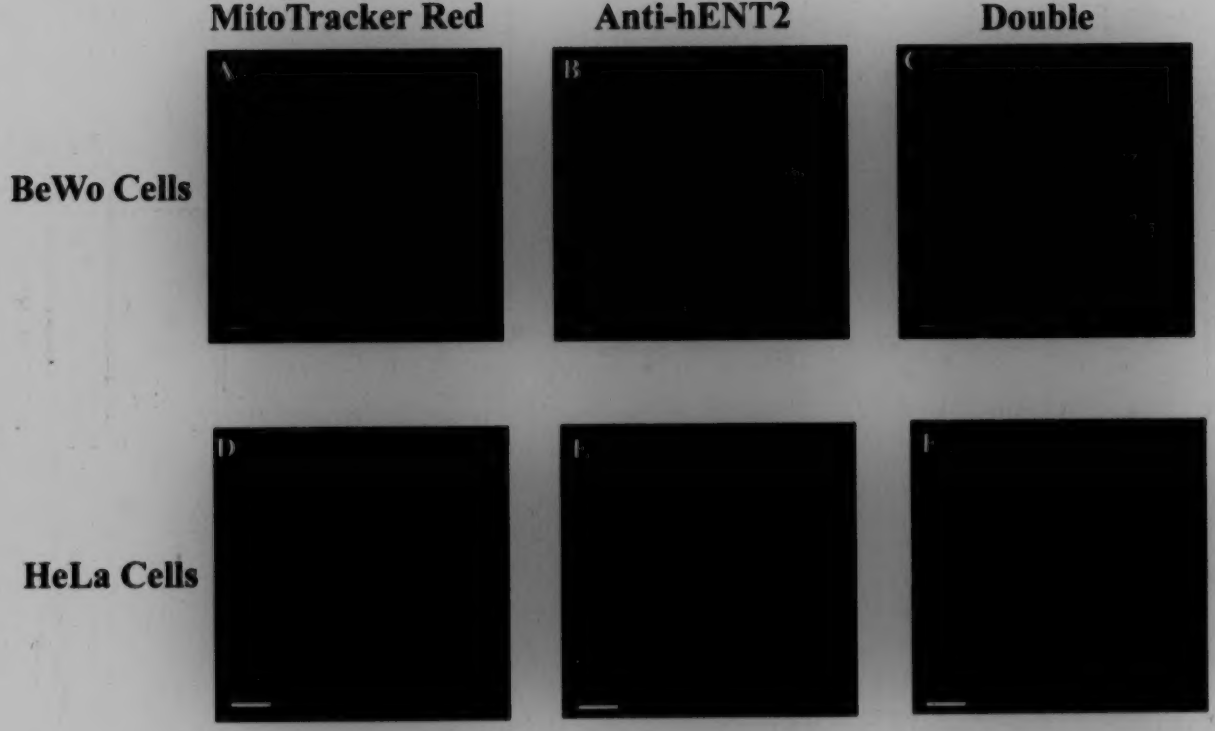
MitoTracker Red
Anti-hENT2
Double
BeWo Cells
HeLa Cells
A
B
C
D
E
F

Figure 5-6. Mitochondrial Co-localization of Anti-hENT2 Staining with Anti-cytochrome oxidase (subunit I) Antibodies in BeWo and HeLa Cells. BeWo and HeLa cells fixed, permeabilized, and incubated first with anti-hENT2 polyclonal (*A*, *C*, *D*, and *F*) and anti-cytochrome oxidase (subunit I) antibodies (*B*, *C*, *E*, and *F*) and then with Alexa 488-conjugated donkey anti-rabbit IgG (*A*, *C*, *D*, and *F*) and Cy5-conjugated donkey anti-mouse IgG antibodies (*B*, *C*, *E*, and *F*). Cells were visualized using laser-scanning confocal microscopy. Overlapping images are shown in Panels *C* and *F*. *Bars*, 10 μm.

Figure 5-6

Anti-cytochrome oxidase (subunit I)
Anti-hENT2
Double
BeWo Cells
HeLa Cells
A
B
C
D
E
F

Figure 5-7. Identification of an Anti-hENT2 Immunoreactive Species in Human Mitochondria. Cell lysates were prepared from CHOK1 cells that had been transfected with pcDNA3/hENT1-HA, pcDNA3/hENT2-VSV-G or pcDNA3 as described in Chapter 2 R. Human erythrocyte ghosts and membranes (hRBC) were prepared as described in Chapter 2 O. Enriched human liver mitochondria were isolated as described in Chapter 2 P. Proteins were resolved by SDS-PAGE and analysed by immunoblotting as described in Chapter 2 R. Panels *A* and *B* depict immunoblots analyses performed in parallel. Equivalent amounts of protein (25 μg) were loaded in the mitochondrial and erythrocyte sample lanes. *A*, The immunoblot was incubated first with anti-hENT1 monoclonal mouse antibodies and then with horseradish peroxidase-conjugated donkey anti-mouse IgG antibodies. *B*, The immunoblot was incubated first with anti-hENT2 monoclonal antibodies and then with horseradish peroxidase-conjugated donkey anti-mouse IgG antibodies. Detection was by ECL as described in Chapter 2 R. In each panel positions of the protein markers (in kDa) are shown on the left.

Figure 5-7

Identification of an Anti-hENT2 Immunoreactive Species in Human Mitochondria

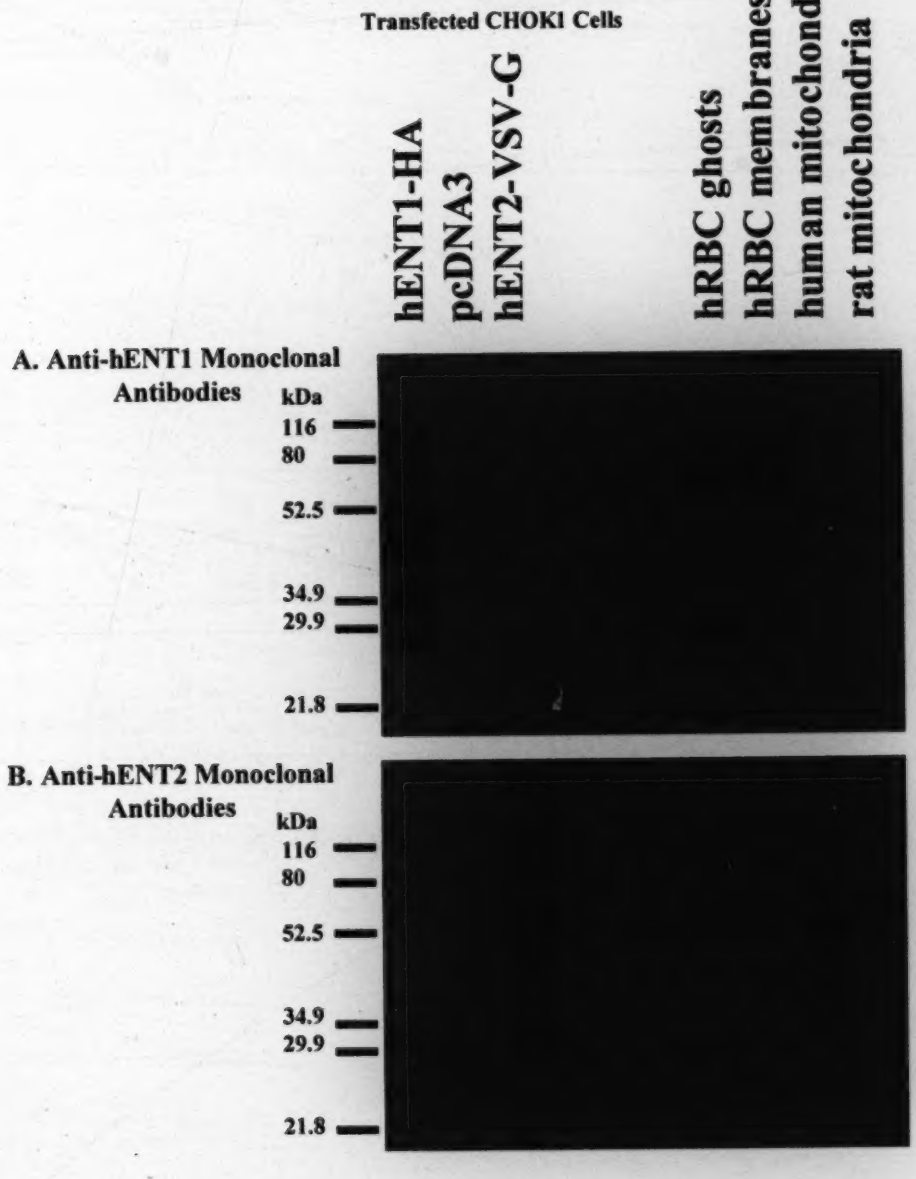

Figure 5-8. Detection of hENT1 in HeLa and BeWo Membranes by Immunoblot Analysis. Cell lysates were prepared from CHOK1 cells that had been transfected with pcDNA3/hENT1-HA or pcDNA3/hENT2-VSV-G as described in Chapter 2 R. hRBC membranes were prepared as described in Chapter 2 O and 15 μg were loaded onto the gels. BeWo crude and HeLa plasma membranes were prepared as described in Chapter 2 N and 25 μg of each was loaded onto the gels. Proteins were resolved by SDS-PAGE and analysed by immunoblotting as described in Chapter 2 R. Panels *A* and *B* depict immunoblots analyses performed in parallel. *A*, The immunoblot was incubated first with anti-hENT1 monoclonal mouse antibodies and then with horseradish peroxidase-conjugated donkey anti-mouse IgG antibodies. *B*, The immunoblot was incubated first with anti-hENT2 monoclonal antibodies and then with horseradish peroxidase-conjugated donkey anti-mouse IgG antibodies. Detection was by ECL as described in Chapter 2 R. In each panel positions of the protein markers (in kDa) are shown on the left.

Figure 5-8

Detection of hENT1 in HeLa and BeWo Membranes by Immunoblot Analysis

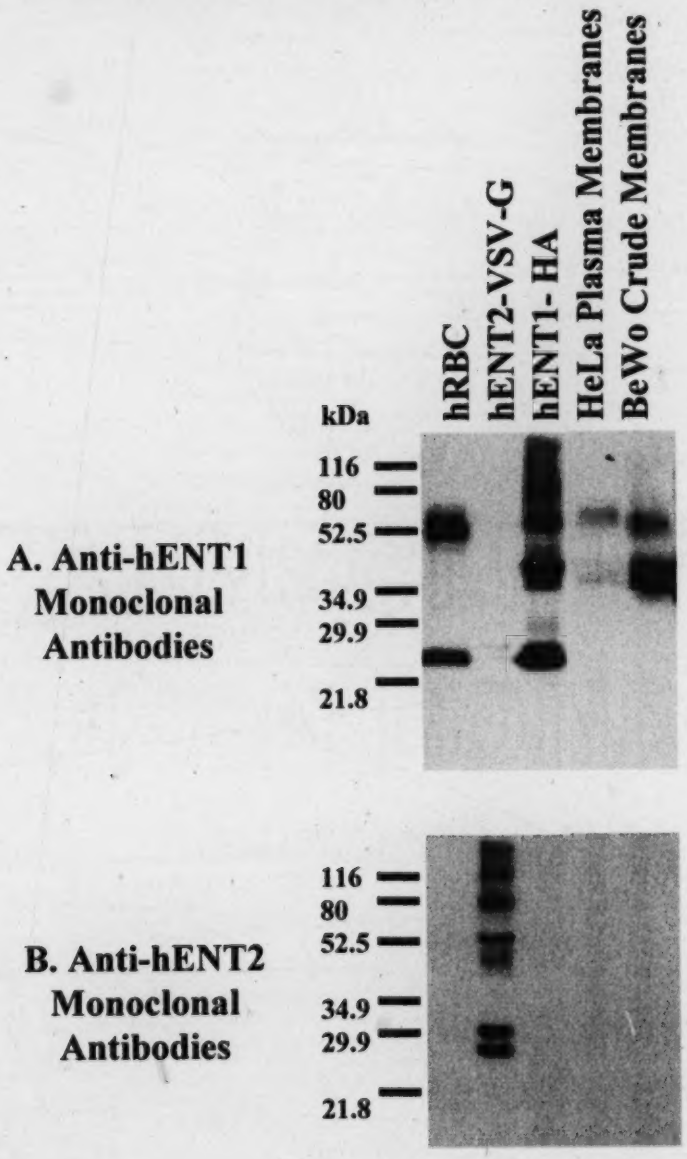

Figure 5-9. GeneScan Analysis of the hENT2/hHNP36 Transcript. *A*. Depicted here is the sequence of the hENT2/hHNP36 cDNA and the position of the primers GShENT2-F and GShENT2-R. The exon/intron boundaries are in bold. The putative alternate splice site is highlighted by asterisks and is in bold print. *B*. Depicted here are the two possible PCR products that can result using the primers described above if both transcripts exist.

Figure 5-9

GeneScan Analysis of the hENT2/hHNP36 Transcript

A. hENT2/hHNP36 cDNA Sequence and Position of GeneScan Primers

Exon2/Exon3

GGGCTGGGCACCCTCCTTCCCTGGAACTTCTTCATCACCGCCATCC**CGTA**CTTCCAGGCGCGACTGGC
CCCGACCCGTGGGAGGAAGGGACCTTGAAGAAGTAGTGGCGGTAGG**GCAT**GAAGGTCCGCGCTGACCG

GShENT2-F

CGGGGCCGGCAACAGCACAGCCAGGA**TCCTGAGCACCAACCACACGGG**TCCCGAGGATGCCTTCAACT
GCCCCGGCCGTTGTCGTGTCGGTCCTAGGACTCGTGGTTGGTGTGCCCAGGGCTCCTACGGAAGTTGA

TCAACAATTGGGTGACGCTGCTGTCCCAGCTGCCCCTGCTGCTCTTCACCCTCCTCAACTCCTTCCTG
AGTTGTTAACCCACTGCGACGACAGGGTCGACGGGGACGACGAGAAGTGGGAGGAGTTGAGGAAGGAC

Exon3/Exon4

TACCAG**TGCG**TCCCGGAGACGGTGCGCATTCTGGGCAGCCTGCTGGCCATACTGCTGCTCTTTGCCCT
ATGGTC**ACGC**AGGGCCTCTGCCACGCGTAAGACCCGTCGGACGACCGGTATGACGACGAGAAACGGGA

****

GACAGC**AGCG**CTGGTCAAGGTGGACATGAGCCCCGGACCCTTCTTCTCCATCACCATGGCCTCCGTCT
CTGTCG**TCGC**GACCAGTTCCACCTGTACTCGGGGCCTGG**GAAGAAGAGGTAGTGGTA**CCGGAGGCAGA

GShENT2-R

Exon4/Exon5

GCTTCATCAA**CTCC**TTCAGTGCAGTCCTACAGGGCAGCCTCTTCGGGCAGCTGGGCACCATGCCCTCC
CGAAGTAGTT**GAGG**AAGTCACGTCAGGATGTCCCGTCGGAGAAGCCCGTCGACCCGTGGTACGGGAGG

ACCTACAGCACCCTCTTCCTCAGCGGCCAGGGCCTGGCTGGG
TGGATGTCGTGGGAGAAGGAGTCGCCGGTCCCGGACCGACCC

B. Possible GeneScan PCR Products

Figure 5-10. GeneScan Analysis Results. Depicted here are the results for the GeneScan RT-PCR Analysis of *A*, HeLa, *B*, CEM *C*, BeWo *D*, HEK293 cells. In all four cases, both the major hENT2 transcript-specific PCR product (~230 bp) and the minor hHNP36 transcript-specific PCR product (~170 bp) are seen (depicted in blue in each electropherogram). The GENESCAN-500 ROX (Applied Biosystems) markers are depicted in red and correspond to 35, 50, 75, 100, 139, 150, 160, 200, 250, 300, 340, 350, 400, 450, 490, 500 bp. The base pair sizes are denoted at the top of each electropherogram. Shown are representative results from one of two separate experiments.

Figure 5-10

GeneScan Analysis Results

A. HeLa Sample

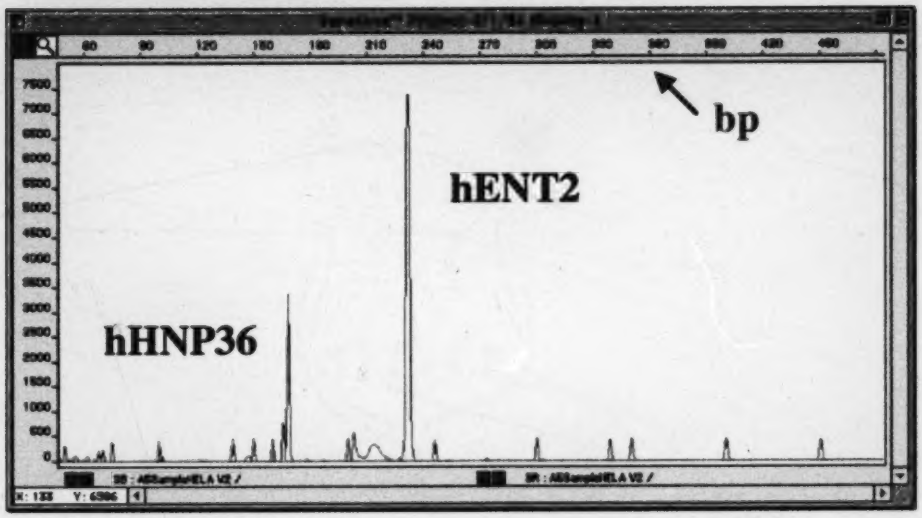

B. CEM Sample

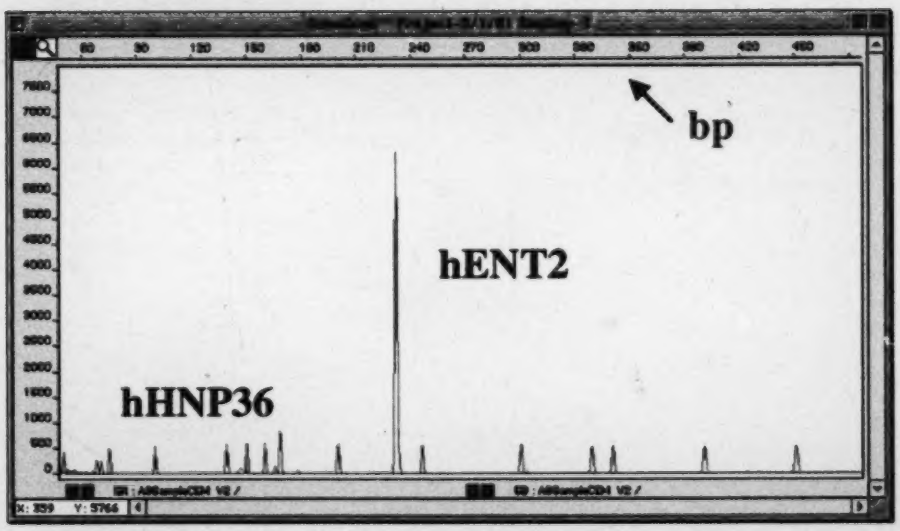

Figure 5-10

GeneScan Analysis Results

C. HEK293 Sample

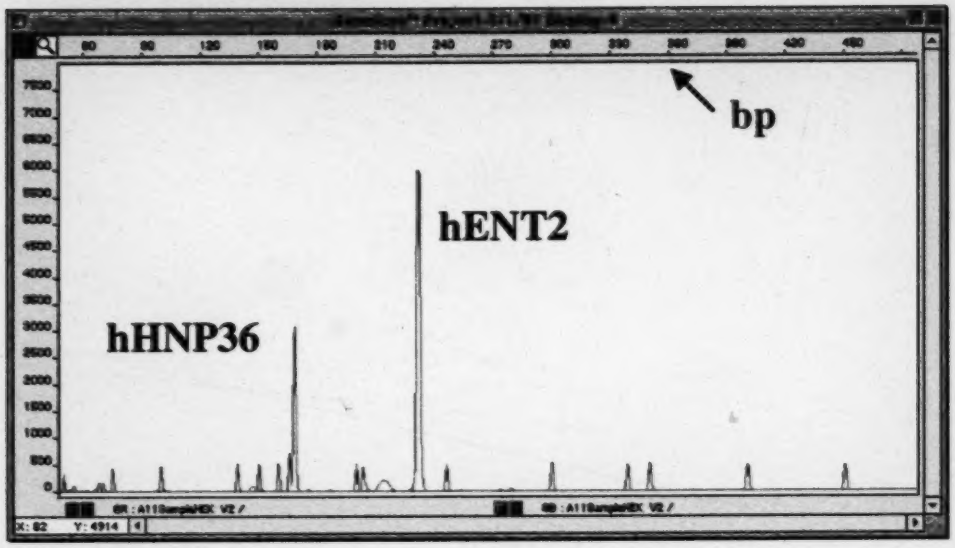

D. BeWo Sample

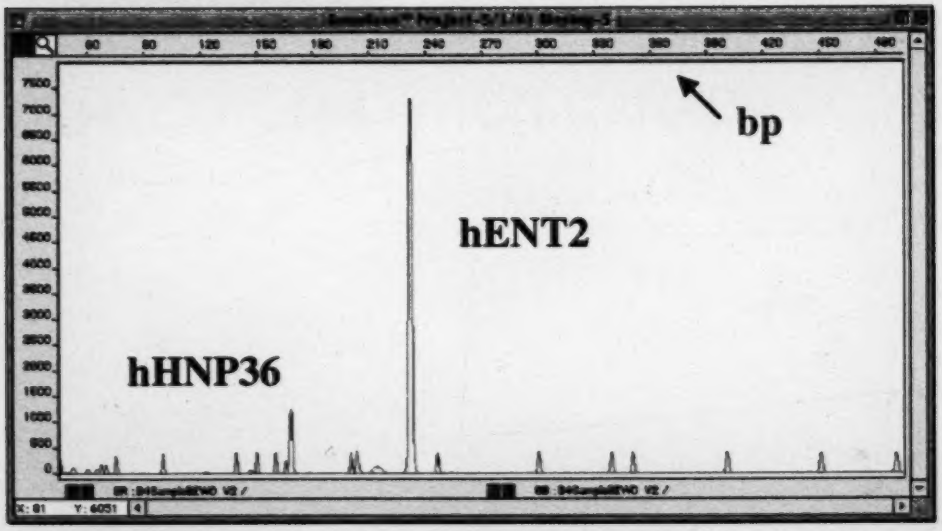

Figure 5-11. Corrected Intron/Exon Boundaries for the hENT2/hHNP36 Gene. ***A.*** The correct intron and exon boundaries are shown for the exon 11/intron 11/exon 12 region of the hENT2 gene. The intron ends are in bold type. The sequence missing from the initial description of the gene [105] is underlined. The sequence that is missing from the hHNP36 genomic sequence [105] yet present in the hHNP36 cDNA sequence [103] is underlined and in bold type. *B*. According to the contig (GenBank accession number NT_009296), the intron acceptor site for intron 6 does have a proper consensus sequence (C/TAG) (in bold type) [310], which was missing from the earlier report [105]. The sequence missing from the Williams *et al.*, paper [105] is underlined. In both *A* and *B*, the exon sequence is shown in uppercase letters, while the intron sequence is in lowercase letters. The stop codon is highlighted in bold type in uppercase letters.

Figure 5-11

Corrected Intron/Exon Boundaries for the hENT2/HNP36 Gene

A. Actual exon 11/intron 11/exon 12 boundary

GTCCCTCACCATGTGC**CTGGCGCCCAG**gtccggggcaatggggtggggtgggggctgggagta…
…ccagatttagacccagcattttctaagagctcctgttcccgggtgttctagGCAGGTGCTGCCACACGAGA
GGGAGGTGGCCGGCGCCCTCATGACCTTCTTCCTGGCCCTGGGACTTTCCT
GTGGAGCCTCCCTCTCCTTCCTCTTCAAGGCGCTGCTC**TGA**

B. Actual intron 6/exon 7 boundary

aggcaagccaggcaggcccaacactttcctgtccttctgcagAAGTTTGCCCGCTACTACCTGGCCAAT
A

Figure 5-12. Identification of the hENT2 Pseudogene on Chromosome 11. The hENT2 cDNA sequence (GenBank accession number AF034102) [99] was used to search the draft human genome (http://www.ncbi.nlm.nih.gov/genome/seq/HsBlast.html). Shown is the graphical result depicting the location of and the identification of the contig containing the hENT2/HNP36 gene and the hENT2 pseudogene. The asterisk denotes the putative exon #1 of the hENT2 pseudogene that contains a sequence discrepancy when compared to the hENT2 gene.

Figure 5-12

Identification of the hENT2 Pseudogene on Chromosome 11

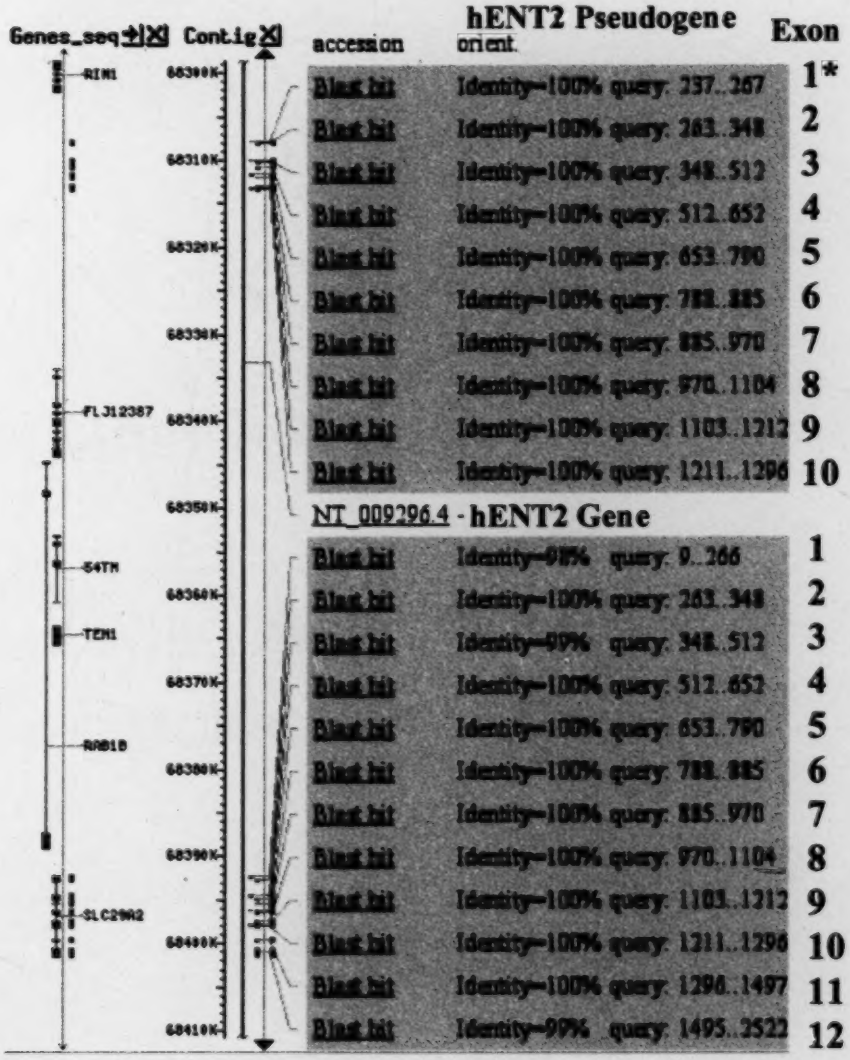

Figure 5-13. Sequence Comparison of the hENT2 Gene and the hENT2 Pseudogene. Shown are the sequences of the homologous regions in the hENT2 gene and hENT2 pseudogene, both found on the same contig (GenBank accession number NT_009296). The pseudogene has an insertion (in bold) at the intron donor splice site, which disrupts the "gt" consensus intron donor site and would prevent splicing from occurring [310]. As a result of this insertion, a different mRNA or no mRNA would result from the pseudogene. Exon sequence is shown in uppercase and intron sequence is shown in lowercase.

Figure 5-13

Comparison of hENT2 Gene and hENT2 Pseudogene

hENT2 Gene

ATGGCGCGAGGAGACGCCCCGCGGGACAGgtgagtgggcccgggtgcgttgcaagtggccgggggc

hENT2 Pseudogene

ATGGCGCGAGGAGACGCCCCGCGGGACAGcgtgagtgggcccgggtgcgttgcaagtggccggggg

Chapter 6

6. Use of Two Perturbative Methods, Hydroxyurea-treatment and hENT Antisense Production, to study Equilibrative Nucleoside Transporter Regulation

6. Abstract

CEM cells were treated with various concentrations of hydroxyurea for 24 h and hENT1 activity and production were assessed by measurements of i) hENT1 abundance on cell surfaces and in whole cells by flow cytometry, ii) [^{3}H]-NBMPR binding, iii) hENT1 mRNA by quantitative RT-PCR analysis and iv) uridine transport to determine if the hydroxyurea-induced decrease in deoxyribonucleotide triphosphate (dNTP) levels modulated transporter protein or mRNA levels. In these experiments, uridine transport rates and [^{3}H]-NBMPR binding increased when computed on a sites per cell basis, but not when protein content was taken into account. Increased fluorescence per cell was observed in flow cytometry experiments performed using probes that either bound to hENT1 located only on the cell surface or to hENT1 bound internally as well as on the cell surface. In contrast, hENT1 mRNA levels remained constant after cells were treated with various concentrations of hydroxyurea for 24 h. When uridine uptake and NBMPR-binding results were based on cell volume or cellular protein content, the hydroxyurea-induced changes in CEM cells were minimal, suggesting that regulation of levels of hENT1 was linked to cell growth.

Antisense constructs of the full-length hENT1 or hENT2 cDNAs were stably transfected into cells to determine what the effect on the other transporter would be. The nucleoside transport profile of human embryonic kidney (HEK293) cells was examined. Only hENT1/*es* and hENT2/*ei* mRNAs and activities were present by both RT-PCR and uridine transport assays, respectively. Stable transfectants expressing either hENT1 antisense or hENT2 antisense were produced and production of antisense was confirmed by RT-PCR. When transport was assessed in the stable transfectants, they were all found to have both hENT1- and hENT2-mediated activity. Thus, the attempt to ablate the activity of the transporters using this methodology was not successful. using different methods and tools.

6 A. Introduction

Numerous studies have demonstrated that equilibrative and concentrative nucleoside transport activities can be modulated in some cell types by growth factors and hormones [176, 312-315], differentiation [179], increases in protein kinase activation, [171, 173-175, 316, 317], adenosine triphosphates [172, 318], nitric oxide [187] and lipopolysaccharide [186, 188].

The work in this chapter attempted to perturb hENT1 and hENT2 function to explore avenues of possible regulation. An hypothesis has emerged that regulation of nucleoside transporters, particularly hENT1, may be linked to cellular levels of deoxynucleotides. dNTPs are used mainly for DNA synthesis and have short half-lives since they are used as quickly as they are synthesized [319]. Thus, decreases in levels of the critical dNTPs may induce an increase in nucleoside transporter levels that is connected to the cellular requirements for more raw materials (*i.e.,* nucleosides) to sustain DNA synthesis.

Recently, Hedley and co-workers [189, 190] reported that the apparent levels of hENT1 were increased by perturbation of dNTP pools with inhibitors of enzymes such as ribonucleotide reductase and thymidylate synthase. In one of these studies [190], the apparent number of hENT1 proteins on the surface of various suspension cells of leukaemic origin, as measured by specific binding of 5-(SAENTA-x_8)-fluorescein in flow cytometry experiments, increased when cells were exposed to a series of anti-metabolite drugs, including hydroxyurea, an inhibitor of ribonucleotide reductase. A series of human hematopoietic-derived cell lines were treated with two different concentrations of hydroxyurea, 50 and 200 μM [190]. When treated CEM cells were compared to untreated cells, a 5-fold increase in the apparent levels of the *es* transporter protein (*i.e.,* hENT1) on cell surfaces was observed. Also, more recently, hydroxyurea-resistant CEM cells were reported to exhibit increased gemcitabine sensitivity that was related to increased gemcitabine uptake and incorporation into DNA [320]. Gemcitabine is an anticancer nucleoside analogue that not only inhibits DNA replication, but also inhibits ribonucleotide reductase [321, 322]. Together, these results suggest that hydroxyurea may increase the activity and/or the amount of nucleoside transporters.

Ribonucleotide reductase is a highly conserved, complex enzyme that converts ribonucleotides to deoxyribonucleotides and therefore is required to maintain intracellular levels of dNTPs for DNA replication [319]. Inhibition of ribonucleotide reductase by hydroxyurea results in cellular dNTP levels decreasing, which causes DNA synthesis to cease. Hydroxyurea is used clinically in the treatment of chronic myelogenous leukaemia, psoriasis, sickle cell anemia [323] and is being tested as an anti-HIV compound in combination with ddI [324]. Hydroxyurea passively diffuses into cells and reversibly binds to a tyrosyl free radical in ribonucleotide reductase, leading to inhibition of the enzyme [319, 323]. In CEM cells, hydroxyurea causes the accumulation of cells in early S phase and inhibits the DNA replication cycle, while protein synthesis is unaffected, thereby resulting in a state of unbalanced growth [325].

The hENT1 protein is an important, and perhaps the most common, transporter

in the nucleoside salvage pathway, and has been found in almost all tissues and cells analysed thus far [1, 2, 4, 76]. NBMPR binds to high-affinity transport-inhibitory exofacial sites on hENT1 [326]. Using radiolabelled NBMPR, the number of NBMPR-binding sites in a cell can be measured by mass-law analysis [90]. The binding of NBMPR has been correlated with the inhibition of transport activity, which led to the presumption that the stoichiometry of binding (NBMPR:protein) is approximately 1:1 [90]. Another compound, 5'-S-(2-aminoethyl)-N6-(4-nitrobenzyl)-5'-thioadenosine (SAENTA), developed as a high-affinity probe for the transport-inhibitory site of hENT1 [327], has subsequently been labelled with fluorescein (5-(SAENTA-x_8)-fluorescein) to enable its use as a flow cytometric probe [249, 250, 328] (Figure 6-1). This probe is also assumed to bind to hENT1 with a 1:1 stoichiometry. However, unlike NBMPR, 5-(SAENTA-x_8)-fluorescein cannot diffuse into the cell and thus in unpermeabilized cells only binds to sites on cell surfaces [326].

The studies described in the first part of this chapter were undertaken to determine whether a decrease in dNTPs influenced hENT1 transport activity and, if so, if it involved changes in protein and/or mRNA levels. The CEM cell line was utilized in the initial experiments because i) it only possesses one transport activity, the hENT1-mediated *es* activity [99, 120, 139], and ii) the study by Pressacco and co-workers had suggested metabolic upregulation of hENT1 activity [190]. In all of the experiments, hydroxyurea, the ribonucleotide reductase inhibitor, was used at concentrations and for exposure times known to deplete the levels of dNTPs in CEM cells [325]. In these experiments, the dNTP concentrations were not measured. To determine the amount of hENT1 on cell surfaces, CEM cells were treated for 24 h with various concentrations of hydroxyurea ranging from 50-500 μM and analysed by flow cytometry using 5-(SAENTA-x_8)-fluorescein [249, 250, 328]. The effect of hydroxyurea treatment on the amount of hENT1 in whole cells was also determined by analysing permeabilized CEM cells by flow cytometry using anti-hENT1 monoclonal antibodies described elsewhere in this thesis (Chapter 4 BI) in conjunction with fluorescently-labelled secondary antibodies. NBMPR binding was also measured in hydroxyurea-treated CEM cells subjected to a high concentration of hydroxyurea as another way to determine if the amounts of total cellular transporter were altered by exposure to hydroxyurea. Quantitative RT-PCR was performed on RNA samples isolated from untreated and hydroxyurea-treated CEM cells to determine the effect of decreased dNTPs on the transcription of hENT1 mRNA. Finally, uridine transport was measured in CEM cells that were untreated or treated with various concentrations of hydroxyurea for 24 h, and in two cell lines, HeLa and BeWo cells, that possess both hENT1 and hENT2, that were untreated or treated with hydroxyurea. The latter experiments were undertaken to assess differences in uridine uptake in cells that have two different nucleoside transporters, hENT1 and hENT2.

The hENT1 and hENT2 proteins are found in most human tissues and cells that have been examined [1, 2, 4, 76]. See Table I-2 for a summary of the distribution of the two transporters. Whenever both transporters are present in the same cell population, the hENT1-mediated *es* activity is the larger component of equilibrative transport. For example, in HeLa and BeWo cells, hENT1-mediated *es* activity is approximately 80-90%,

whereas hENT2-mediated *ei* activity is approximately 10-20%. Some cell types, such as human erythrocytes and CEM, have only one nucleoside transporter, hENT1. To date there are no known examples of cell lines or tissues that naturally possess only hENT2-mediated *ei* activity. However, hENT2 has been transfected into a nucleoside-deficient human cell line when to enable its characterization in isolation from other transporters [99] (T. Lang, J. D. Young and C. E. Cass, unpublished observations). Skeletal muscle has a substantial amount of hENT2 mRNA [99], especially when compared to other tissues that also have hENT1 present [97], but it is not yet known what proportion of equilibrative transport in these cells is due to hENT2-mediated *ei* activity. Little is known about the regulation of the hENT2 protein or why it is such a small component of nucleoside transport.

Why do cells possess two broad specificity nucleoside transporters? This question has become more interesting since it has been recently shown that hENT2, unlike hENT1, transports a wide range of nucleobases as well as nucleosides [87, 88]. While hENT2 has higher apparent affinities for nucleosides than for nucleobases [87, 88], the transporter efficiencies are similar for both types of substrates [88]. Both facilitative and concentrative, sodium-dependent nucleobase transport activities have been described in human cells, but the transporters responsible have not yet been identified [146]. The contribution of hENT2 to nucleobase transport within cells is uncertain.

Does the cell compensate for the loss of one transporter by upregulating the other? To study this question, an antisense approach was undertaken. An easily transfectable human cell line with both hENT proteins and activities was identified. Second, antisense cDNA for one transporter or the other was stably transfected into the cell line and uptake studies were performed in the transfectants to determine the effect of the antisense cDNA on activity of the transporters.

6 B. Results

6 B. I. Flow Cytometric Analysis of Hydroxyurea-treated CEM Cells

To determine if the amount of hENT1 present on the cell surface or in the cell as a whole changed, hydroxyurea-treated cells were analysed by two flow cytometric assays that differed in their ability to detect surface and total cellular hENT1. The 5-(SAENTA-x_8)-fluorescein probe has previously been shown to bind to hENT1 on the surface of unpermeabilized cells and thus can be used to visualize differences in the amount of hENT1 at the cell surface [249]. Anti-hENT1 antibodies, which were generated against the large intracellular loop (residues 254-271) of hENT1 [115] (see Figure I-5), recognize hENT1 in permeabilized cells and thus were used to assess the effect of hydroxyurea treatment on total cellular hENT1.

In the experiments of Figure 6-2 and Table 6-1, CEM cells were untreated or treated with three concentrations of hydroxyurea (50, 200 and 500 μM) for 24 h and then analysed by flow cytometry with 5-(SAENTA-x_8)-fluorescein to determine the amount of hENT1 on the cell surface. The cells used in each analysis belonged to the main

population of cells and were selected by gating (the gate is shown in each fluorescence plot as "M1" in Figure 6-2). The relative mean fluorescence values obtained from the analysis of 10, 000 cells in each experimental condition are given in Table 6-1. The fluorescence due to 5-(SAENTA-x_8)-fluorescein was specific as can be seen in Figure 6-2 by the results obtained with the "control" samples that were analysed alongside the 5-(SAENTA-x_8)-fluorescein samples. First, unlabelled cells showed very little fluorescence. Second, there was little fluorescence when cells were incubated with both 5-(SAENTA-x_8)-fluorescein and excess NBMPR, a competitive inhibitor of 5-(SAENTA-x_8)-fluorescein binding [249]. When the variously treated cells were incubated with 5-(SAENTA-x_8)-fluorescein alone, there was an increase in the amount of fluorescence (as can be seen in the rightward shift of the peaks in Figure 6-2) relative to that observed in unlabelled cells and in cells treated with excess NBMPR.

Increases in fluorescence of ≥150% of control values were observed in hydroxyurea-treated cells. The cells treated with 500 μM hydroxyurea, the highest concentration tested, were unhealthy as can be seen by the appearance of debris in the lower left hand corner of the side and forward light scatter plot (top panel) for this condition in Figure 6-2. The increases in fluorescence demonstrated that the quantity of hENT1 on the surface of cells increased in cells subjected to prolonged exposures to hydroxyurea.

Due to the scarcity of 5-(SAENTA-x_8)-fluorescein, the experiments of Figure 6-2 could not be repeated with permeabilized cells to determine if total cellular binding of 5-(SAENTA-x_8)-fluorescein, and thus hENT1, also increased. An alternative approach to examine the effects of hydroxyurea treatment on total cellular hENT1 protein was to use anti-hENT1 monoclonal antibodies and permeabilized cells. The antibodies were raised against amino acid residues 254-271 [115]; a large loop between transmembrane domains 6 and 7 of hENT1 that is known to be intracellular [304]. Use of the anti-hENT1 monoclonal antibodies requires permeabilization of cells to access the intracellular epitope of hENT1 (see Figure I-5).

In Figure 6-3 and Table 6-2, untreated and hydroxyurea-treated CEM cells were fixed and permeabilized, stained with the anti-hENT1 monoclonal antibodies and analysed using flow cytometry. The fluorescence due to the anti-hENT1 monoclonal antibodies was specific as can be seen in Figure 6-3 by the two control experiments performed alongside the anti-hENT1 experiments. Neither unlabelled, permeabilized cells or permeabilized cells incubated with secondary antibodies alone showed much fluorescence. When cells were incubated with anti-hENT1 antibodies and secondary antibodies, there was an increase in the amount of fluorescence as can be seen in the rightward shift of the peaks in Figure 6-3.

The relative mean fluorescence values obtained for each experimental condition are given in Table 6-2. An increase in mean fluorescence was seen with exposures to hydroxyurea except for the highest concentration (500 μM) at which there appeared to be considerable cell death. Increases in fluorescence of up to 159% of the control value were observed when cells were treated with hydroxyurea. The cells treated with 500 μM

hydroxyurea were probably dying as can be seen by the decrease in fluorescence and the appearance of debris in the lower left hand corner of the side and forward light scatter plot (top panel) for this condition in Figure 6-3. This experiment demonstrated that the total amount of hENT1 proteins increased per cell upon exposure to hydroxyurea. These flow cytometry results suggested that the increase in hENT1 protein abundance was a global phenomenon and was not restricted to the cell surface.

6 B. II. Analysis of NBMPR-Binding Sites in Hydroxyurea-treated CEM Cells

To determine the effects of hydroxyurea treatment on the number of hENT1 proteins in CEM cells, NBMPR-binding sites were quantitated by performing equilibrium binding experiments. The number of NBMPR-binding sites in asynchronously proliferating cultures of CEM cells is known to be approximately 3.3×10^5/cell [120].

A vacuum-filter methodology was employed [7, 94, 329] that was different from the centrifugation method that was previously used [120] to measure NBMPR binding in CEM cells. To validate this methodology, the number of NBMPR-binding sites/cell was determined for cells harvested from actively proliferating cultures and compared to the previously reported results. NBMPR binding was measured by incubating cells with various concentrations of [^{3}H]-NBMPR in the presence or absence of 10 μM unlabelled NBMPR. Specific NBMPR binding was calculated as the difference between total NBMPR binding (absence of excess NBMPR) and non-specific NBMPR-binding (presence of 10 μM NBMPR). Using the vacuum-filter methodology, CEM cells were found to have approximately 1.0×10^5 - 3.0×10^5 NBMPR-binding sites/cell (see Table 6-3) a value similar to the previously reported value of 3.3×10^5 NBMPR-binding sites/cell [120].

To determine the effects of hydroxyurea treatment on NBMPR binding, CEM cells were treated with 200 μM hydroxyurea or were left untreated for 24 h (Table 6-3). The number of NBMPR-binding sites/cell ranged from 1.0×10^5 - 3×10^5 and 2.1×10^5 - 1.2×10^6 for untreated and treated cells, respectively. In Figure 6-4 Panel *A*, untreated CEM cells exhibited a B_{max} value of 1.1 pmol/mg protein, and in Figure 6-4 Panel *C*, hydroxyurea-treated CEM cells had a B_{max} of 1.1 pmol/mg protein. Thus, although treatment with hydroxyurea resulted in an increase in the number of NBMPR-binding sites/cell, the change appeared to be associated with cell growth since the number of NBMPR-binding sites remained nearly constant when total cellular protein content was considered.

6 B. III. Analysis of hENT1 mRNA Levels in Hydroxyurea-treated CEM Cells

Inward transport of nucleosides is the first step in the salvage of preformed deoxynucleosides for deoxynucleotide synthesis. To determine whether the increases in the amounts of hENT1 observed in hydroxyurea-treated cells were due to an increase in hENT1 transcription, the amounts of hENT1 RNA were quantitatively analysed in

hydroxyurea-treated and untreated CEM cells using Taqman RT-PCR. The hypothesis was that the consequences of hydroxyurea treatment (*i.e.*, reduction of deoxynucleotide synthesis) may stimulate an increase in hENT1 transcription to compensate for the decrease in dNTP pool sizes. Such an increase should be detectable by quantitation of hENT1 mRNA.

Total RNA was isolated from CEM cells that were either unexposed or exposed to 50, 200, or 500 μM hydroxyurea for 24 h. The RNA was converted to cDNA by reverse transcriptase and the resulting cDNAs were amplified by real-time quantitative Taqman PCR [133, 217-219] using primer and probes specific for hENT1 as described in Chapter 2 G II (Figure 6-5). For the hENT1 amplification products (Figure 6-5, Panel *A*), the cycle threshold value (approximately 23) was obtained from the linear portion of the amplification curve between cycles 20 and 26. For the control glyceraldehyde-3-phosphate dehydrogenase (GAPDH) products (Figure 6-5, Panel *B*), the cycle threshold value (approximately 16) was obtained from the linear portion of the amplification curve between cycles 16 and 21. GAPDH is commonly used as a control in RNA studies (*e.g.*, northern blot analyses), since its mRNA is presumed to be constitutively produced. The cycle threshold values were then used to calculate the relative amounts of mRNA in untreated and hydroxyurea-treated CEM cells given in Table 6-4. The relative amounts of hENT1 RNA for treated CEM cells remained the same when compared to that of untreated CEM cells. When cells were treated with 200 μM hydroxyurea, the relative amounts of hENT1 mRNA ranged from 0.81 to 1.27 times the amount found in untreated cells. When cells were treated with 500 μM hydroxyurea, the relative amounts of RNA ranged from 1.56 to 2.94 times the amount found in untreated cells. However, the cells treated with 500 μM hydroxyurea were probably dying, as was seen in light scatter patterns observed in the flow cytometry experiments in Figures 6-2 and 6-3, and these changes may not have been meaningful. The Taqman reactions, which were done with equivalent amounts of RNA, would only detect changes in the relative proportions of a target mRNA (in this case, hENT1) and the control (GAPDH) mRNA and would not detect changes in total cellular mRNA content. The Taqman RT-PCR result suggested that the decrease in dNTP levels caused by hydroxyurea did not result in a selective increase in the levels of hENT1 mRNA.

6 B. IV. Characterization of Uridine Transport in Hydroxyurea-treated CEM Cells

Uridine transport was measured in untreated CEM cells and in CEM cells treated with hydroxyurea under conditions demonstrated to deplete dNTP pools and inhibit growth [325]. The nucleoside transport activity found in CEM cells has been characterized and only the hENT1-mediated *es* transport process is present in this cell type [99, 120, 139]. Uridine uptake was measured over 10 s to obtain initial rates. The results were plotted using either pmol/cell number (Figure 6-6, Panel *A)* or pmol/μL cell water (Figure 6-6, Panel *B*) to determine if there were hydroxyurea-induced differences in

transport rates that exceeded the changes in cell size that were associated with unbalanced growth. The initial rates (pmol/cell number and pmol/μL cell water) are shown in Table 6-5. The values increased from 1.03 to 1.61 pmol/10^6 cells/s as the concentration of hydroxyurea increased from 0-200 μM (see Table 6-5). Cells treated with 500 μM hydroxyurea showed a lower rate of transport, however the light scatter patterns observed in the flow cytometry experiments in Figures 6-2 and 6-3 suggested that the cells were probably already dying. When cell volumes were considered, by calculating rates as a function of cell water, the rates of transport of the CEM cells exposed to 50-200 μM hydroxyurea were approximately equal to the rates of transport of untreated CEM cells (see Table 6-5).

6 B. V. Effect of Hydroxyurea Treatment on the Size of CEM Cells

Changes in cell volumes in hydroxyurea-treated cells were determined two different ways either using cell water measurements from transport experiments or Coulter counter measurements of the diameters of the cells. Both methods have been previously demonstrated to correlate to one another [330]. The results are shown in Table 6-6. When CEM cells were treated with hydroxyurea, the cells increased in diameter from 14.4-16.6 μm as the concentration of hydroxyurea increased from 0-200 μM. Although cells treated with 500 μM showed smaller volumes, they were, as noted above, probably already dying. These results suggested that treatment with hydroxyurea at concentrations less than 500 μM increased the volume of CEM cells, probably by a combination of unbalanced growth and accumulation of cells at a particular point in the cell cycle as has been reported earlier [325].

6 B. VI. Characterization of the Nucleoside Transporter Profile of HEK293 Cells.

The human embryonic kidney cell line (HEK293) is an easily transfectable transformed human cell line [331]. No nucleoside transport data existed for this cell line, thus it was necessary to characterize it. Northern blot analysis of HEK293 total RNA using probes specific for hENT1, hENT2, hCNT1 and hCNT2 performed by others in our group (K. A. Graham, D. Mowles and C. E. Cass, unpublished observations) suggested that HEK293 cells possess only hENT1 message. To examine the nucleoside transporter of these cells in greater detail, two more analyses were performed: RT-PCR and uridine uptake assays. RT-PCR revealed that HEK293 cells possessed mRNA for both hENT1 and hENT2. Uridine uptake experiments confirmed that only hENT1- and hENT2-mediated and no Na^+-dependant transport activities were present in these cells.

HEK 293 mRNA was examined more closely by using RT-PCR. BeWo mRNA was used as the positive control since BeWo cells have hENT1 and hENT2 proteins and activities [7]. Following first strand synthesis by reverse transcriptase, specific primers for hENT1 and hENT2 were used in the PCR and hENT1- and hENT2-specific products

were visualized when the PCR products were separated on an agarose gel (Figure 6-7). The RT-PCR analysis revealed the presence of both hENT1- and hENT2-specific PCR products derived from HEK293 mRNA, although hENT2 mRNA had not been observed by northern blot analysis. The hENT1- and hENT2-specific PCR products in the HEK293 lanes were the same sizes as the products in the BeWo control lanes. The PCR products from the hENT2 RT-PCR reactions were isolated and the sequences were shown to correspond to those expected for hENT2 by DNA sequencing.

To determine what types of transport activities were present in HEK293 cells, uridine uptake was measured. Although HEK293 cells are grown as adherent cultures, they were only loosely attached to the plates and were thus easily dislodged. Uridine uptake was measured in single-cell suspensions of HEK293 cells that were produced by treatment with trypsin and EDTA. Initial rates of uptake of 10 μM uridine were measured in NMG buffer to enable distinction between the concentrative and equilibrative transport activities (Figure 6-8). NMG buffer does not contain sodium, which is necessary for CNT activity, since CNTs are sodium nucleoside co-transporters [132]. hENT1-mediated *es* activity can be inhibited by NBMPR and dilazep, while hENT2-mediated *ei* activity can be inhibited by dilazep, but not by NBMPR. HEK293 cells transported uridine in the absence of sodium and this activity was completely inhibited by 100 μM dilazep, indicating that transport was primarily equilibrative. Furthermore, the uridine transport that was observed was sensitive, not only to 100 μM dilazep, but also to 0.1 μM NBMPR, which demonstrated the presence of a major hENT1-mediated *es* component and a minor hENT2-mediated *ei* component. These results were consistent with the RT-PCR results, which demonstrated only ENT mRNAs in HEK293 cells. The presence of only hENT1 and hENT2 in the easily transfectable HEK293 cells made this cell line a candidate for hENT1 and hENT2 antisense studies.

6 B. VII. Characterization of the Nucleoside Transporter Profile of HEK293 Cells Stably Transfected with Sense or Antisense cDNAs for hENT1 and hENT2

hENT1 and hENT2 are often found in the same cell type and, thus far there are no non-transfected cell types that possesses only hENT2 activity. It is unknown why cells have both hENT1 and hENT2 proteins and why hENT1 activity is always the dominant activity of the two. Thus, an antisense strategy was used to attempt to "knock-out" either one of the ENT proteins. These experiments were performed to determine the effects of downregulating one or the other transporter on the remaining ENT activity in the cell. To knock-out either hENT1 or hENT2 in HEK293 cells, the cells were stably transfected with plasmids encoding the antisense cDNA of one or the other of the ENT proteins. Thus, production of one transporter should have been ablated and the activity and production of the remaining transporter could be assessed.

HEK293 cells were stably transfected with one of the following cDNAs: hENT1 sense (contained in plasmid pcDNA3/hENT1), hENT1 antisense (contained in plasmid pcDNA3/hENT1as), hENT2 sense (contained in plasmid pcDNA3/hENT2) hENT2

antisense (contained in plasmid pcDNA3/hENT2as) or β-galactosidase (contained in pcDNA3/β-gal) as described in Chapter 2 H II. The construction of the plasmids is described in Chapter 2 D III. Stable transfectants were selected using Geneticin and four clones were isolated for each transfectant after six weeks of selection. Production of the antisense and sense constructs in the stably-transfected HEK cells was confirmed by RT-PCR analysis for each of the viable clones. RNA was isolated from the cells as described in Chapter 2 F and one-tube RT-PCR was performed using the primers described in Chapter 2 G I (Figure 6-9).

Initial rates of uptake of 10 μM [^{3}H]-uridine were measured in each of the stable antisense transfectants. Shown in Figure 6-10 are the results from a representative experiment with two of the antisense transfectants, one with hENT1 antisense and the other with hENT2 antisense. Uridine uptake was measured in both clones in the presence and in the absence of NBMPR and the rates of transport obtained for both cell lines was similar regardless of the presence of the inhibitor. Three clones from each antisense transfection were examined and gave similar results. In all of the transfectants tested, the production of antisense did not lead to a decrease in either hENT1-mediated or hENT2-mediated activity.

6 C. Discussion

Many examples of regulation of nucleoside transport activity, primarily hENT1-mediated *es* transport, have been reported in the literature over the last 20 years, but the exact nature and mechanism of the regulation has yet to be elucidated. An hypothesis emerged that nucleoside transport activities may be modulated when cells require nucleosides because of metabolic stresses caused by perturbation in nucleotide metabolism. Recent reports in the literature have suggested that this hypothesis may be correct. When human leukaemic cells were treated with drugs that inhibit DNA synthesis either directly (*e.g.*, aphidicolin) or indirectly (*e.g.*, hydroxyurea), an increase in the amount of 5-(SAENTA-x_8)-fluorescein binding at the cell surface was observed [190]. More recently, nucleoside transport was implicated as the mechanism of increased sensitivity to the anticancer nucleoside drug gemcitabine in hydroxyurea-resistant CEM cells [320]. The work presented in this chapter assessed the effects of inhibition of DNA synthesis by treating a human leukaemia cell line, CEM, with a metabolic inhibitor, hydroxyurea, on hENT1 activity.

Hydroxyurea, a reversible inhibitor of ribonucleotide reductase, is used in the treatment of many different disease states [319, 323, 324]. Inhibition of ribonucleotide reductase results in the depletion of dNTPs in the cell, thus inhibiting DNA synthesis. Various hENT1-specific probes, such as NBMPR, 5-(SAENTA-x_8)-fluorescein and anti-hENT1 antibodies were used to monitor the hENT1 protein in CEM cells treated with hydroxyurea. The 5-(SAENTA-x_8)-fluorescein bound only to transporters on the surfaces of cells and the amount bound increased as the concentration of hydroxyurea was increased (up to 200 μM hydroxyurea). The increase seen with 5-(SAENTA-x_8)-

fluorescein was not as great as had been previously reported [190]. The anti-hENT1 antibodies, which were used to analyse permeabilized cells, were used to assess changes in the total cellular hENT1 population. The fluorescence associated with antibody-binding also increased as hydroxyurea concentrations were increased (up to 200 μM hydroxyurea). These observations demonstrated that exposure of cells to hydroxyurea resulted in an increase in the total cellular content of hENT1 as well as the content of hENT1 at cell surfaces.

The classic NBMPR-binding assay [7, 90, 94, 120, 251] was used to quantify changes in transporter numbers in cells subjected to hydroxyurea treatment, since the assay is presumed to correlate NBMPR-binding sites to the amount of hENT1 in each cell. When results were calculated as pmol of specifically bound NBMPR per 10^6 cells, treatment with hydroxyurea produced an increase in the amount of NBMPR bound per cell, suggesting an increase in the number of molecules of hENT1. However, when results were calculated as pmol specifically-bound NBMPR per mg protein, there was little or no change in the amount of NBMPR bound between hydroxyurea-treated and untreated the cells. This result suggested that the unbalanced growth resulting from the decrease in dNTP levels caused by hydroxyurea was accompanied by an increase in hENT1 that was proportional to the increase in cell volume.

Quantitation of hENT1 mRNA was performed to determine if hydroxyurea treatment resulted in an increase in the transcription of hENT1 mRNA, which could be the basis of the increase in hENT1. RNA was isolated from CEM cells that were treated or untreated with hydroxyurea and real-time quantitative RT-PCR was performed using Taqman PCR [217-219]. No change in relative mRNA levels from untreated and hydroxyurea-treated CEM cells was detected. This lack of effect on mRNA levels agrees with previous studies that suggested that mRNA synthesis is not affected by exposure to hydroxyurea [319, 323]. Thus, transcription and translation continued in the absence of DNA synthesis.

When CEM cells were treated with hydroxyurea, an increase in the transport rates was observed when the rates were calculated as pmol per 10^6 cells. However, an increase in the volumes of treated cells was also observed with hydroxyurea exposure, presumably because hydroxyurea treatments results in accumulation of cells in S phase as well as an imbalance in the cellular ratio of DNA and protein [325]. Thus, although hydroxyurea treatment increased the total hENT1 activity per cell, the increase was proportional to the overall increase in cell size, suggesting that hENT1 activity was not upregulated to increase salvage of extracellular nucleosides to compensate for depletion of cellular dNTPs. The CEM cells maintained the same density of hENT1 despite the hydroxyurea treatment.

The results presented in the first part of this chapter suggested that the perturbation of cellular dNTP pools caused by hydroxyurea had no direct effect on the activity or amount of hENT1. The observations that the amounts of hENT1 and uridine transport activities increased in hydroxyurea-treated cells were correlated to the increases in cell size. This change in average cell size was probably due to accumulation of cells in the S phase of the cell cycle as well as to unbalanced growth which changes the

DNA/protein ratio [325]. These findings suggested that this population of larger cells had a larger hENT1 content than untreated smaller cells. A similar observation has previously been made in HeLa synchronized by mitotic detachment cells that were assessed by NBMPR binding, and uridine, thymidine, adenosine uptake studies [177, 178]. In this latter study, the amount of NBMPR specifically bound to cells and the transport rates doubled from G1 to late S phase of the cell cycle in proportion to the increase in cell size. Thus, when the results were calculated considering cell size and/or protein, there were no differences in binding or transport between G1 and the S phase.

The report by Pressacco and colleagues [190] only probed the hENT1 protein using 5-(SAENTA-x_8)-fluorescein and did not assess the more global effects that hydroxyurea treatment has on cells. Thus, they probably prematurely concluded that inhibitors of DNA synthesis could modulate the levels of hENT1. The findings in this study suggested that hydroxyurea-treatment did not upregulate the amount of hENT1 protein on the surface of cells. Similarly, there was no evidence of upregulation of the total cellular amount of hENT1 protein or levels of hENT1 mRNA.

The goal of the antisense study was to determine the effects of downregulating one ENT by antisense production on the other ENT when both ENTs are present within the same cell. The nucleoside transporter profile of HEK293 cells, which are easily transfectable, was assessed to determine if they were acceptable candidates for antisense production of hENT1 and hENT2 cDNAs. It was established that HEK293 cells possess both hENT1 and hENT2 mRNA via RT-PCR experiments. Initial rates of uptake of uridine were measured in the presence and absence of sodium to test for concentrative nucleoside transport activity and in the presence and absence of NBMPR and dilazep to test for equilibrative nucleoside transport activity. These experiments demonstrated that HEK293 cells lacked concentrative nucleoside transport activity and possessed both hENT1-mediated *es* (approximately 80%) and hENT2-mediated *ei* transport activities (approximately 20%).

The production of antisense cDNAs is used to decrease the amount of target mRNAs, which leads to a decrease in the amount of protein being produced and thus less activity. This strategy has been successfully used to reduce and eliminate the activities of other membranes transport proteins such as the insulin-sensitive glucose transporter GLUT4, [332], the glucose transporter GLUT1 [333] and the voltage gated chloride channel, ClC-2 [334] in different cell types. HEK293 cells are easily transfectable and have also been previously used to successfully produce full-length antisense cDNAs. In the latter case, the antisense for the oxygen-regulated protein 150 was used to suppress the activity of the protein to examine the role of the protein in hypoxia-induced apoptosis [335].

Knowing that only the two ENTs were present in HEK293 cells, the cDNAs for both hENT1 and hENT2 were cloned in the antisense direction into the pcDNA3 expression vector. HEK293 were then stably transfected with these constructs. After the establishment of the two cell stable lines, RT-PCR was performed to confirm that either cell line was expressing the hENT1 antisense cDNA or the hENT2 antisense cDNA. Next, uridine transport was performed on the stable cell lines as had been previously for

the wild-type HEK293 cells. Unfortunately, despite the presence of hENT1 or hENT2 antisense mRNA, both stably-transfected cell lines still possessed hENT1 and hENT2 activities. These results indicated that the antisense mRNAs produced did not inhibit the endogenous sense mRNAs sufficiently to reduce transport activity. The antisense mRNAs may have been degraded or the cells may have upregulated the production of endogenous hENT1 and hENT2 mRNAs. To improve the production of antisense in these cells, a different type of plasmid may be necessary. Also, antisense oligonucleotides [336] or ribozymes [337-339] strategies should also be considered as alternatives to the production of full-length antisense cDNAs.

Figure 6-1. hENT1 Probes. Shown are the chemical structures of two tight-binding inhibitors used as probes for hENT1: 5'-S-(2-aminoethyl)-N6-(4-nitrobenzyl)-5'-thioadenosine (SAENTA-x_8)-fluorescein [249, 327, 328], and nitrobenzylthioinosine (NBMPR) [90].

Figure 6-1

hENT1 Probes

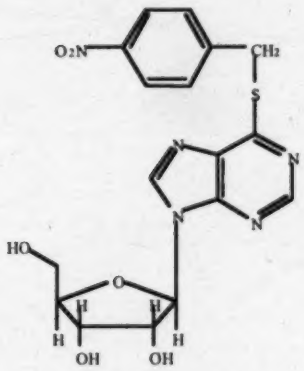

NBMPR

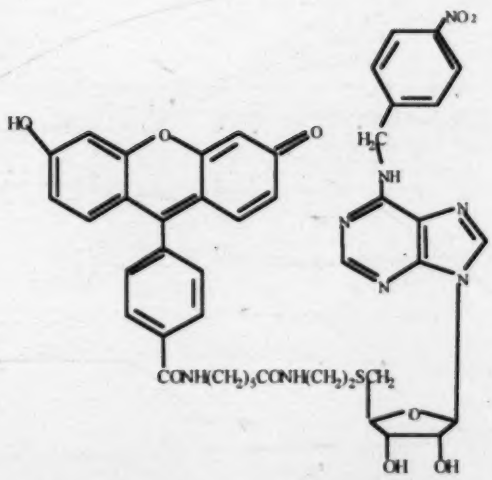

5-(SAENTA-x_8)-fluorescein

Figure 6-2. Analysis of Hydroxyurea-treated CEM Cells using Flow Cytometry and 5-(SAENTA-x_8)-fluorescein. CEM cells were incubated in growth medium for 24 h without or with 50, 200 or 500 μM of hydroxyurea and then analysed by flow cytometry as described in Chapter 2 S. For each concentration (from top to bottom), the four panels are representations of the side and forward light scatter, the fluorescence of unlabelled CEM cells, the fluorescence of CEM cells incubated with 20 nM 5-(SAENTA-x_8)-fluorescein in the presence 6 μM NBMPR, and the fluorescence of CEM cells incubated with 20 nM 5-(SAENTA-x_8)-fluorescein alone. Shown here is a representative result from two experiments (each with replicates) that gave similar results.

Figure 6-2

Analysis of Hydroxyurea-treated CEM Cells using Flow Cytometry and 5-(SAENTA-x_8)-fluorescein

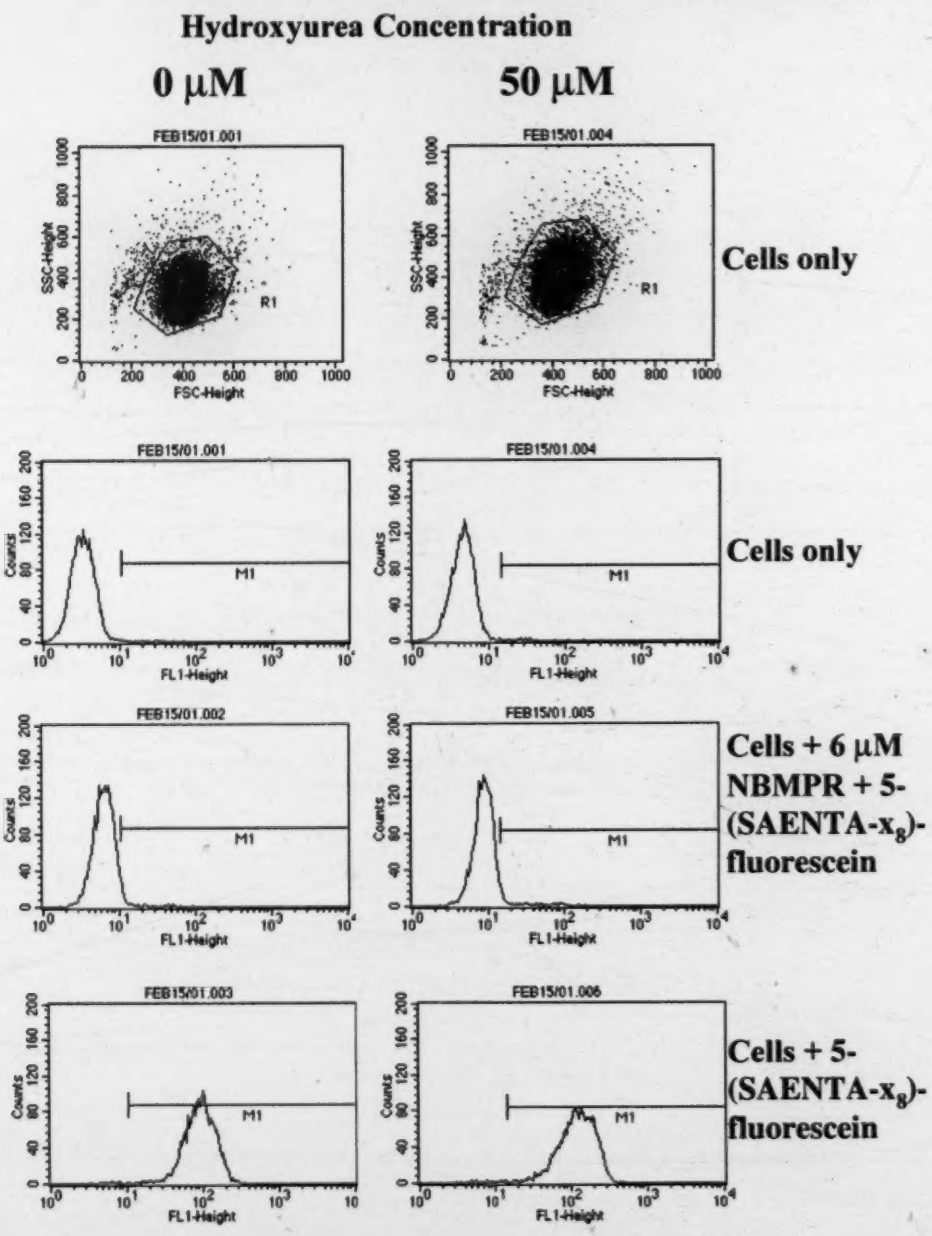

Figure 6-2

Analysis of Hydroxyurea-treated CEM Cells using Flow Cytometry and 5-(SAENTA-x_8)-fluorescein

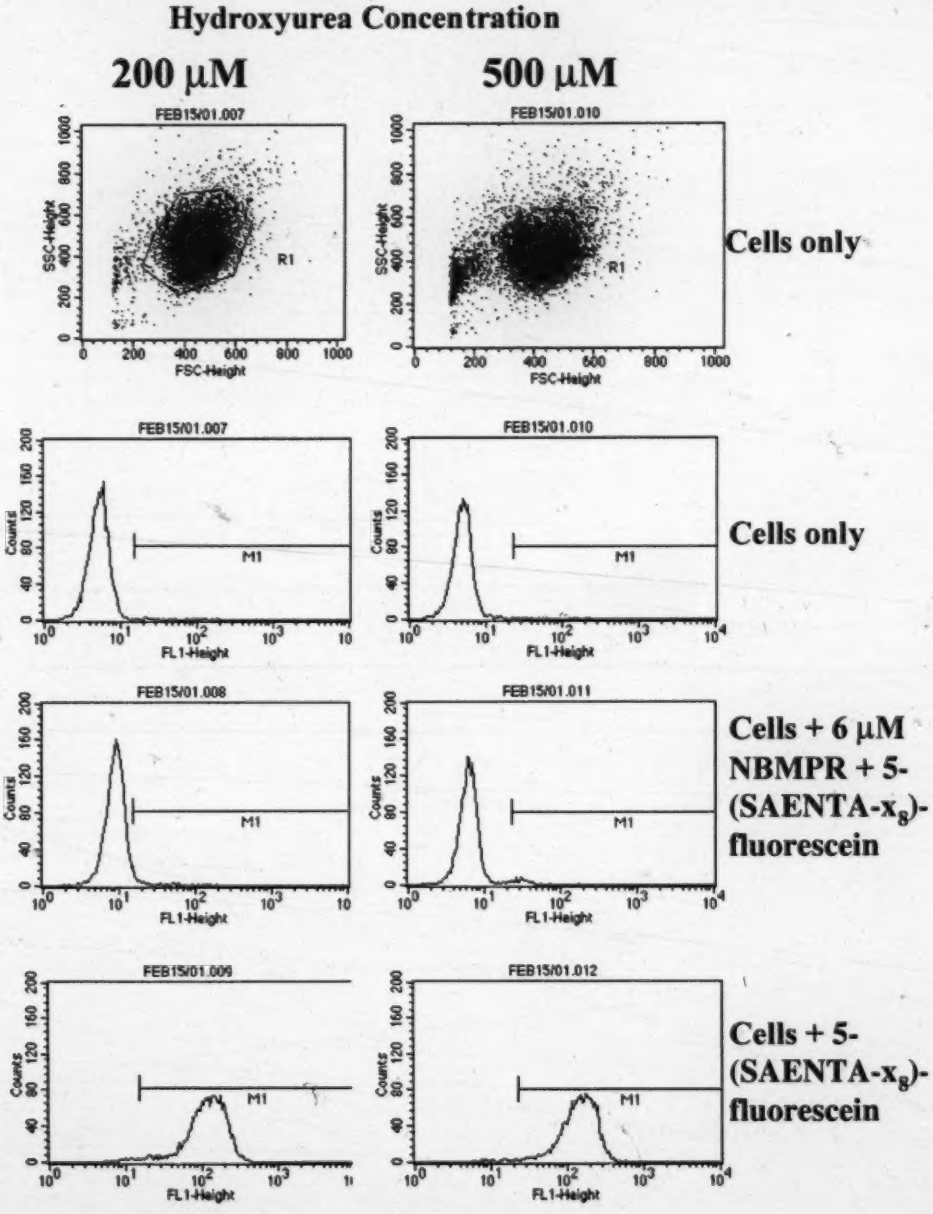

Figure 6-3. Analysis of Hydroxyurea-treated CEM Cells using Flow Cytometry and Anti-hENT1 Monoclonal Antibodies. CEM cells were incubated in growth medium for 24 h without or with 50, 200 or 500 μM of hydroxyurea and then analysed by flow cytometry as described in Chapter 2 S. For each concentration (from top to bottom), the four panels in each are representations of the side and forward light scatter, the fluorescence of unpermeabilized CEM cells, the fluorescence of permeabilized CEM cells incubated with goat anti-mouse Alexa 488 secondary antibodies only, and the fluorescence of CEM cells incubated anti-hENT1 monoclonal antibodies (clone 10D7G2) and goat anti-mouse Alexa 488 secondary antibodies. Shown here is a representative result from two experiments that gave similar results.

Figure 6-3

Analysis of Hydroxyurea-treated CEM Cells using Flow Cytometry and Anti-hENT1 Monoclonal Antibodies

Hydroxyurea Concentration

0 μM **50 μM**

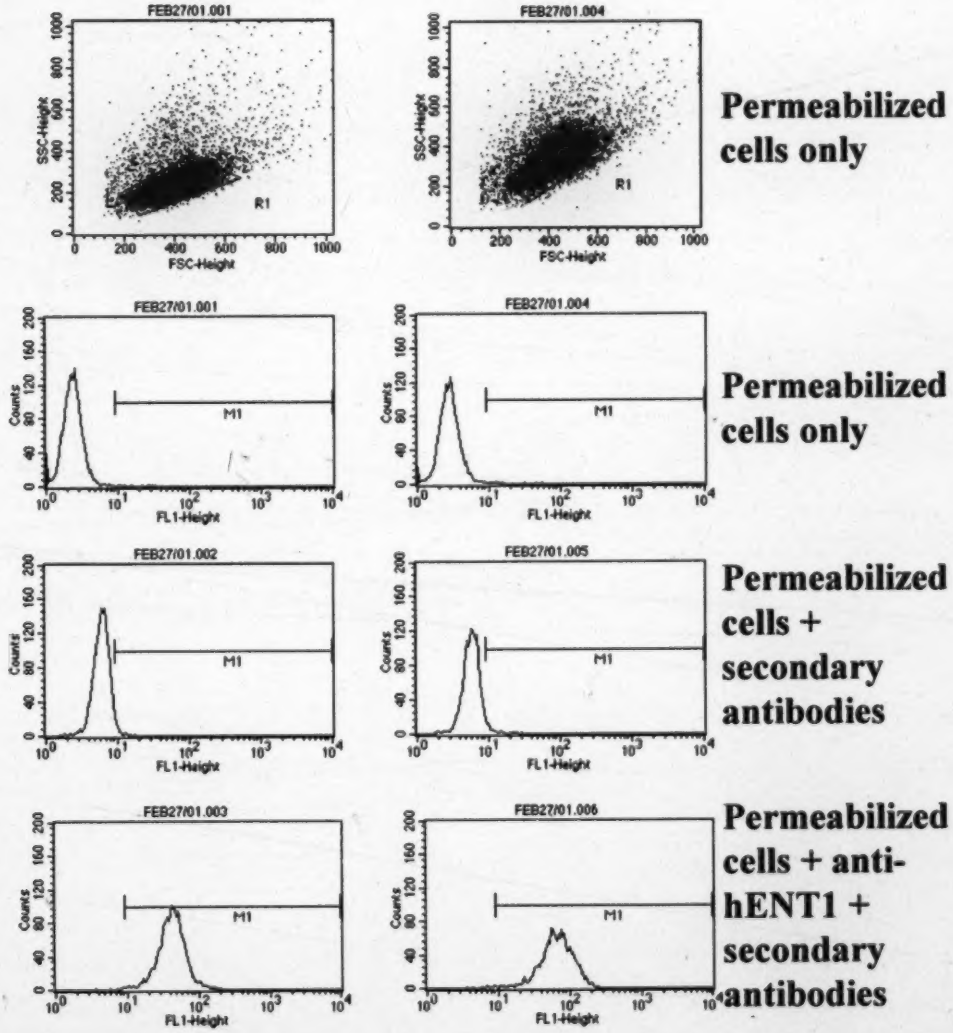

Permeabilized cells only

Permeabilized cells only

Permeabilized cells + secondary antibodies

Permeabilized cells + anti-hENT1 + secondary antibodies

Figure 6-3

Analysis of Hydroxyurea-treated CEM Cells using Flow Cytometry and Anti-hENT1 Monoclonal Antibodies

Hydroxyurea Concentration

200 μM **500 μM**

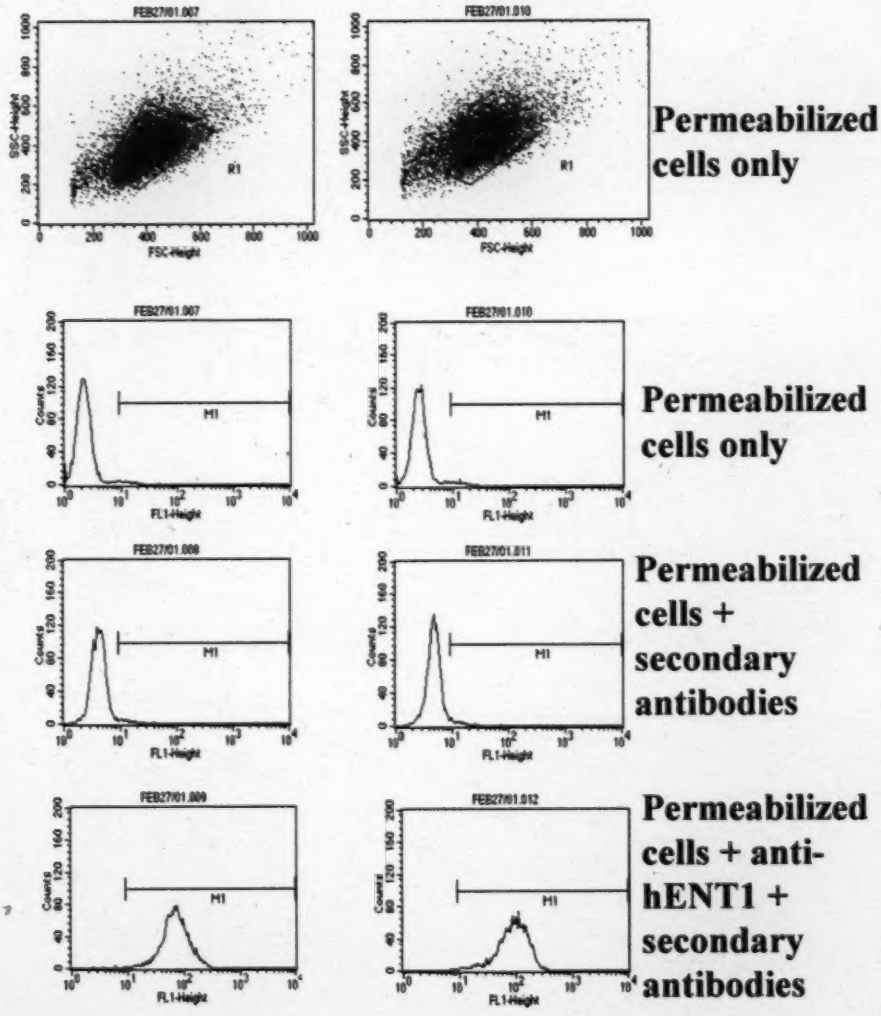
Permeabilized cells only
Permeabilized cells only
Permeabilized cells + secondary antibodies
Permeabilized cells + anti-hENT1 + secondary antibodies

Figure 6-4. NBMPR Binding in Hydroxyurea-treated CEM Cells. CEM cells were incubated in growth medium for 24 h without (Panels *A*, *B*) or with 200 μM of hydroxyurea (Panels *C*, *D*). Site-specific binding of NBMPR-binding was measured in CEM cells under equilibrium conditions as described in Chapter 2 T. In panels *A* and *C*, the binding isotherms are presented as pmol/mg protein. In panels *B* and *D*, the Scatchard analyses are presented. Error bars represent standard error of the mean for replicate values determined in individual experiments and thus indicate the precision with which the experiment was performed; some error bars are not visible because the values were too small. Shown here is a representative result from three experiments that gave similar results.

Figure 6-4

NBMPR Binding in Hydroxyurea-treated CEM Cells

A. 0 μM Binding Isotherm

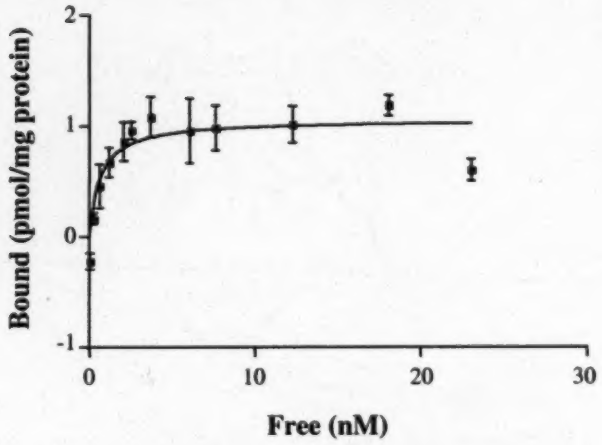

B. 0 μM Scatchard Analysis

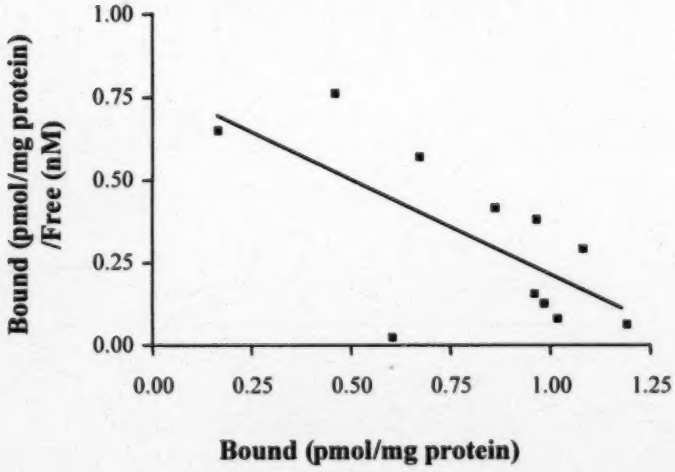

Figure 6-4

NBMPR Binding in Hydroxyurea-treated CEM Cells

C. 200 μM Binding Isotherm

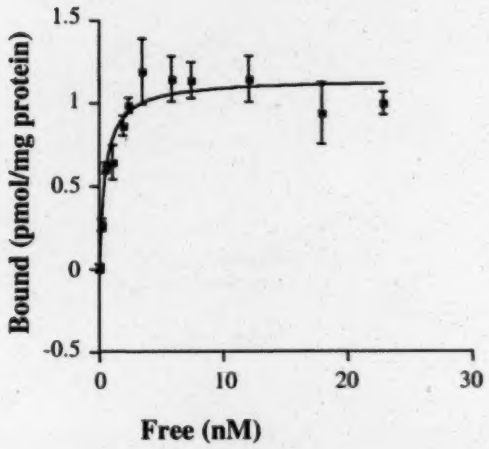

D. 200 μM Scatchard Analysis

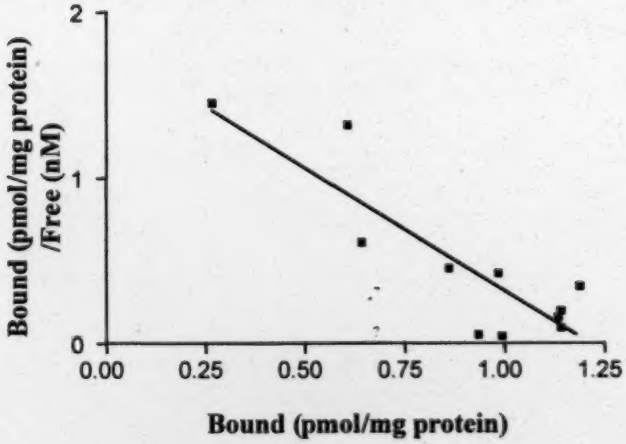

Figure 6-5. Taqman Real-time Quantitative RT-PCR Analysis of hENT1 in Hydroxyurea-treated CEM Cells. CEM cells were treated with hydroxyurea for 24 h and RNA was isolated as described in Chapter 2 F. Taqman RT-PCR was performed as described in Chapter 2 G. Depicted here is the visual representation of the fluorescence emitted by the formation of hENT1- and GAPDH)-specific products. Two reactions per sample were prepared for each experimental condition (0, 50, 200, 500 μM hydroxyurea). Shown here is a representative result of three experiments which gave similar results. *A*, hENT1 results *B*, GAPDH results.

Figure 6-5

Taqman Real-time Quantitative RT-PCR Analysis of hENT1 in Hydroxyurea-treated CEM Cells

A. hENT1 Analysis

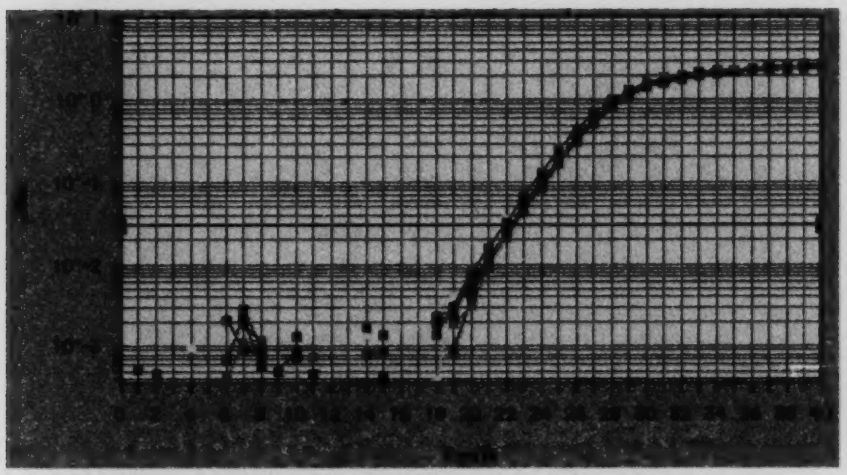

B. GAPDH Control Analysis

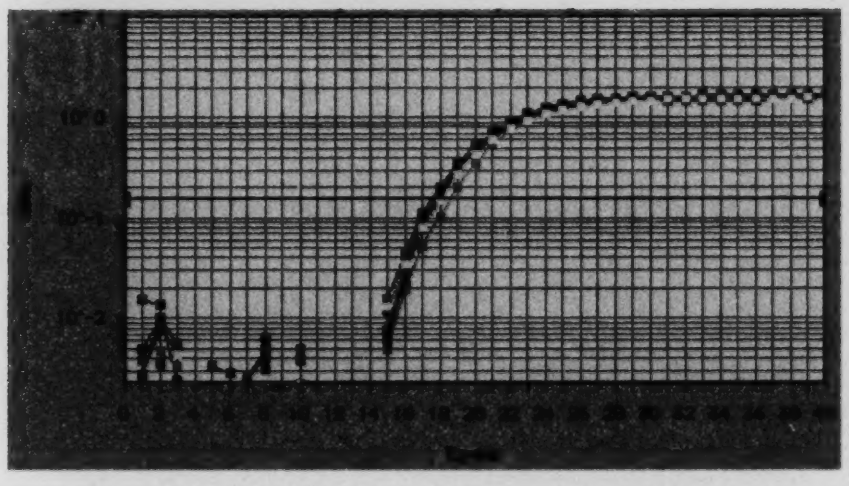

Figure 6-6. Uridine Transport in Hydroxyurea-treated CEM Cells. CEM cells were incubated in growth medium for 24 h without or with 50, 200 or 500 μM of hydroxyurea. Subsequently, cells were harvested and initial rates of cellular uptake of 10 μM [^{3}H]-uridine were measured as described in Chapter 2 C. Results are presented as pmol/cell number (Panel *A*) and pmol/μL cell water (Panel *B*). Error bars represent standard error of the mean for replicate values determined in individual experiments and thus indicate the precision with which the experiment was performed; some error bars are not visible because the values were too small. Shown here are representative results from six experiments, two of which involved measurements of cell numbers and cell volumes on the cell preparations.

Figure 6-6
Uridine Transport in Hydroxyurea-treated CEM Cells

A. Results plotted as pmol/10^6 cells

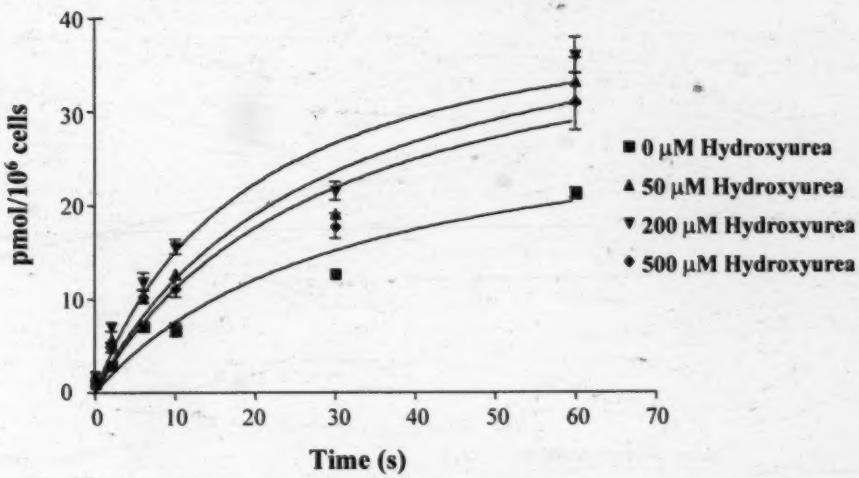

B. Results plotted as pmol/μL cell water

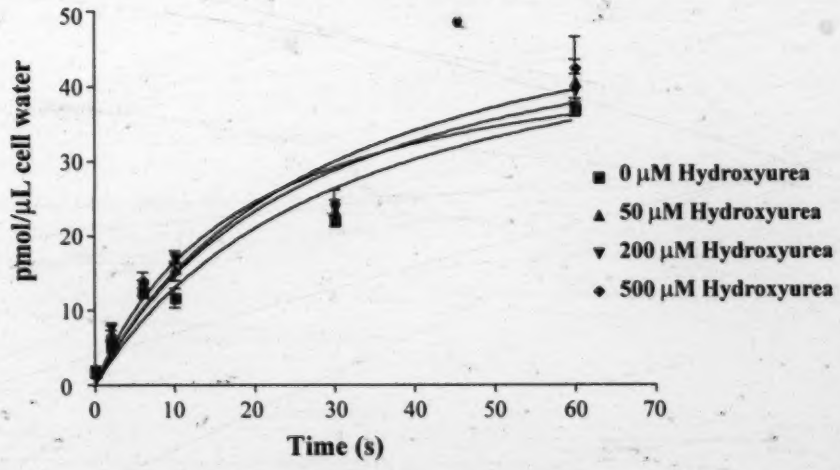

NO TEXT ON PAGE

Figure 6-7. RT-PCR Analysis of HEK293 Cells. HEK293 cells were grown as described in Chapter 2 B. Messenger RNA (mRNA) was isolated from cells using the FASTTrack mRNA isolation protocol as described in Chapter 2 F. RT-PCR was performed using the Gibco/BRL Life Technologies Superscript RT-PCR kit and primers specific for hENT1 and hENT2 as described in Chapter 2 G I. BeWo total RNA was used as a positive control. The PCR products were run out on a 1% agarose gel. Lanes *1*, Control PCR *2*, RT-PCR from BeWo (hENT1) *3*, RT-PCR from BeWo (hENT2) *4*, RT-PCR from HEK293 (hENT1 #1) *5*, RT-PCR from HEK 293 (hENT2 #1) *6*, RT-PCR from HEK 293 (hENT1 #2) *7*, RT-PCR from HEK293 (hENT2 #2) *M* 123-bp ladder (Gibco/BRL Life Technologies). Shown here is a representative result from 3 experiments.

Figure 6-7 RT-PCR Analysis of HEK293 Cells

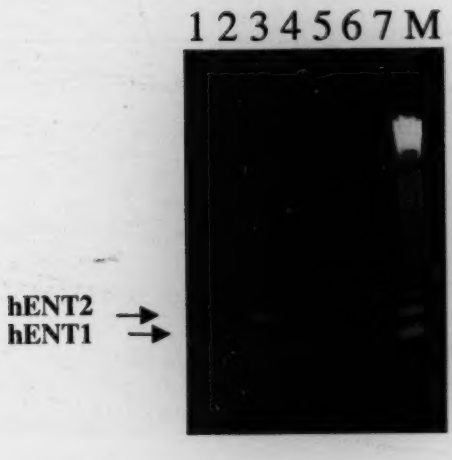

Figure 6-8. Characterization of Nucleoside Transport in HEK293 Cells. HEK293 cells were grown as described in Chapter 2 B. Briefly, HEK293 cells (approximately 8 x 10^8 cells) were trypsinized, centrifuged and then resuspended (1 x 10^7 cells/mL) in either sodium buffer, sodium buffer with 100 μM diiazep, sodium buffer with 0.1 μM NBMPR, NMG buffer or NMG buffer with 100 μM dilazep. Subsequently, 10 μM uridine transport was measured as described in Chapter 2 C. Results were graphed as pmol/μL cell water. Error bars represent standard error of the mean for replicate values determined in individual experiments and thus indicate the precision with which the experiment was performed; some error bars are not visible because the values were too small. Shown here is a representative result from 4 experiments.

Figure 6-8

Characterization of Nucleoside Transport in HEK293 Cells

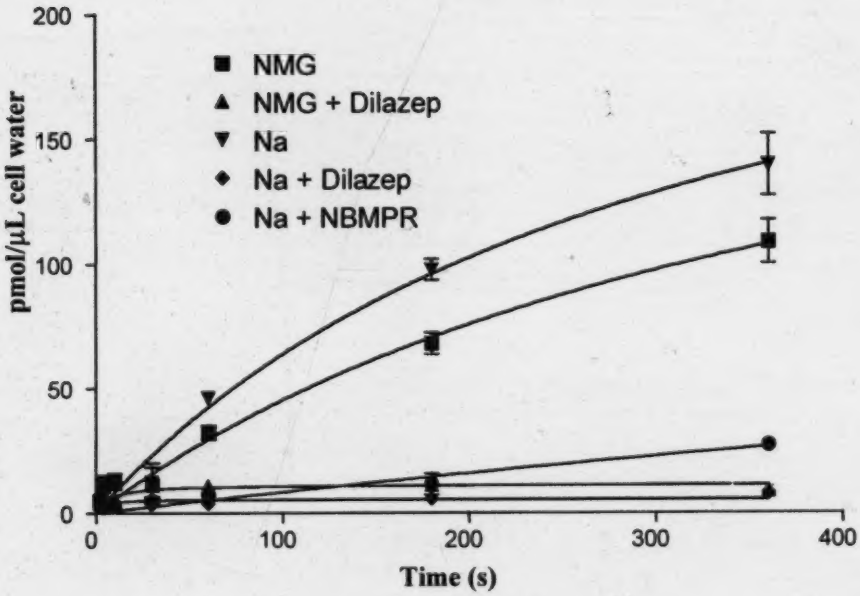

Figure 6-9. RT-PCR Analysis of HEK293 Cells Stably Transfected with Plasmids containing Sense and Antisense hENT1 and hENT2 cDNAs. HEK293 cells were grown as described in Chapter 2 B. Total RNA was isolated from cells using the Qiagen RNeasy isolation protocol as described in Chapter 2 F. RT-PCR was performed using single tube RT-PCR as described in Chapter 2 G I. and the PCR products were separated on a 1% agarose gel. *A*. RT-PCR from hENT1-transfected cells. Lanes *1*, hENT1 clone #1; *2*, hENT1 clone #2; *3*, hENT1 clone #3; *M*, 123-bp ladder. *B*. RT-PCR from hENT2-transfected cells. Lanes *1*, hENT2 clone #2; *2*, hENT2 clone #4; *M*, 123-bp ladder. *C*. RT-PCR from hENT1as-transfected cells. Lanes *1*, hENT1as clone #2; *2*, hENT1as clones #3; *3*, hENT1as clone #4; *M*, 123-bp ladder. *D*. RT-PCR from hENT2as-transfected cells. Lanes *1*, hENT2as clone #1; *2*, hENT2as clones #2; *3*, hENT2as clone #3; *4*, hENT2as clone #4; *M*, 123-bp ladder.

Figure 6-9

RT-PCR Analysis of HEK293 Cells Stably Transfected with Plasmids containing Sense and Antisense hENT1 and hENT2 cDNAs

Figure 6-10. Characterization of Nucleoside Transport in HEK293 Cells Stably Transfected with Plasmids containing Antisense hENT1 and hENT2 cDNAs. HEK293 cells were grown as described in Chapter 2 B. For uptake assays, approximately 8×10^8 cells were trypsinized, centrifuged and then resuspended (1×10^7 cells/mL) in either sodium buffer or sodium buffer with 0.1 μM NBMPR. Subsequently, 10 μM [^{3}H]-uridine transport was measured as described in Chapter 2 C. Results were graphed as pmol/10^6 cells. Error bars represent standard error of the mean for replicate values determined in individual experiments and thus indicate the precision with which the experiment was performed; some error bars are not visible because the values were too small. Shown here is a single experiment. Qualitatively similar results were obtained in three other experiments performed with uncloned transfectants as well as with two different clones transfected with each antisense-containing plasmid.

Figure 6-10

Characterization of Nucleoside Transport in HEK293 Cells Stably Transfected with Plasmids containing Antisense hENT1 and hENT2 cDNAs

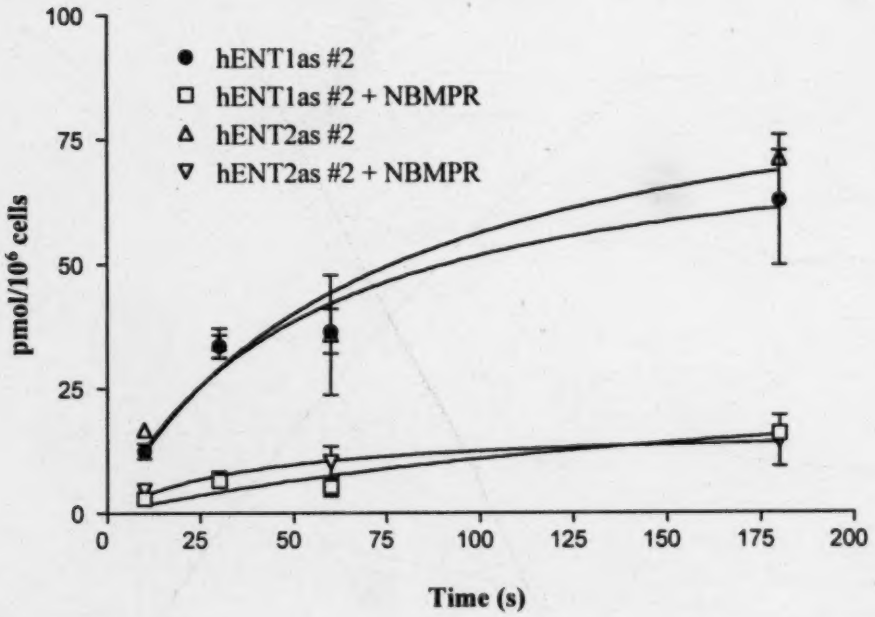

Table 6-1. Flow Cytometry using 5-(SAENTA-x_8)-fluorescein. CEM cells were incubated in growth media with hydroxyurea at the concentrations indicated for 24 h and analysed by flow cytometry as described in Chapter 2 S. Each experimental condition was controlled for non-specific binding (using 10 μM NBMPR) and autofluorescence (using cells that were not incubated with SAENTA-FITC) according to the protocol described in Chapter 2 S. The relative mean fluorescence values for the gated population (10, 000 cells) for each condition are shown in the table. The results of two separate experiments are shown below.

Hydroxyurea (μM)	Experiment #1		Experiment #2	
	Relative Mean Fluorescence	Percent of Control	Relative Mean Fluorescence	Percent of Control
0	94.07	100	73.62	100
50	127.43	135.5	92.50	125.6
200	125.30	133.2	110.68	150.3
500	150.59	160.1	115.13	156.4

Table 6-2. Flow Cytometry using Anti-hENT1 Monoclonal Antibodies. CEM cells were incubated in growth media with hydroxyurea at the concentrations indicated for 24 h and analysed by flow cytometry as described in Chapter 2 S. Each experimental condition was controlled for non-specific binding (using cells incubated only with secondary antibodies) and autofluorescence (using cells incubated without any antibodies). The relative mean fluorescence values for the gated population (10, 000 cells) for each condition are shown in the table. The data shown are for one of three experiments that gave qualitatively similar results.

Hydroxyurea (μM)	Relative Mean Fluorescence	Percent of Control
0	392.32	100
50	535.21	136.4
200	621.69	158.5
500	460.74	117.4

Table 6-3. Effects of Hydroxyurea on Site-specific Binding of NBMPR to CEM Cells. CEM cells were incubated in growth media without or with 200 μM hydroxyurea at the concentrations indicated for 24 h and NBMPR binding was assessed as described in Chapter 2 T. NBMPR-binding sites/cell were calculated by determining the amount of mol/cell and then multiplying by Avogadro's number (6.022×10^{23}). B_{max}, K_d and sites/cell values are shown below ± standard error. Error bars represent standard error of the mean for replicate values determined in individual experiments and thus indicate the precision with which the experiment was performed; some error bars are not visible because the values were too small. The results of three separate experiments are shown below.

Hydroxyurea (μM)		**0**	**200**
Experiment #1			
	B_{max} (pmol/10^6 cells)	0.49 ± 0.01	0.78 ± 0.02
	sites/cell	$3.0 \times 10^5 \pm 6.0 \times 10^3$	$1.2 \times 10^6 \pm 8.4 \times 10^4$
	K_d	0.29 ± 0.04	0.35 ± 0.05
Experiment #2			
	B_{max} (pmol/mg protein)	0.91 ± 0.07	1.13 ± 0.06
	sites/cell	$1.1 \times 10^5 \pm 8.9 \times 10^3$	$4.7 \times 10^5 \pm 1.1 \times 10^4$
	K_d	1.25 ±0.40	0.33 ± 0.11
Experiment #3			
	B_{max} (pmol/mg protein)	1.06 ± 0.09	1.14 ± 0.06
	sites/cell	$1.0 \times 10^5 \pm 1.1 \times 10^4$	$2.1 \times 10^5 \pm 1.0 \times 10^3$
	K_d	0.64 ± 0.29	0.49 ± 0.14

Table 6-4. Taqman Real-time Quantitative RT-PCR Analysis of hENT1 in Hydroxyurea-treated CEM Cells. CEM cells were treated with hydroxyurea for 24 h and RNA was isolated as described in Chapter 2 F. Taqman RT-PCR, which was performed as described in Chapter 2 G (see Figure 6-5), was used to analyse the relative quantities of hENT1 in CEM cells treated with various concentrations of hydroxyurea. The results of three independent experiments are shown below.

Hydroxyurea (μM)	Relative Amount of hENT1 mRNA		
	Experiment #1	Experiment #2	Experiment #3
0	1	1	1
50	1.01	1.23	0.76
200	1.27	1.44	0.81
500	2.94	1.67	1.56

Table 6-5. Comparison of Uridine Transport Rates in Hydroxyurea-treated CEM Cells. CEM cells were incubated in growth media with hydroxyurea at the concentrations indicated for 24 h. Uptake of 10 [^{3}H]-uridine transport was measured as shown in Figure 6-6. Transport rates were calculated from linear initial rates of uptake determined during the first 6 seconds using the GraphPad Prism program. Shown here are representative results from six experiments, two of which involved measurements of cell numbers and cell volumes on the cell preparations. Presented below are the values obtained from the results (mean ± standard error) of Figure 6-6. Error bars represent standard error of the mean for replicate values determined in individual experiments and thus indicate the precision with which the experiment was performed; some error bars are not visible because the values were too small.

	Rate of Transport (pmol/10^6 cells/s)[1]	**Rate of Transport (pmol/μL cell water/s)[2]**
Hydroxyurea (μM)		
0	1.03 ± 0.03	1.78 ± 0.06
50	1.42 ± 0.15	1.73 ± 0.18
200	1.61 ± 0.19	1.77 ± 0.20
500	1.44 ± 0.12	1.97 ± 0.16

[1]n=6
[2]n=2

Table 6-6. Comparison of Volumes of Hydroxyurea-treated CEM Cells. CEM cells were incubated in growth media with hydroxyurea at the concentrations indicated for 24 h. Cells were enumerated and the diameter measurements (mean ± standard deviation) were obtained by using a Coulter Counter as described in Chapter 2 B. Cell water was determined as described in Chapter 2 C. Volume is expressed µL cell water.

	Coulter counter diameter[1] (µm)	Volume (µL cell water)[2]
Hydroxyurea (µM)		
0	14.40 ± 0.90	0.555
50	16.40 ± 0.24	0.647
200	16.66 ± 0.31	0.705
500	15.82 ± 0.36	0.805

[1]n=3 (4 or 6 different measurements from 3 different experiments)
[2]n=2

Chapter 7

7. Summary and Conclusions

The goals of this study were quite diverse and dealt with members of two different transport protein families. The overall objective was to determine the subcellular localization of membrane transporter proteins of the LAPTm4 and ENT families. It was hoped that revealing the intracellular location of these proteins would provide insights into their biological roles. Potential regulatory mechanisms of equilibrative nucleoside transporters were also analysed using metabolic and translational perturbatory methods.

7 A. The mLAPTm4 Protein is a Lysosomal/Endosomal Transporter

The first objective was to determine the substrate specificity of a then newly characterized four-transmembrane domain protein, originally termed MTP and now known as mLAPTm4. However, despite repeated and varied efforts to improve production of mLAPTm4 in *X. laevis* oocytes, the transport activities observed were very low. No insights into potential nucleoside substrates of the transporter were gained by these studies in oocytes. Thus, the subcellular localization of mLAPTm4 was determined in the hopes that the intracellular location of the mLAPTm4 might provide clues to its function.

Recombinant epitope-tagged mLAPTm4 was localized to lysosomes and endosomes in transiently transfected cells using double-label immunofluorescence confocal microscopy. Subsequently, it was discovered that mLAPTm4 is involved in drug sequestration and that the full-length protein differed from the truncated versions in that it did not transport nucleosides when expressed in yeast [168]. Drug sequestration is an important mechanism of drug resistance [260-271] and weakly basic chemotherapeutic drugs, such as anthracyclines and vinca alkaloids, have been shown to compartmentalize in lysosomes [264-268, 270]. The highly conserved LAPTm4 family may play a critical role in this process. Studies describing interacting proteins, mouse and fruit fly mutants, and site-directed mutagenesis of LAPTm4 and LAPTm5 family members are underway to further elucidate the role of these transporters (Douglas Hogue, Dalhousie University, personal communication).

7 B. Detection and Visualization of Recombinant and Endogenous hENT1 and hENT2

hENT1 and hENT2 are the predominant mediators of equilibrative nucleoside transport in human cells. This study focussed on generating the tools necessary to visualize hENT1 and hENT2 by immunoblot and immunofluorescence analysis to enable biochemical and cell biological studies. Although efforts to raise antibodies against an epitope in the large extracellular loop of hENT1 between transmembrane domains 1 and 2 were not successful, collaborative studies led by Jennings *et al.*, [115] produced polyclonal and monoclonal antibodies against an epitope in the large intracellular loop of hENT1 between transmembrane domains 6 and 7. Anti-hENT2 polyclonal and monoclonal antibodies were raised in this study against the large intracellular loop of

hENT2. The hENT1 and hENT2 sequences in this loop region have low amino acid identities and the antibodies produced were, therefore, expected to distinguish between the two proteins. The anti-hENT1 and anti-hENT2 antibodies were used to recognize recombinant and endogenous hENT proteins in transiently transfected hamster cells and in human cells, respectively.

In immunoblotting experiments, the anti-hENT1 antibodies recognized recombinant proteins of ~50 kDa from cells transiently transfected with plasmids encoding hENT1-HA and endogenous proteins of ~50 kDa from HeLa and BeWo membrane preparations. In immunofluorescence experiments, the anti-hENT1 antibodies stained mostly the plasma membranes of HeLa and BeWo cells, but intracellular membrane staining was also seen in most cells. Determination of the subcellular location of this intracellular staining is currently being pursued by examining other organelles, such as the endoplasmic reticulum and lysosomes.

The anti-hENT2 antibodies recognized recombinant proteins of ~50 kDa in immunoblots of cells transfected with plasmids encoding hENT2-VSV-G, but were unable to detect endogenous hENT2 from BeWo and HeLa crude membranes. The anti-hENT2 polyclonal antibodies reacted with intracellular epitopes in HeLa and BeWo cells that were shown to be mitochondrial in nature. It is not known whether the mitochondrial entity was hENT2, hHNP36 or a hENT2-like protein. It could also have been a non-related protein with a conformationally similar epitope, since the mitochondrial staining observed using the anti-hENT2 polyclonal antibodies could not be diminished by blocking with GST-eif polypeptides in immunofluorescence experiments, suggesting that the mitochondrial staining may not have been specific. The preimmune sera from the same animal did not stain cells. However, the anti-hENT2 monoclonal antibodies detected a species of ~45 kDa from enriched human liver mitochondria in immunoblot analyses. Competition experiments will be attempted to ascertain whether or not the anti-hENT2 monoclonal antibodies are specifically recognizing this mitochondrial protein in immunoblots. The lack of plasma membrane staining and the lack of immunoreactive species in immunoblots with the anti-hENT2 antibodies suggests that there were very small amounts of hENT2 in BeWo and HeLa cells or that the antibodies are of low affinity. Another approach would be to isolate the hENT2-like protein from enriched mitochondria. Immunoprecipitation experiments using enriched human liver mitochondrial fractions are currently underway with the goal of using mass spectrometry as a way to identify the immunoreactive mitochondrial species.

Another informative experiment would be to determine the glycosylation state of the protein species detected by the anti-hENT2 antibodies in mitochondria. The enriched mitochondria could be treated with deglycosylation enzymes and analysed by immunoblotting. If the proteins are glycosylated, this result would suggest that the protein is a contaminant from another intracellular membrane (*e.g.*, endoplasmic reticulum). If the proteins are not glycosylated, this results would suggest that the proteins are in fact mitochondrial.

The availability of anti-hENT1 and anti-hENT2 antibodies enable the isolation of hENT1 and hENT2 via immunoprecipitation reactions. In this study,

immunoprecipitation of hENT1 was demonstrated; it is not yet known if the anti-hENT2 antibodies can immunoprecipitate hENT2. An informative experiment would be to determine the half-life of hENT1 and of hENT2 in tissue culture cells by metabolic-labelling [210]. This information may provide clues to how the proteins are turned over and possible routes of ENT protein regulation.

The anti-hENT1 monoclonal antibodies have been used to detect hENT1 by immunohistochemistry in samples of breast tissue [340] with the goal being to use the anti-hENT1 antibodies as a predictive tool to guide clinicians in their use of anticancer nucleoside analogues such as gemcitabine. In some cancer samples, increased levels of hENT1 have been observed. For example, high levels of specific NBMPR binding have been detected in many types of tumours, when compared to normal tissues [341] and hENT1 cDNA has been isolated in a screen of upregulated genes in 5-fluorouracil-resistant tumours [342]. It is not known if this reflects the proliferation state of the cells or enhanced drug sensitivity. It is not yet known whether or not the anti-hENT2 monoclonal antibodies can be used in immunohistochemistry experiments. The role of hENT2 in drug resistance in human diseases is not well understood, since the ability to detect it did not exist until this study. However, in the future, immunohistochemistry experiments, probably using skeletal muscle first since this tissue possesses an abundance of hENT2 mRNA, will be attempted with the anti-hENT2 monoclonal antibodies to assess their suitability for this application. Only then will tumour tissues be examined using this methodology to know if the anti-hENT2 antibodies will also be useful as predictive tools for therapy.

The GST-esf and GST-eif fusion proteins produced in this study (i.e., fusions with the large intracellular loops of hENT1 and hENT2, respectively) and the anti-hENT1 and anti-hENT2 antibodies may be useful in identifying interacting proteins by GST-pull down assays [210] and immunoprecipitation reactions, respectively. If interacting proteins do bind to either hENT1 or hENT2 at the large intracellular loop regions between transmembrane domains 6 and 7, the GST fusion proteins are potentially useful tools, since the hENT1 and hENT2 fusion proteins are comprised of amino acids from the large intracellular loop region. Since both the anti-hENT1 and anti-hENT2 antibodies bind in the large intracellular loop regions, they may interfere with potentially interacting proteins and thus would not be good tools to look for interacting proteins. However, this can only be determined by experimentation.

More anti-hENT1-specific and anti-hENT2-specific antibodies will be necessary to properly study these important proteins of the salvage pathway. For example, antibodies directed against extracellular epitopes of hENT1 and hENT2 are desirable for analysis of intact cells. By making more antibodies to different sequences on hENT1 and hENT2, different types of analyses can be used to examine hENT in human cells and tissues.

7 C. The hENT2 Gene and Alternate Splice Products

This study demonstrated that hHNP36 is a splice product of the hENT2/hHNP36

gene that results from the usage of an alternative splice site in exon 3. The amount of hHNP36 transcripts when compared to the amount of hENT2 transcripts was very small in four human tissue culture cell lines. Also, the anti-hENT2 antibodies recognized recombinant hHNP36-VSV-G in immunoblot and immunofluorescence analyses. In the study of human brain membrane samples [115], anti-hENT2 immunoblots show mainly two proteins, one of ~50 kDa and another of ~36 kDa, suggesting that endogenous hHNP36 can be detected. At the moment, there is no way to distinguish between the two endogenous proteins in immunofluorescence studies, since the anti-hENT2 antibodies were raised against a region that is found in both proteins, thus any differences in the localization of the endogenous proteins cannot yet be determined, if they are detectable in cell lines.

hHNP36 is a truncated version of hENT2, comprised of the last 326 amino acids and 8 transmembrane domains of hENT2. However, the hydropathy predictions suggested that it could have either 7 or 8 transmembrane domains [147, 148, 157]. If it is produced, what is its orientation in the membrane? Topology studies such as those undertaken with hENT1 [304] could be used to answer this question.

The generation of specific anti-hENT2 antibodies would be necessary to distinguish between the two protein products of the hENT2 gene in immunofluorescence experiments. An N-terminal antigen, such as the one suggested by the Alberta Peptide Institute for hENT2 (see Table 4-1), may generate antibodies that could distinguish between hENT2 and hHNP36 to this end. Transfection studies using two different epitope tags on hENT2 and hHNP36 may also be fruitful in determining if these proteins reside in different intracellular locations.

How much hHNP36 is found in cells? The GeneScan RT-PCR results suggested that the amounts of HNP36 differed among cell lines. mRNA isolated from different human tissues could be analysed to determine whether some tissues have more hHNP36 transcripts than others. If endogenous hHNP36 is present in cells, what is its function? Studies in heterologous systems may provide clues to the function of this truncated version of hENT2. Also, purification and reconstitution of the recombinant protein into proteoliposomes could be used to establish the function of hHNP36.

7 D. Potential Regulatory Mechanisms of the ENT family

The regulation of the ENT proteins was probed using two perturbatory methods. The first method involved treating CEM cells with hydroxyurea. CEM cells treated with hydroxyurea suffer from unbalanced growth, a condition characterized by the inhibition of DNA synthesis while mRNA and protein synthesis continues [325]. When the amounts of hENT1 were measured by flow cytometry or by NBMPR-binding, the amounts increased on a per cell basis. This increase in the amount of hENT1 was proportional to the increase in cell size as a result of the unbalanced growth and indicated that treatment of CEM cells with hydroxyurea did not affect hENT1 levels.

Other reagents that perturb dNTP pools, such as thymidine, 5-fluorouracil, gemcitabine, cytarabine and aphidicolin should be tested. However, cells should be

analysed after shorter exposure times, since any attempts by cells to increase the amount of dNTPs may be short-lived and reactionary. Also, any further analyses performed with a flow cytometer should include DNA-binding dyes to allow for assessment of the cell cycle state.

The second perturbation method involved the production of hENT1 or hENT2 antisense mRNA. The HEK293 cell line was characterized for the first time with respect to nucleoside transport activity. HEK293 cells only possess the hENT1-mediated *es* and the hENT2-mediated *ei* activities. Stable transfectants producing either hENT1 antisense or hENT2 antisense were established. The hope was that ablation of either ENT activity would be observed. However, the stable transfectants producing either antisense exhibited both transport activities, suggesting that the production of the antisense was not successful. A different approach using either a different expression vector, specific antisense oligonucleotides [336] or specific ribozymes [337-339] should be attempted. Such experiments may reveal if the activity of the two ENT transporters is somehow linked.

Other ways could be used to study if the ENT activities are co-ordinated. For example, pharmacological inhibitors could be used to specifically inhibit the activity of one of the ENT proteins. Presently, only a hENT1-specific inhibitor, NBMPR, exists that would allow for this type of experiment. A search for hENT2-specific inhibitors could be initiated using the *S. cerevisiae* complementation system as a screen.

The rationale for having at least two ENT proteins on the plasma membrane of cells with different levels of activity and different substrate specificities is not yet understood except that perhaps for evolutionary purposes protection from cytotoxic chemicals and redundant functions are beneficial to survival. Further experimentation utilizing new and old molecular and pharmacological tools, will enable these questions to be answered and undoubtedly create more questions.

Chapter 8

8. Bibliography

1. Baldwin, S.A., et al., *Nucleoside transporters: molecular biology and implications for therapeutic development.* Mol Med Today, 1999. **5**(5): p. 216-224.
2. Cass, C.E., J.D. Young, and S.A. Baldwin, *Recent advances in the molecular biology of nucleoside transporters of mammalian cells.* Biochem Cell Biol, 1998. **76**(5): p. 761-70.
3. Cass, C.E., *Nucleoside Transport*, in *Drug Transport in Antimicrobial and Anticancer Chemotherapy*, N.H. Georgopapadakou, Editor. 1995, Marcel Deker: New York, NY. p. 403-451.
4. Cass, C.E., et al., *Nucleoside transporters of mammalian cells*, in *Membrane Transporters as Drug Targets*, G.L. Amidon and W. Sadée, Editors. 1999, Kluwer Academic/Plenum Publishers: New York, NY. p. 313-52.
5. Griffith, D.A. and S.M. Jarvis, *Nucleoside and nucleobase transport systems of mammalian cells.* Biochimica et Biophysica Acta, 1996. **1286**(3): p. 153-181.
6. Young, J.D., et al., *Molecular Mechanisms of Nucleoside and Nucleoside Drug Transport*, in *Gastrointestinal Transport: Molecular Physiology*, K.E. Barrett and M. Donowitz, Editors. 2001, Academic Press: San Diego, CA. p. 329-378.
7. Mani, R.S., et al., *Demonstration of equilibrative nucleoside transporters (hENT1 and hENT2) in nuclear envelopes of cultured human choriocarcinoma (BeWo) cells by functional reconstitution in proteoliposomes.* J Biol Chem, 1998. **273**(46): p. 30818-25.
8. Pisoni, R.L. and J.G. Thoene, *Detection and characterization of a nucleoside transport system in human fibroblast lysosomes.* J Biol Chem, 1989. **264**(9): p. 4850-6.
9. Arner, E.S.J. and S. Eriksson, *Mammalian deoxyribonucleoside kinases.* Pharmacology and Therapeutics, 1995. **67**: p. 155-186.
10. Landfear, S.M., *Molecular genetics of nucleoside transporters in Leishmania and African trypanosomes.* Biochem Pharmacol, 2001. **62**(2): p. 149-55.
11. Landfear, S.M., *Genetics and biochemistry of Leishmania membrane transporters.* Curr Opin Microbiol, 2000. **3**(4): p. 417-21.
12. Carter, N.S., S.M. Landfear, and B. Ullman, *Nucleoside transporters of parasitic protozoa.* Trends Parasitol, 2001. **17**(3): p. 142-5.
13. Murray, A.W., *The biological significance of purine salvage.* Annu Rev Biochem, 1971. **40**: p. 811-26.
14. Hu, M., *Comparison of uptake characteristics of thymidine and zidovudine in a human intestinal epithelial model system.* Journal of Pharmaceutical Sciences, 1993. **82**(8): p. 829-833.
15. Zimmerman, T.P., W.B. Mahony, and K.L. Prus, *3'-azido-3'-deoxythymidine. An unusual nucleoside analogue that permeates the membrane of human erythrocytes and lymphocytes by nonfacilitated diffusion.* J Biol Chem, 1987. **262**(12): p. 5748-54.
16. Gourdeau, H., et al., *Mechanisms of Uptake and Resistance to Troxacitabine, a Novel Deoxycytidine Nucleoside Analogue, in Human Leukemic and Solid Tumour*

Cell Lines. Cancer Res, 2001. **in press.**

17. Dunwiddie, T.V. and S.A. Masino, *The role and regulation of adenosine in the central nervous system.* Annu Rev Neurosci, 2001. **24**: p. 31-55.
18. Jin, X., et al., *Inosine binds to A3 adenosine receptors and stimulates mast cell degranulation.* J Clin Invest, 1997. **100**(11): p. 2849-57.
19. Olah, M.E., H. Ren, and G.L. Stiles, *Adenosine receptors: protein and gene structure.* Arch Int Pharmacodyn Ther, 1995. **329**(1): p. 135-50.
20. Abd-Elfattah, A.S., et al., *Differential cardioprotection with selective inhibitors of adenosine metabolism and transport: role of purine release in ischemic and reperfusion injury.* Mol Cell Biochem, 1998. **180**(1-2): p. 179-91.
21. Abd-Elfattah, A.S., et al., *Nucleoside transport protein: Properties and regulation,* in *Purines and Myocardial Protection,* A.S. Abd-Elfattah and A.S. Wechsler, Editors. 1996, Kluwer Academic Publishers. p. 151-163.
22. Brown, J.R., K. Cornell, and P.W. Cook, *Adenosine- and adenine-nucleotide-mediated inhibition of normal and transformed keratinocyte proliferation is dependent upon dipyridamole- sensitive adenosine transport.* J Invest Dermatol, 2000. **115**(5): p. 849-59.
23. Cook, P.W., N.M. Ashton, and M.R. Pittelkow, *Adenosine and adenine nucleotides inhibit the autonomous and epidermal growth factor-mediated proliferation of cultured human keratinocytes.* J Invest Dermatol, 1995. **104**(6): p. 976-81.
24. Sellers, L.A., et al., *Adenosine nucleotides acting at the human P2Y1 receptor stimulate mitogen-activated protein kinases and induce apoptosis.* J Biol Chem, 2001. **276**(19): p. 16379-90.
25. Peyot, M.L., et al., *Extracellular Adenosine Induces Apoptosis of Human Arterial Smooth Muscle Cells via A(2b)-Purinoceptor.* Circ Res, 2000. **86**(1): p. 76-85.
26. Barry, C.P. and S.E. Lind, *Adenosine-mediated killing of cultured epithelial cancer cells.* Cancer Res, 2000. **60**(7): p. 1887-94.
27. Schrier, S.M., et al., *Extracellular adenosine-induced apoptosis in mouse neuroblastoma cells: studies on involvement of adenosine receptors and adenosine uptake.* Biochem Pharmacol, 2001. **61**(4): p. 417-25.
28. Blay, J., T.D. White, and D.W. Hoskin, *The extracellular fluid of solid carcinomas contains immunosuppressive concentrations of adenosine.* Cancer Res, 1997. **57**(13): p. 2602-5.
29. Spychala, J., *Tumor-promoting functions of adenosine.* Pharmacol Ther, 2000. **87**(2-3): p. 161-73.
30. Pearson, T., et al., *A depletable pool of adenosine in area CA1 of the rat hippocampus.* J Neurosci, 2001. **21**(7): p. 2298-307.
31. Imura, T. and S. Shimohama, *Opposing effects of adenosine on the survival of glial cells exposed to chemical ischemia.* J Neurosci Res, 2000. **62**(4): p. 539-46.
32. Frizzo, M.E., et al., *Activation of glutamate uptake by guanosine in primary astrocyte cultures.* Neuroreport, 2001. **12**(4): p. 879-81.
33. Thomson, S., et al., *Adenosine formed by 5'-nucleotidase mediates*

tubuloglomerular feedback. J Clin Invest, 2000. **106**(2): p. 289-98.

34. Szkotak, A.J., et al., *Regulation of whole-cell current in human airway epithelial cells by exogenous and autocrine adenosine.* American Journal of Physiology, 2001. **in press**.
35. Thorn, J.A. and S.M. Jarvis, *Adenosine transporters.* General Pharmacology, 1996. **27**(4): p. 613-20.
36. Geiger, J.D., F.E. Parkinson, and E.A. Kowaluk, *Regulators of Endogenous Adenosine Levels as Therapeutics Agents*, in *Purinergic Approaches in Experimental Therapeutics*, K.A. Jacobson and M.F. Jarvis, Editors. 1997, Wiley-Liss: New York, NY. p. 55-84.
37. Anderson, C.M. and F.E. Parkinson, *Potential signalling roles for UTP and UDP: sources, regulation and release of uracil nucleotides.* Trends Pharmacol Sci, 1997. **18**(10): p. 387-92.
38. Connolly, G.P. and J.A. Duley, *Uridine and its nucleotides: biological actions, therapeutic potentials.* Trends Pharmacol Sci, 1999. **20**(5): p. 218-25.
39. Silei, V., V. Politi, and G.M. Lauro, *Uridine induces differentiation in human neuroblastoma cells via protein kinase C epsilon.* J Neurosci Res, 2000. **61**(2): p. 206-11.
40. Communi, D. and J.M. Boeynaems, *Receptors responsive to extracellular pyrimidine nucleotides.* Trends Pharmacol Sci, 1997. **18**(3): p. 83-6.
41. O'Dwyer, P.J., et al., *Role of thymidine in biochemical modulation: a review.* Cancer Res, 1987. **47**(15): p. 3911-9.
42. Mackey, J.R., et al., *Nucleoside transport and its significance for anticancer drug resistance.* Drug Resist Updates, 1998. **1**(1): p. 310-324.
43. Mackey, J.R., et al., *Functional nucleoside transporters are required for gemcitabine influx and manifestation of toxicity in cancer cell lines.* Cancer Res, 1998. **58**(19): p. 4349-57.
44. Pastor-Anglada, M., A. Felipe, and F.J. Casado, *Transport and mode of action of nucleoside derivatives used in chemical and antiviral therapies.* Trends Pharmacol Sci, 1998. **19**(10): p. 424-30.
45. Cass, C.E., *Membrane transport of anticancer drugs and drug resistance*, in *Pharmacological sciences: perspective for research and therapy in the late 1990s*, A.C. Cuello and B. Collier, Editors. 1995, Birkhauser Verlag Basel: Switzerland. p. 413-431.
46. Galmarini, C.M., J.R. Mackey, and C. Dumontet, *Nucleoside analogues: mechanisms of drug resistance and reversal strategies.* Leukemia, 2001. **15**(6): p. 875-90.
47. Plunkett, W. and V. Gandhi, *Nucleoside Analogs: Cellular Pharamacology, Mechanisms of Action, and Strategies for Combination Therapy*, in *Nucleoside Analogs in Cancer Therapy*, B.D. Cheson, M.J. Keating, and W. Plunkett, Editors. 1997, Marcel Dekker: New York, NY. p. 1-35.
48. Carmichael, J., *The role of gemcitabine in the treatment of other tumours.* Br J Cancer, 1998. **78**(Suppl 3): p. 21-5.

49. Hammond, J.R., S. Lee, and P.J. Ferguson, *[3H]Gemcitabine Uptake by Nucleoside Transporters in a Human Head and Neck Squamous Carcinoma Cell Line.* J Pharmacol Exp Ther, 1999. **288**(3): p. 1185-1191.
50. Rando, R.F. and N. Nguyen-Ba, *Development of novel nucleoside analogues for use against drug resistant strains of HIV-1.* Drug Discov. Today, 2000. **5**(10): p. 465-476.
51. Nevens, F., et al., *Lamivudine therapy for chronic hepatitis B: a six-month randomized dose- ranging study.* Gastroenterology, 1997. **113**(4): p. 1258-63.
52. Mathews, C.K. and v.H.K. E., *Nucleotide Metabolism*, in *Biochemistry.* 1990, Benjamin/Cummings Publishing Company, Inc.: Redwood City, CA. p. 742-778.
53. Hatse, S., E. De Clercq, and J. Balzarini, *Role of antimetabolites of purine and pyrimidine nucleotide metabolism in tumor cell differentiation.* Biochem Pharmacol, 1999. **58**(4): p. 539-55.
54. Gero, A.M. and W.J. O'Sullivan, *Purines and pyrmidines in malarial parasites.* Blood Cells, 1990. **16**: p. 467-484.
55. Maser, P., et al., *Identification and characterization of trypanocides by functional expression of an adenosine transporter from Trypanosoma brucei in yeast.* J Mol Med, 2001. **79**(2-): p. 121-7.
56. Afifi, M.A., H.S. el-Wakil, and M.M. Abdel-Ghaffar, *A novel chemotherapeutic combination for Trichomonas vaginalis targeting purine salvage pathways of the parasite.* J Egypt Soc Parasitol, 2000. **30**(3): p. 735-46.
57. el Kouni, M.H., P.M. Knopf, and S. Cha, *Combination therapy of SCHISTOSOMA JAPONICUM by tubercidin and nitrobenzylthioinosine 5'-monophosphate.* Biochem. Pharmacol., 1985. **34**: p. 3921 - 3923.
58. el Kouni, M.H., N.J. Messier, and S. Cha, *Treatment of schistosomiasis by purine nucleoside analogues in combination with nucleoside transport inhibitors.* Biochemical Pharmacology, 1987. **36**(22): p. 3815-21.
59. el Kouni, M.H., et al., *Metabolism and selective toxicity of 6-nitrobenzylthioinosine in Toxoplasma gondii.* Antimicrob Agents Chemother, 1999. **43**(10): p. 2437-43.
60. el Kouni, M.H., *Efficacy of combination therapy with tubercidin and nitrobenzylthioinosine 5'-monophosphate against chronic and advanced stages of schistosomiasis.* Biochemical Pharmacology, 1991. **41**(5): p. 815-20.
61. el Kouni, M.H. and S. Cha, *Metabolism of adenosine analogues by Schistosoma mansoni and the effect of nucleoside transport inhibitors.* Biochemical Pharmacology, 1987. **36**(7): p. 1099-106.
62. Ginsburg, H., *Transport pathways in the malaria-infected erythrocyte. Their characterization and their use as potential targets for chemotherapy.* Biochemical Pharmacology, 1994. **48**(10): p. 1847-1856.
63. Gero, A.M., et al., *Antimalarial action of nitrobenzylthioinosine in combination with purine nucleoside antimetabolites.* Molecular and Biochemical Parasitology, 1989. **34**(1): p. 87-97.
64. Gero, A.M., *Induction of nucleoside transport sites into the host cell membrane of Babesia bovis infected erythrocytes.* Molecular and Biochemical Parasitology,

1989. **35**(3): p. 269-76.

65. Gero, A.M. and J.M. Upston, *Altered membrane permeability: A new approach to malaria chemotherapy.* Parasitology Today, 1992. **8**(8): p. 283-286.
66. Lander, E.S., et al., *Initial sequencing and analysis of the human genome.* Nature, 2001. **409**(6822): p. 860-921.
67. Venter, J.C., et al., *The sequence of the human genome.* Science, 2001. **291**(5507): p. 1304-51.
68. Griffiths, M., et al., *Cloning of a human nucleoside transporter implicated in the cellular uptake of adenosine and chemotherapeutic drugs [see comments].* Nature Medicine, 1997. **3**(1): p. 89-93.
69. Vickers, M.F., et al., *Nucleoside transporter proteins of Saccharomyces cerevisiae. DEMONSTRATION OF A TRANSPORTER (FUI1) WITH HIGH URIDINE SELECTIVITY IN PLASMA MEMBRANES AND A TRANSPORTER (FUN26) WITH BROAD NUCLEOSIDE SELECTIVITY IN INTRACELLULAR MEMBRANES.* J Biol Chem, 2000. **275**(34): p. 25931-8.
70. Vasudevan, G., et al., *Cloning of Leishmania nucleoside transporter genes by rescue of a transport-deficient mutant.* Proc Natl Acad Sci U S A, 1998. **95**(17): p. 9873-8.
71. Sanchez, M.A., et al., *Cloning and Functional Expression of a Gene Encoding a P1 Type Nucleoside Transporter from Trypanosoma brucei.* J Biol Chem, 1999. **274**(42): p. 30244-30249.
72. Chiang, C.W., et al., *The adenosine transporter of Toxoplasma gondii. Identification by insertional mutagenesis, cloning, and recombinant expression.* J Biol Chem, 1999. **274**(49): p. 35255-61.
73. Carter, N.S., et al., *Cloning of a Novel Inosine-Guanosine Transporter Gene from Leishmania donovani by Functional Rescue of a Transport-deficient Mutant.* J Biol Chem, 2000. **275**(27): p. 20935-20941.
74. Carter, N.S., et al., *Isolation and functional characterization of the PfNT1 nucleoside transporter gene from plasmodium falciparum.* J Biol Chem, 2000. **275**(14): p. 10683-91.
75. Hyde, R.J., et al., *The ENT family of eukaryote nucleoside and nucleobase transporters: recent advances in the investigation of structure/function relationships and the identification of novel isoforms.* Mol Membr Biol, 2001. **18**(1): p. 53-63.
76. Vickers, M.F., et al., *Nucleoside transporter proteins: emerging targets for drug discovery.* Emerg. Ther. Targets, 2000. **4**(4): p. 515-539.
77. Li, J. and D.W. Wang, *Cloning and in vitro expression of the cDNA encoding a putative nucleoside transporter from Arabidopsis thaliana.* Plant Science, 2000. **157**(1): p. 23-32.
78. Griffiths, M., et al., *Molecular cloning and characterization of a nitrobenzylthioinosine- insensitive (ei) equilibrative nucleoside transporter from human placenta.* Biochem J, 1997. **328**(Pt 3): p. 739-43.
79. Yao, S.Y., et al., *Molecular cloning and functional characterization of*

nitrobenzylthioinosine (NBMPR)-sensitive (es) and NBMPR-insensitive (ei) equilibrative nucleoside transporter proteins (rENT1 and rENT2) from rat tissues. J Biol Chem, 1997. **272**(45): p. 28423-30.

80. Handa, M., et al., *Cloning of a novel isoform of the mouse NBMPR-sensitive equilibrative nucleoside transporter (ENT1) lacking a putative phosphorylation site.* Gene, 2001. **262**(1-2): p. 301-307.
81. Kiss, A., et al., *Molecular cloning and functional characterization of inhibitor-sensitive (mENT1) and inhibitor-resistant (mENT2) equilibrative nucleoside transporters from mouse brain.* Biochem J, 2000. **352**(Pt 2): p. 363-372.
82. Boleti, H., et al., *Molecular identification of the equilibrative NBMPR-sensitive (es) nucleoside transporter and demonstration of an equilibrative NBMPR- insensitive (ei) transport activity in human erythroleukemia (K562) cells.* Neuropharmacology, 1997. **36**(9): p. 1167-79.
83. Wohlhueter, R.M., et al., *A rapid-mixing technique to measure transport in suspended animal cells: Applications to nucleoside transport in Novikoff rat hepatoma cells.* Methods in Cell Biol., 1978. **20**: p. 211-236.
84. Belt, J.A., *Heterogeneity of nucleoside transport in mammalian cells. Two types of transport activity in L1210 and other cultured neoplastic cells.* Molecular Pharmacology, 1983. **24**(3): p. 479-84.
85. Shi, M.M. and J.D. Young, *[3H]dipyridamole binding to nucleoside transporters from guinea-pig and rat lung.* Biochemical Journal, 1986. **240**(3): p. 879-83.
86. Parker, M.D., et al., *Identification of a nucleoside/nucleobase transporter from Plasmodium falciparum, a novel target for anti-malarial chemotherapy.* Biochem J, 2000. **349**(Pt 1): p. 67-75.
87. Osses, N., et al., *Hypoxanthine enters human vascular endothelial cells (ECV 304) via the nitrobenzylthioinosine-insensitive equilibrative nucleoside transporter.* Biochemical Journal, 1996. **317**(Pt 3): p. 843-8.
88. Yao, S.Y., et al., *Functional and Molecular Characterization of Nucleobase Transport by Recombinant Human and Rat ENT1 and ENT2 Equilibrative Nucleoside Transport Proteins Produced in Xenopus Oocytes: Chimeric Constructs Reveal a Role for the ENT2 Helix 5-6 Region in Nucleobase Translocation.* submitted to J. Biol. Chem, 2001.
89. Oliver, J.M. and A.R. Paterson, *Nucleoside transport. I. A mediated process in human erythrocytes.* Canadian Journal of Biochemistry, 1971. **49**(2): p. 262-70.
90. Cass, C.E., L.A. Gaudette, and A.R. Paterson, *Mediated transport of nucleosides in human erythrocytes. Specific binding of the inhibitor nitrobenzylthioinosine to nucleoside transport sites in the erythrocyte membrane.* Biochimica et Biophysica Acta, 1974. **345**(1): p. 1-10.
91. Coe, I.R., et al., *Assignment of the human equilibrative nucleoside transporter (hENT1) to 6p21.1-p21.2.* Genomics, 1997. **45**(2): p. 459-60.
92. Kwong, F.Y., et al., *Purification of the human erythrocyte nucleoside transporter by immunoaffinity chromatography.* Biochemical Journal, 1988. **255**(1): p. 243-9.
93. Kwong, F.Y., et al., *Enzymic cleavage as a probe of the molecular structures of*

mammalian equilibrative nucleoside transporters. Journal of Biological Chemistry, 1993. **268**(29): p. 22127-34.

94. Vickers, M.F., et al., *Functional production and reconstitution of the human equilibrative nucleoside transporter (hENT1) in Saccharomyces cerevisiae. Interaction of inhibitors of nucleoside transport with recombinant hent1 and a glycosylation-defective derivative (hent1/n48q).* Biochem J, 1999. **339**(Pt 1): p. 21-32.
95. Sundaram, M., et al., *Equilibrative nucleoside transporters: mapping regions of interaction for the substrate analogue nitrobenzylthioinosine (nbmpr) using rat chimeric proteins.* Biochemistry, 2001. **40**(27): p. 8146-51.
96. Hogue, D.L., K.C. Hodgson, and C.E. Cass, *Effects of inhibition of N-linked glycosylation by tunicamycin on nucleoside transport polypeptides of L1210 leukemia cells.* Biochemistry and Cell Biology, 1990. **68**(1): p. 199-209.
97. Pennycooke, M., et al., *Differential Expression of Human Nucleoside Transporters in Normal and Tumor Tissue.* Biochem Biophys Res Commun, 2001. **280**(3): p. 951-959.
98. Crawford, C., D. Patel, and J. Belt, *Isolation of a human cDNA that confers equilibrative, nitrobenzylmercaptopurine riboside-insensitive nucleoside transport activity (ei) to a transport deficient human leukemia cell line.* Proc. Annu. Meet. Am. Assoc. Cancer Res., 1997. **38**: p. A406.
99. Crawford, C.R., et al., *Cloning of the Human Equilibrative, Nitrobenzylmercaptopurine Riboside (NBMPR)-insensitive Nucleoside Transporter ei by Functional Expression in a Transport-deficient Cell Line.* J Biol Chem, 1998. **273**(9): p. 5288-93.
100. Belt, J.A., *Nitrobenzylthioinosine-insensitive uridine transport in human lymphoblastoid and murine leukemia cells.* Biochemical and Biophysical Research Communications, 1983. **110**(2): p. 417-23.
101. Belt, J.A. and L.D. Noel, *Nucleoside transport in Walker 256 rat carcinosarcoma and S49 mouse lymphoma cells. Differences in sensitivity to nitrobenzylthioinosine and thiol reagents.* Biochemical Journal, 1985. **232**(3): p. 681-8.
102. Belt, J.A., et al., *Nucleoside transport in normal and neoplastic cells.* Advances in Enzyme Regulation, 1993. **33**: p. 235-52.
103. Williams, J.B. and A.A. Lanahan, *A mammalian delayed-early response gene encodes HNP36, a novel, conserved nucleolar protein.* Biochem Biophys Res Commun, 1995. **213**(1): p. 325-33.
104. Lanahan, A., et al., *Growth factor-induced delayed early response genes.* Mol Cell Biol, 1992. **12**(9): p. 3919-29.
105. Williams, J.B., et al., *The human HNP36 gene is localized to chromosome 11q13 and produces alternative transcripts that are not mutated in multiple endocrine neoplasia, type 1 (MEN I) syndrome.* Genomics, 1997. **42**(2): p. 325-30.
106. Yao, S.Y., et al., *Identification of Cys140 in helix 4 as an exofacial cysteine residue within the substrate-translocation channel of rat equilibrative nitrobenzylthioinosine (NBMPR)-insensitive nucleoside transporter rENT2.*

Biochem J, 2001. **353**(Pt 2): p. 387-393.

107. Yao, S.Y., et al., *Transport of antiviral 3'-deoxy-nucleoside drugs by recombinant human and rat equilibrative, nitrobenzylthioinosine (NBMPR)-insensitive (ENT2) nucleoside transporter proteins produced in Xenopus oocytes.* Mol Membr Biol, 2001. **18**(2): p. 161-7.
108. Zimmerman, T.P., B.A. Domin, and W.B. Mahony, *Inhibition of thymidine transport by 3'-azido-3'-deoxythymidine and its metabolites.* Oncol Res, 1993. **5**(12): p. 483-7.
109. Sandoval, I.V., et al., *Distinct reading of different structural determinants modulates the dileucine-mediated transport steps of the lysosomal membrane protein LIMPII and the insulin-sensitive glucose transporter GLUT4.* J Biol Chem, 2000. **275**(51): p. 39874-85.
110. Sundaram, M., et al., *Chimeric constructs between human and rat equilibrative nucleoside transporters (hENT1 and rENT1) reveal hENT1 structural domains interacting with coronary vasoactive drugs.* J Biol Chem, 1998. **273**(34): p. 21519-25.
111. Pastor Anglada, M. and S.A. Baldwin, *Recent advances in the molecular biology and physiology of nucleoside and nucleobase transporters.* Drug Development Research, 2001. **52**(1-2): p. 431-437.
112. Visser, F., et al., *Mutation of Residue 33 of Human Equilibrative Nucleoside Transporters 1 and 2 (hENT1 and hENT2) Alters Sensitivity to Inhibition of Transport by Dilazep and Dipyridamole.* submitted to J. Biol. Chem, 2001.
113. Boumah, C.E., D.L. Hogue, and C.E. Cass, *Expression of high levels of nitrobenzylthioinosine-sensitive nucleoside transport in cultured human choriocarcinoma (BeWo) cells.* Biochemical Journal, 1992. **288**(Pt 3): p. 987-96.
114. Dahlig-Harley, E., et al., *Binding of nitrobenzylthioinosine to high-affinity sites on the nucleoside-transport mechanism of HeLa cells.* Biochemical Journal, 1981. **200**(2): p. 295-305.
115. Jennings, L.L., et al., *Distinct regional distribution of human equilibrative nucleoside transporter proteins 1 and 2 (hENT1 and hENT2) in the central nervous system.* Neuropharmacology, 2001. **40**(5): p. 722-31.
116. Anderson, C.M., et al., *Distribution of mRNA encoding a nitrobenzylthioinosine-insensitive nucleoside transporter (ENT2) in rat brain.* Brain Res Mol Brain Res, 1999. **70**(2): p. 293-297.
117. Anderson, C.M., et al., *Distribution of equilibrative, nitrobenzylthioinosine-sensitive nucleoside transporters (ENT1) in brain.* J Neurochem, 1999. **73**(2): p. 867-73.
118. Chandrasena, G., et al., *Functional Expression of Human Intestinal Na+ Dependent and Na+ Independent Nucleoside Transporters in Xenopus Laevis Oocytes.* Biochemical Pharmacology, 1997. **53 (12)**: p. 1909-1918.
119. Lum, P.Y., et al., *Human intestinal es nucleoside transporter: molecular characterization and nucleoside inhibitory profiles.* Cancer Chemother Pharmacol, 2000. **45**(4): p. 273-8.

120. Cass, C.E., et al., *A comparison of the abilities of nitrobenzylthioinosine, dilazep, and dipyridamole to protect human hematopoietic cells from 7-deazaadenosine (tubercidin).* Cancer Research, 1992. **52**(21): p. 5879-86.
121. Huang, Q.Q., et al., *Cloning and functional expression of a complementary DNA encoding a mammalian nucleoside transport protein.* Journal of Biological Chemistry, 1994. **269**(27): p. 17757-60.
122. Hamilton, S.R., et al., *Sub-cellular Distribution and Membrane Topology of the Mammalian Concentrative Na{super+}-Nucleoside Co-Transporter rCNT1.* J Biol Chem, 2001. **25**: p. 25.
123. Craig, J.E., Y. Zhang, and M.P. Gallagher, *Cloning of the nupC gene of Escherichia coli encoding a nucleoside transport system, and identification of an adjacent insertion element, IS 186.* Molecular Microbiology, 1994. **11**(6): p. 1159-68.
124. Zhang, Y., J.E. Craig, and M.P. Gallagher, *Location of the nupC gene on the physical map of Escherichia coli K-12.* Journal of Bacteriology, 1992. **174**(17): p. 5758-5759.
125. Vickers, M.F., et al., *Functional production of mammalian concentrative nucleoside transporters in Saccharomyces cerevisiae.* Mol Membr Biol, 2001. **18**(1): p. 73-9.
126. Flanagan, S.A. and K.A. Meckling-Gill, *Characterization of a Novel Na+ Dependent, Guanosine Specific, Nitrobenzylthioinosine Sensitive Transporter in Acute Promyelocytic Leukemia Cells.* Journal of Biological Chemistry, 1997. **272 (29)**: p. 18026-18032.
127. Gutierrez, M.M., et al., *Nucleoside transport in brush border membrane vesicles from human kidney.* Biochim Biophys Acta, 1992. **1105**(1): p. 1-9.
128. Gutierrez, M.M. and K.M. Giacomini, *Substrate selectivity, potential sensitivity and stoichiometry of Na(+)- nucleoside transport in brush border membrane vesicles from human kidney.* Biochim Biophys Acta, 1993. **1149**(2): p. 202-8.
129. Gutierrez, M.M. and K.M. Giacomini, *Expression of a human renal sodium nucleoside cotransporter in Xenopus laevis oocytes.* Biochem Pharmacol, 1994. **48**(12): p. 2251-3.
130. Paterson, A.R., et al., *Inhibitor-sensitive, Na(+)-linked transport of nucleoside analogs in leukemia cells from patients.* Proc. Annu. Meet. Am. Assoc. Cancer Res., 1993. **34**: p. A84.
131. Ritzel, M.W.L., et al., *Molecular cloning and functional expression of cDNAs encoding a human Na+-nucleoside cotransporter (hCNT1).* American Journal of Physiology, 1997. **272**(2 41-2): p. C707-C714.
132. Ritzel, M.W., et al., *Recent molecular advances in studies of the concentrative Na+-dependent nucleoside transporter (CNT) family: identification and characterization of novel human and mouse proteins (hCNT3 and mCNT3) broadly selective for purine and pyrimidine nucleosides (system cib).* Mol Membr Biol, 2001. **18**(1): p. 65-72.
133. Ritzel, M.W., et al., *Molecular identification and characterization of novel human and mouse concentrative Na{super+}-nucleoside cotransporter proteins (hCNT3*

and mCNT3) broadly selective for purine and pyrimidine nucleosides (system cib). J Biol Chem, 2000. **13**: p. 13.

134. Ritzel, M.W., et al., *Molecular cloning, functional expression and chromosomal localization of a cDNA encoding a human Na+/nucleoside cotransporter (hCNT2) selective for purine nucleosides and uridine.* Mol Membr Biol, 1998. **15**(4): p. 203-11.
135. Gerstin, K.M., et al., *Molecular cloning of a Na+-dependent nucleoside transporter from rabbit intestine.* Pharm Res, 2000. **17**(8): p. 906-10.
136. Wang, J., et al., *Na(+)-dependent purine nucleoside transporter from human kidney: cloning and functional characterization.* Am J Physiol, 1997. **273**(6 Pt 2): p. F1058-65.
137. Che, M., D.F. Ortiz, and I.M. Arias, *Primary structure and functional expression of a cDNA encoding the bile canalicular, purine-specific Na+-nucleoside cotransporter.* Journal of Biological Chemistry, 1995. **270**(23): p. 13596-13599.
138. Loewen, S.K., et al., *Identification of amino acid residues responsible for the pyrimidine and purine nucleoside specificities of human concentrative Na(+) nucleoside cotransporters hCNT1 and hCNT2.* J Biol Chem, 1999. **274**(35): p. 24475-84.
139. Lang, T.L., et al., *Acquisition of human concentrative nucleoside transporter 2 (hCNT2) activity by gene transfer confers sensitivity to fluoropyrimidine nucleosides in drug-resistant leukemia cells.* Mol. Pharmacol., 2001. **in press**.
140. Wang, J. and K.M. Giacomini, *Characterization of a bioengineered chimeric Na+-nucleoside transporter.* Mol Pharmacol, 1999. **55**(2): p. 234-40.
141. Wang, J. and K.M. Giacomini, *Serine 318 is essential for the pyrimidine selectivity of the N2 Na+- nucleoside transporter.* J Biol Chem, 1999. **274**(4): p. 2298-302.
142. Patil, S.D. and J.D. Unadkat, *Sodium Dependent Nucleoside Transport in the Human Intestinal Brush Border Membrane.* American Journal of Physiology, 1997. **35 (6)**: p. G1314-G1320.
143. Ngo, L.Y., S.D. Patil, and J.D. Unadkat, *Ontogenic and longitudinal activity of Na(+)-nucleoside transporters in the human intestine.* American Journal of Physiology, 2001. **280**(3): p. G475-G481.
144. Mangravite, L.M., et al., *Localization of GFP-tagged concentrative nucleoside transporters in a renal polarized epithelial cell line.* American Journal of Physiology, 2001. **280**(5): p. F879-85.
145. Jund, R., E. Weber, and M.R. Chevallier, *Primary structure of the uracil transport protein of Saccharomyces cerevisiae.* Eur J Biochem, 1988. **171**(1-2): p. 417-24.
146. de Koning, H. and G. Diallinas, *Nucleobase transporters (review).* Mol Membr Biol, 2000. **17**(2): p. 75-94.
147. Sonnhammer, E.L., G. von Heijne, and A. Krogh, *A hidden Markov model for predicting transmembrane helices in protein sequences.* Proc Int Conf Intell Syst Mol Biol, 1998. **6**: p. 175-82.
148. Krogh, A., et al., *Predicting transmembrane protein topology with a hidden Markov model: application to complete genomes.* J Mol Biol, 2001. **305**(3): p.

567-80.

149. Jund, R. and F. Lacroute, *Genetic and physiological aspects of resistance to 5-fluoropyrimidines in Saccharomyces cerevisiae.* J Bacteriol, 1970. **102**(3): p. 607-15.

150. Wagner, R., et al., *The ORF YBL042 of Saccharomyces cerevisiae encodes a uridine permease.* FEMS Microbiol Lett, 1998. **159**(1): p. 69-75.

151. Munch-Petersen, A. and N. Jensen, *Analysis of the regulatory region of the Escherichia coli nupG gene, encoding a nucleoside-transport protein.* Eur J Biochem, 1990. **190**(3): p. 547-51.

152. Westh Hansen, S.E., N. Jensen, and A. Munch-Petersen, *Studies on the sequence and structure of the Escherichia coli K-12 nupG gene, encoding a nucleoside-transport system.* Eur J Biochem, 1987. **168**(2): p. 385-91.

153. Seeger, C., C. Poulsen, and G. Dandanell, *Identification and characterization of genes (xapA, xapB, and xapR) involved in xanthosine catabolism in Escherichia coli.* J Bacteriol, 1995. **177**(19): p. 5506-16.

154. Detke, S., *Cloning of the Candida albicans nucleoside transporter by complementation of nucleoside transport-deficient Saccharomyces.* Yeast, 1998. **14**(14): p. 1257-65.

155. Hogue, D.L., et al., *Functional complementation of a membrane transport deficiency in Saccharomyces cerevisiae by recombinant ND4 fusion protein.* Biochem Biophys Res Commun, 1997. **238**(3): p. 811-6.

156. Hogue, D.L., et al., *Identification of a novel membrane transporter associated with intracellular membranes by phenotypic complementation in the yeast Saccharomyces cerevisiae.* Journal of Biological Chemistry, 1996. **271**(16): p. 9801-8.

157. Claros, M.G. and G. von Heijne, *TopPred II: an improved software for membrane protein structure predictions.* Comput Appl Biosci, 1994. **10**(6): p. 685-6.

158. Jullig, M. and S. Eriksson, *Mitochondrial and submitochondrial localization of human deoxyguanosine kinase.* Eur J Biochem, 2000. **267**(17): p. 5466-72.

159. Wang, L., et al., *Human thymidine kinase 2: molecular cloning and characterisation of the enzyme activity with antiviral and cytostatic nucleoside substrates.* FEBS Lett, 1999. **443**(2): p. 170-4.

160. Lewis, W. and M.C. Dalakas, *Mitochondrial toxicity of antiviral drugs.* Nature Medicine, 1995. **1**: p. 417-422.

161. Hentosh, P. and M. Tibudan, *2-Chloro-2'-deoxyadenosine, an antileukemic drug, has an early effect on cellular mitochondrial function.* Mol Pharmacol, 1997. **51**(4): p. 613-9.

162. Camins, A., et al., *Characterization of nitrobenzylthioinosine binding sites in the mitochondrial fraction of rat testis.* Life Sciences, 1996. **58**(9): p. 753-9.

163. Jimenez, A., et al., *Further characterization of an adenosine transport system in the mitochondrial fraction of rat testis.* Eur J Pharmacol, 2000. **398**(1): p. 31-39.

164. Liang, L. and R.M. Johnstone, *Evidence for an internal pool of nucleoside transporters in mammalian reticulocytes.* Biochimica et Biophysica Acta, 1992.

1106(1): p. 189-196.

165. Delicado, E.G., R.P. Sen, and M.T. Miras Portugal, *Effects of phorbol esters and secretagogues on nitrobenzylthioinosine binding to nucleoside transporters and nucleoside uptake in cultured chromaffin cells.* Biochemical Journal, 1991. **279**(Pt 3): p. 651-5.
166. Cabrita, M.A., et al., *Mouse transporter protein, a membrane protein that regulates cellular multidrug resistance, is localized to lysosomes.* Cancer Res, 1999. **59**(19): p. 4890-7.
167. Cabrita, M.A., et al., *Localization of a Nucleoside Transporter to Late Endosomes and/or Lysosomes.* Mol Biol Cell, 1996. **7**(Suppl.): p. 135a.
168. Hogue, D.L., L. Kerby, and V. Ling, *A mammalian lysosomal membrane protein confers multidrug resistance upon expression in Saccharomyces cerevisiae.* J Biol Chem, 1999. **274**(18): p. 12877-82.
169. Sadee, W., V. Drubbisch, and G.L. Amidon, *Biology of membrane transport proteins.* Pharmaceutical Research, 1995. **12**(12): p. 1823-37.
170. Bradbury, N.A. and R.J. Bridges, *Role of membrane trafficking in plasma membrane solute transport.* American Journal of Physiology, 1994. **267**(1 Pt 1): p. C1-24.
171. Meckling-Gill, K.A. and C.E. Cass, *Effects of transformation by v-fps on nucleoside transport in Rat-2 fibroblasts.* Biochemical Journal, 1992. **282**(Pt 1): p. 147-54.
172. Delicado, E.G., et al., *Evidence that adenine nucleotides modulate nucleoside-transporter function. Characterization of uridine transport in chromaffin cells and plasma membrane vesicles.* European Journal of Biochemistry, 1994. **225**(1): p. 355-62.
173. Coe, I.R., et al., *Activation of cyclic AMP-dependent protein kinase reverses tolerance of a nucleoside transporter to ethanol.* J Pharmacol Exp Ther, 1996. **276**(2): p. 365-9.
174. Coe, I.R., et al., *The role of protein kinase C in cellular tolerance to ethanol.* Journal of Biological Chemistry, 1996. **271**(46): p. 29468-29472.
175. Sinclair, C.J., et al., *Stimulation of nucleoside efflux and inhibition of adenosine kinase by A1 adenosine receptor activation.* Biochem Pharmacol, 2000. **59**(5): p. 477-83.
176. Meckling-Gill, K.A., L. Guilbert, and C.E. Cass, *CSF-1 stimulates nucleoside transport in S1 macrophages.* Journal of Cellular Physiology, 1993. **155**(3): p. 530-8.
177. Cass, C.E., J.A. Belt, and A.R. Paterson, *Adenosine transport in cultured cells and erythrocytes.* Progress in Clinical and Biological Research, 1987. **230**: p. 13-40.
178. Cass, C.E., et al., *Fluctuations in nucleoside uptake and binding of the inhibitor of nucleoside transport, nitrobenzylthioinosine, during the replication cycle of HeLa cells.* Cancer Research, 1979. **39**(4): p. 1245-52.
179. Chen, S.F., et al., *Changes in nucleoside transport of HL-60 human promyelocytic cells during N,N-dimethylformamide induced differentiation.* Cancer Research,

1986. **46**(7): p. 3449-55.
180. Takimoto, T., et al., *Cell cycle related change of Ara-C transport in HL-60 cells after differentiation induction.* FEBS Lett, 1989. **247**(2): p. 173-6.
181. Sokoloski, J.A., et al., *Effects of uridine on the growth and differentiation of HL-60 leukemia cells.* Leuk-Res, 1991. **15**(11): p. 1051-8.
182. Lee, C.W., et al., *Induction of the differentiation of HL-60 cells by phorbol 12-myristate 13-acetate activates a Na(+)-dependent uridine-transport system. Involvement of protein kinase C.* Biochemical Journal, 1991. **274**(Pt 1): p. 85-90.
183. Lee, C.W., et al., *Differentiation of HL-60 cells by dimethylsulfoxide activates a Na(+)-dependent nucleoside transport system.* In Vivo, 1994. **8**(5): p. 795-801.
184. Lee, C.W., *Decrease in equilibrative uridine transport during monocytic differentiation of HL-60 leukaemia: involvement of protein kinase C.* Biochemical Journal, 1994. **300**(Pt 2): p. 407-12.
185. Jones, K.W., R.J. Rylett, and J.R. Hammond, *Effect of cellular differentiation on nucleoside transport in human neuroblastoma cells.* Brain Research, 1994. **660**(1): p. 104-12.
186. Soler, C., et al., *Regulation of nucleoside transport by lipopolysaccharide, phorbol esters, and tumor necrosis factor-alpha in human B-lymphocytes.* J Biol Chem, 1998. **273**(41): p. 26939-45.
187. Soler, C., et al., *Nitric oxide regulates nucleoside transport in activated B lymphocytes.* J Leukoc Biol, 2000. **67**(3): p. 345-9.
188. Soler, C., et al., *Lipopolysaccharide (LPS)-induced apoptosis of macrophages determines the up-regulation of concentrative nucleoside transporters CNT1 and CNT2 through TNF-alpha-dependent and -independent mechanisms.* J Biol Chem, 2001. **9**: p. 9.
189. Pressacco, J., et al., *Effects of thymidylate synthase inhibition on thymidine kinase activity and nucleoside transporter expression.* Cancer Research, 1995. **55**(7): p. 1505-1508.
190. Pressacco, J., et al., *Modulation of the equilibrative nucleoside transporter by inhibitors of DNA synthesis.* British Journal of Cancer, 1995. **72**(4): p. 939-942.
191. Choi, D.S., et al., *Genomic organization and expression of the mouse equilibrative, nitrobenzylthioinosine-sensitive nucleoside transporter 1 (ENT1) gene.* Biochem Biophys Res Commun, 2000. **277**(1): p. 200-8.
192. Maser, P., et al., *A nucleoside transporter from trypanosoma brucei involved in drug resistance.* Science, 1999. **285**(5425): p. 242-4.
193. Dhalla, A.K., et al., *Characterization of an NBTI-sensitive Equilibrative Nucleoside Transporter in Vascular Smooth Muscle.* J Mol Cell Cardiol, 2001. **33**(6): p. 1143-52.
194. Geiger, J.D. and J.I. Nagy, *Heterogeneous distribution of adenosine transport sites labelled by [3H]nitrobenzylthioinosine in rat brain: an autoradiographic and membrane binding study.* Brain Res. Bull., 1984. **13**: p. 657 - 666.
195. Leung, G.P., et al., *Characterization of nucleoside transport systems in cultured rat epididymal epithelium.* American Journal of Physiology, 2001. **280**(5): p.

C1076-82.

196. Xiao, G., et al., *A Novel Proton-Dependent Nucleoside Transporter, CeCNT3, from Caenorhabditis elegans.* Mol Pharmacol, 2001. **59**(2): p. 339-348.

197. Patel, D.H., et al., *Cloning, genomic organization and chromosomal localization of the gene encoding the murine sodium-dependent, purine-selective, concentrative nucleoside transporter (CNT2).* Gene, 2000. **242**(1-2): p. 51-8.

198. Pajor, A.M., *Sequence of a pyrimidine-selective Na+/nucleoside cotransporter from pig kidney, pkCNT1.* Biochim Biophys Acta, 1998. **1415**(1): p. 266-9.

199. Huang, Q.Q., et al., *Functional expression of Na(+)-dependent nucleoside transport systems of rat intestine in isolated oocytes of Xenopus laevis. Demonstration that rat jejunum expresses the purine-selective system N1 (cif) and a second, novel system N3 having broad specificity for purine and pyrimidine nucleosides.* Journal of Biological Chemistry, 1993. **268**(27): p. 20613-9.

200. Anderson, C.M., et al., *Demonstration of the existence of mRNAs encoding N1/cif and N2/cit sodium/nucleoside cotransporters in rat brain.* Brain Research. Molecular Brain Research, 1996. **42**(2): p. 358-61.

201. Li, J.Y., R.J. Boado, and W.M. Pardridge, *Cloned blood-brain barrier adenosine transporter is identical to the rat concentrative na+ nucleoside cotransporter cnt2.* J Cereb Blood Flow Metab, 2001. **21**(8): p. 929-36.

202. Patel, D., et al., *Molecular cloning and characterization of a mouse purine-selective concentrative nucleoside transporter.* Proc. Annu. Meet. Am. Assoc. Cancer Res., 1997. **38**: p. A405.

203. Enjo, F., et al., *Isolation and characterization of a thiamin transport gene, THI10, from Saccharomyces cerevisiae.* J Biol Chem, 1997. **272**(31): p. 19165-70.

204. Yoo, H.S., T.S. Cunningham, and T.G. Cooper, *The allantoin and uracil permease gene sequences of Saccharomyces cerevisiae are nearly identical.* Yeast, 1992. **8**(12): p. 997-1006.

205. de Montigny, J., et al., *The uracil permease of Schizosaccharomyces pombe: a representative of a family of 10 transmembrane helix transporter proteins of yeasts.* Yeast, 1998. **14**(11): p. 1051-9.

206. Weber, E., et al., *The purine-cytosine permease gene of Saccharomyces cerevisiae: primary structure and deduced protein sequence of the FCY2 gene product.* Mol Microbiol, 1990. **4**(4): p. 585-96.

207. Danielsen, S., et al., *Characterization of the Escherichia coli codBA operon encoding cytosine permease and cytosine deaminase.* Mol Microbiol, 1992. **6**(10): p. 1335-44.

208. Yao, S.Y.M., C.E. Cass, and J.D. Young, *The Xenopus oocyte expression system for the cDNA cloning and characterization of plasma membrane transport proteins*, in *Membrane Transport*, S.A. Baldwin, Editor. 2000, Oxford University Press: Oxford.

209. Harley, E.R., A.R. Paterson, and C.E. Cass, *Initial rate kinetics of the transport of adenosine and 4-amino-7-(beta-D-ribofuranosyl)pyrrolo[2,3-d]pyrimidine (tubercidin) in cultured cells.* Cancer Research, 1982. **42**(4): p. 1289-95.

210. Ausubel, F.M., et al., eds. *Current Protocols in Molecular Biology.* Current Protocols, ed. V.B. Chanda. 1997, John Wiley & Sons, Inc.: New York, N.Y.
211. Kozak, M., *An analysis of vertebrate mRNA sequences: intimations of translational control.* J Cell Biol, 1991. **115**(4): p. 887-903.
212. Krieg, P.A. and D.A. Melton, *Functional messenger RNAs are produced by SP6 in vitro transcription of cloned cDNAs.* Nucleic Acids Research, 1984. **12**(18): p. 7057-70.
213. Melton, D.A., et al., *Efficient in vitro synthesis of biologically active RNA and RNA hybridization probes from plasmids containing a bacteriophage SP6 promoter.* Nucleic Acids Research, 1984. **12**(18): p. 7035-56.
214. Kolodziej, P.A. and R.A. Young, *Epitope tagging and protein surveillance.* Methods Enzymol, 1991. **194**: p. 508-19.
215. Wilson, I.A., et al., *The structure of an antigenic determinant in a protein.* Cell, 1984. **37**(3): p. 767-78.
216. Kreis, T.E., *Microinjected antibodies against the cytoplasmic domain of vesicular stomatitis virus glycoprotein block its transport to the cell surface.* Embo J, 1986. **5**(5): p. 931-41.
217. Heid, C.A., et al., *Real time quantitative PCR.* Genome Res, 1996. **6**(10): p. 986-94.
218. Gibson, U.E., C.A. Heid, and P.M. Williams, *A novel method for real time quantitative RT-PCR.* Genome Res, 1996. **6**(10): p. 995-1001.
219. Fink, L., et al., *Real-time quantitative RT-PCR after laser-assisted cell picking.* Nat Med, 1998. **4**(11): p. 1329-33.
220. Renshaw, M.A., et al., *Fluorescent multiplex polymerase chain reaction analysis of four genes associated with inpaired fibrinolysis and myocardial infarction.* Blood Coagulation and Fibrinolysis, 2001. **12**(4): p. 245-51.
221. Brown, W.J., J. Goodhouse, and M.G. Farquhar, *Mannose-6-phosphate receptors for lysosomal enzymes cycle between the Golgi complex and endosomes.* J Cell Biol, 1986. **103**(4): p. 1235-47.
222. Brown, W.J. and M.G. Farquhar, *The mannose-6-phosphate receptor for lysosomal enzymes is concentrated in cis Golgi cisternae.* Cell, 1984. **36**(2): p. 295-307.
223. Matovcik, L.M., J. Goodhouse, and M.G. Farquhar, *The recycling itinerary of the 46 kDa mannose 6-phosphate receptor-- Golgi to late endosomes--coincides with that of the 215 kDa M6PR.* Eur J Cell Biol, 1990. **53**(2): p. 203-11.
224. Lin, W.C. and L.A. Culp, *Selectable plasmid vectors with alternative and ultrasensitive histochemical marker genes.* Biotechniques, 1991. **11**(3): p. 344-8, 350-1.
225. Karin, N.J., *Cloning of transfected cells without cloning rings.* Biotechniques, 1999. **27**(4): p. 681-2.
226. Boleti, H., E. Karsenti, and I. Vernos, *Xklp2, a novel Xenopus centrosomal kinesin-like protein required for centrosome separation during mitosis.* Cell, 1996. **84**(1): p. 49-59.

227. Robinson, K.M., A. von Kieckebusch-Guck, and B.D. Lemire, *Isolation and characterization of a Saccharomyces cerevisiae mutant disrupted for the succinate dehydrogenase flavoprotein subunit.* J Biol Chem, 1991. **266**(32): p. 21347-50.
228. Harlow, E. and D. Lane, *Antibodies: A Laboratory Manual.* 1988, Cold Spring Harbor, NY: Cold Spring Harbor Laboratory.
229. Barnstable, C.J., et al., *Production of monoclonal antibodies to group A erythrocytes, HLA and other human cell surface antigens-new tools for genetic analysis.* Cell, 1978. **14**(1): p. 9-20.
230. Kohler, G. and C. Milstein, *Derivation of specific antibody-producing tissue culture and tumor lines by cell fusion.* Eur J Immunol, 1976. **6**(7): p. 511-9.
231. Harlow, E. and D. Lane, *Using Antibodies: A Laboratory Manual.* 1999, Cold Spring Harbor, NY: Cold Spring Harbor Laboratory Press.
232. De Strooper, B., et al., *Phosphorylation, subcellular localization, and membrane orientation of the Alzheimer's disease-associated presenilins.* J Biol Chem, 1997. **272**(6): p. 3590-8.
233. Otto, J.C. and W.L. Smith, *The orientation of prostaglandin endoperoxide synthases-1 and -2 in the endoplasmic reticulum.* J Biol Chem, 1994. **269**(31): p. 19868-75.
234. Dan, N., R.B. Middleton, and M.A. Lehrman, *Hamster UDP-N-acetylglucosamine:dolichol-P N-acetylglucosamine-1-P transferase has multiple transmembrane spans and a critical cytosolic loop.* J Biol Chem, 1996. **271**(48): p. 30717-24.
235. Johnson, P.A. and R.M. Johnstone, *Partial purification of amino acid transport systems in Ehrlich ascites tumor cell plasma membranes.* Membr Biochem, 1982. **4**(3): p. 189-218.
236. Bardin, C. and R.M. Johnstone, *Sodium-dependent amino acid transport in reconstituted membrane vesicles from Ehrlich ascites cell plasma membranes.* J Biol Chem, 1978. **253**(5): p. 1725-32.
237. Colombini, M. and R.M. Johnstone, *Preparation and properties of the (Na+ + K+)-ATPase of plasma membranes from Ehrlich ascites cells.* Biochim Biophys Acta, 1973. **323**(1): p. 69-86.
238. Hanahan, D.J. and J.E. Ekholm, *The preparation of red cell ghosts (membranes).* Methods Enzymol, 1974. **31(Pt**(A)): p. 168-72.
239. Morré, D.J. and D.M. Morré, *Isolation of the Golgi Apparatus from rat liver*, in *Cells: a laboratory manual*, D.L. Spector, R.D. Goldman, and L.A. Leinwand, Editors. 1998, Cold Spring Harbor Laboratory Press: Cold Spring Harbor. p. 39.3-39.7.
240. Graham, J.M., T. Ford, and D. Rickwood, *Isolation of the major subcellular organelles from mouse liver using Nycodenz gradients without the use of an ultracentrifuge.* Anal Biochem, 1990. **187**(2): p. 318-23.
241. Rickwood, D., M.T. Wilson, and V.M. Darley-Usmar, *Isolation and characteristics of intact mitochondria*, in *Mitochondria: a practical approach*, V.M. Darley-Usmar, D. Rickwood, and M.T. Wilson, Editors. 1987, IRL Press,

Ltd.: Oxford.
242. Fleischer, S., J.O. McIntyre, and J.C. Vidal, *Large-scale preparation of rat liver mitochondria in high yield.* Methods Enzymol, 1979. **55**: p. 32-9.
243. Bergeron, J.J., et al., *Galactose transfer to endogenous acceptors within Golgi fractions of rat liver.* J Cell Biol, 1982. **92**(1): p. 139-46.
244. Smith, P.K., et al., *Measurement of protein using bicinchoninic acid [published erratum appears in Anal Biochem 1987 May 15;163(1):279].* Anal Biochem, 1985. **150**(1): p. 76-85.
245. Bradford, M.M., *A rapid and sensitive method for the quantitation of microgram quantities of protein utilizing the principle of protein-dye binding.* Anal Biochem, 1976. **72**: p. 248-54.
246. Maniatis, T., E.F. Fritsch, and J. Sambrook, *Molecular cloning: a laboratory manual.* 1989, Cold Spring Harbor Laboratory: Cold Spring Harbor Laboratory Press.
247. Laemmli, U.K., *Cleavage of structural proteins during the assembly of the head of bacteriophage T4.* Nature, 1970. **227**(259): p. 680-5.
248. Sen, R.P., et al., *Flow cytometric studies of nucleoside transport regulation in single chromaffin cells.* FEBS Lett, 1998. **422**(3): p. 368-72.
249. Jamieson, G.P., et al., *Flow cytometric quantitation of nucleoside transporter sites on human leukemic cells.* Cytometry, 1993. **14**(1): p. 32-38.
250. Wiley, J.S., et al., *A new fluorescent probe for the equilibrative inhibitor-sensitive nucleoside transporter. 5'-S-(2-aminoethyl)-N6-(4-nitrobenzyl)-5'- thioadenosine (SAENTA)-chi 2-fluorescein.* Biochem J, 1991. **273**(Pt 3): p. 667-72.
251. Hammond, J.R., *Kinetic analysis of ligand binding to the Ehrlich cell nucleoside transporter: pharmacological characterization of allosteric interactions with the [3H]nitrobenzylthioinosine binding site.* Molecular Pharmacology, 1991. **39**(6): p. 771-9.
252. Hammond, J.R. and M. Zarenda, *Effect of detergents on ligand binding and translocation activities of solubilized/reconstituted nucleoside transporters.* Archives of Biochemistry and Biophysics, 1996. **332**(2): p. 313-22.
253. Reaves, B.J., et al., *The effect of wortmannin on the localisation of lysosomal type I integral membrane glycoproteins suggests a role for phosphoinositide 3- kinase activity in regulating membrane traffic late in the endocytic pathway.* J Cell Sci, 1996. **109**(Pt 4): p. 749-62.
254. Velasco, A., et al., *Cell type-dependent variations in the subcellular distribution of alpha- mannosidase I and II.* J Cell Biol, 1993. **122**(1): p. 39-51.
255. Ferro-Novick, S. and P. Novick, *The role of GTP-binding proteins in transport along the exocytic pathway.* Annu Rev Cell Biol, 1993. **9**: p. 575-99.
256. Nagase, T., et al., *Prediction of the coding sequences of unidentified human genes. III. The coding sequences of 40 new genes (KIAA0081-KIAA0120) deduced by analysis of cDNA clones from human cell line KG-1 (supplement).* DNA Res, 1995. **2**(1): p. 51-9.
257. Nagase, T., et al., *Prediction of the coding sequences of unidentified human genes.*

III. The coding sequences of 40 new genes (KIAA0081-KIAA0120) deduced by analysis of cDNA clones from human cell line KG-1. DNA Res, 1995. **2**(1): p. 37-43.

258. Simon, S.M. and M. Schindler, *Cell biological mechanisms of multidrug resistance in tumors.* Proc Natl Acad Sci U S A, 1994. **91**(9): p. 3497-504.
259. Gottesman, M.M. and I. Pastan, *Biochemistry of multidrug resistance mediated by the multidrug transporter.* Annu Rev Biochem, 1993. **62**: p. 385-427.
260. Breuninger, L.M., et al., *Expression of multidrug resistance-associated protein in NIH/3T3 cells confers multidrug resistance associated with increased drug efflux and altered intracellular drug distribution.* Cancer Res, 1995. **55**(22): p. 5342-7.
261. Beck, W.T., *The cell biology of multiple drug resistance.* Biochem Pharmacol, 1987. **36**(18): p. 2879-87.
262. Cleary, I., et al., *The multidrug-resistant human lung tumour cell line, DLKP-A10, expresses novel drug accumulation and sequestration systems.* Biochem Pharmacol, 1997. **53**(10): p. 1493-502.
263. Daniel, W.A. and J. Wojcikowski, *Contribution of lysosomal trapping to the total tissue uptake of psychotropic drugs.* Pharmacol Toxicol, 1997. **80**(2): p. 62-8.
264. Altan, N., et al., *Defective acidification in human breast tumor cells and implications for chemotherapy.* J Exp Med, 1998. **187**(10): p. 1583-98.
265. Gervasoni, J.E., Jr., et al., *Subcellular distribution of daunorubicin in P-glycoprotein-positive and -negative drug-resistant cell lines using laser-assisted confocal microscopy.* Cancer Res, 1991. **51**(18): p. 4955-63.
266. Hindenburg, A.A., et al., *Intracellular distribution and pharmacokinetics of daunorubicin in anthracycline-sensitive and -resistant HL-60 cells.* Cancer Res, 1989. **49**(16): p. 4607-14.
267. Kramer, D.L., et al., *Lysosomal sequestration of polyamine analogues in Chinese hamster ovary cells resistant to the S-adenosylmethionine decarboxylase inhibitor, CGP-48664.* Cancer Res, 1998. **58**(17): p. 3883-90.
268. Hurwitz, S.J., et al., *Vesicular anthracycline accumulation in doxorubicin-selected U-937 cells: participation of lysosomes.* Blood, 1997. **89**(10): p. 3745-54.
269. Lautier, D., et al., *Altered intracellular distribution of daunorubicin in immature acute myeloid leukemia cells.* Int J Cancer, 1997. **71**(2): p. 292-9.
270. Slapak, C.A., et al., *Energy-dependent accumulation of daunorubicin into subcellular compartments of human leukemia cells and cytoplasts.* J Biol Chem, 1992. **267**(15): p. 10638-44.
271. Simon, S., D. Roy, and M. Schindler, *Intracellular pH and the control of multidrug resistance [published erratum appears in Proc Natl Acad Sci U S A 1994 Apr 26;91(9):4101].* Proc Natl Acad Sci U S A, 1994. **91**(3): p. 1128-32.
272. Moriyama, Y., *Membrane energization by proton pumps is important for compartmentalization of drugs and toxins: a new type of active transport.* J Exp Biol, 1996. **199**(Pt 7): p. 1447-54.
273. Ishizaki, J., et al., *Contribution of lysosomes to the subcellular distribution of basic drugs in the rat liver.* Pharm Res, 1996. **13**(6): p. 902-6.

274. Lee, N.H., et al., *Comparative expressed-sequence-tag analysis of differential gene expression profiles in PC-12 cells before and after nerve growth factor treatment.* Proc Natl Acad Sci U S A, 1995. **92**(18): p. 8303-7.
275. Sakai, D., H.S. Tong, and C. Minkin, *Osteoclast molecular phenotyping by random cDNA sequencing.* 1995.
276. Granger, B.L., et al., *Characterization and cloning of lgp110, a lysosomal membrane glycoprotein from mouse and rat cells.* J Biol Chem, 1990. **265**(20): p. 12036-43.
277. Cha, Y., S.M. Holland, and J.T. August, *The cDNA sequence of mouse LAMP-2. Evidence for two classes of lysosomal membrane glycoproteins.* J Biol Chem, 1990. **265**(9): p. 5008-13.
278. Kirschner, M.A., et al., *Mouse excitatory amino acid transporter EAAT2: isolation, characterization, and proximity to neuroexcitability loci on mouse chromosome 2.* Genomics, 1994. **24**(2): p. 218-24.
279. Naciff, J.M., H. Misawa, and J.R. Dedman, *Molecular characterization of the mouse vesicular acetylcholine transporter gene.* Neuroreport, 1997. **8**(16): p. 3467-73.
280. Hunziker, W. and H.J. Geuze, *Intracellular trafficking of lysosomal membrane proteins.* Bioessays, 1996. **18**(5): p. 379-89.
281. Altschul, S.F., et al., *Gapped BLAST and PSI-BLAST: a new generation of protein database search programs.* Nucleic Acids Res, 1997. **25**(17): p. 3389-402.
282. Adra, C.N., et al., *LAPTM5: a novel lysosomal-associated multispanning membrane protein preferentially expressed in hematopoietic cells.* Genomics, 1996. **35**(2): p. 328-37.
283. Scott, L.M., L. Mueller, and S.J. Collins, *E3, a hematopoietic-specific transcript directly regulated by the retinoic acid receptor alpha.* Blood, 1996. **88**(7): p. 2517-30.
284. Origasa, M., et al., *Activation of a novel microglial gene encoding a lysosomal membrane protein in response to neuronal apoptosis.* Brain Res Mol Brain Res, 2001. **88**(1-2): p. 1-13.
285. Honing, S., et al., *The tyrosine-based lysosomal targeting signal in lamp-1 mediates sorting into Golgi-derived clathrin-coated vesicles.* Embo J, 1996. **15**(19): p. 5230-9.
286. Marks, M.S., et al., *Protein sorting by tyrosine-based signals: adapting to the Y's and wherefores.* Trends Cell Biol, 1997. **7**(3): p. 124-128.
287. Marks, M.S., et al., *Protein targeting by tyrosine- and di-leucine-based signals: evidence for distinct saturable components.* J Cell Biol, 1996. **135**(2): p. 341-54.
288. Rohrer, J., et al., *The targeting of Lamp1 to lysosomes is dependent on the spacing of its cytoplasmic tail tyrosine sorting motif relative to the membrane.* J Cell Biol, 1996. **132**(4): p. 565-76.
289. Sandoval, I.V. and O. Bakke, *Targeting of membrane proteins to endosomes and lysosomes.* Trends Cell Biol, 1994. **4**(8): p. 292-297.
290. Cherqui, S., et al., *The targeting of cystinosin to the lysosomal membrane requires*

a tyrosine-based signal and a novel sorting motif. J Biol Chem, 2001. **276**(16): p. 13314-21.

291. Rouille, Y., W. Rohn, and B. Hoflack, *Targeting of lysosomal proteins.* Semin Cell Dev Biol, 2000. **11**(3): p. 165-71.
292. Staub, O., et al., *WW domains of Nedd4 bind to the proline-rich PY motifs in the epithelial Na+ channel deleted in Liddle's syndrome.* Embo J, 1996. **15**(10): p. 2371-80.
293. Rotin, D., O. Staub, and R. Haguenauer-Tsapis, *Ubiquitination and endocytosis of plasma membrane proteins: role of Nedd4/Rsp5p family of ubiquitin-protein ligases.* J Membr Biol, 2000. **176**(1): p. 1-17.
294. Rotin, D., *Regulation of the epithelial sodium channel (ENaC) by accessory proteins.* Curr Opin Nephrol Hypertens, 2000. **9**(5): p. 529-34.
295. Staub, O., et al., *Regulation of the epithelial Na+ channel by Nedd4 and ubiquitination.* Kidney Int, 2000. **57**(3): p. 809-15.
296. Staub, O., et al., *Regulation of stability and function of the epithelial Na+ channel (ENaC) by ubiquitination.* Embo J, 1997. **16**(21): p. 6325-36.
297. Pisoni, R.L. and J.G. Thoene, *The transport systems of mammalian lysosomes.* Biochim Biophys Acta, 1991. **1071**(4): p. 351-73.
298. Sandoval, R., J. Leiser, and B.A. Molitoris, *Aminoglycoside antibiotics traffic to the Golgi complex in LLC-PK1 cells.* J Am Soc Nephrol, 1998. **9**(2): p. 167-74.
299. Craik, J.D., et al., *Identification of glucose and nucleoside transport proteins in neonatal pig erythrocytes using monoclonal antibodies against band 4.5 polypeptides of adult human and pig erythrocytes.* Biochemistry and Cell Biology, 1988. **66**(8): p. 839-52.
300. Good, A.H., et al., *Characterization of monoclonal antibodies that recognize band 4.5 polypeptides associated with nucleoside transport in pig erythrocytes.* Biochemical Journal, 1987. **244**(3): p. 749-55.
301. Kwong, F.Y., et al., *Mammalian nitrobenzylthioinosine-sensitive nucleoside transport proteins. Immunological evidence that transporters differing in size and inhibitor specificity share sequence homology.* Journal of Biological Chemistry, 1992. **267**(30): p. 21954-60.
302. Beaumont, N., et al., *Antibodies as probes of nitrobenzylthionosine-sensitive nucleoside transporters*, in *Adenosine and adenine nucleotides*, L. Belardinolli and A. Pilkg, Editors. 1994. p. 55-60.
303. Barros, L.F., et al., *Immunolocalisation of nucleoside transporters in human placental trophoblast and endothelial cells: Evidence for multiple transporter isoforms.* Pflugers Archiv. European Journal of Physiology, 1995. **429**(3): p. 394-399.
304. Sundaram, M., et al., *Topology of a human nucleoside transporter implicated in cellular uptake of adenosine and anti-cancer drugs.* J. Biol. Chem., 2001. **submitted**.
305. Niman, H.L., et al., *Generation of protein-reactive antibodies by short peptides is an event of high frequency: implications for the structural basis of immune*

recognition. Proc Natl Acad Sci U S A, 1983. **80**(16): p. 4949-53.

306. Parker, J.M., D. Guo, and R.S. Hodges, *New hydrophilicity scale derived from high-performance liquid chromatography peptide retention data: correlation of predicted surface residues with antigenicity and X-ray-derived accessible sites.* Biochemistry, 1986. **25**(19): p. 5425-32.
307. Parker, J.M. and R.S. Hodges, *Prediction of surface and interior regions in proteins--Part I: Linear tripeptide sequences identify structural boundaries in proteins.* Pept Res, 1991. **4**(6): p. 347-54.
308. Wohlheuter, R.M., W.E. Brown, and P.G.W. Plagemann, *Kinetic and thermodynamic studies on nitrobenzylthioinosine binding to the nucleoside transporter of Chinese hamster ovary cells.* Biochim. Biophys. Acta, 1983. **731**: p. 168 - 176.
309. Plagemann, P.G. and R.M. Wohlhueter, *Nucleoside transport in cultured mammalian cells. Multiple forms with different sensitivity to inhibition by nitrobenzylthioinosine or hypoxanthine.* Biochimica et Biophysica Acta, 1984. **773**(1): p. 39-52.
310. Padgett, R.A., et al., *Splicing of messenger RNA precursors.* Annu Rev Biochem, 1986. **55**: p. 1119-50.
311. Mighell, A.J., et al., *Vertebrate pseudogenes.* FEBS Lett, 2000. **468**(2-3): p. 109-14.
312. Fideu, M.D. and M.T. Miras-Portugal, *Long term regulation of nucleoside transport by thyroid hormone (T3) in cultured chromaffin cells.* Neurochemical Research, 1992. **17**(11): p. 1099-104.
313. Aguayo, C. and L. Sobrevia, *Nitric oxide, cGMP and cAMP modulate nitrobenzylthioinosine-sensitive adenosine transport in human umbilical artery smooth muscle cells from subjects with gestational diabetes.* Experimental Physiology, 2000. **85**(4): p. 399-409.
314. Aguayo, C., et al., *Modulation of adenosine transport by insulin in human umbilical artery smooth muscle cells from normal or gestational diabetic pregnancies.* Journal of Physiology, 2001. **534**(Pt 1): p. 243-54.
315. Fideu, M.D., et al., *Prolactin and cyclosporine modulate adenosine transporters and adenosine A1 receptors in the rat brain.* J Physiol Biochem, 2000. **56**(2): p. 83-90.
316. Sen, R.P., E.G. Delicado, and M.T. Miras-Portugal, *Differential modulation of nucleoside transport types in neuroblastoma cells by protein kinase activation.* Neuropharmacology, 1999. **38**(7): p. 1009-15.
317. Sen, R.P., et al., *Effect of P(2Y) agonists on adenosine transport in cultured chromaffin cells.* Journal of Neurochemistry, 1993. **60**(2): p. 613-619.
318. Casillas, T., E.G. Delicado, and M.T. Miras-Portugal, *Adenosine 5'-triphosphate modulation of nitrobenzylthioinosine binding sites in plasma membranes of bovine chromaffin cells.* Neuroscience Letters, 1993. **164**(1-2): p. 51-4.
319. Jordan, A. and P. Reichard, *Ribonucleotide reductases.* Annu Rev Biochem, 1998. **67**: p. 71-98.

320. Wong, S.J., et al., *Increased sensitivity of hydroxyurea-resistant leukemic cells to gemcitabine.* Clin Cancer Res, 1999. **5**(2): p. 439-43.
321. Plunkett, W., P. Huang, and V. Gandhi, *Preclinical characteristics of gemcitabine.* Anticancer Drugs, 1995. **6**(SUPPL. 6): p. 7-13.
322. Plunkett, W., et al., *Gemcitabine: preclinical pharmacology and mechanisms of action.* Semin Oncol, 1996. **23**(5 Suppl 10): p. 3-15.
323. Yarbro, J.W., *Mechanism of action of hydroxyurea.* Semin Oncol, 1992. **19**(3 Suppl 9): p. 1-10.
324. Balzarini, J., *Effect of antimetabolite drugs of nucleotide metabolism on the anti-human immunodeficiency virus activity of nucleoside reverse transcriptase inhibitors.* Pharmacol Ther, 2000. **87**(2-3): p. 175-87.
325. Skog, S., et al., *Hydroxyurea-induced cell death in human T lymphoma cells as related to imbalance in DNA/protein cycle and deoxyribonucleotide pools and DNA strand breaks.* Anticancer Drugs, 1992. **3**(4): p. 379-86.
326. Agbanyo, F.R., C.E. Cass, and A.R. Paterson, *External location of sites on pig erythrocyte membranes that bind nitrobenzylthioinosine.* Molecular Pharmacology, 1988. **33**(3): p. 332-7.
327. Agbanyo, F.R., et al., *5'-S-(2-aminoethyl)-N6-(4-nitrobenzyl)-5'-thioadenosine (SAENTA), a novel ligand with high affinity for polypeptides associated with nucleoside transport. Partial purification of the nitrobenzylthioinosine-binding protein of pig erythrocytes by affinity chromatography.* Biochemical Journal, 1990. **270**(3): p. 605-14.
328. Buolamwini, J.K., et al., *Conjugates of fluorescein and SAENTA (5'-S-(2-aminoethyl)-N6-(4- nitrobenzyl)-5'-thioadenosine): Flow cytometry probes for the es nucleoside transporter elements of the plasma membrane.* Nucleosides and Nucleotides, 1994. **13**(1-3): p. 737-751.
329. Hammond, J.R., *Enhancement of the Functional Stability of Solubilized Nucleoside Transporters By Substrates and Inhibitors.* Biochemical Pharmacology, 1997. **53 (5)**: p. 623-629.
330. Burres, N.S. and C.E. Cass, *Comparison of Coulter volumes with radiometrically determined intracellular water volumes for cultured cells.* In Vitro Cell Dev Biol, 1989. **25**(5): p. 419-23.
331. Graham, F.L., et al., *Characteristics of a human cell line transformed by DNA from human adenovirus type 5.* J Gen Virol, 1977. **36**(1): p. 59-74.
332. Broydell, M., et al., *The role of the GLUT 4 transporter in regulating rat myoblast glucose transport processes.* Biochim Biophys Acta, 1998. **1371**(2): p. 295-308.
333. Chan, J.Y., et al., *Inhibition of glucose transporter gene expression by antisense nucleic acids in HL-60 leukemia cells.* Life Sci, 1999. **65**(1): p. 63-70.
334. Schwiebert, E.M., et al., *Analysis of ClC-2 channels as an alternative pathway for chloride conduction in cystic fibrosis airway cells.* Proc Natl Acad Sci U S A, 1998. **95**(7): p. 3879-84.
335. Ozawa, K., et al., *150-kDa oxygen-regulated protein (ORP150) suppresses hypoxia-induced apoptotic cell death.* J Biol Chem, 1999. **274**(10): p. 6397-404.

336. Bristol, L.A. and J.D. Rothstein, *Use of antisense oligodeoxynucleotides to inhibit expression of glutamate transporter subtypes.* Methods Enzymol, 1998. **296**: p. 514-29.
337. Kitazono, M., et al., *Multidrug resistance and the lung resistance-related protein in human colon carcinoma SW-620 cells.* J Natl Cancer Inst, 1999. **91**(19): p. 1647-53.
338. Materna, V., et al., *Kinetic characterization of ribozymes directed against the cisplatin resistance-associated ABC transporter cMOAT/MRP2/ABCC2.* Cancer Gene Therapy, 2001. **8**(3): p. 176-84.
339. Kowalski, P., et al., *Selection and characterization of a high-activity ribozyme directed against the antineoplastic drug resistance-associated ABC transporter BCRP/MXR/ABCG2.* Cancer Gene Ther, 2001. **8**(3): p. 185-92.
340. Mackey, J.R., et al., *Immunohistochemical Variation of Human Equilibrative Nucleoside Transporter 1 (hENT1) Protein in Primary Breast Cancers.* Clin Cancer Res, 2001. **in press**.
341. Goh, L.B., P. Mack, and C.W. Lee, *Nitrobenzylthioinosine-binding protein overexpression in human breast, liver, stomach and colorectal tumour tissues.* Anticancer Res, 1995. **15**(6B): p. 2575-9.
342. Takechi, T., et al., *Screening of differentially expressed genes in 5-fluorouracil-resistant human gastrointestinal tumor cells.* Jpn J Cancer Res, 2001. **92**(6): p. 696-703.